1-11-2016

Defining the Microglia Response to Ischemic Stroke Injury: The Role of CD200-CD200R1 Signaling

Rodney M. Ritzel
University of Connecticut - Storrs, rritzel@uchc.edu

Defining the Microglia Response to Ischemic Stroke Injury:

The Role of CD200-CD200R1 Signaling

Rodney M. Ritzel, Ph.D.

University of Connecticut, 2016

Abstract

The work presented herein details our efforts at characterizing and understanding the mechanisms that govern microglia homeostasis and activation in the central nervous system (CNS). These studies have focused on the microglial response to aging and ischemic stroke, highlighting the importance of neuro-immune interactions and inflammatory signaling in the brain (Chapters 1 and 2). We begin with our investigations into microglial activity following ischemic brain injury and how these responses differ from that of other bone marrow-derived monocyte populations (Chapter 3). Then we define the role of the CD200-CD200R1 immuno-inhibitory signaling axis in ischemic stroke (Chapter 4), highlighting the importance of neuronal-glial interactions in maintaining immune privilege and attenuating post-stroke inflammation. Lastly, our work on the effects of aging on microglia function (Chapter 5) and immune surveillance (Chapter 6) in the CNS furthers our understanding of microglia senescence and the phenomenon of 'inflamm-aging'.

Defining the Microglia Response to Ischemic Stroke Injury:

The Role of CD200-CD200R1 Signaling

Rodney M. Ritzel

B.S., Millersville University, 2007

Ph.D., University of Connecticut, 2016

A Dissertation

Submitted in Partial Fulfillment of the

Requirements for the degree of

Doctor of Philosophy

at the

University of Connecticut

2016

APPROVAL PAGE

Doctor of Philosophy Dissertation

Defining the Microglia Response to Ischemic Stroke Injury:

The Role of CD200-CD200R1 Signaling

Presented by:

Rodney M. Ritzel

Major Advisor _____
Louise D. McCullough, M.D., Ph.D.

Associate Advisor _____
Stefan Brocke, M.D., Ph.D.

Associate Advisor _____
Stephen J. Crocker, Ph.D.

Associate Advisor _____
Betty A. Eipper, Ph.D.

Associate Advisor _____
Lynn Puddington, Ph.D.

University of Connecticut

2016

Acknowledgements

First and foremost, I would like to thank my thesis advisor Dr. Louise McCullough. One quickly understands the mentoring challenges posed by the busy schedule of a physician scientist, yet Louise has displayed a remarkable ability to advise at every available opportunity and has remained committed to fostering my growth and development as a scientist. Louise takes seriously her role as mentor and her impressive time management skills, unparalleled grantsmanship and one-of-a-kind communication skills have made her the type of role model that not just inspires but empowers others to reach their full potential. Perhaps this is most evident in her open-minded, hands-off approach to fostering trainee independence, which has enabled me to chart my own intellectual pursuits in addition to my central thesis project. Louise has many redeemable mentoring qualities, however none have been more critical to fueling my passion for science than her willingness to let me pursue my own interests. For these reasons alone, I am incredibly grateful to her and proud to call her my mentor.

I must also thank all of the other members of my lab for their support and camaraderie along the way. Many of the findings presented in this dissertation may not have been possible if it weren't for the dedication of a select group of highly motivated research technicians that have assisted me during this time. Despite having spent countless hours training these amazing students, I feel forever indebted to the following individuals: Anita Patel, Joshua Crapser, Sarah Pan, and Brittany Knight. I wish them great success in their future endeavors and thank them for their cooperation and friendship during my tenure as a graduate student.

I would like to thank my fellow colleagues, Dr. Matthew Hammond, Dr. Rajkumar Verma, and Jeremy Grenier for engaging in critical thinking sessions, rigorous scientific debate, and off-the-wall 'thought' experiments. These interactions were not taken for granted, as this intellectual stimulation has been vital to my survival as a scientist.

I feel extremely fortunate to have been a part of such a youthful and energetic group. I would especially like to thank Sharon Dimauro and Lori Capozzi for their administrative support. Like any productive graduate student, I have made numerous purchase requests in my time, and being regularly reminded how expensive my graduate studies have been has enabled me to prioritize my ideas and be more economic in my scientific thinking. Dr. Evan Jellison, the director of the flow cytometry core, has been an enormous asset to both my development and the institution. Indeed, I am very appreciative to all of the brilliant members of Dr. Leo Lefrancois' laboratory, especially Dr. Brian Sheridan and Dr. Jellison for providing me with hands-on training and for helping me navigate the technical aspects of immunology research. I would also like to thank my thesis committee members, Dr. Brocke, Dr. Puddington, Dr. Crocker, Dr. Eipper, and Dr. Lauren Sansing (presently at Yale) for their valuable feedback over the years.

Of course none of this would have been possible without the UConn Health Center Biomedical Science PhD program, the Graduate Programs Committee, the Department of Neuroscience and graduate program and all of the individuals who work so hard to assure an excellent educational experience for students. In particular, I would like to thank Dr. Barbara Kream, Stephanie Rauch, Swapna Das, Jody Gridley and Diana Mikulak for their continued dedication. I would also like to thank Mary Nordgren for her

assistance with grant submissions, and Anna Sagan and Ella Sun for their assistance in organizing my travel expenses.

Lastly, I would like to thank my parents and my sister for their patience these last few years. I look forward to being more involved in their lives. My relationship with my fiancé has also been tested during this time, yet throughout it all we have persevered together. Her unflappable patience, understanding, and compassion has served as the foundation on which my well-being and success stands.

Table of Contents

Chapter 1……..……1

Introduction……..……....1

Stroke and inflammation……..……...1

Role of microglia in stroke injury……..……..2

CD200 regulation of microglia……..……..3

Inflammation in the aging brain……..……7

Chapter 2……..……..11

Microglia and ischemic stroke: a double-edged sword…….…….....11

Abstract……..……12

Introduction…….…….....13

Origin and development of microglia……..……..15

Markers and methods for identification……..……..15

Iba-1 expression by immunohistochemistry……..…….....15

CD45/CD11b expression by flow cytometry……..……..18

Transgenic mice…….....20

Chimeras……..21

Resting Microglia……..……..22

Resting phenotype……..……..22

Inhibitory signaling of microglia……..…….24

CD200/CD200R1……24

Fractalkine (CX3CL1)/CX3CR1……25

SIRPα/CD47……..……..……26

Triggering receptor expressed on myeloid cells 2 (TREM2)……...…27

Activation of microglia…….……...…27

Microglial activation phenotypes: M1 and M2……..…….……29

Migration……..…..……31

Phagocytosis by microglia and macrophages……32

Purinergic receptors……..……33

Toll like receptor (TLR)……..……..……33

Functional insights into resident microglia and peripheral macrophages……35

Microglial proliferation and renewal……35

MMPs……..……36

TNF……..……37

iNOS……37

Peroxiredoxin……..……38

Summary……..…….38

Chapter 3……..…….40

Functional differences between microglia and monocytes after ischemic stroke……40

Abstract…….….40

Introduction……..…….40

Materials and Methods……...……43

Mice/Animals……..……..……43

Ischemic Stroke Model…….……43

Tissue harvesting……..44

Flow cytometry……..……44

Phagocytosis bead assay…….……45

Reactive oxygen species measurement…..……45

BRDU labeling and analysis…….……46

Intracellular cytokine production…….……46

Bone marrow chimera generation…….……46

Statistical analyses…….……47

Results……47

Ischemic stroke induces microglial death, bone marrow production of monocytes, and recruitment of monocytes to the injured brain……..…47

Differential oxidative stress and cytokine production by microglia and monocytes after stroke……..…48

Monocytes are the predominant phagocytes in the brain at 72hrs after stroke……50

Discussion……56

Supplemental Material……..……..67

Author Contributions……..……68

Acknowledgements……..……68

Chapter 4……..…….69

CD200R1 immune inhibitory signaling attenuates brain inflammation and promotes behavioral recovery after stroke……..……69

Abstract……..……69

Introduction……70

Materials and Methods……72

Mice/Animals……..……72

Ischemic stroke model……..……73

Clinical assessment……73

Behavioral testing……..……73

Hanging wire……74

Open Field……..……74

Y maze spontaneous alternation……75

Static rod……..……75

Rotarod……..……76

Nesting activity……76

Terminal histopathology……76

Immunohistochemistry……..……77

Enzyme-linked immunoabsorbant assay……77

Tissue processing for flow cytometry……..……78

Intracellular cytokine production……..……80

Statistical analyses……..……80

Results……..……81

Characterization of CD200- and CD200R1-expressing cells in the healthy adult brain……81

CD200R1 mediates T cell entry into the un-injured brain and regulates basal cytokine production in CNS-specific T cells but not microglia……..84

CD200R1 immune-inhibitory signaling promotes better outcomes after ischemic stroke……..……89

Loss of CD200R1-mediated immune inhibition worsens behavioral recovery following stroke……..……90

CD200-CD200R1 signaling attenuates leukocyte infiltration into the ischemic brain…… 95

Lack of CD200R1-mediated inhibition results in exacerbated peripheral immune dysfunction at 7 days after stroke……..……101

CD200 protein expression is exaggerated after stroke with age……..…104

Discussion……...……106

Supplemental Material……..……118

Author Contributions……119

Acknowledgements……..……119

Chapter 5……120

Age- and location-related changes in microglia function……..……120

Abstract……..……120

Introduction……121

Materials and Methods……123

Mice/Animals……123

Tissue harvesting……124

Flow cytometry…… ……124

Assessment of blood-brain barrier permeability……..……126

ELISA cytokine measurement……127

RNA isolation and qPCR……128

Statistical analyses……128

Results.....129

Age- and location-related changes were seen in the physical properties and CD45/CD11b expression of microglia……129

Age- and location-related increases in mitochondrial activity, reactive oxygen species (ROS) production, and expression of the pro-inflammatory cytokines……131

Age- and location-related changes in phagocytic potential of microglia are associated with changes in the expression of immunoregulatory molecules……133

The blood-spinal cord barrier exhibits a relatively high degree of vascular leakage……134

Tissue cytokine production in the CNS is profoundly affected by the regional environment……139

Discussion……142

Supplemental Material……149

Author Contributions……151

Acknowledgements……151

Chapter 6……152

Opposing roles for immune surveillant CD8 T cells in the aging central nervous system……152

Abstract……152

Introduction……153

Materials and Methods……156

Mice/Animals……156

Tissue harvesting……156

Flow cytometry……157

ELISA cytokine measurement……159

Intravascular staining and cell isolation……159

Immunohistochemistry……160

Middle cerebral artery occlusion (MCAO) model of ischemic stroke……161

Statistical analyses……161

Results……162

Aging increases the number of peripheral leukocytes in the CNS……162

Age-related chemokine production is associated with active recruitment of CD8 T cells into the aging brain……162

CD8 T cells are present in perivascular and parenchymal regions throughout the aging CNS……165

Age-related, CNS-specific CD8 T cells have memory/effector phenotype and expression markers of T cell-receptor activation……168

Age-related recruitment of CNS-specific CD8 T cells is mostly stochastic……170

Increased immune surveillance by CD8 T cells in the aging brain is associated with healthier microglial function……173

Basal and stimulus-driven production of cytokines and chemokines associated with neutrophil chemotaxis following ischemic stroke.....173

Discussion……..……180

Supplemental Material……..190

Author Contributions……192

Acknowledgements……..……192

Chapter 7……..…193

Significance and Future Directions……193

Significance……..……..193

Future Directions……..……196

Conclusion……..…….200

References……..…….201

Chapter 1:

Introduction

Stroke and inflammation

Stroke affects 15 million people worldwide each year[1]. Increasing life expectancy together with an expanding aging population will place a profound burden on the economy well beyond the current estimate of $69 billion annually[1]. In recent years, major advances in the area of ischemic injury have highlighted the importance of the inflammatory response to stroke. This view is supported by growing evidence showing an association between inflammation, brain damage, and poor outcome in ischemic stroke patients[2,3]. The sterile inflammatory response to stroke is robust and characterized by a stereotypic sequence of events involving the brain, its vasculature, and the peripheral immune system. Oxidative stress and the release of pro-inflammatory mediators induce expression of adhesion molecules (e.g., ICAM, VCAM-1, selectins) on brain endothelial cells, promoting leukocyte entry into the brain[4]. Infiltrating leukocytes amplify the immune response further by releasing a variety of cytotoxic agents including cytokines, reactive oxygen species (ROS), and extracellular proteases (e.g., MMP-9), ultimately leading to extensive neuronal death, blood brain barrier (BBB) breakdown, and further influx of leukocytes[5]. Many investigators have

demonstrated experimentally that by antagonizing these features of the post-ischemic response, infarct damage can be salvaged, and survival outcomes improved[6,7]. As key players in the initiation and maintenance of this response, microglia have become increasingly recognized as cellular targets for therapeutic drug development[7,8].

Role of microglia in stroke injury

The hallmark of neuroinflammation is microglial activation. Microglia express many pattern recognition receptors like toll-like receptors, that when activated, as in stroke, shift phenotype from a resting, ramified morphology to an activated, amoeboid state (**Figure 1-1**). Activation is often accompanied by an increase in protein synthesis (e.g., production of cytokines), proliferation, migration, and MHCII/CD40 expression[7]. The release of chemokines, cytokines, and ROS further activate microglia and amplify the local inflammatory response. Excessive activation can result in collateral damage (e.g., neuronal death), alter the neurovascular unit, and exacerbate tissue injury, potentially leading to a chronic inflammatory state[9,10]. Indeed, severe ischemic insults are generally associated with increased numbers of microglia[11]. However, when appropriately kept in check, microglia activation can be regarded as a beneficial host response to ischemic injury, responsible for resolving inflammation and restoring function by migrating to the site of injury, clearing apoptotic neutrophils, and releasing various growth factors (e.g., BDNF, VEGF) and anti-inflammatory mediators[12-15]. Thus, the regulation of microglia following stroke is crucial in determining the extent of neuronal injury and disease progression.

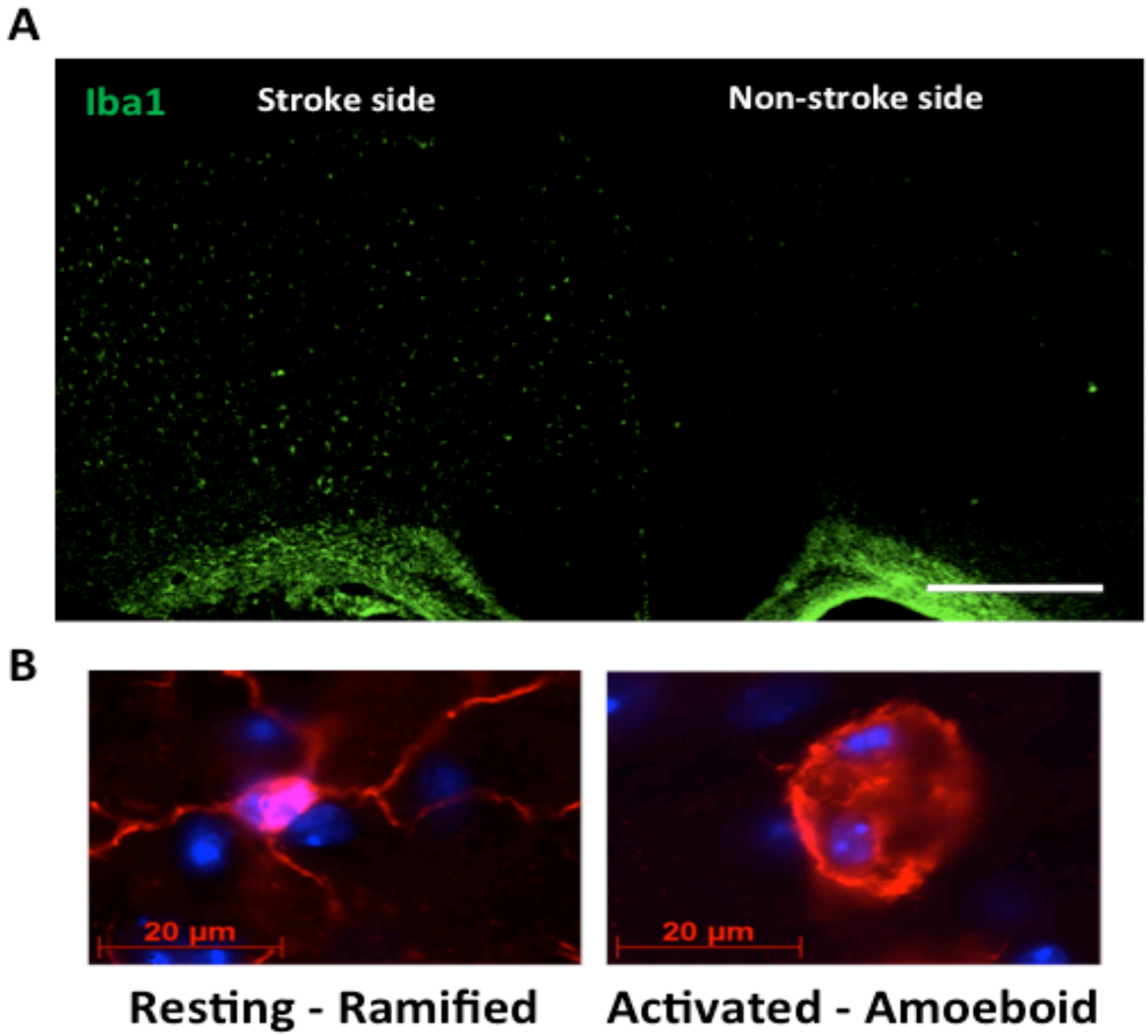

Figure 1-1. Microglia activation after ischemic stroke.

Microglia can be visualized as Iba1-positive cells (A, green; and B, red) in the brain using immunohistochemistry. Activation of microglia (green) can be observed as early as 6 hours in the ipsilateral (ischemic) cortex after MCAO (A). After injury, microglia exhibit a morphological shift from a ramified (resting) state to an activated, amoeboid state (B). Abbreviation: Iba1 ionized calcium-binding adaptor molecule 1, MCAO middle cerebral artery occlusion

CD200 regulation of microglia

The CNS also has several endogenous neuroprotective mechanisms that ensure inhibition of central immune responses, but these have been less studied. These inhibitory signals are provided in the form of neuronal-glial interactions, which act to suppress microglial activation when neurons are healthy. One such mechanism involves the immunosuppressant interaction between CD200 (OX-2), which is highly expressed on neurons and CD200 receptor 1 (CD200R1/OX-2R), a myeloid immune inhibitory receptor expressed at low levels on resting microglia. Under normal conditions, activation of CD200R1 by its CD200 ligand prevents immune activation by inhibiting signaling pathways involved in the production of pro-inflammatory mediators[16-18]. Following CNS injury, this interaction is disrupted (**Figure 1-2**). Reduced activation of CD200R1 allows a pro-inflammatory response to ensue. The functional significance of this disruption is best evidenced in CD200-deficient mice, which have an enhanced susceptibility to autoimmune disease and worsened outcome in several models of neuroinflammation[19-21]. CD200-deficient mice exhibit widespread microglial activation as indicated by increased aggregation, CD40/MHCII expression, and amoeboid morphology[19,21,22]. To date, few studies have examined the role of the CD200-CD200R1 axis as it relates to experimental stroke; the literature is limited to two studies which report an early decrease in CD200 gene expression in the infarct core and an increase in CD200R1-positive cells in the brain[23,24]. What accounts for these changes in CD200/CD200R1 expression, and how they impact the central immune response is the focus of this thesis work.

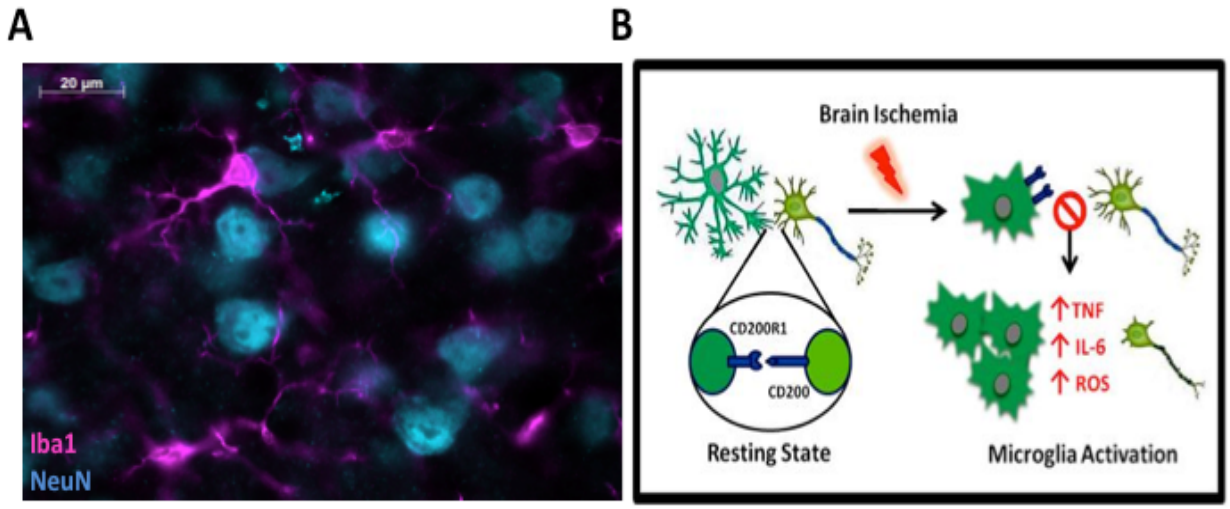

Figure 1-2. Neuronal-glial Interactions in the healthy and diseased brain. Immunostaining shows Iba1-positive microglia (pink) and NeuN-positive neurons (blue) in the healthy brain (A). Microglial extensions can be observed in close contact with neuronal cell bodies in every region throughout the brain. A schematic of CD200-CD200R1 signaling in the healthy brain and after stroke (B). Under normal conditions, neurons maintain contact-dependent inhibition of microglia by engagement of CD200R1 by CD200. The proposed model demonstrates how ischemic injury results in microglia activation. Neuronal death and remodeling of the extracellular matrix disrupts CD200-CD200R1 interactions, thereby releasing the brake on microglia activation resulting in the release of pro-inflammatory mediators.

CD200 is ubiquitously expressed throughout the body including the CNS, whereas CD200R1 is primarily expressed on leukocytes of the myeloid lineage (e.g., microglia, monocytes, macrophages, dendritic cells, neutrophils). CD200 and CD200R1 are structurally similar, type I transmembrane glycoprotein members of the immunoglobulin superfamily. These genes are located on the same chromosome and are highly conserved in structure and function across rodents and humans[25]. CD200 lacks a cytoplasmic motif capable of recruiting adapter proteins, and thus imparts a unidirectional inhibitory signal to CD200R1-expressing cells. Both in vivo and in vitro studies have demonstrated that CD200R1 activation suppresses TLR-4- , IL-17- , and IFN-γ-mediated inflammatory pathways, resulting in the downregulation of many important cytokines (e.g., TNF, IL-1β) and chemokines (e.g., CXCL8), and a biased shift towards a Th2 response (i.e., IL-4, IL-10)[26-29]. Interestingly, many of these pathways have been shown to be detrimental in stroke, leading us to speculate (Aim 3), that targeting of CD200-CD200R1 signaling by a CD200R1 agonist will provide protection by reducing the microglial response to injury[30-34].

Given that inflammation can be detrimental to stroke outcome[35,36], recent efforts have targeted the immune system to develop novel neuroprotective therapies. Inflammation is an attractive target for therapy due to its wide therapeutic window. In many stroke survivors, elevated levels of acute-phase markers and circulating leukocytes persist for weeks, even months after a stroke event, increasing the risk of recurrent events[37-39]. Indeed, higher CSF and serum levels of IL-6 and IL-1 have been shown to correlate with larger infarcts in humans[40-42]. To date, several clinical trials have examined the effectiveness of blocking antibodies directed against adhesion

molecules (e.g., ICAM-1 and CD11b/CD18); however, these drugs have proven unsuccessful due to lack of efficacy and adverse side effects[43,44]. Although it is unclear why these therapies failed to translate, one explanation is that post-ischemic inflammation acts through multiple redundant pathways that cannot be effectively treated by targeting a single adhesion molecule or cytokine[45]. The therapeutic potential of CD200R1 manipulation offers a promising new approach, as its activation is known to suppress several important pro-inflammatory mediators involved in multiple signaling pathways [46].

Inflammation in the aging brain

Acute ischemic stroke is a disease that primarily affects the elderly [47]. Indeed, the strongest independent risk factor for stroke is age, as elderly patients have the highest mortality and morbidity. With increasing life expectancy, the world is facing a rapid expansion in its elderly population. In addition to the looming economic toll, the concurrent rise in age-related disease and disability will also put a burden on the healthcare system. Currently, there is no treatment beyond the four-hour window with which a patient must present to be eligible for TPA. To date, most treatments that have been successful in experimental models have failed to translate in clinical trials. The reason for this lack of efficacy is not understood, although may be associated with the design of commonly used models [48]. For instance, the vast majority of rodent stroke studies are performed using 2 month-old young mice, roughly equivalent to that of a 10-year-old human child. Like humans, aged mice are profoundly different from their

younger counterparts. Aging is associated with the following changes: epigenetic modifications, mitochondrial and DNA damage, redox stress, endocrinosenescence, immunosenescence, replicative senescence, and diminished regeneration capacity [49]. As a consequence, aging individuals display considerable variation in normal physiology, response to injury, and facilitative recovery. At the molecular level, aging induces significant changes in the CNS transcriptome and proteome. At the cellular level, blood-brain barrier integrity is compromised and immune privilege is broken [50,51]. Microglia in aged mice display a higher basal activated state, altered responsivity, and dysregulated responses to stimuli [52] (**Figure 1-3**). Microglia dystrophy is a hallmark of CNS aging [53,54]. The gradual increase in basal inflammatory processes that occurs with age is a phenomenon known as 'inflamm-aging' and is believed to contribute to the etiology of several neurodegenerative diseases [55,56]. Thus, understanding how the aged CNS environment influences the response and subsequent recovery following stroke injury is critical to developing reliable targets and efficacious treatments.

The present dearth of studies exploiting the use of aged mice may explain why past therapeutic targets have failed to translate in the clinic, where the majority of enrolled patients are elderly. By utilizing aged mice with varying degrees of disease state researchers may better model the pathological setting in which this disease occurs in humans. The identification of age-specific targets and treatment paradigms may eventually yield more effective treatments for older populations. In this work, we examine the functional contributions of microglia and monocytes to ischemia and identify novel inflammatory mechanisms that may help explain why older individuals are

A

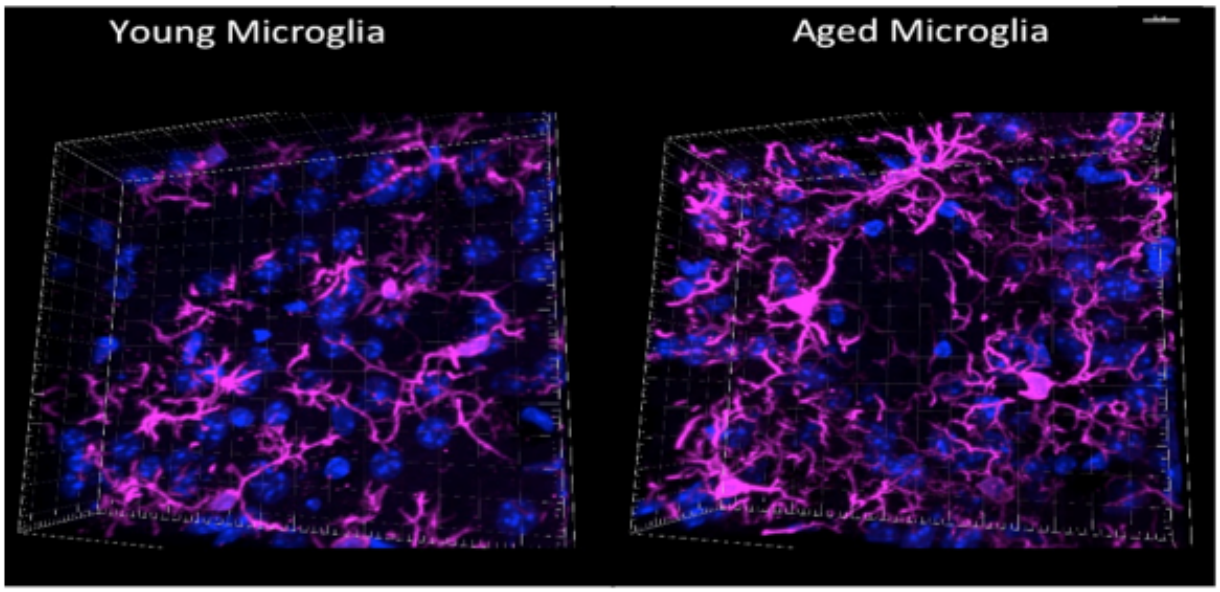

Figure 1-3. Age-related changes in microglia.

The effects of normal aging on microglia morphology is shown (A). Aging is associated with an increase in activated microglia with enlarged somas and pronounced morphological heterogeneity in branching patterns.

more prone to chronic inflammatory responses and worse outcomes following traumatic brain injury.

Chapter 2:

Microglia and ischemic stroke: a double-edged sword

Anita R. Patel, Rodney M. Ritzel, Louise D. McCullough, and Fudong Liu

This chapter was published as a literature review in International Journal of Physiology, Pathophysiology, and Pharmacology. 2013 May; 5(2): 73-90.

Abstract

Inflammatory processes have a fundamental role in the pathophysiology of stroke. A key initial event is the rapid activation of resident immune cells, primarily the microglia. This cell population is an important target for new therapeutic approaches to limit stroke damage. Activation of microglia is normally held in check by strictly controlled mechanisms involving neuronal-glial communication. Ischemic stroke is a powerful stimulus that disables the endogenous inhibitory signaling and triggers microglial activation. Once activated, microglia exhibit a spectrum of phenotypes, release both pro- and anti-inflammatory mediators, and function to either exacerbate ischemic injury or help repair depending on different molecular signals the microglial receptors receive. Various ligands and receptors have been identified for microglial activation. Experimental tools to detect these inflammatory signals are being increasingly

developed in an effort to define the functional roles of microglia. Fine-tuning immunomodulatory interventions based on the heterogeneous profiles of microglia are urgently needed for ischemic stroke.

Introduction

Inflammation plays a critical role in mediating post-ischemic injury. The activation of microglia, the major resident immune cells in the brain, is a key element in triggering the innate immune response [30]. When ischemia occurs, cessation of cerebral blood flow leads to deprivation of oxygen and glucose to areas supplied by the occluded vessel. Resultantly, vulnerable neurons are subject to death and the endogenous signaling that inhibits inflammatory responses under physiological conditions compromises, leading to microglial activation. Once activated, microglia develop macrophage-like capabilities including phagocytosis, cytokine production, antigen presentation and the release of matrix metalloproteinases (MMPs) that weaken the blood brain barrier (BBB) [57]. As a result, peripheral leukocytes infiltrate into the brain and the normally immune-privileged brain environment is exposed to systemic responses that further exacerbate inflammation and brain damage.

The inflammatory response has dual effects on ischemic injury [58]. Stroke-induced microglial activation causes a release of variety of inflammatory mediators many of which are cytotoxic and/or cytoprotective [59]. Phagocytosis of cellular debris and harmful substances along with the release of anti-inflammatory cytokines by microglia occurs in an effort to defend against damaging substances and restore tissue

homeostasis by clearing pathogens or necrotic cells, and consequently attenuate the detrimental effects of inflammation and aid in tissue repair [60,61]. Because of their critical roles in the immune response to stroke, microglia have become a recent target of interest for many stroke scientists. This review focuses on current findings, providing an update on microglial activation, phenotype identification, and the roles of microglia in the pathophysiology of cerebral ischemia.

Origin and development of microglia

There has been much controversy over the characterization of the cell lineage of microglia. The most significant hypotheses of the development of microglia debate their embryonic neuroectodermal or mesodermal origin. Unlike the ectodermal development of macroglia (astrocytes and oligodendrocytes) and neurons, a consensus in favor of the mesodermal hematopoietic origin of microglia is currently held [62,63]. A subset of primitive myeloid precursors, localized in the extra-embryonic yolk sac (YS) at embryonic day 8 (E8) was shown to contribute to the rise of yolk sac microglia that persists into adulthood [64]. This cellular subset of primitive hematopoiesis contributes little to blood leukocyte development, which is largely specific to definitive hematopoiesis of hematopoetic stem cells (HSCs) [64-66]. Microglia precursors originate in the embryonic yolk sac before the emergence of definitive HSCs from the aorto-gonad-mesenephros (AGM). The direct precursors of microglia that travel to the neural tube at E8 are exclusively the $CD45^{-}cKit^{+}$ cells. This subpopulation of erythromyeloid cells eventually begins expressing CX3CR1 and CD45 and travels into the

neuroectoderm in a matrix metalloproteinase 8 (MMP 8) and MMP 9 dependent manner to develop into microglia [67,68]. These precursor cells are seen seeding the brain rudiment by E10 in rodents [64] and have a full microglial morphology beginning at E14[67].

The transcription factor *Myb* is essential for the development of HSCs [69,70] and can be found in the AGM during embryogenesis [63,71]. By using *Myb* knockout (KO) mice, Schulz et al. [70]found that yolk sac-derived $CD45^{+}CX_3CR1^{hi}F4/80^{hi}$ macrophages and microglia still develop in normal numbers and remain independent of *Myb* into adulthood; however, $CD45^{+}CX_3CR1^{+}F4/80^{low}CD11b^{hi}$ monocytic phagocytes continually replaced by bone marrow (BM) in an adult are unable to develop without *Myb*. The transcription factor PU.1, on the other hand, is necessary for myelopoiesis of the YS but dispensable for the development of definitive HSCs [66,70]. This further suggests two separate myeloid lineages of peripheral macrophages and resident microglia.

Moreover, colony stimulating factor (CSF) and its receptor CSF-1R are necessary for the differentiation of most macrophages/microglia [72]. Recent studies showed that in CSF-1R KO mice, yolk sac-derived microglia do not develop and are deficient throughout life, but HSC-derived monocytes are able to differentiate and circulate without dependence on CSF-1R [63,64,73]. Fate mapping analysis of *Flt3*-Cre x $Rosa^{LSL\text{-}YFP}$ mice also shows that yolk sac-derived microglia are independent of *Flt3*, a chemokine present on multipotent hematopoetic progenitors in the blood and brain [70]. Taken together, the separation between HSCs and yolk sac derivations is evident and allows insight into microglial ontogeny.

Markers and methods for Identification

To date, no single microglial-specific marker has been identified, keeping the cell type indistinguishable from macrophages and various myeloid-derived cells that infiltrate the brain during pathological states [74]. Changes in microglial activation in response to central nervous system (CNS) injury are illustrated by diverse phenotypes and unique expression of cell surface proteins. Microglial activation stages can be detected by characterizations of these changes, but the similarities with other cell types pose a major hurdle for their definitive characterization and detection.

Ionized calcium binding adaptor molecule-1 (Iba-1) expression by immunohistochemistry (IHC)

Iba-1 is amongst the most useful proteins for distinguishing microglia through IHC and immunocytochemistry (ICC) staining [75,76], especially for studies of cerebral ischemia where the expression of Iba-1 is upregulated [77] (**Figure. 2-1**) . However, Iba-1 has also been shown to bind various cells of monocytic lineage [75], and thus its specificity for microglia staining is limited in injured brain tissue where peripheral macrophages may infiltrate. Other markers, such as CD11b, Isolectin (IB4), and F4/80, have also been used for *in vivo* and *in vitro* microglial staining. Although the benefits of IHC include the ability to create a spatiotemporal and morphological profile of microglia within the CNS, it lacks in specificity and may be inconsistent depending on the type of histological preparation.

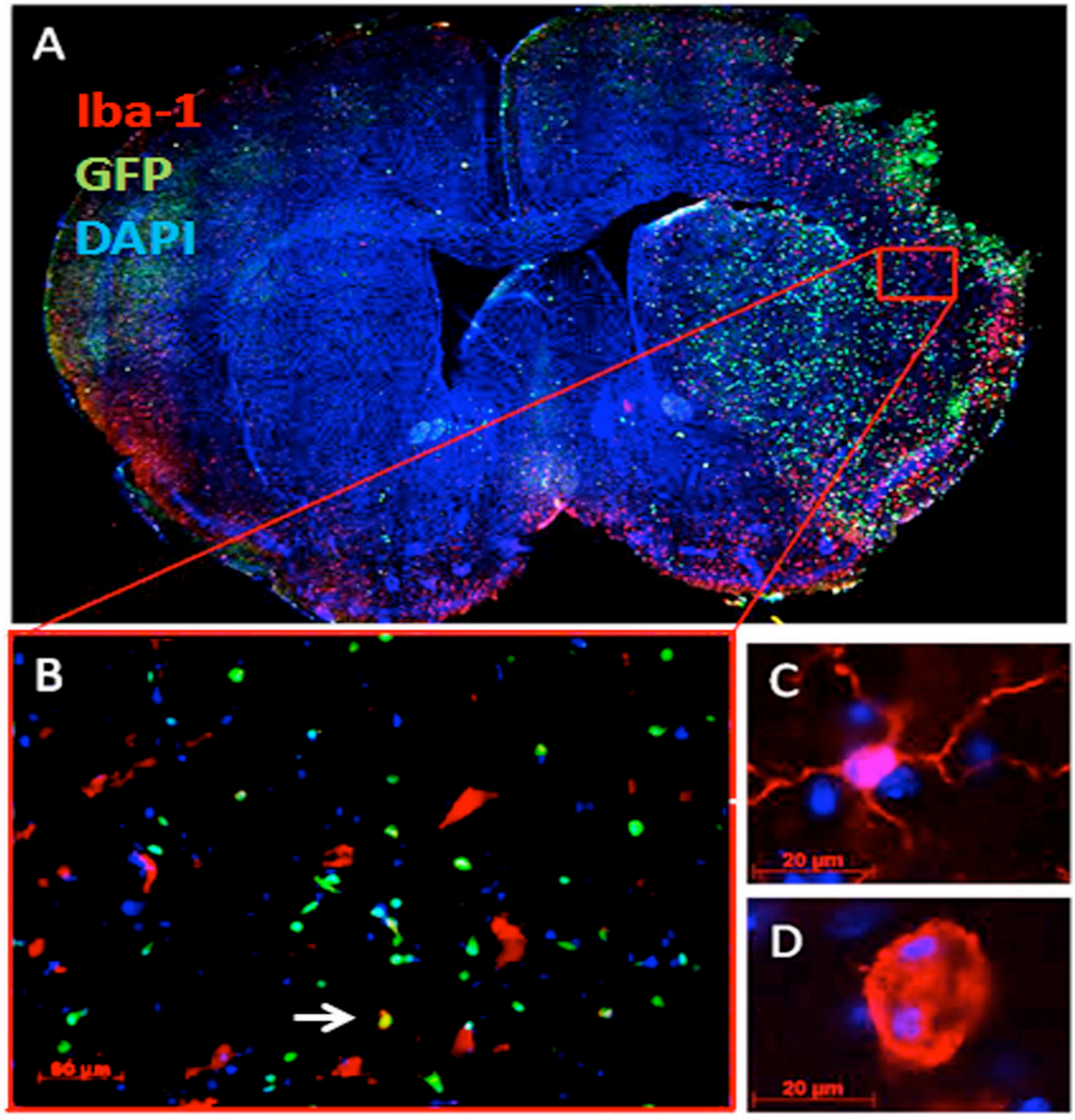

Figure 2-1. (Legend on following page)

Figure 2-1: Microglia activation and leukocyte infiltration in the ischemic brain. **(A)** Representative brain slice stained with Iba-1 (red), GFP (green) and DAPI (blue) from a chimeric mouse after stroke (10x magnification). The chimeric mouse model was made by transferring GFP^+ bone marrow of a donor mouse to an irradiated WT mouse. Eight weeks after reconstitution, the chimeric mouse was subjected to 90 min MCAO. The mouse was reperfused for 72 hours before sacrifice. GFP^+ cells represent bone marrow-derived peripheral leukocyte infiltrates. Green fluorescence is localized to the region of injured tissue in the striatum and cortex. **(B)** 20x magnification of the box area in (A). The arrow indicates a cell co-labeled with IbA-1 and GFP. **(C)** Resting microglia morphology with thin, ramified processes in the non-injured brain hemisphere. 63x. **(D)** Activated microglia with large, ameboid cell body in the ischemic cortex. 63x.

CD45/CD11b expression by flow cytometry

Flow cytometry provides a sensitive means to detect various markers and create a multiparameter characterization of different cell types. In 1991, Sedgewick et al [78]observed differences in the expression of the hematopoietic cell surface marker CD45 on resident microglia and infiltrating peripheral leukocytes. To date, the most common characterization profile derived from flow cytometry sorting still holds that resident microglial cells are CD45 ^{low} CD11b^{+}, while infiltrating hematogenous leukocytes are CD45^{high}CD11b^{+} [79]. Experimental stroke studies with two photon imaging [80] and IHC [81] also demonstrated that infiltrating leukocytes in the ischemic hemisphere showed a higher expression of CD45, which is consistent with our flow cytometry data (**Figure. 2-2**). Although CD11c ^{high} and CD14^{-} have sometimes been used to label microglia in flow cytometry, their similarity in expression on other peripheral cell types makes it difficult to justify resident microglial specificity [79,82].

There are, however, limitations to using variable levels of CD45 expression to distinguish between microglia and other monocyte/macrophage populations. CD45 on microglia can be upregulated in mouse models of EAE in spinal cord towards a CD45 high phenotype [83]. Inflammation in the periphery of humans also may upregulate CD45 in CNS resident microglia with no changes in CD11b expression [84] . The possible instability of this marker's levels during pathological states reiterates the need for a better method of tracking resident microglia and peripheral monocyte/macrophages.

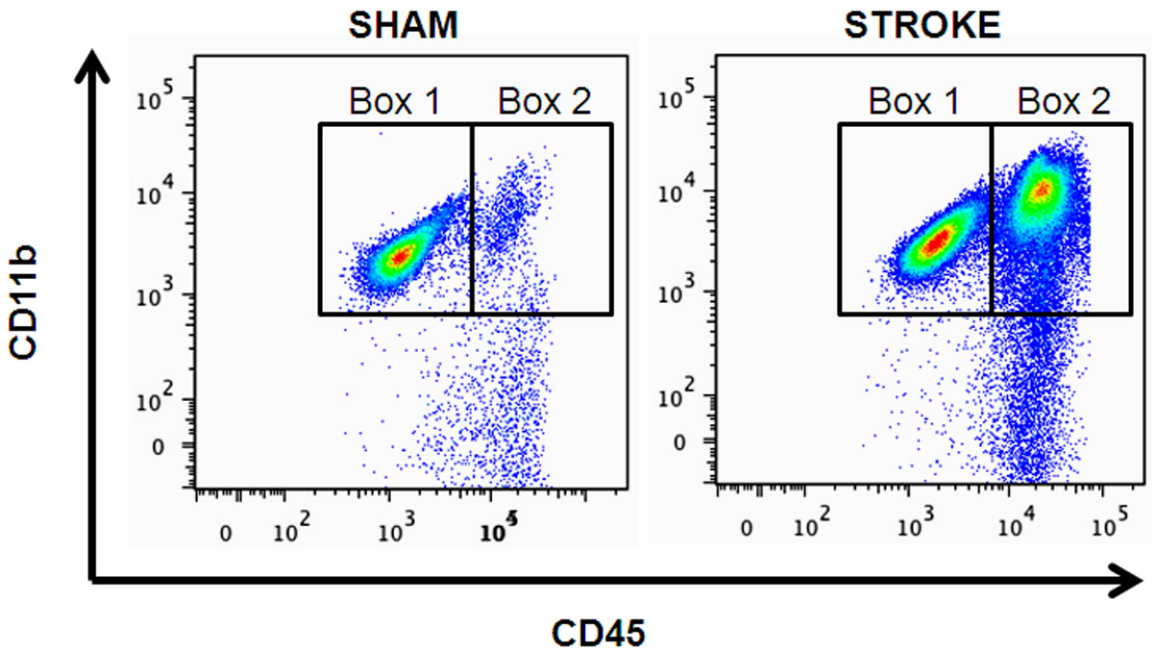

Figure 2-2: Representative flow cytometry plots of resident microglia and peripheral leukocytes in the mouse brain.

In the brains of sham mice (left), $CD45^{low}CD11b^{+}$ (box 1) and $CD45^{high}CD11b^{+}$ (box 2) cells were identified as resident microglia and peripheral leukocytes respectively. 72 hours after 90 min MCAO (right), both $CD45^{low}CD11b^{+}$ and $CD45^{high}CD11b^{+}$ cells were increased in the brain.

Transgenic mice

A multitude of transgenic mice can also be used to label cell populations by attaching a fluorescent reporter to a myeloid promoter. For example, CD11b-GFP can label all cells of myeloid origin including microglia in the mouse brain [85]. Similarly, Iba-1-EGFP transgenic mice have shown successful fluorescent labeling of CNS microglia/macrophages in tissue samples [86]. More recently, a fluorescent knock-in transgenic mice line created using CX3CR1-GFP and CCR2-RFP has shown to be the most useful to the field to differentiate resident microglia from peripheral monocytes. It is now known that CCR2, though differentially expressed, is specific to the periphery in naïve and EAE mouse [87], and unlike CD45, is not upregulated significantly in pathological states. In addition, fractalkine receptor (CX3CR1) is present on microglial progenitors in the yolk sac and, in the CNS, remains specific to microglia into adulthood[68].

Studies using systemic and region-specific depletion of myeloid cells or macrophages can be done using DTR-CD11b transgenic mice. These mice have diphtheria toxin receptors (DTR) linked to the CD11b promoter. Administration of diphtheria toxin will deplete $CD11b^+$ (myeloid) cells [85,88]. Another commonly used technique to selectively ablate $CD11b^+$ cells involves treating CD11b-HSV TK transgenic mice with injection of ganciclovir (GCV) [89]. Inducible death of $CD11b^+$ cells has more recently become a useful technique in the field.

Chimeras

Irradiation chimera models are a popular technique to differentiate microglia from peripheral myeloid cells since there is no exclusive antigenic marker [90]. To generate a BM chimera (**Figure. 2-1**), BM cells of a mouse with ubiquitously expressing fluorescent (GFP^+, YFP^+, RFP^+, etc) protein is extracted and injected into a mouse of interest whose own marrow is first irradiated and eliminated. After weeks to months of reconstitution of the new cell population, it is possible to track the origins of cells in CNS tissue, particularly after neurological diseases, where cells from the periphery that cross the BBB have been labeled with fluorescence. BM chimeras can be performed with transgenic knockout or knockin mice to selectively target cells of the CNS or of the periphery. Unfortunately, the effects of irradiation are confounding and have been implicated in physiological alterations such as weakening of the BBB, potential cell death and activation of microglia [91-95]. Though microglia are mostly radio-resistant, their numbers in the CNS may also be altered in uninjured and ischemic chimeric mice compared to nonchimeric mice in the hippocampus and the cortex [96]. Changes in gene regulation with higher expression of proinflammatory cytokine and CCL2 can also accompany irradiation [93,97]. These undesireable effects of irradiation pose a caveat to the technique. However, preventive measures can be taken to study the brain using chimeras. For example, targeted, instead of whole body irradiation using lead shielding of mouse heads is now often used in an effort to prevent damage or brain environmental changes due to radiation exposure [91,98].

Resting Microglia

Resting phenotype

Resting microglia in a healthy brain, more representatively known as “surveying microglia,” are constantly extending and retracting their thin ramified processes in an effort to inspect the CNS microenvironment (**Table. 2-1**) [99,100]. As the central macrophages of the brain, microglia are implicated in controlling synapse number and remodeling in the developing brain, and function to prevent accumulation of debris in the healthy adult CNS. They are not present uniformly in the adult brain and express differences in location, protein expression, and morphology [101]. Heterogeneity of morphology and location of microglia translates to differences in microglial responses to injuries and in activation states [102]. The majority of microglia are found in the gray matter and express more ramified structure with radial branches than those found in the white matter with longitudinal processes [101]. In the ischemic lesion induced by MCAO modeling, the penumbral area (the border zone of dead and living tissue) showed highly ramified cells (resting), while the ischemic core housed amoeboid bodies with thick ramifications (activated) [80]. To conclude, resting microglia are not “sleeping”; instead they are poised to respond to stimuli resulting from disturbances in the CNS environment by drastically altering their phenotypes and functions.

Phenotype	Identification Markers	References
Resting State	Iba-1 $CD45^{int}$ $CD11b^{+}$ F4/80 Isolectin (IB4)	76,103 78,79 101,104
Classical Activation (M1)	MHCII CD16 (FcγR III) CD 32 (FcγR II) CD80(B7-1) CD86 (B7-2) CD40 (TNFR)	83,100,105 106,107 106 108,109 108,109 110
Alternative Activation (M2)	Arg-1 CD68 (ED1) Fizz1(Relmα) Ym-1 CD206 (MR) Dectin-1	111 112 111,113 111,113 114,115 114

Table 2-1: Phenotypes of microglia.

Abbreviations: MHC, major histocompatibility complex; Arg, arginase; TNFR, tumor necrosis factor receptor; Fizz1: resting-like molecule alpha; MR, mannose receptor.

Inhibitory signaling of microglia

In the healthy brain, microglia express numerous inhibitory proteins, and interact with neurons to form a "brake" on inflammation [103]. The endogenous mechanisms in the form of neuronal-glial interactions may prevent excess microglial activation in the CNS. Following injury, these interactions may be disrupted due to neuronal cell death and structural tissue damage. Regulating these inhibitions to keep microglia from acquiring a proinflammatory phenotype has been shown to prevent uncontrolled damage in models of Alzheimers Disease (AD), multiple sclerosis (MS), and neurodegeneration [19,104-107]. Similarly, regulation of these inhibitory proteins may also have beneficial effects on ischemic stroke.

CD200/CD200R1

CD200 is a transmembrane glycoprotein mainly expressed on neurons [108,109]. The cell-cell contact between CD200 and its receptor (CD200R1), expressed on the surface of all myeloid origin cells, provides microglia with stability to remain in a resting state under normal CNS conditions [110,111]. Cleavage of this interaction and subsequent microglial activation leads to the upregulation of proinflammatory cytokines and an inflammatory profile [108]. Increased tissue damage was related to a decrease of CD200 level in mouse models of EAE, suggesting a detrimental effect of the activated microglia unbound from CD200/CD200R1 interaction [112]. Aging is also associated with a reduced level of CD200 and long-term potentiation (LTP), as well as an increased microglial activation in

the brain; however, treatment of CD200R1 agonist (CD200Fc) can attenuate the LTP deficit and ameliorate microglial activation, even after Lipopolysaccharide (LPS) stimulation[113]. Little is known about the role of CD200/ CD200R1 signaling in ischemic stroke, but a primarily descriptive study of CD200 on Iba^+ cells showed a decrease in gene transcripts of CD200 in the ischemic hemisphere [23].

Fractalkine (CX3CL1)/CX3CR1

Much like the immunoglobulin superfamily member CD200R1, fractalkine receptor (CX3CR1) on microglia can bind the soluble and membrane bound forms of CX3CL1, to keep microglia quiescent [114]. However, under injury, neurons significantly decrease CX3CL1 release thereby enabling microglial activation [115]. Loss of this contact has been shown to be neurotoxic in many disease models including Parkinson's disease and ALS by exacerbating neuronal loss [104]. Similarly, LPS stimulation of microglia on CX3CR1 $^{(-/-)}$ mice led to greater IL1- β secretion compared to CX3CR1 $^{(+/-)}$ mice[104].

However, the effect of CX3CL1/CX3CR1 signaling in neuroinflammation is controversial as deleterious roles for the CX3CL1/ CX3CR1pair were reported in rodent models of AD and cerebral ischemia [105,106]. Twenty four hours after a transient MCAO, CX3CR1 $^{(gfp/gfp)}$ mice (GFP is inserted into both alleles of the CX3CR1 locus) were noted to have less severe cerebral infarct volumes than WT mice, possibly associated with a coinciding decrease in IL-1β and TNF-α gene transcripts [116], as in the case of fractalkine knockout mice [117]. Similar results were seen in a recent study by Ciprani et al with a pMCAO model in CX3CL1 $^{-/-}$ and CX3CR1 $^{(gfp/gfp)}$ rodents, both of which showed

less severe ischemic damage than WT mice [106]. Furthermore, CX3CL1$^{-/-}$ animals have increased damage after ischemia with exogenous intracerebroventricular CX3CL1 administration. Interestingly, WT rodents show less severe infarct volumes and better functional outcomes with the addition of CX3CL1 in a dose dependent manner [106]. The disparity in the effect of exogenous CX3CL1between KO and WT animals suggests that CX3CL1may be protective only when microglia exhibited a normal constitutive CX3CR1-mediated signaling throughout development in the WT brain [106].

SIRPα/CD47

SIRPα (CD147, signal regulatory alpha, SHPS-1, P84), expressed on myeloid cells including microglia, binds integrin associated protein CD47 on neurons to activate an intracellular immunotyrosine inhibitory motif [118,119], keeping microglia silenced and thereby suppressing phagocytosis [120,121]. Human MS lesions have shown a decrease in CD47 expression [107], though little is known to date about the role of CD47 and SIRPα in ischemia specifically. A reduction of infarct was seen 24 and 72 hours after 90 min MCAO in CD47 knockout mice, potentially due to a decrease in peripheral inflammatory cell infiltration [122]. Wang et al recently also reported a reduction of infarct and improvement of behavior deficit after transient MCAO in SIRPα mutant mice [123].

Triggering receptor expressed on myeloid cells 2 (TREM2)

The neuronal-microglial connection of heat shock protein 60 (HSP60)-TREM2 is important for the clearance of apoptotic neurons by microglial phagocytosis [124]. Microglia, via its intracellular adaptor protein DAP12, prevent the release of proinflammatory cytokines and maintain an anti-inflammatory microglial profile [125,126]. In EAE, mice lacking TREM-2 by antibody blockage suffered worse pathology, but are rescued with greater recovery and tissue repair by injection of myeloid cells expressing TREM-2 [126]. Contrarily, TREM -2 KO mice showed a decrease in amoeboid $Iba1^+$ and $CD68^+$ microglial activation and an overall decreased inflammatory response 7 days post-reperfusion after a 30 minute MCAO model that did not translate into a decreased infarct volume [127]. The inhibitory effect of TREM-2 on microglial activation following stroke is still uncertain at this time.

Activation of microglia

A commonly held assertion is that distinct activation states (based on protein expression signatures) impart defined functional roles of microglia and may account for heterogenic responses to CNS injury. These activation states are generally described in terms of the class of activating signals and selectively induced expression of unique markers. Microglia can change patterns of migration, cell surface protein expression, and functions in response to tissue damage or dysfunction (**Figure. 2-3**). The rapid

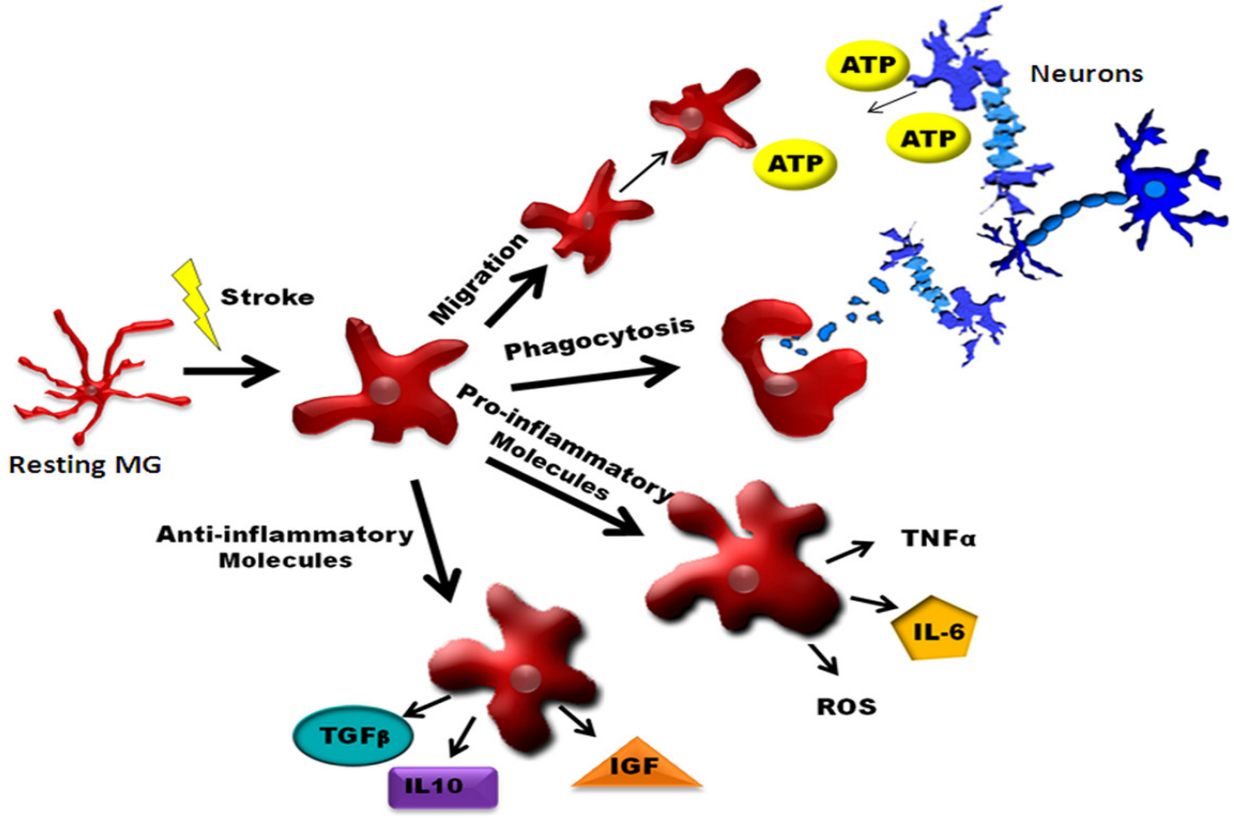

Figure 2-3: Schematic of Microglia Activation after Ischemic Brain Injury.
In the ischemic brain, microglia display prominent changes in morphology associated with various functional states. Activation results in upregulation of transcriptional machinery which serves to increase the production of inflammatory mediators. In response to chemotaxic factors, microglia can migrate to sites of ischemic tissue injury to increase phagocytic uptake of cellular debris and cytotoxic substances. Depending on their activation state, microglia may promote a proinflammatory environment (via M1 activation) or regenerative milieu (via M2 activation). IL-10: interleukin 10; TGFβ: Transforming growth factor beta; IGF-1: Insulin like growth factor 1; IL-1β: interleukin 1 beta; ROS: reactive oxidative species; IL-6: interleukin 6; TNFα : Tumor necrosis factor alpha.

responses to altered homeostasis of the brain parenchyma can be visualized in two photon imaging to show immediate (within minutes) increase in the motility of microglial processes towards area of injury in a chemical gradient dependent manner, while the cell bodies remain stationary [99,100]. *In vivo* data suggest that ATP signaling of P_2Y_{12} receptors on the cell surface is responsible for such extensions and directional guidance [99,128,129].

Microglial activation phenotypes: M1 and M2

Changes in microglial phenotype during activation may be analogous to that of peripheral macrophages, as the two cell types are indistinguishable without definitive surface markers for either. Microglial responses to stimuli from a changing brain environment are characterized as either M1, classical activation, or M2, alternative activation (**Table. 2-1**). M1 is a proinflammatory cellular state associated with an increase in protein synthesis of pro-inflammatory mediators (IFNγ, Il-1β, TNFα, Il-6, CXCL10, etc.), ROS and NO production, and proteolytic enzymes (MMP 9, MMP3) that act on the extracellular matrix leading to BBB breakdown [7,130]. M1 phenotype can lead to increased neuronal death compared to alternatively activated M2 microglia [131]; therefore, there is a growing interest to pharmacologically interfere with the signaling mechanisms that give rise to the classical activation phenotype of microglia. M2 microglia release anti-inflammatory mediators (IL-10, TGF-β, IL-4, IL-13, IGF-1, CD206, etc.) [132], leading to enhanced expression of genes associated with inflammation resolution, scavenging, and homeostasis [130,133-135]. Levels of IL-10, TGF-β and CD206

mRNA increased as early as day 1 after ischemic injury and peaked at 4-6 days. In addition, TGF-β released by microglia promotes an anti-inflammatory profile associated with increased proliferation and neuroprotection in the ischemic brain [136] . This may be therapeutically relevant because TGF-β1 is specifically found in the salvageable peri-infarcted region of the cortex 24 hours after a 60 min MCAO and involved in distinct spatiotemporally regulated inflammatory and neuroprotective processes [137].

During disease progression and in normal ageing, microglial activation phenotypes can switch from M2 to M1 [138]. One recent study suggested that microglia first alternatively activate early after MCAO and morph into a reactive M1 phenotype by 7 days [131]. The balance between the M1 and M2 states is dynamic in inflammatory responses and may be offset in chronic disease states such as stroke, representing a novel mechanistic target for therapy [130]. Several proteins have been identified as markers for M1 or M2. MHC II, implicated in antigen presentation as an immune reaction, is upregulated on classically activated microglia, and is commonly used as a marker for M1 [83]. The alternatively activated M2 up-regulates presentation of several antigens. Ym-1 (Chitinase 3-like 3), for example, has been found to be associated with the protective, pre-phagocytic state of macrophages after ischemia [80]. Some of Ym-1$^+$ cells co-express CD206 (mannose receptor), which is another marker for M2 activation known to be involved in antigen internalization and processing [80]. CD68 (macrosialin) glycoprotein is another accepted marker for phagocytotic cells and is often used to distinguish the M2 debris clearing state of microglia [80]. Stroke-induced changes in the expression of specific cell surface proteins probably reflect a continuum of the microglial activation spectrum. There is a growing need to identify subpopulations of M1/M2

microglia versus those of peripheral myeloid cells and the relative percentages of each over time to determine the overall functional contribution to stroke injury.

Migration

Microglia, as the first immune responders in the CNS, migrate to areas of injury through detection of chemoattractant gradient, and phagocytize debris, damaged tissue, neutrophils, and apoptotic cells that have the potential to release damaging molecules [99,139,140]. CX3CL1 and ATP released from dying neurons can act on microglial receptors to induce chemotaxis. In addition, monocyte attractant protein 1 (MCP-1, CCL2) is a chemokine expressed both in the brain and in some peripheral organs that can induce migration of leukocytes and macrophages/microglia to the ischemic area [141,142]. After MCAO, MCP-1 expression increases at injured region and peaks at 2-3 days [143] when monocytes/macrophages also start to peak in the ischemic brain [144]. Transgenic CCL2 knockout mice show decreased ischemic injury [145], suggesting that the recruitment of monocytes/macrophages to the injured area may be detrimental and that therapies designed to block the migration of leukocytes may have translational value. Microglia at the border region of the infarct, "penumbral" microglia, may be the major targets of therapy given their large numbers, and activated status after stroke [146]. Unlike microglia of the ischemic core, which appear to be dying with increased disease severity, penumbral microglia are presumably living and highly activated [102]. This suggests a regional target of interest to deliver treatments.

Phagocytosis by microglia and macrophages

As the primary phagocytes in the brain, activated microglia phagocytize and uptake damaging components in an effort to reestablish homeostasis after insults [60]. Microglial phagocytosis of neuronal cells begins early even before peripheral macrophages infiltrate into the brain after stroke [147]. These phagocytotic cells were seen interacting with neurons and show neuron engulfment in the ischemic brain. CD68 is a commonly used marker of macrophage phagocytosis and expressed as early as 6h after pMCAO on ramified $CD11b^+$ cells in the penumbra, and continues to increase later in the hypertrophic ameboid cells of the ischemic core [80]. However, the phgocytosis marker can be expressed on both the resident and infiltrating phagocytes, and therefore may not be exclusive to microglia [80].

Phagocytosis is able to attenuate inflammation but can also be implicated in neuronal damage. A recent study of primary microglial cultures assessed the sequence of events from microglial activation to the phagocytosis of neurons [148]. Production of peroxynitrite during a microglial immune response to TLR4 and TLR2 activation leads neurons to externalize phosphatidylserine on the outer membrane to act as an “eat me” signal to elicit phagocytosis. Interestingly, inhibition of this process at any stage not only leads to the decrease in phagocytosis of the neurons, as would be suspected, but also prevents 90% of neuronal cell death [148]. The potential for microglia to phagocytize viable neurons illustrates the importance of microglial modulation in ischemic stroke [148].

Purinergic receptors

Purinergic receptors ($P2X_7$, etc.) are upregulated on microglia in the periinfarct region of injury [149] and have been shown to interact with ATP that is accumulated extracellularly in the ischemic brain [150], subsequently leading to microglial activation [151]. Activation of these receptors leads to cell death [152]and the prominent release of proinflammatory cytokine IL-1β through caspase-1 pathway [153]. ATP leaked from dying neuronal cells and released by astrocytes [99,154] can act as a chemoattractant on microglia by interacting with $P2Y_{12}$ receptor [155]; the microglia attracted to sites of ischemic injury can further amplify activation by autocrine signaling of ATP [156]. This positive feedback loop leads to increased proliferation and secretion of IL-1β, TNF-α, and ROS [151], and exacerbate inflammatory responses. Blocking $P2X_7$ receptors was shown to improve behavior deficits in a model of transient global ischemia where decreases in microglial activation and proinflammatory cytokines (TNF-α, IL1-β, and IL-6) were noted [157]. A nonselective P2 blocker, Reactive Blue 2, was shown to reduce infarction in a focal pMCAO model; however, $P2X_7$ receptors are also expressed on neurons and astrocytes, therefore the function may not be solely attributed to microglia [158].

Toll like receptor (TLR)

The stroke-induced innate immune response is also associated with the release of various damage associated molecular patterns (DAMPs), which can further activate pattern recognition receptors (PRRs), including members of the TLR family on microglia

[159,160]. TLRs are important in innate immunity in both the central and peripheral systems. TLR4 is the prominent LPS receptor that can lead to activation of LPS-responsive cells, such as monocytes and macrophages, and subsequently causes upregulation of proinflammatory genes via NFκB signaling [161]. The most prominent TLRs on microglia are TLR4 and TLR2, both of which are upregulated after ischemia [160,162-165]. TLR4 deficient mice have smaller infarct sizes, better neurological scores and decreased downstream NFκB signaling in experimental stroke studies [164,166]. Recent studies have shown that CNS preconditioning with TLR4 agonist can lead to tolerance, eliciting a diminished proinflammatory response with subsequent less ischemic injury [167,168]. Although there has been controversy as to the role of TLR2 deficiency in cerebral ischemia, recent studies have shown an exacerbation of injury in TLR2 KO mice [160,163,169]. Some endogenous ligands of TLRs have recently been identified. Purines and peroxiredoxin (prx) released to the extracellular space from dying cells can bind TLRs on macrophages and produce proinflammatory cytokines IL-23 and IL-17 [170]. Heat shock proteins (HSP) and High mobility group box 1 (HMGB1) are other endogenous ligands for TLRs that result in upregulation of NOS and proinflammatory cytokines (TNF-α, IL-6, and IL-1β) [171,172].

Functional insights of resident microglia and peripheral macrophages

Microglial proliferation and renewal

There is evidence that activated microglia are proliferative in the ischemic brain. Using carboxyfluorescein diacetate succinimidyl ester (CSFE) to intracellularly label peripheral cells before a 30-60min MCAO, one study found higher amounts of $BrdU^+$ $Iba1^+$ $CSFE^-$ colabeling microglia after stroke indicating increased proliferation [140]. Interestingly accumulating data show microglial proliferation is beneficial after ischemia. *In vitro* studies have shown that increased microglial proliferation by stimulation of CSF-1R, which is upregulated in ischemia, is neuroprotective [83,173]. An in vivo study also showed that defective microglial proliferation was associated with significant increase in the size of ischemic lesion and a 2-fold increase in the number of apoptotic neurons [174].

In addition to microglia, choroid plexus macrophages, perivascular macrophages, and meningeal macrophages inhabit various regions around the CNS [175]. This heterogeneous population of tissue macrophages is continuously replenished by circulating and peripheral monocytes, unlike microglia that are largely thought to be resident in the adult CNS from early development [93,176,177]. Theories of another wave of microglial establishment postembryonic from peripheral monocytic precursers that last into adulthood are part of an ongoing debate [93,178]. It is uncertain whether these monocytic precursors become integrated into the microglial population or remain bone marrow-derived monocytes. Nevertheless, Varvel et al. [179] suggest yet another mode of microglial replacement apart from proliferation exists in the adult brain. They ablated

microglia using intracerebroventricular ganciclovir treatment in Tk^{+} /*Ccr2*$^{+/rfp}$ mice and found abundant levels of $CD45^{high}$ monocytes in neocortical areas of microglial depletion before engraftment. In addition, there were increased levels of *Ccr2 RFP* expression which returned to normal levels after engraftment. These infiltrating cells of monocytic origin are morphologically similar to microglia and functionally active in surveying the microenvironment of the brain, without changes in number over time [179]. It's possible that a population of dying microglia in the ischemic brain could be replenished by peripheral monocyte/macrophages infiltrating into the injured region and downregulating CCR2 and CD45 to morph into microglia. The topic of microglial renewal and proliferation, however, is still controversial.

MMPs

Macrophages, including microglia, are major contributors to the release of MMPs (mainly MMP3 and MMP9) which are responsible for the breakdown of the extracellular matrix and the BBB after ischemia [140,180]. MMP-3 and MMP-9 knockout mice were shown to suffer less neuronal injury after an ischemic episode [181,182]. Since MMP-9 can be derived from both brain and peripheral immune cells, its origin after ischemia has been debated. Recently, chimeric studies showed that the increased damage from MMP-9 toxicity in the ischemic brain are attributed to bone marrow cells as opposed to resident microglia [182,183]. This suggests that infiltrating monocytes/macrophages can also release MMPs and modulate their own entry into the CNS by weakening BBB.

TNF

TNF-α can be released from both microglia and peripheral leukocytes. TNF-α has been largely regarded as neurotoxic [184]; however, chimeric studies have found that TNF-α produced locally by resident brain microglia (but not by peripheral macrophages and leukocytes) exerted neuroprotection in pMCAO model via TNF-p55 signaling [185]. The disparity in implications may be attributed to different signaling mechanisms between the neuroprotective TNF-p55 and neurotoxic TNF-p75 pathways [186] .

iNOS

Local accumulation of nitric oxide (NO) is also involved in the inflammatory cascade after cerebral ischemia [187]. Equipped with inducible nitric oxide synthase (iNOS), M1 microglia are partially responsible for the changes in expression level of NO. The role of iNOS in ischemia is inconsistent in literature as both protective and deleterious roles have been reported [188-190]. Pruss et al [191] found that in chimeric iNOS-deficient mice transplanted with WT bone marrow (BM) cells and wild-type mice transplanted with iNOS-deficient BM cells, no difference in cerebral iNOS expression or in infarct volumes can be seen between the chimeric animals after MCAO, suggesting iNOS from microglia and peripheral myeloid cells may not be a significant regulator of ischemic injury.

Peroxiredoxin

The peroxiredoxin family of proteins (Prxs) are intracellular antioxidant enzymes that are needed for cell survival in the brain [192,193] . However, once released from necrotic brain cells, extracellular Prxs promote neural cell death in ischemia by inducing expression of inflammatory cytokines including IL-23 in macrophages [170]. This study also utilized chimeric mice models and further showed that the infiltrating bone marrow-derived macrophages but not the resident microglia, are responsible for increased ischemic volume and inflammatory response triggered by Prxs release [170]. In addition, they found that neutralization of the released extracellular Prxs with a prx antibody is protective.

Summary

Despite more than one century of research since they were first investigated by Rio Del Hortega [194], "the father of microglia," the precise role of microglia is still shrouded in mystery due to a current lack of tools and fundamental understanding of the heterogeneity of their observed activation spectrum. The nature of the microglial response to stroke is multi-faceted and complicated by the aggregate immune response. The significance of the local and systemic inflammatory response as well as the interplay between the two is widely argued. While many studies suggested that anti-inflammatory agents confer neuroprotection following ischemic brain injury, others

pointed to a requirement for pro-inflammatory cytokines and leukocyte activation in orchestrating repair. Enhancing repair may be possible by targeting distinct populations of microglia with special attention to temporal and spatial specific therapeutic intervention in ischemic stroke and other neurological disorders. There is room for improvements of methods for better identification and manipulation of microglia. The roles of microglia in stroke-induced inflammatory responses merit further investigation, in hope that fine-tuning immunomodulatory therapies could be available to avoid the deleterious effects of total immunosuppression and the possible detrimental effects of chronic microglial inhibition.

Chapter 3:

Functional differences between microglia and monocytes after ischemic stroke

Rodney M. Ritzel[1], Anita R. Patel, Jeremy M. Grenier, Joshua Crapser, Rajkumar Verma, Evan R. Jellison, and Louise D. McCullough

This chapter was published in its present form in Journal of Neuroinflammation; 2015 May 29;12: 106.

Abstract

The brain's initial innate response to stroke is primarily mediated by microglia, the resident macrophage of the CNS. However, as early as four hours after stroke the blood-brain barrier is compromised and monocyte infiltration occurs. The lack of discriminating markers between these two myeloid populations has led many studies to generate conclusions based on the grouping of these two populations. A growing body of evidence now supports the distinct roles played by microglia and monocytes in many disease models. Using a flow cytometry approach, combined with ex-vivo functional assays, we were able to distinguish microglia from monocytes using the relative

expression of CD45, and assess the function of each cell type following stroke over the course of 7 days. We found that at 72hrs after a 90-minute middle cerebral artery occlusion (MCAO), microglia populations decrease whereas monocytes significantly increase in the stroke brain compared to sham. After stroke, BRDU incorporation into monocytes in the bone marrow increased. After recruitment to the ischemic brain these monocytes accounted for nearly all BRDU-positive macrophages. Inflammatory activity peaked at 72hrs. Microglia produced relatively higher reactive oxygen species and TNF, whereas monocytes were the predominant IL-1β producer. Although microglia showed enhanced phagocytic activity after stroke, monocytes had significantly higher phagocytic capacity at 72hrs. Interestingly, we found a positive correlation between TNF expression levels and phagocytic activity of microglia after stroke. In summary, the resident microglia population is vulnerable to the effects of severe ischemia, show compromised cell cycle progression, and adopt a largely pro-inflammatory phenotype after stroke. Infiltrating monocytes are primarily involved with early debris clearance of dying cells. These findings suggest that the early wave of infiltrating monocytes may be beneficial to stroke repair and future therapies aimed first at mitigating microglia cell death may prove more effective than attempting to elicit targeted anti-inflammatory responses from damaged cells.

Introduction

Inflammation is a key component of stroke-induced injury and elevated levels of inflammatory markers are associated with poor outcome in stroke patients [35,195-197]. Inflammation in the brain is generally mediated by microglia, the resident macrophage of the CNS [198]. In the protected confines of the blood-brain barrier microglia maintain healthy brain function by clearing debris, pruning synapses, and producing growth/repair factors [199]. These cells stand poised to respond to injuries in the CNS such as ischemic stroke. Numerous experimental studies have shown that microglia become activated following stroke, notably shifting their morphology from a thin, ramified state to a large, amoeboid structure [200]. This change is generally thought to be accompanied by an increase in proliferation and production of inflammatory mediators. Yet despite the evidence for widespread recruitment of bone marrow-derived monocytes (and their derivatives) to injured brain regions, and a lack of discriminate cell markers, little is known regarding the functional differences between these two myeloid populations in ischemic stroke. Given the high degree of macrophage heterogeneity that comprises our innate immune system, the functional role of these populations is likely distinct and of translational importance [201-204]. CNS-resident microglia are the first responders to ischemia, these cells likely serve a unique role in injury repair relative to monocytes, which have a finite lifespan and are recruited in higher numbers during the post-reperfusion phase from the periphery. These differences have been made evident in recent studies that utilize transgenic bone marrow chimeras to distinguish between local and circulating myeloid populations [205]. These potentially disparate roles suggest

that drugs designed to modulate microglia function may adversely impact that of the infiltrating monocyte population.

In this study, we investigated functional differences between brain-resident microglia and infiltrating monocytes in acute ischemic injury to better understand the contribution of each population to the recovery phase of stroke. Using flow cytometry to discriminate between these two populations, we applied ex-vivo functional assays to ascertain their functional roles during stroke and early recovery. By identifying the distinct function of microglia and monocytes early after ischemic stroke, the potential for targeting these specific cell populations will allow for the development of more effective therapeutic interventions.

Materials and Methods

Mice/Animals: Young adult C57BL/6J male mice (10-12 weeks) of age were pair-housed on sawdust bedding in a pathogen free facility (light cycle 12/12 h light/dark). All animals had access to chow and water ad libitium. All procedures were performed in accordance with NIH guidelines for the care and use of laboratory animals and approved by the Institutional Animal Care and Use Committee of the University of Connecticut Health Center. All analysis was performed blinded to surgical conditions.

Ischemic Stroke Model: Cerebral ischemia was induced by 90 minutes of reversible middle cerebral artery occlusion (MCAO, 20–25 gm mice) under Isoflurane anesthesia

as previously described [206]. Rectal temperatures were maintained at approximately 37°C during surgery and ischemia with an automated temperature control feedback system. A midline ventral neck incision was made, and unilateral MCAO was performed by inserting a 6.0 Doccol monofilament (Doccol Corp, Redland, CA) into the right internal carotid artery 6 mm from the internal carotid/pterygopalatine artery bifurcation via an external carotid artery stump. Following reperfusion mice were sacrificed at 24hrs, 72hrs, and 7 days. Sham-operated animals underwent the same surgical procedure, but the suture was not advanced into the internal carotid artery.

Tissue Harvesting: Mice were euthanized, transcardially perfused with 60 mL cold, sterile PBS, and the brains were harvested. The brainstem, cerebellum, and optic nerve were removed. The brain was then divided along the interhemispheric fissure into two hemispheres and subsequently rinsed with PBS to remove contaminant cells.

Flow Cytometry: Brains were placed in complete RPMI 1640 (Lonza) medium and mechanically and enzymatically digested in collagenase/dispase (1 mg/mL) and DNAse (10mg/mL; both Roche Diagnostics) for 1hr at 37C. The cell suspension was filtered through a 70um filter. Leukocytes were harvested from the interphase of a 70%/30% Percoll gradient. Cells were washed and blocked with mouse Fc Block (ebioscience) prior to staining with primary antibody-conjugated flourophores: CD45-eF450, CD11b-APCeF780, Ly6C-PerCP-Cy5.5, Ly6G-PE, and SIRPα-APC. All antibodies were commercially purchased from eBioscience. For live/dead discrimination, a fixable viability dye, carboxylic acid succinimidyl ester (CASE-AF350, Invitrogen), was diluted

at 1:300 from a working stock of 0.3mg/mL. Cells were briefly fixed in 2% paraformaldehyde (PFA). Data were acquired on a LSRII using FACsDiva 6.0 (BD Biosciences) and analyzed using FlowJo (Treestar Inc.). No less than 100,000 events were recorded for each sample. Resident microglia were identified as the $CD45^{int}$ $CD11b^{+}Ly6C^{-}$ population, whereas bone marrow-derived leukocytes were identified as $CD45^{hi}CD11b^{+}Ly6C^{+}Ly6G^{-}$. Cell type-matched fluorescence minus one (FMO) controls were used to determine the positivity of each antibody. Prior to assessment on the cytometer, isolated cells were briefly probed to determine phagocytosis activity, oxidative stress level, cell proliferation status, and cytokine production as described below.

Phagocytosis Bead Assay: To study the phagocytic activity of microglia, fluorescent latex beads (Fluoresbrite Yellow Green (YG) carboxylate microspheres; 1um diameter; Polysciences) were added to sorted microglia in a final dilution of 1:100 as described [207]. After 1-hour incubation at 37°C the cells were washed three times with FACS buffer, re-suspended in FACS buffer, stained for surface markers, and fixed in PFA (N=6/group). Mean fluorescence was determined from the YG bead+ microglia population, and used to measure the amount of beads per phagocytosing cell [208].

Reactive Oxygen Species Measurement: For detection of reactive oxygen species, microglial cells were incubated with redox-sensitive DHR (5uM; Ex/Em: 495/520) fluorogenic cell-permeant dye (Life Technologies, Invitrogen). Cells were incubated for 20min at 37C, washed three times with FACS buffer (without NaAz), and then stained

for surface markers including CASE (N=5/group). After loading cells with DHR, each sample was separated into two tubes, one kept on ice and one at 37ºC.

BRDU Labeling and Analysis: For cell proliferation studies, 50mg/kg of BRDU (Sigma) was injected interperitoneally starting at 12hrs after reperfusion and again at 24hrs and 48hrs. BRDU staining was assessed using a BRDU Flow Kit (BD Biosciences). In brief, cells were permeabilized with detergent and treated with DNAse prior to the addition of both anti-BRDU-FITC antibody and Ki67-PE (eBioscience).

Intracellular Cytokine Production: For intracellular cytokine staining, an *in vivo* brefeldin A (BFA) protocol was followed. Briefly, 10mL/kg of BFA (Sigma, 0.5mg/mL in DMSO) was injected via tail vein. Ten hours later, animals were sacrificed and tissue was harvested as noted above. Prior to staining, 1ul of GolgiPlug containing brefeldin A (BD Biosciences) was added to 800ul complete RPMI and cells were incubated for 2h at 37C (5% CO2). Afterward, cells were re-suspended in Fc Block, stained for surface antigens and washed in 100ul of fixation/permeabilization solution (BD Biosciences) for 20 min. Microglia were then washed twice in 300ul permeabilization/wash buffer (BD Biosciences) and re-suspended in an intracellular antibody cocktail containing TNF-PE-Cy7 (eBioscience) and IL-1β-FITC (eBioscience), and subsequently fixed (N=5-7/group).

Bone Marrow Chimera Generation: Wildtype C57BL/6J mice (8 weeks old) were lethally irradiated (two doses of 5-6 Gy) in a Gammacell 40 research irradiator and 5 x

10^5 nucleated GFP-expressing donor bone marrow cells were injected retro-orbitally [209]. Chimeras were maintained on sulfamethoxazole/trimethoprim antibiotics in their drinking water one day prior- and two weeks following irradiation. Chimeras were used for experiments 10 weeks following transplantation.

Statistical Analyses: Data from individual experiments are presented as mean ± SEM and assessed by Student t test or One-way ANOVA with Tukey post-hoc test for multiple comparisons (GraphPad Prism Software Inc, San Diego, CA, USA). For Two-way ANOVA, significant differences between paired comparisons were conducted with the Holm-Sidak test. The Spearman's rank correlation test was used to ascertain the correlation between cytokine production and phagocytic activity. Significance was set at $p < 0.05$.

Results

Ischemic stroke induces microglial death, bone marrow production of monocytes, and recruitment of monocytes to the injured brain

We confirmed the ability to reliably distinguish $CD45^{int}$ microglia from $CD45^{hi}$ monocyte populations in the ischemic brain by generating GFP bone marrow chimeras, in which all bone marrow-derived cells were GFP-positive (**Supplementary Figure 3-1A**). We demonstrated that the two populations did not significantly overlap after stroke,

validating this approach. Absolute leukocyte counts were obtained by flow cytometry at 24 and 72 hours after MCAO in non-irradiated, intact wild type mice using the gating strategy shown in **Figures 3-1A-B**. A significant reduction in the number of microglia ($CD45^{int}CD11b^{+}Ly6C^{-}$) after stroke was found after 24hrs ($p<0.05$; **Figure 3-1C**). Conversely, we found a dramatic increase in monocyte ($CD45^{hi}CD11b^{+}Ly6C^{+}Ly6G^{-}$) counts in the stroke hemisphere compared to sham brain (**Figure 3-1D**). At 72hrs, Microglia expressed increased levels of Ki67, a marker of actively cycling cells ($p=0.017$; **Figures 3-2A-B**). DNA synthesis, an indicator of cell proliferation, was then measured by BRDU incorporation. Following repeated BRDU injections starting at 12hrs, microglia showed little BRDU incorporation by 72hrs, whereas ~90% of monocytes in the ischemic brain were BRDU-positive (**Figures 3-2C-D**). Stroke is known to stimulate bone marrow production of myeloid cells that are subsequently recruited to the brain [210]. We found a significant increase in the percentage of $BRDU^{+}$ monocytes in the bone marrow following stroke ($p=0.016$; **Figures 3-2E-F**). These data suggest that after 90-minute tMCAO, there is a significant loss of resident microglia, impaired cell cycle progression, and an increased number of newly produced, bone marrow-derived monocytes.

Differential oxidative stress and cytokine production by microglia and monocytes after stroke

Reactive oxygen species production drives the oxidative stress response to stroke and is critical to injury progression [211]. We examined free radical formation in microglia and

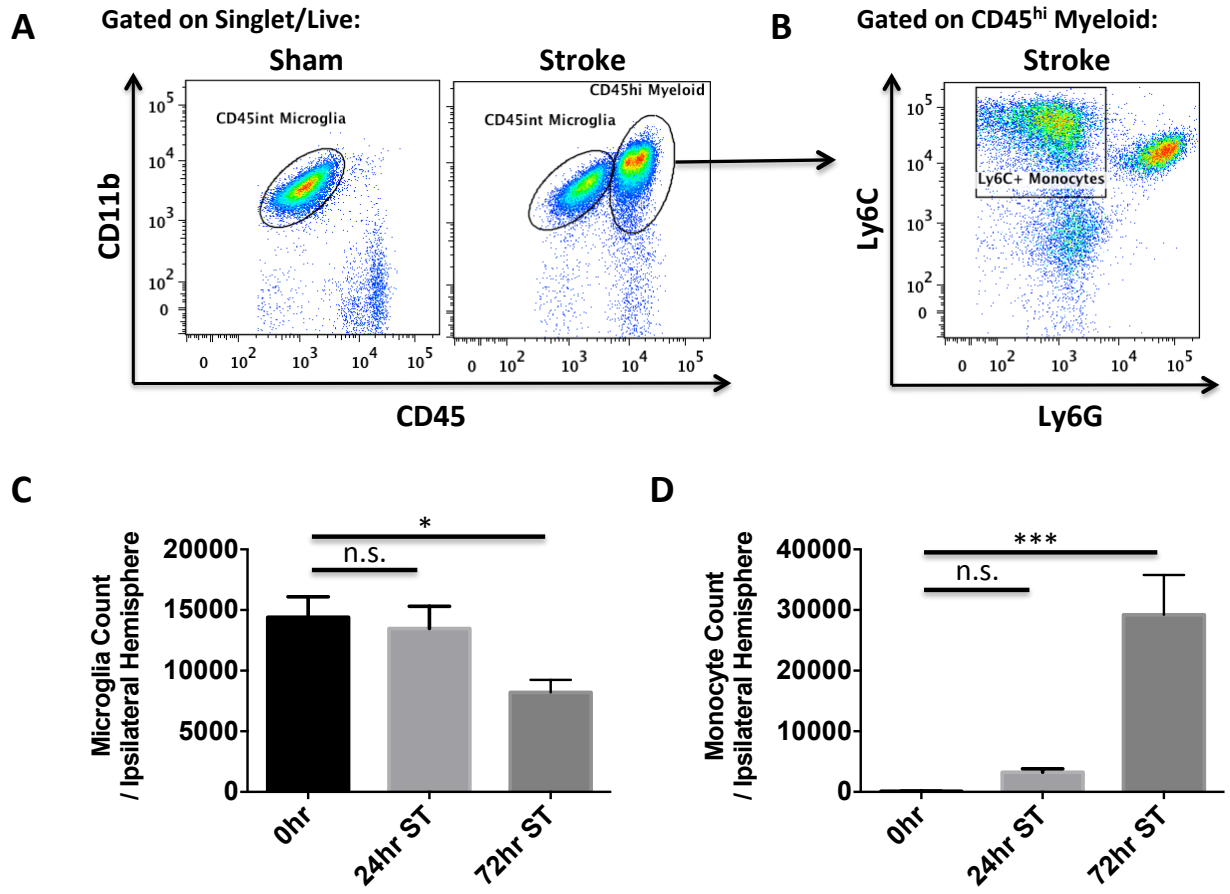

Figure 3-1. Number of microglia and monocytes in the ischemic hemisphere in the early period after stroke.

A representative dot plot depicts the gating strategy used to identify both brain-resident microglia and Ly6C^{+} monocytes at 72hrs after 90-minute MCAO (A-B). Absolute cell counts of microglia (C) and monocytes (D) were quantified at 0-, 24- and 72hrs after stroke. For all experiments, N=9/group. Error bars show mean SEM. Abbreviation: SEM, standard error of the mean.

monocytes after stroke. Resident microglia expressed significantly more ROS relative to the infiltrating monocytes ($p<0.01$), as evidenced by increased DHR123 staining intensity (**Figures 3-3A-B**). Because oxidative stress precipitates cytokine production, we next evaluated pro-inflammatory cytokine levels in these cells. Newly recruited monocytes expressed higher levels of TNF at 24hrs; however, microglia expressed significantly greater levels by 72hrs (**Figures 3-3C-D**). Infiltrating monocytes expressed relatively higher levels of IL-1β at all time-points ($p<0.001$; **Figures 3-3E-F**). The number of microglia expressing TNF remained elevated above sham levels at 7 days, whereas those expressing IL-1β did not differ. Neither microglia nor brain-recruited monocytes expressed detectable levels of the anti-inflammatory cytokines IL-4 and IL-10 after stroke (data not shown). These results suggest that microglia play a critical role in oxidative injury and that these two cell types may mediate cell death via distinct signaling pathways.

Monocytes are the predominant phagocytes in the brain at 72hrs after stroke.

Microglia in the ischemic hemisphere were significantly more activated based on side scatter (granularity) properties compared to sham, suggesting enhanced uptake of dying cells and debris (**Figures 3-4A-B**). Phagocytosis is important in debris clearance and injury repair. Using a bead assay, we measured phagocytic activity of microglia and monocytes (**Figure 3-4C**). After stroke, the percentage of microglia that phagocytosed beads significantly increased at 24hrs ($p<0.001$) and peaked at a near four-fold increase by 72hrs ($p<0.01$; **Figure 3-4D**). The phagocytic activity of microglia is

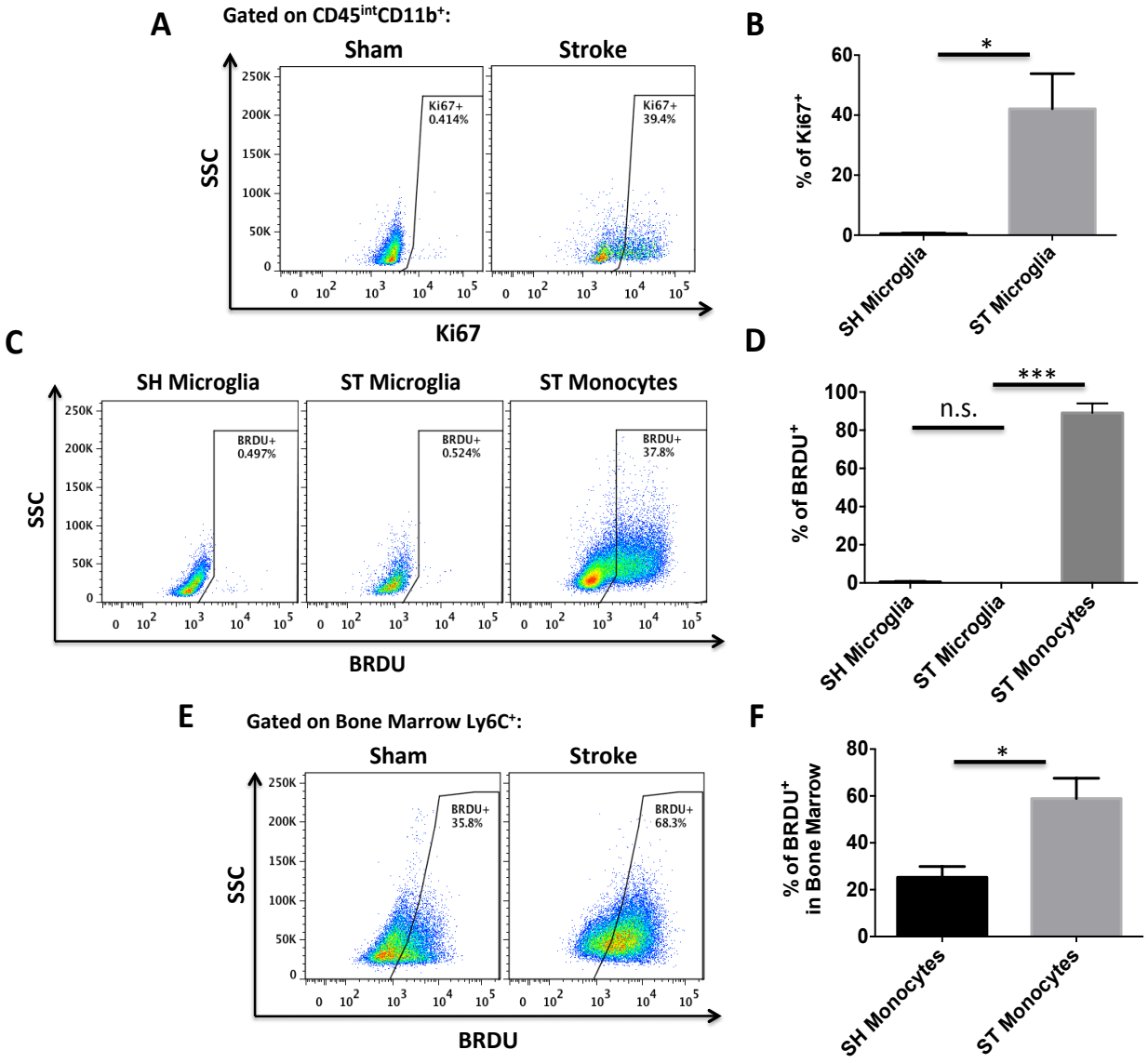

Figure 3-2. (Legend on following page)

Figure 3-2. Assessment of microglia proliferation and monocyte production by 72hrs after stroke.

A representative dot plot shows Ki67 expression by microglia at 72hrs after stroke (A). The percentages of $Ki67^+$ microglia were quantified (B). BRDU incorporation of myeloid cells was assessed in the brain using flow cytometry. A representative dot plot illustrates that resident microglia had not undergone DNA synthesis by 72hrs in the ischemic brain (C). Quantification of $BRDU^+$ cells revealed that nearly all monocytes had entered S phase of proliferation (D). Analysis of bone marrow revealed that stroke-induced production of monocytes likely account for $BRDU^+$ monocytes in the brain (E-F). For all experiments, N=5/group. Cell-specific FMO controls were used to determine positive gating. Error bars show mean SEM. Abbreviation: SEM, standard error of the mean; SH, sham; ST, stroke.

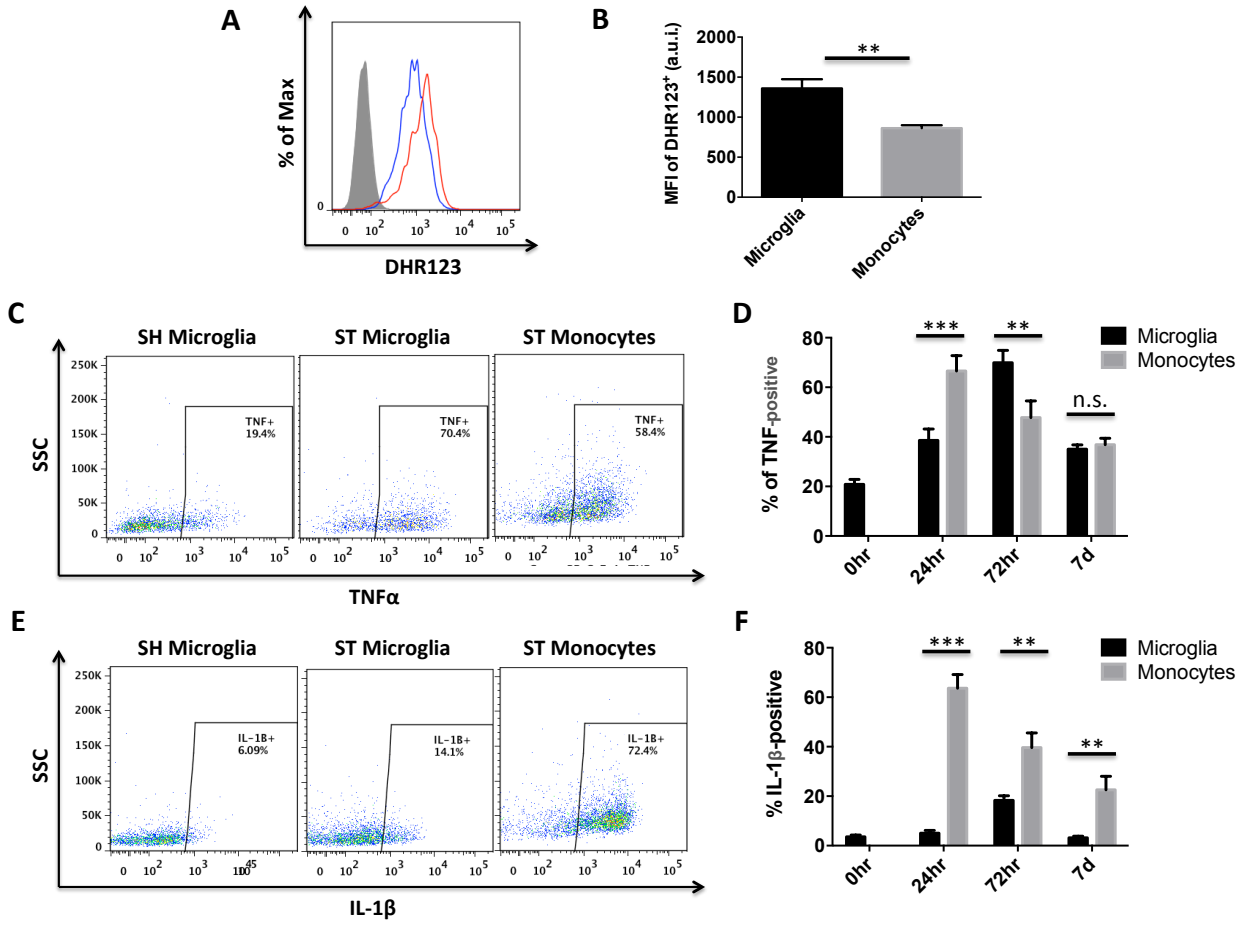

Figure 3-3. Measurement of cytokine production by microglia and monocytes at 24 hours, 72 hours, and 7 days following stroke.

A representative histogram showing microglia (red) have relatively higher reactive oxygen species levels than monocytes (blue) at 72hrs after stroke as measured with dihydrorhodamine (DHR) 123 (A). The mean fluorescence intensity of DHR123 was quantified (B). Representative dot plots showing microglia and monocyte production of TNF (C) and IL-1β (E) at 72hrs reveals differential expression patterns after stroke. The respective percentages of cells positive for these cytokines are quantified at 0hrs, 24hrs, 72hrs, and 7 days (D and F). For all experiments, N=5-7/group. Cell-specific FMO controls were used to determine positive gating. Error bars show mean SEM. Abbreviation: SEM, standard error of the mean; SH, sham; ST, stroke

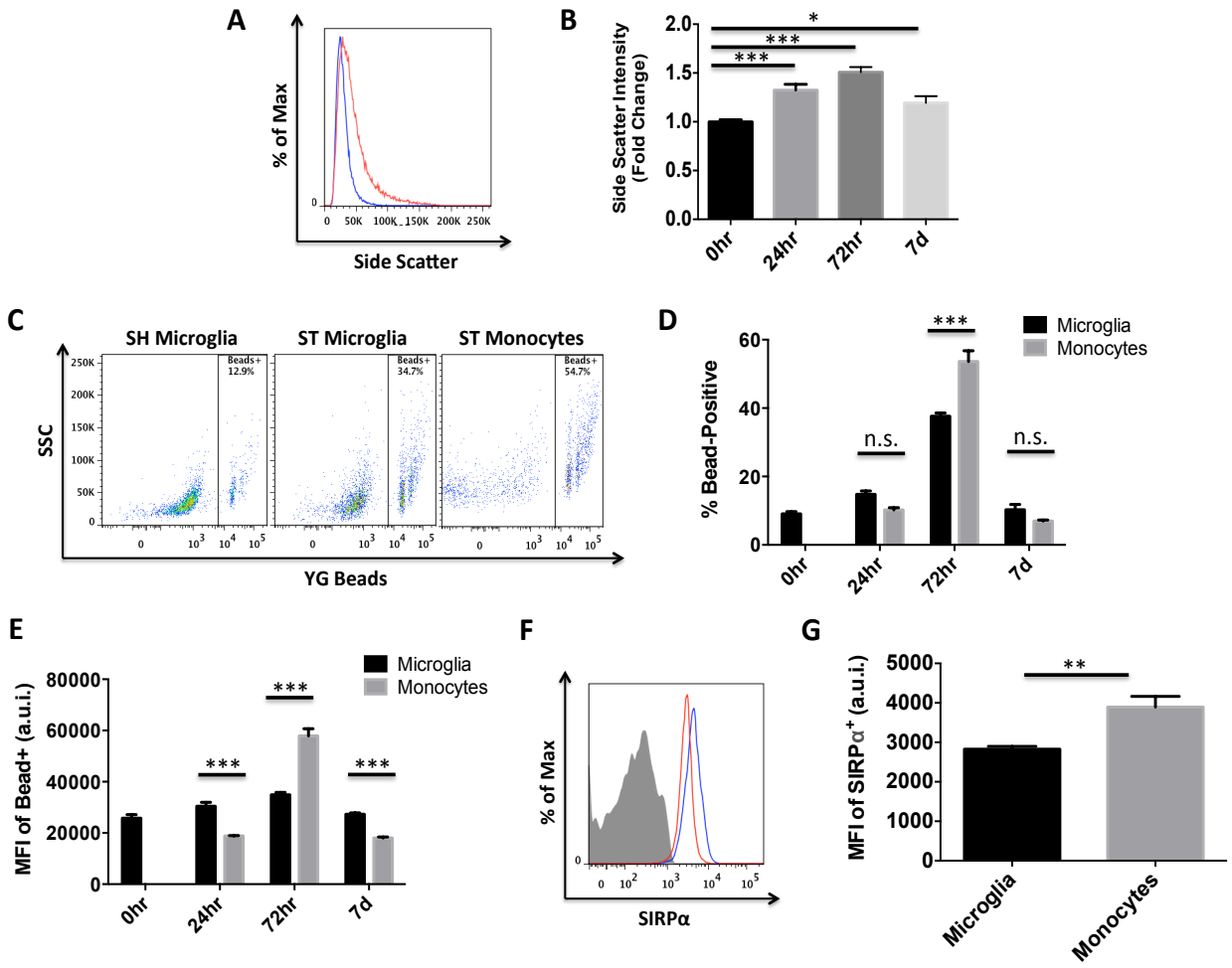

Figure 3-4. Phagocytic activity of microglia and monocytes at 24hrs, 72hrs, and 7 days following stroke.

Representative histogram showing a relative increase in side scatter (granularity) properties of microglia at 72hrs after stroke (red) compared to sham (blue; A). Mean side scatter intensity of microglia was quantified at different time points after MCAO (N=5/group; B). Phagocytic activity after stroke was measured by bead assay using flow cytometry (C). The percentages and mean fluorescence intensity (MFI) of bead$^+$ cells were quantified at 0hrs, 24hrs, 72hrs, and 7 days (N=6/group; D-E). A representative histogram shows higher expression of the phagocytic marker SIRPα on monocytes (blue) compared to microglia (red) at 72hrs in the ischemic hemisphere (F). The MFI of SIRPα$^+$ cells are quantified (N=5/group; G). Cell-specific FMO controls were used to determine positive gating. Error bars show mean SEM. Abbreviation: SEM, standard error of the mean; SH, sham; ST, stroke; SSC, side scatter; YG, yellow green

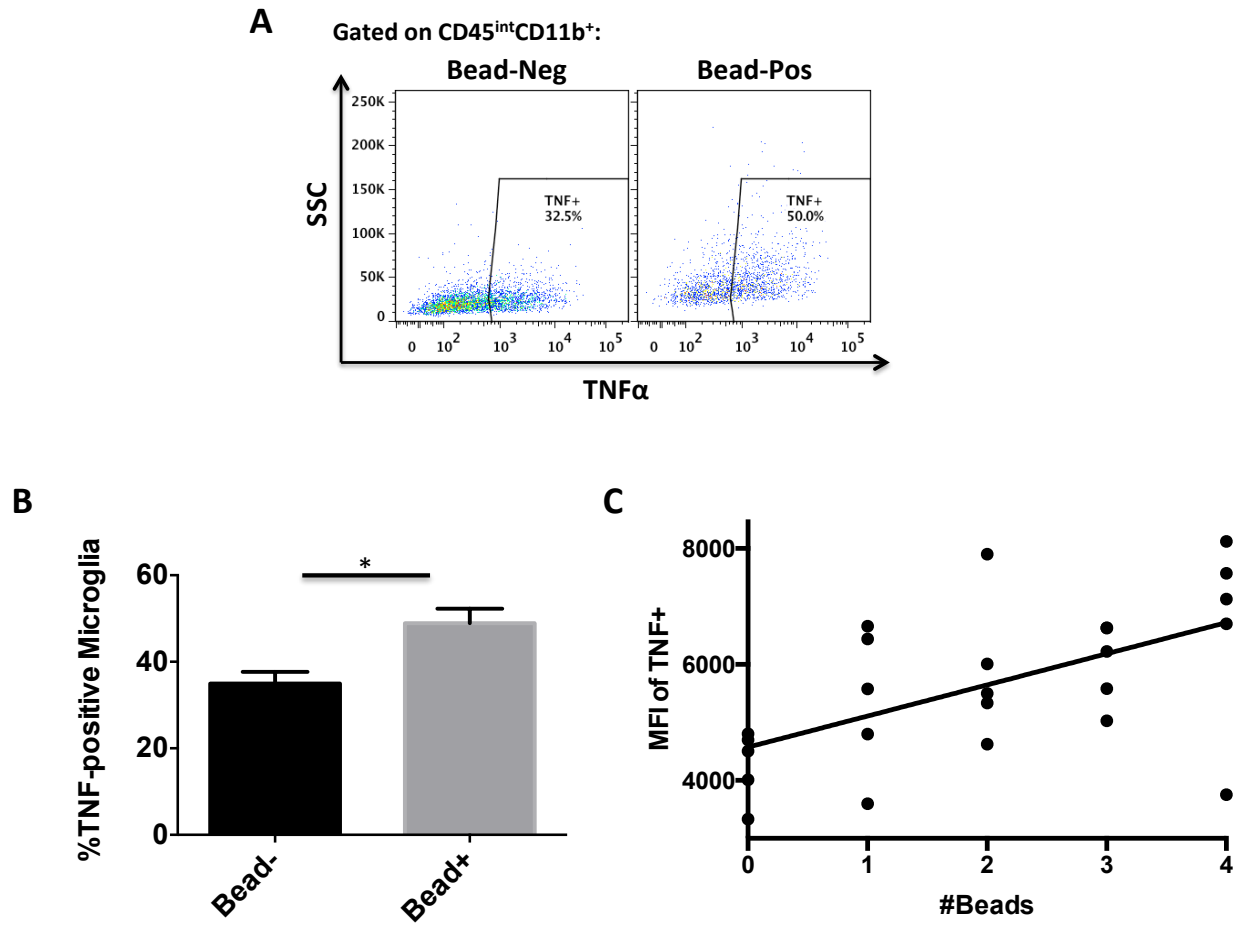

Figure 3-5. Relationship between TNF production and phagocytic activity of microglia after stroke.

A representative dot plot shows the relationship between microglial TNF production and phagocytic activity at 24hrs (A). The percentage of TNF^+ microglia is significantly higher in the phagocytic subset of microglia compared to the non-phagocytic subset (N=5/group; B). A positive correlation was found between the MFI of TNF expression in microglia and number of beads they phagocytosed after stroke (C). Cell-specific FMO controls were used to determine positive gating. Error bars show mean SEM. Abbreviation: SEM, standard error of the mean; SSC, side scatter; MFI, mean fluorescence intensity; a.u.i., arbitrary units of intensity.

restored back to baseline levels by 7 days. Compared to microglia, however, infiltrating monocytes exhibited far greater capacity for phagocytosis. Significantly more monocytes were bead-positive as were the number of beads phagocytosed per cell as evidenced by MFI ($p<0.001$; **Figure 3-4E**). Monocytes at 72 hrs also expressed significantly higher levels of the phagocytic marker SIRPα than did microglia ($p=0.005$; **Figures 3-4F-G**). Interestingly, phagocytic microglia were more likely to express TNF and at higher levels than non-phagocytic microglia, indicating that pro-inflammatory (M1) markers may overlap with anti-inflammatory (M2) function (**Figures 3-5A-B**). Moreover, a positive correlation was found between the level of TNF production and the number of beads phagocytosed by microglia after stroke ($p=0.0167$; **Figure 3-5C**). Taken together, these data imply that microglia do increase phagocytic activity following stroke stimulus, albeit at significantly lower levels than recruited monocytes.

Discussion

We demonstrate for the first time that the increase in macrophage proliferation in the brain following severe tMCAO is a result of stimulus-driven bone marrow production of migrant monocytes rather than proliferation of microglia. Resident microglia, as bystanders to ischemia, are similarly vulnerable to its detrimental effects. We found that after a 90-minute MCA occlusion, the number of microglia is significantly less than that seen in sham brain. Traditionally, the use of standard immunohistochemistry could not make this distinction; possibly overestimating the microglial response leading to the

concept that microglia are highly proliferative, even after severe ischemic injuries. Indeed, the microglia population in general appears to be severely compromised after stroke. It is not known whether the microglial population replenishes itself during recovery, or if invading monocytes establish permanent residence and take over the microglial niche [93,179].

Although microglia and monocytes exhibit several features of pro-inflammatory activation after stroke, several studies suggest a supportive and even beneficial role for each in stroke outcome [12,14,212-216]. These outcomes are likely influenced by the degree of ischemic severity and the ischemic setting/conditions. Distinguishing brain-resident microglia from monocyte populations in ischemic brains that have high numbers of infiltrating leukocytes can be challenging. Due to the lack of available microglia-specific markers, the absolute identification of microglia can be hampered by up-regulation of CD45 expression on activated microglia after injury, which can cause overlap with bone marrow-derived macrophage populations [83,102,217]. Bone marrow chimeras allowed us to differentiate between all fluorescently tagged bone marrow-derived leukocytes from resident microglia, definitively confirming that microglial expression of CD45 is relatively stable after stroke. However, to further ensure the purity of our microglial gating strategy, we selected out any contaminating monocytes using Ly6C antibody, which is not expressed on adult microglia. These findings enabled us to provide a reliable functional assessment of resident microglia and recruited monocyte populations by ex-vivo flow cytometry.

Recent work from the Merad laboratory has elegantly demonstrated that there is little bone marrow or systemic contribution to the resident microglia pool under normal

conditions [64,218]. These observations were made using donor-tagged bone marrow chimeras and parabiotic mice. Consistent with these findings, our group has also found that as far out as one year following radiation, uninjured chimeras had less than 5% 'microglia-like' monocytes as evidenced by their $CD45^{int}CD11b^{+}GFP^{+}Ly6C^{+}$ phenotype, reminiscent of the resident $CD45^{int}CD11b^{+}GFP^{-}$ microglia population (data not shown). Although these findings imply there is a low frequency of monocyte mixing in the resident $CD45^{int}$ microglia population of irradiated chimeras, these bone marrow-derived GFP^{+} cells can still be distinguished by the expression of Ly6C. Although useful, chimera development and parabiotic manipulation have limitations, including the potential for radiation injury and immune activation from the invasive surgical stress, respectively. Importantly, other studies have found that following an injury to the CNS, recruited monocytes can down-regulate Ly6C expression and establish permanent residence, thereby replenishing the attenuated microglia pool [179,219]. The acute time points described in our study are unlikely to be affected by the down-regulation of Ly6C on monocytes as earlier studies have shown this does not occur until after 7 days post-injury. While the genotoxic elimination of the microglia in mice appears to be non-deleterious in the short-term, the long-term consequences of microglia removal are likely detrimental to CNS homeostasis as evidenced in several neurodegenerative models [220-223]. The long-term consequences of microglia elimination in necrotic regions following ischemic stroke warrants further investigation.

We show that microglia numbers are decreased at 72hrs after a 90-minute tMCAO, and noted an inverse correlation between microglia and infiltrating monocyte counts. This is in contrast to several reports that have shown significant increases in

microglia proliferation [61,163,224]. However it is likely the severity of the ischemic injury plays a major role in the microglial response as other work has shown reduced microglial populations with more severe injury (e.g., longer occlusion times) [140]. Previous work has shown that the morphological changes that accompany glial cell activation after stroke are not dependent on or coincident with neuronal death, but rather the duration of ischemia [225]. Microglia are more ischemia-resistant than neurons and oligodendrocytes, but clearly they are also vulnerable to severe ischemia [226-228]. The inability to distinguish microglia from infiltrating monocytes, which increase in number with injury severity using histological methods may further obfuscate this issue. Flow cytometry may provide a more sensitive means of identification of cell type based on the well-accepted relative surface expression of CD45. Depending on the compensation setup, overlapping of these cell populations may also occur with flow cytometry. However, we have shown that it is extremely useful to use Ly6C as a monocyte marker to achieve maximal separation of these two populations, as infiltrating monocytes may down-regulate CD45 and MHCII levels over time, adopting a microglia-like phenotype ($CD45^{int}CD11b^{+}$) [219].

Increased production of bone marrow derived myeloid cells after stroke has been described [210]. We found that BRDU is incorporated into many newly produced monocytes in the bone marrow, which are subsequently recruited into the brain. This is consistent with recent work showing ischemic stroke activates hematopoietic stem cells in the bone marrow, resulting in a myeloid bias and greater output of monocytes [229]. The number of BRDU-positive myeloid cells in the brain reaches its peak by 72hrs [140,163]. This parallels the time course of leukocyte infiltration

into the brain, which also peaks at 72hrs. Although microglia did not enter S-phase in our study, many were $Ki67^{+}$, indicating that they were actively cycling at 72hrs. Ki67 expression in activated microglia after stroke has also been documented [230]. The failure of most cells to progress through later stages of the cell cycle may also be due to altered length of G1 and/or cellular stress [231]. Based on this earlier work and given the differential effects of ischemia of microglia populations located throughout the hemisphere, we hypothesized that some of these cells would enter the S-phase of cell cycle to begin dividing prior to 72hrs. Surprisingly, we did not observe this trend. An earlier study using GFP bone marrow chimeras revealed that the vast majority of macrophages in the infarct area after 30min tMCAO were derived from local microglia [232]. Despite the smaller injuries and altered leukocyte kinetics that result from shorter occlusion times, the ability to assess microglia numbers after stroke in an unbiased fashion using immunohistochemistry can be challenging due to the subtle difficulty of identifying microglia in their ramified state relative to those with amoeboid morphology, and given the rapid migration of activated microglia into the penumbral region often present in the field of view. As such, shifts in population densities due to migration towards injury sites could be misinterpreted as local microglia proliferation. It should be noted, however, that our data do not exclude the possibility that microglia proliferation occurs beyond 72hrs in the 90-minute tMCAO model.

A recent study of microglia proliferation after stroke was elegantly approached by implementing the parabiosis model using wild type and $CX3CR1^{GFP/-}$ mice [233]. The authors concluded that microglia proliferation accounted for the majority of microgliosis observed after stroke, rather than monocyte infiltration. However, there are several

possible explanations for the disparate results. The CX3CR1-GFP signal in these reporter mice is not specific only to microglia, especially following an injury stimulus, as it has been shown that Ly6C^{lo} monocytes also express GFP [217,234,235]. As histological analyses would not be able to distinguish GFP^{+} microglia from GFP^{+} monocytes (or vice versa in non-GFP WT mice), these cells largely go undetected as they typically begin migrating to the brain within 12-24 hours of injury. In addition, this study used a smaller, more localized injury induced photothrombosis, resulting in a milder inflammatory response. The stimulus-driven production of monocytes in bone marrow in this milder injury would likely be less and further diluted following egress into the blood due to the ~50% equilibrium of circulating cells in parabiotic (GFP-WT) mice. These studies provide valuable information in the context of both the specific model of stroke being employed, the severity of ischemia, and the time points being investigated. Taken together, these authors nicely demonstrate that microglia proliferation occurs early after stroke under mild or modest ischemic conditions, whereas our data implies this function is likely compromised after severe ischemic injury.

Oxidative stress and cytokine-induced cell death are key components of ischemic injury. Reperfusion after ischemia produces a burst in ROS formation [236]. Oxidative stress increases within the first hour after reperfusion and delivers signals that promote necrosis and apoptosis. The generation of ROS burst activity results from impaired mitochondrial respiratory chain function and activation of cytoplasmic oxidases. As a result, oxidative stress contributes directly to necrosis and apoptosis through a number of pathways in ischemic tissue. Although neurons and endothelial cells are important sources of ROS, all cells subject to ischemic injury are vulnerable to ROS-mediated cell

death signaling [237]. The massive influx of ROS-producing infiltrating leukocytes adds considerably to the overall ROS levels in the brain after stroke. Using bone marrow chimeras, a recent study demonstrated that NADPH oxidase (NOX2)-mediated ROS production in circulating leukocytes contributed to exacerbated infarct volumes compared to that produced by resident microglia after stroke [238]. Although we found ROS levels were higher in microglia after stroke, we did not evaluate the other subsets of infiltrating myeloid cells, namely neutrophils. Instead, we show that on cell-to-cell basis, monocytes produce significantly less ROS after stroke than resident microglia. This may reflect the severely compromised state of microglia following ischemic reperfusion.

Injury-driven production of ROS can further amplify the inflammatory response by driving cytokine production. TNF and IL-1β are produced by both microglia and monocytes after stroke. Numerous studies using transgenic mice and pharmacological agents have demonstrated a neurotoxic role for each of these pro-inflammatory cytokines in ischemic injury [185,239]. Our finding that microglia produced higher levels of ROS and TNF after stroke than monocytes suggest that the resident cells may be the more detrimental macrophage early after injury. Excessive insult to resident microglia may impair their primary function to maintain brain homeostasis during recovery. These findings build on previous work which described the expression of these cytokines in different subsets of microglia and macrophages 24hrs after permanent MCAO using a bone marrow chimera approach combined with immunohistochemistry and flow cytometry [240]. The authors reported that a greater number of $CD11b^{+}$ $CD45^{hi}$ macrophages/granulocytes expressed TNF and IL-1β at 24hrs compared to $CD11b^{+}$

$CD45^{dim}$ microglia. While innovative in its design, the use of GR-1 to distinguish between and identify monocytes/macrophages and neutrophils is not as accurate as Ly6C/Ly6G markers [234]. Despite this discrepancy, we found similar expression profiles in these two populations at 24hrs, whereas microglia became the predominant TNF producers by peak leukocyte infiltration at 72hrs. The importance of TNF signaling to ischemic injury was recently evaluated [170]. Using bone marrow chimeras it was found that TLR2- and TLR4-mediated injury is primarily driven by infiltrating leukocytes rather than resident microglia. However, TNF is also produced by microglia early after ischemia prior to monocyte infiltration, and TNF-directed therapies at these early time points are neuroprotective [31,241]. However, it must also be noted that infiltrating monocytes expressed higher levels of IL-1β, a cytokine associated with inflammasome-signaling [242,243]. This implies that inflammatory signaling in macrophage populations is incredibly robust and complex. Further understanding of these differences between these two cell subtypes and their inflammatory function after stroke may provide better insight on the targeted effects of known drug treatments, allowing for the development of more effective, cell-specific drugs.

Following ischemia, injured areas of the brain undergo apoptosis. Dead and dying cells generate a vast amount of debris that requires clearance for regenerative processes to ensue. As the ischemic/reperfusion injury core evolves after 24hrs, amoeboid microglia migrate from the core to the transition zone of the penumbral area following reperfusion and adopt an M1 phenotype [131,244]. The importance of debris clearance by phagocytes is evident in rodents and humans lacking the scavenger receptor gene CD36, resulting in exacerbated injury and hematoma absorption in

models of ICH [245,246]. MRI imaging has demonstrated that USPIO particles can be tracked and localized to ED1+ microglia/macrophages with the highest signal intensities found in striatal and cortical penumbral regions at day 2 after 30min tMCAO in rats [247]. Using GFP bone marrow chimeras, an earlier study had shown that activated microglia phagocytose neuronal material as early as 24hrs and are the predominant phagocyte by day 7 [147]. While an early preponderance of phagocytic microglia would be expected given the delayed recruitment of monocytes, their use of a less severe, 30 min tMCA occlusion resulted in attenuated numbers of infiltrating monocytes. In another study, rats that had underwent 3hr tMCAO exhibited poor microglial phagocytosis of caspase-3-expressing neurons at 24hrs [14]. Moreover, the number of apoptotic neurons was not increased following liposome-mediated ablation of microglia, indicating a limited contribution to debris clearance in environments that are significantly impacted by ischemia. Injury-related defects in migration and increased cytokine repulsion signals may halt microglia phagocytic activity under increasing ischemic stress.

We provide the first functional evidence that microglia increase capacity for phagocytosis in acute ischemic stroke. The number of phagocytic microglia initially increased at 24hrs, peaked at 72hrs, and returned to baseline by 7 days. These data paralleled the increase in microglia side scatter properties (granularity) in separate experiments, further indication of phagocytic uptake. Interestingly, however, infiltrating monocytes were significantly more efficient at phagocytosing material during the peak response at 72hrs. Following tissue entry, monocytes may further mature into macrophage or dendritic cell subsets with tissue-specialized functions. Monocyte-derivatives retain the expression of lineage markers and have enhanced phagocytic

ability [248]. Our findings indicate that while these tissue phagocytes exhibit many classical pro-inflammatory features deemed destructive, they appear to play a critical role in debris clearance and post-stroke recovery. It may be that in addition to being injured, many resident microglia had already exhausted their capacity to phagocytize surplus debris prior to ex-vivo phagocytosis assessment. However, by 7 days after stroke when monocytes diminish in the ischemic brain, resident microglia again become the predominant phagocyte, highlighting the importance of microglia in the long-term recovery and repair process. Unpublished results from our laboratory suggest that circulating phagocyte populations are generally more efficient than microglia at phagocytizing material under non-stimulated conditions. Recent work demonstrating the importance of monocytes to hemorrhage clearance in a model of intracerebral hemorrhage highlights their ability to significantly improve long-term outcomes through phagocytic function early after stroke [249]. This may relate in part to the degree of adaptive functionality associated with their different lifespans, as monocyte function may be more robust given their 'boom and bust' half-life, whereas the phagocytic activity of microglia likely endures at a steady rate throughout life. It is important to note that monocyte-targeted therapies aimed at inhibiting the function of these cells may inadvertently affect their phagocytic activity. Moreover, strategies to exploit this capacity should be considered, especially during the early stages of injury when the blood-brain barrier is susceptible to monocyte entry.

Finally, we showed a positive correlation between TNF expression levels and the level of phagocytic activity of microglia after injury. ROS and pro-inflammatory cytokine signaling is thought to hamper phagocytic activity and debris clearance [250,251]. Our

finding suggests that dichotomizing function into M1/M2 polarization, in which cells are polarized to become either pro-inflammatory/detrimental (M1) or anti-inflammatory/injury resolving (M2) may be too simplistic [252]. This concept more aptly applies to microglia *in vitro* and is polarization may be better appreciated as a continuum of activation *in vivo* due the combination of factors and diverse cell types present in intact tissue. Indeed, the polarization dynamics of microglia and monocytes during stroke appear to be mixed and complex. As mentioned, anti-inflammatory markers such as IL-4 and IL-10 were not expressed by either myeloid cell at any timepoint in this study. However, we acknowledge that transitioning between M1 and M2 phases may occur weeks after injury as has been reported by others [131,198]. Whether there is a requirement for pro-inflammatory signaling to induce or enhance phagocytic activity and debris clearance is currently not known. These findings point to a possible side effect of microglia/macrophage inhibition that could hamper the removal of dead cells and slow recovery.

In conclusion, we have identified distinct functional roles for brain-resident and infiltrating macrophages after stroke. To better both the interpretation of failed clinical trials and the development of more efficacious drugs to treat sterile inflammation in the CNS requires a better understanding of potential cellular targets. We believe that functional assessment of immune cells after stroke ex-vivo could be a powerful tool in screening and validating the targeted cellular effects of drugs and various therapeutic interventions.

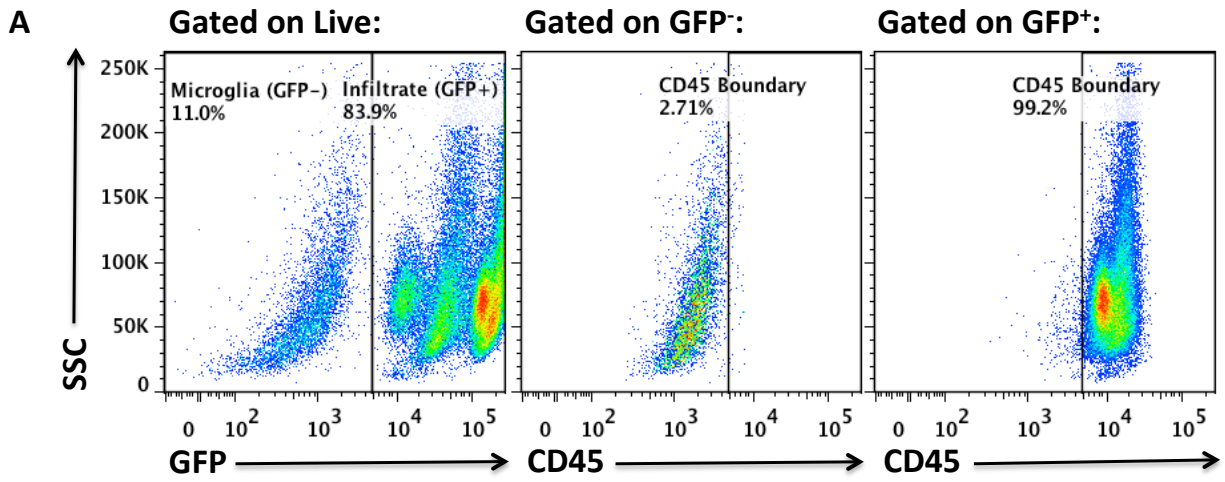

Supplemental Figure 3-1. Relative stability of CD45 expression by microglia at 72hrs after stroke.

Bone marrow chimeras were generated using GFP^+ donors and wildtype recipient mice. Microglial CD45 expression level was evaluated to determine if their CD45-intermediate expression level is increased after stroke, potentially overlapping with the CD45-high expressing bone marrow-derived myeloid population. A representative dot plot of the ischemic brain at 72hrs illustrates that GFP^- (wildtype) microglia do not substantially increase CD45 expression to CD45-high levels associated with GFP^+ bone marrow-derived populations (98% GFP reconstitution in this wildtype host; A). Cell-specific FMO controls were used to determine positive gating.

Authors' Contributions

RMR and LDM conceived the project. RMR performed most of the experiments and ARP, JMG, and JG assisted with the flow cytometry preparations. RMR and ARP performed FACS analysis and interpretation. RV assisted with the statistical analyses. RMR and LDM wrote the paper. All authors read and made comments on the manuscript draft and approved the final manuscript.

Acknowledgements

This work was supported by National Institutes of Health grants R21 NS082906-02 (Louise D. McCullough), R21 NS076293-01A1 (Louise D. McCullough), and F31 NS083244-01A1 (Rodney M. Ritzel).

Chapter 4:

CD200R1 immune inhibitory signaling attenuates brain inflammation and promotes behavioral recovery after stroke

Rodney M. Ritzel[1], Joshua Crapser, Rajkumar Verma, Anita R. Patel, Brittany Knight, Jeremy M. Grenier, Brett Freidler, and Louise D. McCullough

Abstract

In ischemic stroke injury homeostatic pathways are dysregulated in the CNS, which leads to a sterile inflammatory response, subsequent cell death, and impaired survival. The CD200-CD200R1 pathway is a key regulator of inflammation and CNS homeostasis, and is perturbed in the brain following injury. Given the immune-inhibitory properties of CD200, we investigated the role of CD200R1-mediated signaling in post-acute brain inflammation and recovery following transient middle cerebral artery occlusion (tMCAO) using CD200R1-deficient mice. At baseline, CD200R1 knockout mice had significantly more T cells with an activated, effector memory phenotype present in the brain compared to wild type littermates. No changes in the microglial compartment were found, however CNS-specific T cells from CD200R1 knockout mice showed altered cytokine production. Following ischemia, CD200R1 knockout mice had

significantly greater mortality by day 7. These mice also displayed severe body weight loss, impaired motor recovery and decreased nesting activity compared to wild type mice. Nearly thrice as many infiltrating leukocytes were found in the ischemic brain of CD200R1 knockout mice, with subtle differences in leukocyte composition. Taken together, these data suggest that the immune-inhibitory effects of CD200R1 signaling in the CNS serve to attenuate the level of immune-surveillance by T cells, while having a negligible effect on microglia under normal conditions. More importantly, CD200R1 is up-regulated on the surface of activated leukocytes after stroke, where it serves an important compensatory function required to quell immune cell activation and transmigration, and thus, the amplitude of the overall inflammatory response. The cellular basis for the observed protective effects of CD200-CD200R1 signaling on stroke recovery warrants further investigation.

Introduction

Inflammation plays a key role in the pathophysiology of stroke, the fourth leading cause of mortality and primary cause of disability in the United States [253]. Mounting evidence suggests that stroke-induced inflammation significantly contributes to neuronal injury, disease progression, and clinical outcome [57]. The innate immune system plays a pivotal role in the brain's response to injury, including activation of microglia and macrophages. Microglia are of myeloid origin and represent the resident immune cells of the CNS, where their primary function is to maintain tissue homeostasis [254]. As constant

surveyors of the environment, microglia are uniquely predisposed to both effectively initiate and subsequently quell inflammatory signaling in an effort to restore tissue structure and function back to steady state. Thus, microglial activation is a tightly regulated process. However, in a pathological setting signaling may become overactive or dysregulated leading to neuronal cell death and loss of function [198].

Among the homeostatic mechanisms that regulate the activation state of microglia/macrophages, are a select group of membrane-associated glycoproteins collectively known as immune inhibitory receptors that regulate inflammation via neuronal-glial interactions. One known example involves the interaction between CD200R1 (expressed on myeloid cells) and CD200 ligand (expressed on neurons). In this paradigm, CD200R1 is activated upon binding to CD200 ligand resulting in downstream inhibition of pro-inflammatory pathways, thereby maintaining microglia in an inactive, resting state [19,27]. CD200-CD200R1 interactions depend upon a NPXY motif, leading to phosphorylation of Dok1 and Dok2 proteins, binding of RasGAP and SHIP, and subsequent downstream inhibition of the RasMAPK pathways [46,255-257]. Following tissue injury, these interactions between neurons and microglia are disrupted, thus lifting the 'brake' on inflammation and enabling a pro-inflammatory response. Recent studies investigating the imbalance of CD200-CD200R1 signaling in models of neurodegenerative disease support the hypothesis that this interaction may also be disrupted after stroke [23,112,258-260]. To date, the functional role of the CD200-CD200R1 signaling axis in sterile brain injuries such as stroke is not known.

We therein proposed to investigate the role of CD200-CD200R1 signaling in experimental stroke. CD200R1 knockout and littermate control mice were subject to 60-

minute tMCAO and evaluated at day 7 for post-acute changes in neuroinflammation and behavioral recovery. We report a novel role for the CD200-CD200R1 pathway in regulating the homeostatic control of T cell immunosurveillance in the CNS under normal conditions. Moreover, we demonstrate that following an ischemic insult, CD200R1 inhibitory signaling functions as a critical regulator of inflammation. Lack of CD200R1-mediated immunoregulation resulted in poor survival and worse outcomes following stroke. Given the immunoregulatory role of the CD200R1 signaling pathway, its relevance to ischemic stroke is of great interest, as it serves as a potential therapeutic target for suppressing the deleterious effects of leukocyte activation.

Materials and Methods

Mice/Animals: CD200R1$^{+/-}$ mice (bred on a C57BL/6J background) were generously provided by Professor R. Gorczynski (Toronto, Canada) [261]. Heterozygous CD200R1$^{+/-}$ mice were bred to obtain CD200R1$^{-/-}$ mutants and CD200R1$^{+/+}$ wildtype littermates. Young adult male mice (12-14 weeks) of age were pair-housed on sawdust bedding in a pathogen free facility (light cycle 12/12 h light/dark). C57BL/6J male mice 10-12 weeks (young adult; 24.5 ± 0.8 grams) and 18-20 months (aged; 33.1 ± 1.5 grams,) of age were obtained from Charles River Laboratories (Wilmington, MA) and the NIA breeding colony, respectively. All animals had access to chow and water ad libitium. All procedures were performed in accordance with NIH guidelines for the care and use of laboratory animals and approved by the Institutional Animal Care and Use Committee of

the University of Connecticut Health Center. All analysis was performed blinded to surgical conditions.

Ischemic Stroke Model: Cerebral ischemia was induced by 60 minutes of reversible middle cerebral artery occlusion (MCAO, 25–32 gm mice) under Isoflurane anesthesia as previously described [206]. Rectal temperatures were maintained at approximately 37°C during surgery and ischemia with an automated temperature control feedback system. A midline ventral neck incision was made, and unilateral MCAO was performed by inserting a 6.0 Doccol monofilament (Doccol Corp, Redland, CA) into the right internal carotid artery 6 mm from the internal carotid/pterygopalatine artery bifurcation via an external carotid artery stump. Following reperfusion mice were sacrificed at 7 days. In a separate cohort, young and aged wildtype mice were subject to 90 minutes of MCAO and 72 hours of reperfusion prior to sacrifice. 0.21 mm and 0.23 mm silicone coated sutures were utilized in young and aged mice respectively to achieve occlusion. Sham-operated animals underwent the same surgical procedure, but the suture was not advanced into the internal carotid artery.

Clinical assessment: Before and after ischemia body weight was monitored daily. Rectal temperatures were recorded during ischemia and immediately prior to sacrifice. Neurological deficits were assessed by Bederson-score from 0 (no deficit) to 4 (severe deficit) with minor modifications [262].

Behavioral Testing: All the animals were tested on each behavioral task twice, three days prior to surgery to establish a baseline reference and again on the day of sacrifice.

The mice enrolled for surgeries did not demonstrate any behavioral deficits in any test (prior to surgery). The testing was done at a fixed time in the morning. All behavioral testing equipment and surfaces were cleaned with 70% ethanol before and after testing for each animal. Mice were tested in the following order: nesting activity (overnight), neurological scoring, open field, Y maze, static rod, rotarod, and wirehang.

Hanging Wire: The hanging wire tests both limb strength and balance after stroke [263,264]. This test was performed as described by [265], with slight modification. A wire cage top, dimensions, 18 inch × 9 inch with its edges taped off was used for this experiment. The mouse was placed on the center of the wire lid and the lid was slowly inverted and placed on top of cage. The wire lid was 9 inch above the cage bedding. Latency to fall from the wire was recorded. The average time of three trials was taken. Mice with a latency of less than 3 seconds were excluded from the study, whereas a maximum cut-off of 120 seconds was assigned this value. Mice were alternately tested to allow for a rest period of at least 5 minutes between trials.

Open Field: Open Field measures spontaneous locomoter activity in a novel environment and has been used in stroke models [266]. In this task, the total ambulatory activity of the mouse was assessed. The mouse was placed in the open field chamber (15″ × 15″) in a dark room in Scoville Neurobehavioral Suite at UCHC. Locomotor activity was quantified as the total number of beam breaks by a computer operated PAS Open Field system (San Diego Instruments, San Diego, CA). Each testing session was 20 minutes long and the data was collected in 60 second intervals. All the mice were acclimatized to the dark testing room for 1 hour before the beginning of the test and the activity was recorded immediately after the mice were placed in the open field

apparatus.

Y maze spontaneous alternation: The Y maze test was used to evaluate cognitive function, especially working memory in a new environment [266]. All the mice were acclimatized to the testing room for 60 minutes prior to the beginning of the test and the activity was recorded immediately after the mice were placed in the maze. The number of entries, spontaneous alteration and percentage of alteration were recorded for one 5 min trial per test day. Entry is defined as a complete placement of hind paws within the arm of the maze. Spontaneous alteration is considered when a subject visits a new arm and does not return to one of previously-visited two arms. The percentage of alteration was calculated as follows: [number of spontaneous alteration/(number of entry − 2)] × 100. No difference in the number of arm entries was found between groups either before or after stroke.

Static rod: Balance and coordination of movement were assessed using a wooden rod of 60 cm in length and 2.8 cm in diameter as described by [267] with minor modification. Briefly, the rod was fixed by a G-clamp to a laboratory table such that the rod horizontally protruded into space 60 cm above a cotton-padded floor. Mice were placed at the free end of the rod facing away from the home table (nose tip one head's length from the edge) and were allowed a maximum period of 180 seconds to turn 180 degrees. The time taken to achieve this orientation was scored for each mouse and taken as average of three trials. The number of falls and successful turns was also tallied for each trial and the percentage was calculated. Subjects that turned upside down or fell off were arbitrarily assigned (for statistical purposes) the maximum

orientation score of 180 seconds. If it fell off in less than 3 seconds it was presumed to be due to faulty placement by the experimenter and allowed another attempt. This test has been validated for the assessment of motor balance in models of Down syndrome and Huntington's disease [268,269].

Rotarod: Mice were placed on a rotating cylindrical rod accelerating from 2 rotations per minute (rpm) to 20 rpm, over a span of 5 min [270,271]. Subjects were given 4 trials on the rotarod on day -3 and 7 of testing. A 5-minute break was given between the trials. The latency of the subject to fall from the rotating rod was recorded for each trial (in seconds), and the average latency was used for further analysis. No differences were found between groups at baseline.

Nesting activity: Two hours prior to the onset of the dark phase, mice were separated into individual cages and supplied with a ~5 × 5 cm pressed cotton squared piece. Nesting activity was assessed as described by [272,273] with minor modifications. In brief, each cotton pad was weighed prior to placing into cages for reference. After mice had habituated for 15 min in a novel empty cage, the cotton pad was placed in a random cage corner. The next morning (approximately 12 hours later) cages were inspected for nest construction. Any loose, shredded material was gently brushed off the intact nesting pad. Nesting activity was calculated as follows: [1 – (post-pad wt. (g) / pre-pad wt. (g))] x 100 = % nested material.

Terminal histopathology: All animals were sacrificed at 7 days after stroke with

avertin overdose (i.p). A separate cohort of animals (n=7-9/group) was sacrificed at for immunohistochemistry. Transcardial perfusion was performed with cold PBS followed by 4% paraformaldehyde; the brain was fixed for 24 hours and placed in cyroprotectant (30% sucrose). The brains were cut into 40-µm free-floating sections on a freezing microtome and every eighth slice was stained by cresyl violet staining to evaluate ischemic cell damage. The images were digitalized and cerebral atrophy was analyzed using computer software (Sigma scan Pro5) as previously described [264,274].

Immunohistochemistry (IHC): Immunohistochemical staining of fixed-frozen sections (40µm-thickness) was performed as described previously [275]. Briefly, brain slices were mounted onto gelatin-coated slides, allowed to air dry, and then blocked in 0.1 M phosphate buffer (PB) with 0.3% Triton X-100 (sigma) and 10% donkey serum (PBTDS) for an hour. Primary antibody (CD200, R&D Systems, 1:500; NeuN, Abcam, 1:200; GFAP, Dako, 1:200) was added overnight. After washes, the sections were incubated with secondary antibody (1:1000) and 4′,6-diamidino-2-phenylindole, dihydrochloride (DAPI, 1:1000, Invitrogen, Carlsbad, CA). Secondary antibody (1:1000, goat anti-mouse IgG conjugated to Alexa-488 or -594) was removed with three consecutive washes in PBTDS, 0.1 M PB, and 0.05 M PB respectively. Images were acquired with a Zeiss Axiovert 200M microscope (Carl Zeiss, Oberkochen, Germany) using a X-Cite 120Q fluorescence illumination system (Lumen Dynamics Group Inc., Mississauga, ON, Canada) and Zeiss image acquisition software (Zeiss LSM 510).

Enzyme-linked immunoabsorbant assay (ELISA): Plasma cytokine concentrations were determined by ELISA (Bio-Plex Pro Mouse Cytokine Assay, Bio-Rad

Laboratories). In brief, mice were euthanized by avertin injection and blood was collected by cardiac puncture into heparin-coated syringes. Samples were centrifuged (13,000g for 10min at 4C) and plasma was collected and stored frozen (-80C) until assaying. Samples were assayed according to the manufacturer's instructions using a Luminex 200 (Luminex Corporation, Austin, TX, USA) magnetic bead array platform. Inter-and intra-assay coefficients of variation were than less than 10%. CD200 protein concentrations were assayed using a mouse CD200 PicoKine ELISA kit (Boster Bio, Pleasanton, CA). Brain hemispheres were collected and homogenized in ice-cold lysis buffer containing a protease inhibitor cocktail (Roche Diagnositics). Homogenates were sonicated and centrifuged at 4C for 15 min at 14,000 rpm, and supernatants were assayed for total protein using a BCA protein assay kit (Pierce, Thermo scientific). Plasma and brain protein was assayed according to the manufacturer's instructions using a microplate reader (EnSpire 2300 Multilabel Reader, Perkin Elmer). Briefly, 50ul of plasma and 100ug of whole cell lysate brain protein were plated in triplicate for each sample. CD200 protein concentration was quantitatively determined by measuring the optical density absorbance at 450 nm.

Tissue processing for flow cytometry: Mice were euthanized, transcardially perfused with 60 mL cold, sterile PBS, and the brains were harvested. Blood was drawn by cardiac puncture with heparinized needles. Red blood cell lysis was achieved by three consecutive 10-minute incubations with Tris-ammonium chloride (Stem Cell Technologies). The brainstem and cerebellum were removed. The brain was then divided along the interhemispheric fissure to isolate the ipsilateral hemisphere and

subsequently rinsed with PBS to remove contaminant cells. Brains were placed in complete RPMI 1640 (Lonza) medium and mechanically and enzymatically digested in collagenase/dispase (1 mg/mL) and DNAse (10mg/mL; both Roche Diagnostics) for 1hr at 37C. The cell suspension was filtered through a 70um filter. Leukocytes were harvested from the interphase of a 70%/30% Percoll gradient. Cells were washed and blocked with mouse Fc Block (CD16/CD32, ebioscience) prior to staining with primary antibody-conjugated flourophores: CD45-eF450, CD11b-APCeF780, CD3e-APC, Ly6C-PerCP-Cy5.5, and Ly6G-PE. All antibodies were commercially purchased from eBioscience. For live/dead discrimination, a fixable viability dye, carboxylic acid succinimidyl ester (CASE-AF350, Invitrogen), was diluted at 1:300 from a working stock of 0.3mg/mL. Cells were briefly fixed in 2% paraformaldehyde (PFA). Data were acquired on a LSRII using FACsDiva 6.0 (BD Biosciences) and analyzed using FlowJo (Treestar Inc.). No less than 100,000 events were recorded for each sample. A gating strategy was designed as described in [276]. Resident microglia were identified as the $CD45^{int}$ $CD11b^{+}Ly6C^{-}$ population, whereas bone marrow-derived leukocytes were identified as $CD45^{hi}$. Cell type-matched fluorescence minus one (FMO) controls were used to determine the positive gating for each antibody. The following antibodies were used in this study: CD69-APC (eBioscience), CD4-PE-Cy7 (eBioscience), CD8-Bv510 (Biolegend), CD44-FITC (Biolegend), CD62L-PE (eBioscience), CD200R1-FITC (Biolegend), CD19-AF700 (eBioscience), MHCII-Bv510 (Biolegend), NKp46-PerCPeF710 (eBioscience), and DX5-PE (Biolegend).

To determine TCRvβ usage, we used a mouse vβ TCR screening panel (BD Pharmingen) according to the manufacturers instructions. Briefly, after collecting blood

leukocytes each sample was divided into 15 separate FACS tubes and stained for the antibody cocktail including one of 15 respective TCRvβ FITC-conjugated monoclonal antibodies.

Intracellular cytokine production: For intracellular cytokine staining, a stock solution of brefeldin A (Sigma) was prepared at 20mg/mL in DMSO, and diluted with PBS to obtain a working solution of 0.5mg/mL. Mice were euthanized 12 hours after intravenous injection of brefeldin A (250ul). Leukocytes were collected as described above, and 1ul of GolgiPlug containing brefeldin A (BD Biosciences) was added to 800ul complete RPMI. To assess T cell cytokine production, cells were subsequently stimulated with Cell Stimulation Cocktail (eBioscience) containing PMA/ionomycin and incubated for 4 hours at 37C (5% CO2). Cells were resuspended in Fc Block, stained for surface antigens and washed in 100ul of fixation/permeabilization solution (BD Biosciences) for 20 minutes. Cells were then washed twice in 300ul Permeabilization/Wash buffer (BD Biosciences) and resuspended in an intracellular antibody cocktail containing TNF-PE-Cy7 (eBioscience), IL-1β –FITC (eBioscience), MMP-9-PE (StressMarq Biosciences), and IFNγ-PerCP-Cy5.5 (Biolegend) and then fixed.

Statistical analyses: Data from individual experiments are presented as mean ± SEM and assessed by Student t test or One-way ANOVA with Tukey post-hoc test for multiple comparisons (GraphPad Prism Software Inc, San Diego, CA, USA). For Two-way ANOVA, significant differences between paired comparisons were conducted with

the Holm-Sidak test. Kaplan-Meier survival curves were compared using Cox-Mantel analysis to determine statistical significance between groups. The neurological deficit scores, being ordinal in nature, were analyzed using the Mann-Whitney U test. The Spearman's rank correlation test was used to ascertain the correlation between leukocyte infiltration and neurological deficit score. Significance was set at $p \leq 0.05$.

Results

Characterization of CD200- and CD200R1-expressing cells in the healthy adult brain

To begin our investigation into the functional role of CD200-CD200R1 immune inhibitory signaling in the brain we first characterized the cells that express CD200 or CD200R1 protein in the wildtype brain using immunohistochemistry and flow cytometry. CD200 protein was ubiquitously expressed throughout the central nervous system (**Figure 4-1A**). The staining pattern in the cerebral cortex was diffuse, largely confined to gray matter regions, and mostly localized to the cell membrane of neurons (**Figure 4-1B**). Using flow cytometry, we assessed CD200R1 expression on leukocytes present in the healthy wildtype adult brain. We identified the presence of resident $CD45^{int}CD11b^{+}$ microglia, a small population of $CD45^{hi}CD11b^{+}$ peripheral myeloid cells, and a population of $CD45^{hi}CD11b^{-}$ putative lymphocytes (**Figure 4-2A**), of which the majority were $CD3^{+}$ T cells (**Figure 4-2B**). Surprisingly, very few resident microglia expressed CD200R1 (**Figure 4-2C**). However, 20-30% of brain-specific $CD3^{+}$ T cells were

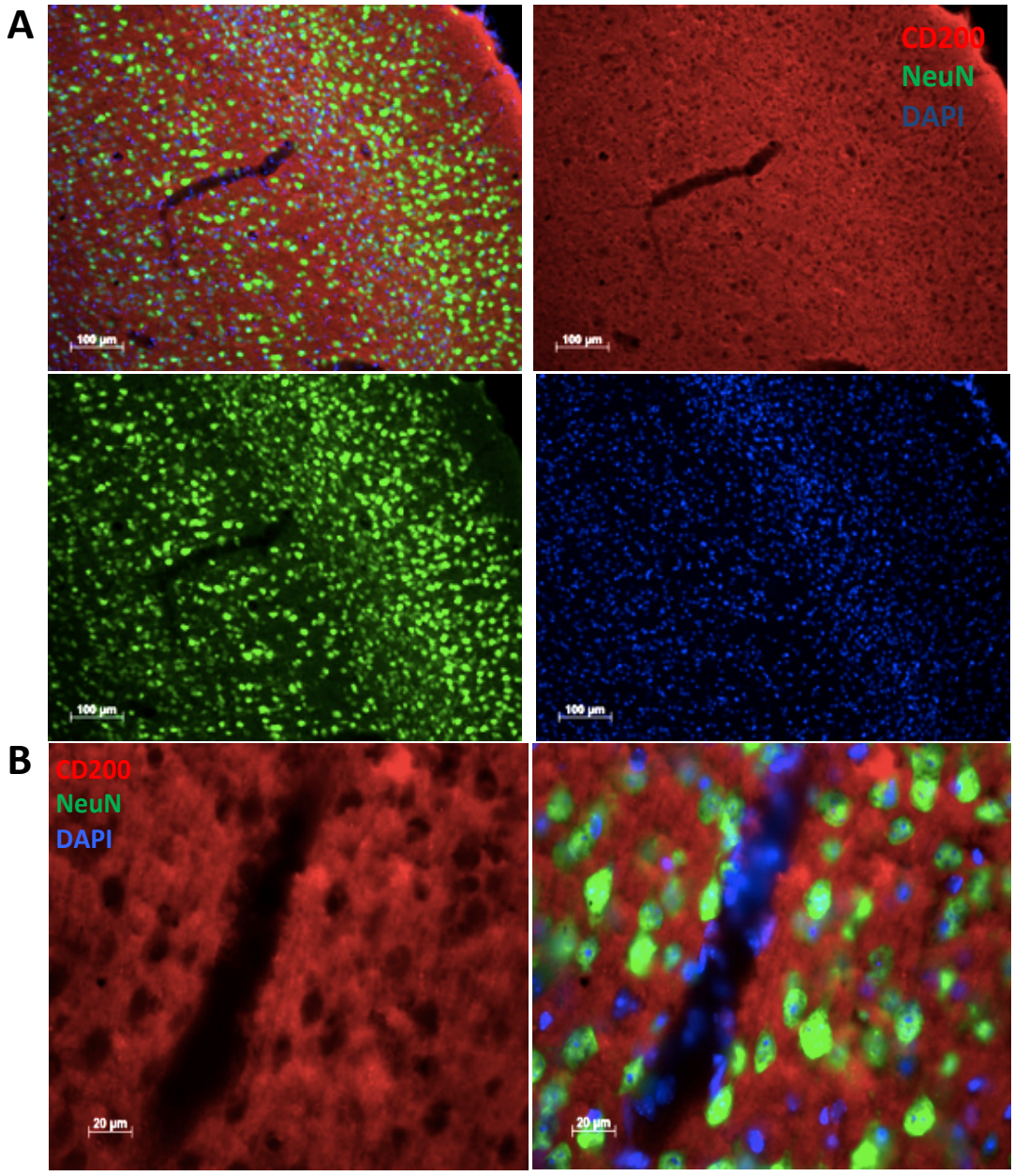

Figure 4-1. CD200 protein expression in the normal adult cerebral cortex. Representative 40um-thick brain tissue sections illustrating the diffuse, ubiquitous expression of CD200 (red) surrounding DAPI-positive (blue) neurons (green) in the grey matter of the healthy, wildtype adult cortex (A; N=3). Higher magnification shows CD200 is expressed on the cell membrane of neurons and secreted in the extracellular space (B). Abbreviation: DAPI 4',6-diamidino-2-phenylindole, NeuN neuronal nuclei.

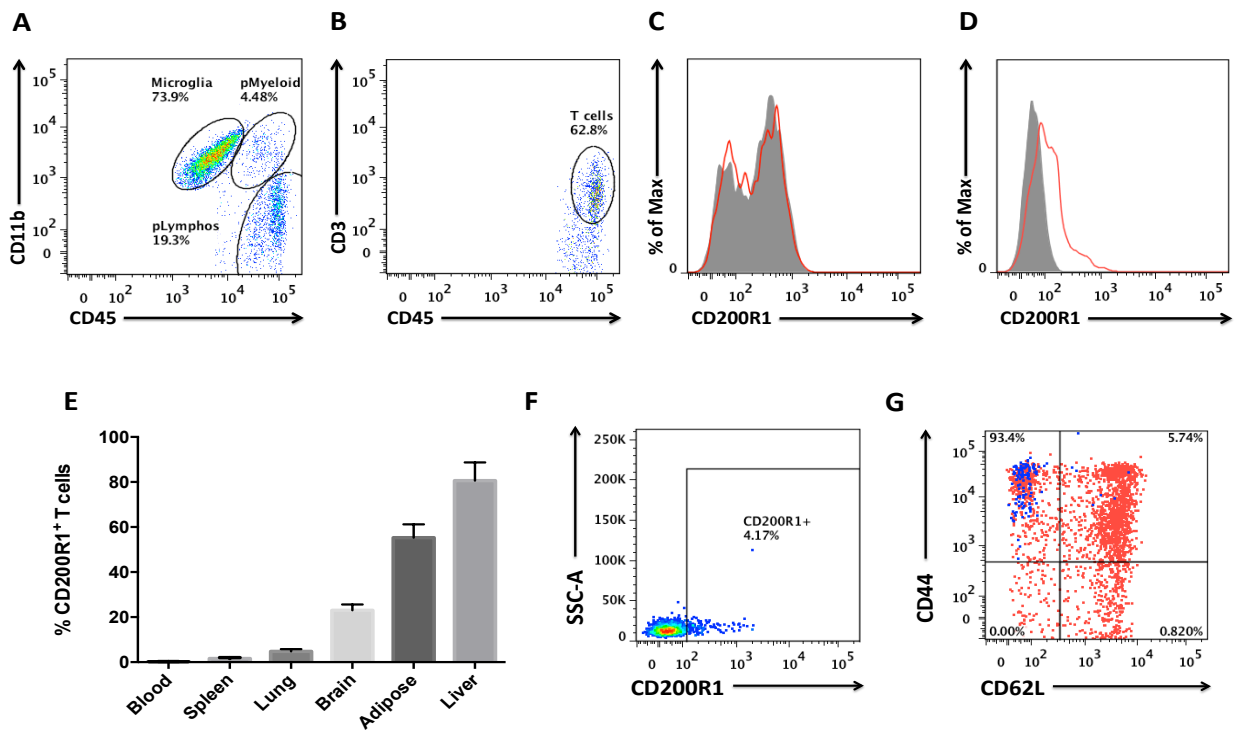

Figure 4-2. Surface expression of CD200R1 by tissue-resident T cells with effector memory phenotype.

A representative dot plot shows the identification of $CD45^{int}CD11b^{+}$ resident microglia, $CD45^{hi}CD11b^{+}$ peripheral myeloid cells, and $CD45^{hi}CD11b^{-}$ peripheral lymphocytes in the PBS-perfused brain of healthy adult wildtype mice (A). A representative dot plot shows that $CD3^{+}$ T cells compose the majority of the $CD45^{hi}CD11b^{-}$ peripheral lymphocyte population in the brain (B). A representative histogram illustrates the lack of CD200R1 protein expression on the cell surface of wildtype microglia in the adult brain (C). A histogram depicts the presence of CD200R1 on the surface of CNS-resident T cells (D). The percentage of CD200R1-positive T cells was quantified in lymphoid and tertiary tissues (E). A representative dot plot depicts the CD200R1 expression on circulating blood T cells (F). An overlay dot plot reveals that the majority of CD200R1-positive $CD3^{+}$ T cells (blue) in the blood have an effector memory phenotype ($CD44^{hi}CD62L^{lo}$) compared to CD200R1-negative (red) T cells (G). For all experiments, N= 5-8/group. Cell-specific FMO controls and genotype-confirmed $CD200R1^{-/-}$ controls were used to determine positive gating (shaded gray). Error bars show mean SEM.

positive for CD200R1 (**Figure 4-2D**). Interestingly, CD200R1 was expressed largely on $CD3^+$ T cells present in tertiary tissues rather than lymphoid tissues (**Figure 4-2E**). CD200R1-positive $CD3^+$ T cells in the blood were identified as those with an effector memory ($CD44^{hi}CD62L^{lo}$) phenotype indicating that they are antigen-experienced and activated (**Figures 4-2F**-**G**). These data suggest that the migration and/or activation of CNS-resident (or circulating) T cells in the healthy brain are potentially regulated by CD200-mediated inhibition either through direct interactions with neurons or by soluble CD200 present in the extracellular environment.

CD200R1 mediates T cell entry into the un-injured brain and regulates basal cytokine production in CNS-specific T cells but not microglia

To determine the functional role of CD200R1 signaling in CNS-specific T cells we assessed changes in T cell migration and activation in CD200R1 (global) knockout mice and control wildtype littermates. We observed no changes in the absolute number of resident microglia between groups, however CD200R1 knockout mice had a significantly greater number of $CD45^{hi}$ peripheral leukocytes per brain hemisphere compared to wildtype (**Figures 4-3A** and **4-4A-B**, p=0.040). Although no changes in peripheral myeloid cell counts were found, CD200R1 knockout mice showed a significant increase in the number of $CD3^+$ T cells present in the brain (p=0.0004), of which the majority were identified as $CD8^+$ subset of T cells (**Figures 4-3B** and **4-4C-F**). Both CD4 and CD8 subsets of CNS-specific $CD3^+$ T cells had an effector memory

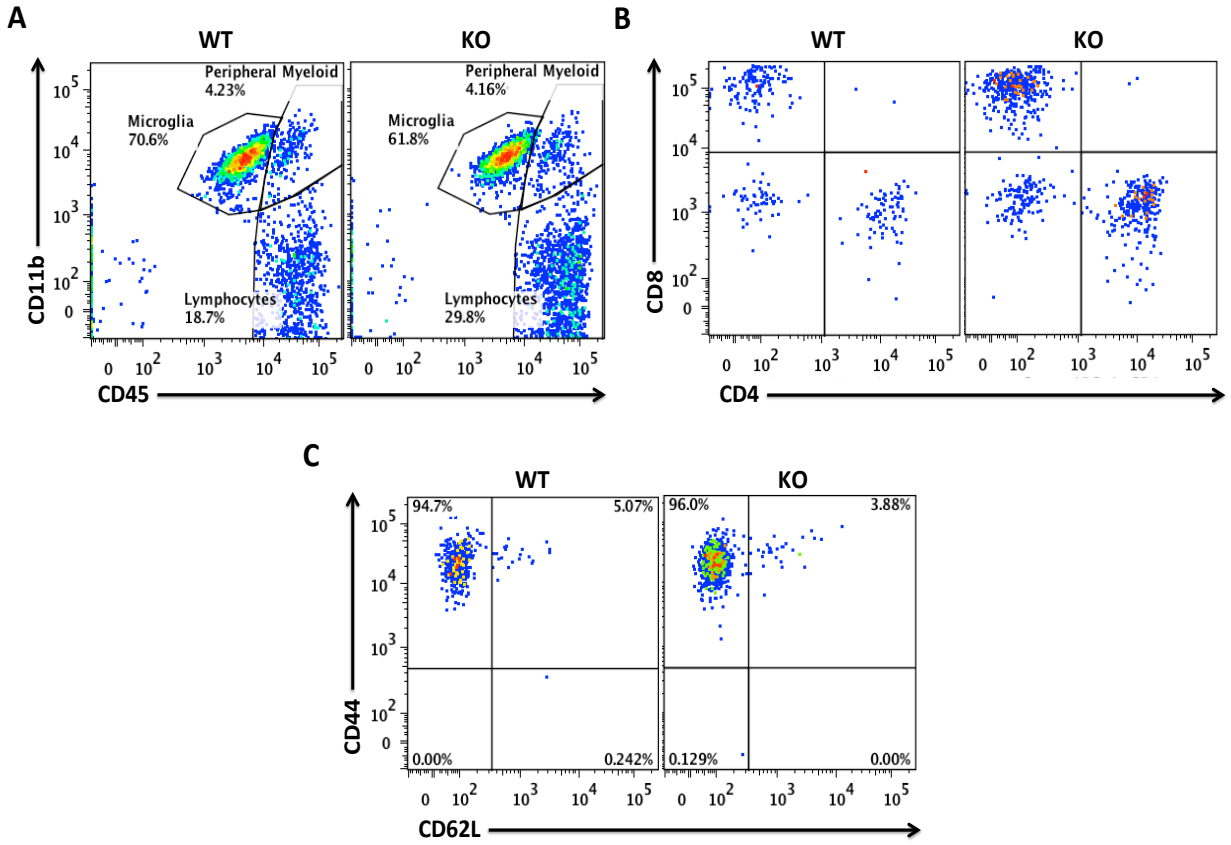

Figure 4-3. Characterization of brain leukocytes in naive CD200R1 wildtype and knockout mice by flow cytometry.

Representative dot plots illustrate the differences in resident microglia ($CD45^{int}CD11b^{+}$) and peripheral leukocytes ($CD45^{hi}$) in the normal brain of CD200R1 wildtype and knockout mice (A). A representative dot plot shows that the $CD45^{hi}CD11b^{-}$ lymphocyte population is largely composed of CD4 and CD8 subsets of $CD3^{+}$ T cells (B). Brain-specific $CD3^{+}$ T cells have an effector memory ($CD44^{hi}CD62L^{lo}$) phenotype (C). For all experiments, N= 5-12/group. Cell-specific FMO controls were used to determine positive gating. Abbreviation: WT wildtype, KO knockout.

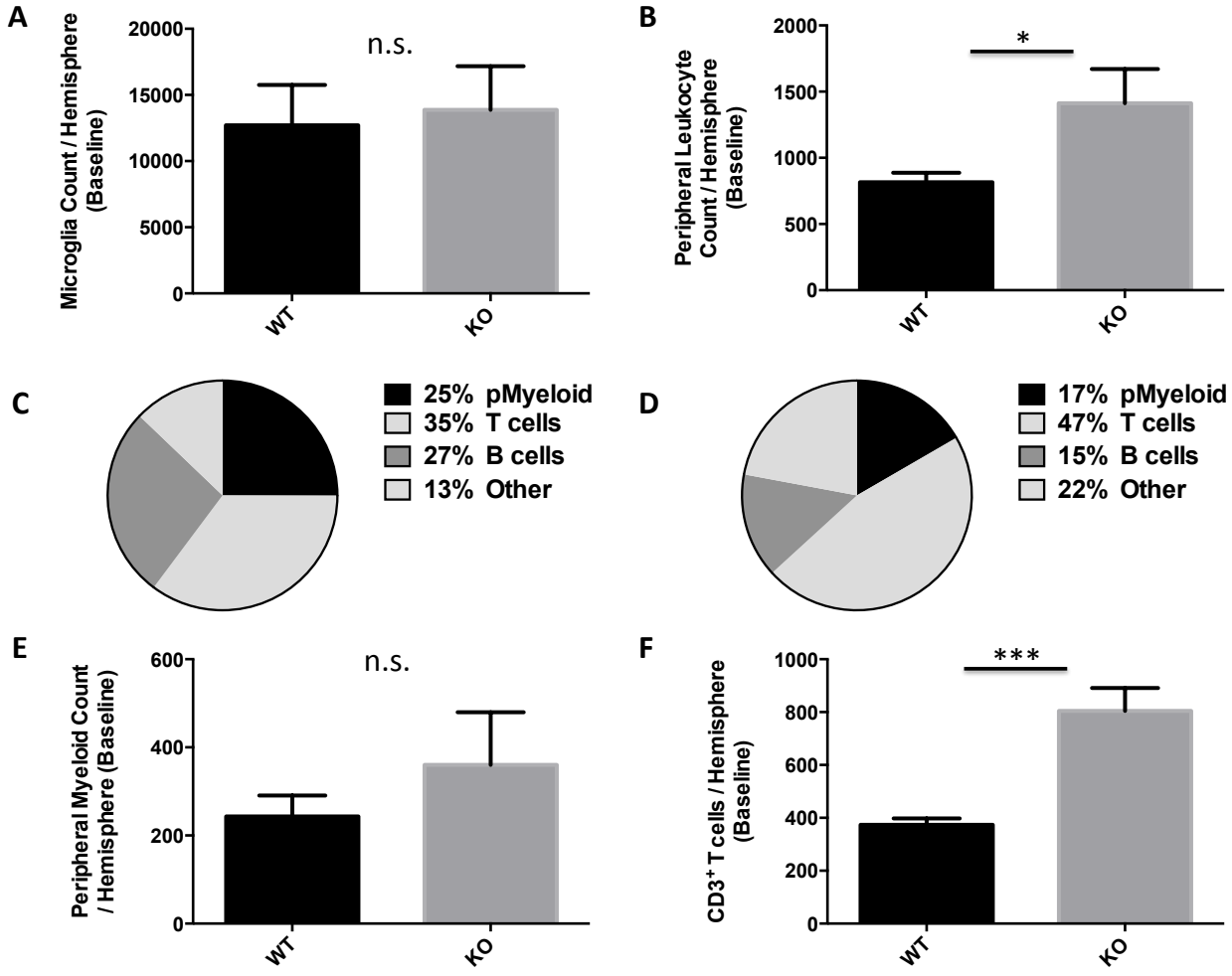

Figure 4-4. Effect of CD200R1 deletion on microglia and peripheral leukocyte counts in the normal brain.

The absolute number of microglia (A) and peripheral leukocytes (B) per brain hemisphere was quantified in CD200R1 wildtype and knockout mice (N=7/group). The relative cellular composition of $CD45^{hi}$ peripheral leukocytes in the CD200R1 wildtype (C) and knockout (D) brain are shown. The absolute number of $CD45^{hi}CD11b^{+}$ peripheral myeloid cells (E) and $CD45^{hi}CD11b^{-}$ lymphocytes (F) are quantified. Error bars show mean SEM. Abbreviation: SEM standard error of mean, WT wildtype, KO knockout, n.s. not significant. *p≤0.05; **p≤0.01; ***p≤0.001

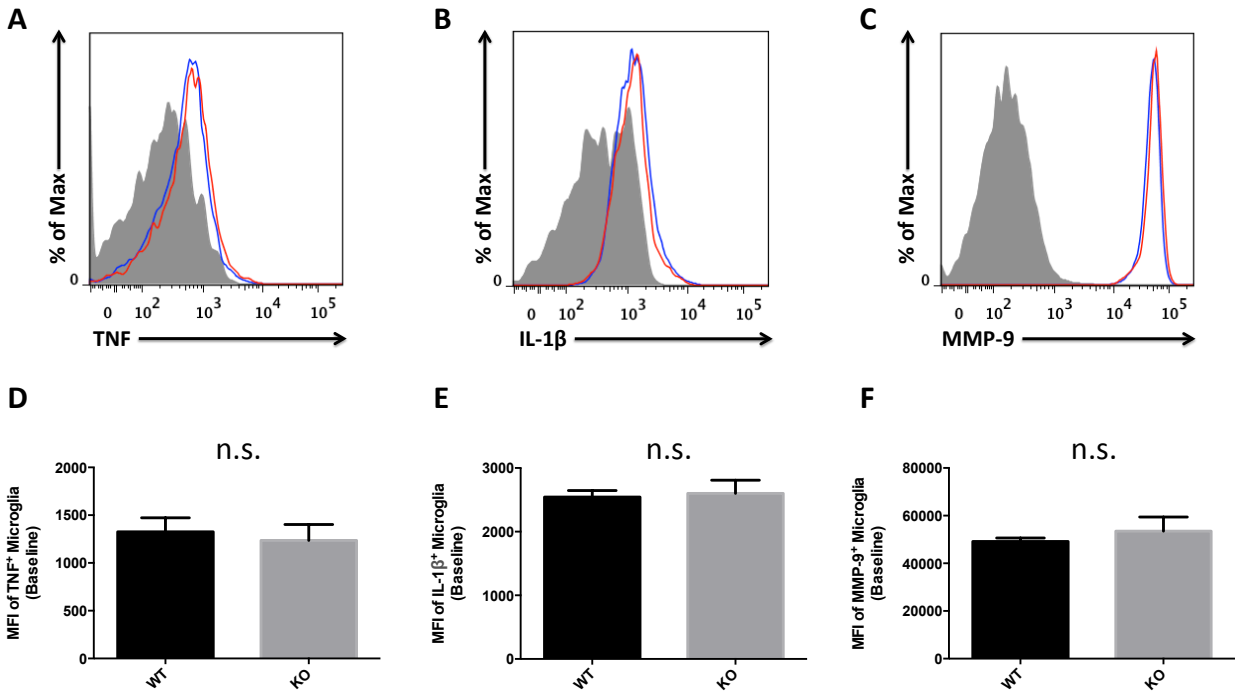

Figure 4-5. Effect of CD200R1 deletion on basal production of pro-inflammatory cytokines by microglia.

Representative dot plots show basal production of TNF (A), IL-1β (B), and MMP-9 (C) by microglia in the healthy adult brain of CD200R1 wildtype (red) and knockout (blue) mice. The respective mean fluorescence intensities of these cytokines (D, E, and F) were quantified (arbitrary units of intensity, N=5-10/group). Microglia-specific FMO controls were used to determine positive gating. Error bars show mean SEM. Abbreviation: SEM standard error of mean, MFI mean fluorescence intensity, WT wildtype, KO knockout, TNF tumor necrosis factor, IL-1β interleukin-1 beta, MMP-9 matrix metalloproteinase-9, Max maximum, n.s. not significant. *p≤0.05; **p≤0.01; ***p≤0.001

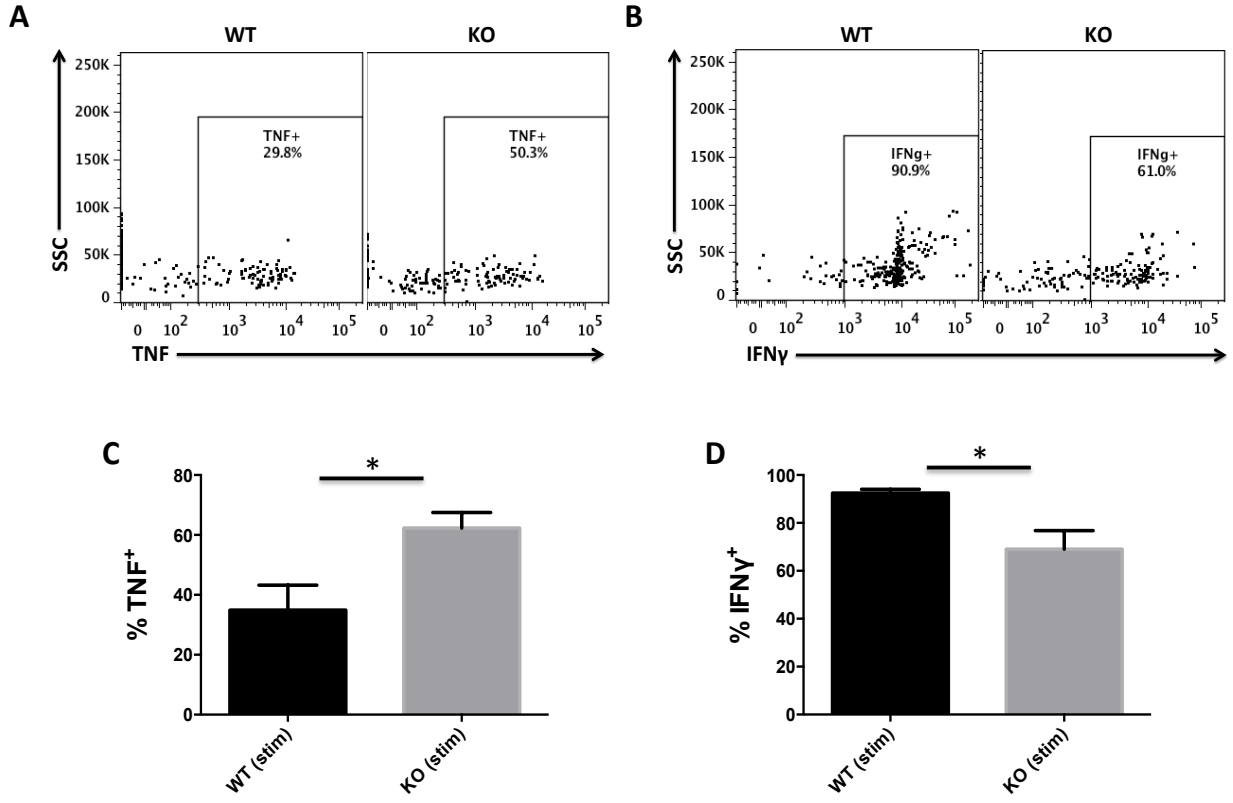

Figure 4-6. Effect of CD200R1 deletion on cytokine production by brain-resident T cells.

Representative dot plots show PMA/ionomycin-induced CD8 T cell expression of TNF (A) and IFNγ (B) from the healthy adult brain of CD200R1 wildtype and knockout mice. The respective percentages (C and D) were quantified (N=6/group). Cell-specific FMO controls were used to determine positive gating. Error bars show mean SEM. Abbreviation: SEM standard error of mean, SSC side scatter, WT wildtype, KO knockout, TNF tumor necrosis factor, IFNγ interferon gamma, Stim stimulation. *p≤0.05; **p≤0.01; ***p≤0.001

phenotype (**Figure 4-3C**). No differences in the gross vasculature of the circle of Willis were found between groups (**Supplemental Figure 4-1A**). Intracellular cytokine staining revealed that the basal production level of several pro-inflammatory mediators (TNF, IL-1β, and MMP-9) expressed by resident microglia in un-injured brains did not significantly differ between groups (**Figures 4-5A-F**). However, CNS-specific CD8 T cells from CD200R1 knockout mice exhibited a significant increase in the number of cells expressing TNF following PMA/ionomycin stimulation (**Figures 4-6A** and **4-6C**). Interestingly, IFNγ production was significantly diminished after stimulation of CNS-specific CD8 T cells lacking CD200R1 compared to wildtype controls (**Figures 4-6B** and **4-6D**). Taken together, our results suggest that the effects of CD200R1 immune-inhibitory signaling are largely confined to the T cell population in the un-injured brain, rather than the resident microglia. These data indicate that CD200R1 immune-inhibitory signaling regulates both T cell migration into the brain and effector cytokine production.

CD200R1 immune-inhibitory signaling promotes better outcomes after ischemic stroke

Next we investigated the functional role of CD200R1-mediated immune regulation following sterile brain injury using the middle cerebral artery occlusion (MCAO) model of ischemic stroke. Given that our earlier findings showed an increase in CNS-specific T cell numbers in the brain of otherwise healthy mice lacking CD200R1, we designed our study to extend out to 7 days after stroke due to the well-accepted delayed-recruitment of T cells into the ischemic brain [61,277-279]. Following 60 minutes of MCAO, we

observed a 52.4% survival rate for CD200R1 knockout mice by day 7, significantly lower than was seen for wildtype (83.3%, **Figure 4-7A**, p=0.049). CD200R1 knockout mice had significantly worse neurological deficit scores at day 7 compared to controls, as measured using the Bederson scoring system (**Figure 4-7B**, p=0.003). In addition to exacerbated hemiparesis, CD200R1 knockout mice exhibited a dramatic increase in body weight loss following stroke, nearly twice as much as wildtype controls (**Figure 4-7C**, p=0.003). This depletion of fat stores was accompanied by a significant decrease in body temperature (**Figure 4-7D**). CD200R1 knockout mice had a significant increase in thymic atrophy at day 7 (p=0.05); however, no differences in splenic atrophy were found between groups (**Figures 4-7E-F**). In sum, these results indicate that CD200R1-mediated inhibition of immune cells is required for survival and better neurological and physiological outcomes following ischemic stroke.

Loss of CD200R1-mediated immune inhibition worsens behavioral recovery following stroke

To see whether these outcomes were associated with changes in behavioral recovery, we ran a battery of behavioral tests to measure cognitive and sensorimotor deficits after stroke. We found no difference in short-term spatial memory function between groups using a Y-maze spontaneous alternation test (**Figure 4-8A**). Using one-way ANOVA analysis, spontaneous locomotor activity was significantly decreased in CD200R1 knockout mice, albeit modestly in comparison to the change in wildtype after stroke (**Figure 4-8B**). Motor coordination and endurance were measured using a rotarod

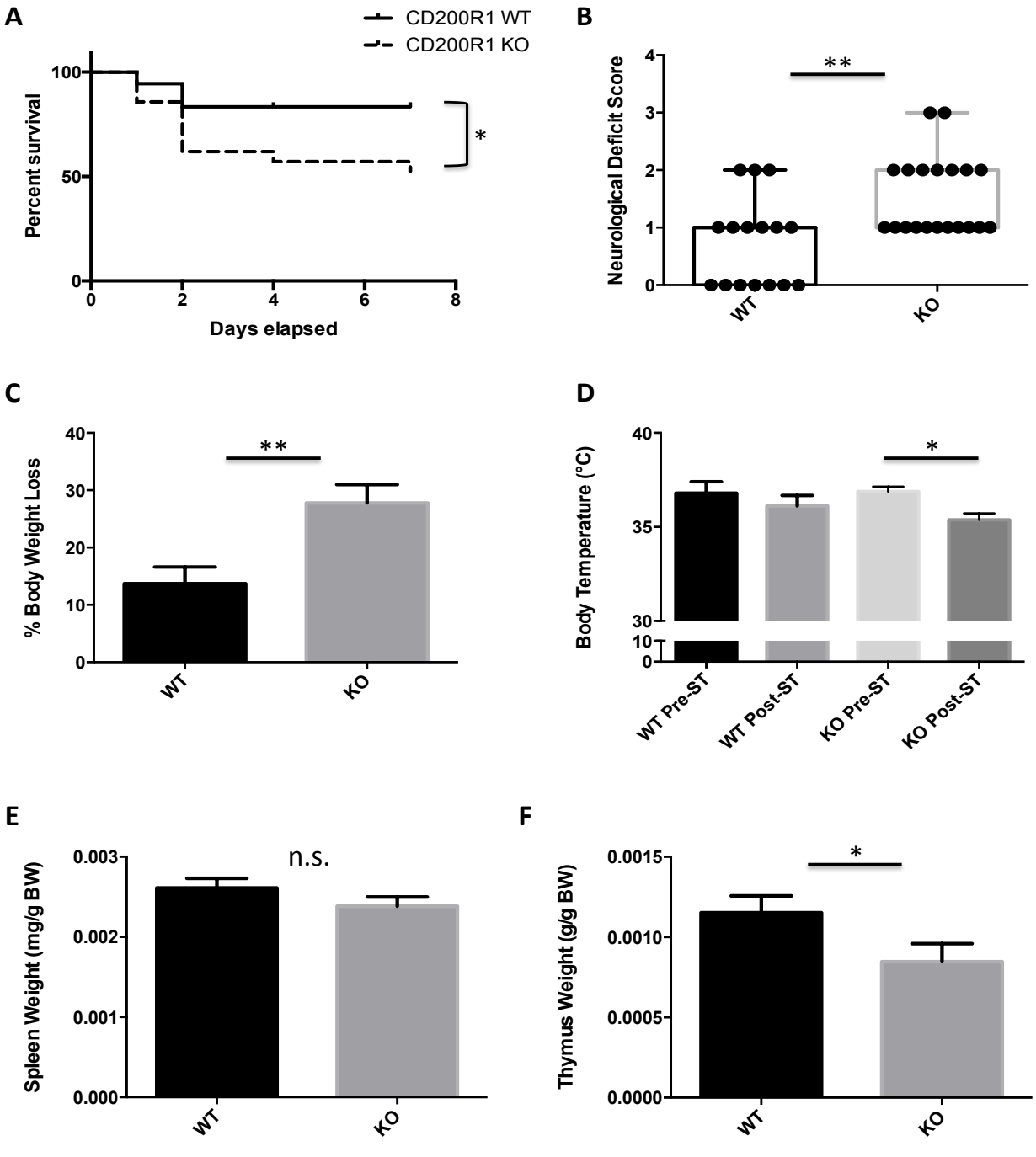

Figure 4-7. (Legend on following page)

Figure 4-7. Effect of CD200R1 deletion on stroke outcome at 7 days.

The survival rate for CD200R1 wildtype and knockout mice was quantified after stroke (A). Neurological deficit scores at day 7 are shown (B). The percentage of body weight loss was measured at sacrifice (from baseline) and quantified (C). Changes in rectal temperature were monitored at day 0 (Pre-ST) and day 7 (Post-ST) and quantified (D). Spleen (E) and thymus (F) weights were measured at day 7 and normalized to body weight. For all experiments, N=16-24/group. Error bars show mean SEM. Abbreviation: SEM standard error of mean, WT wildtype, KO knockout, ST stroke, BW body weight. *p≤0.05; **p≤0.01; ***p≤0.001

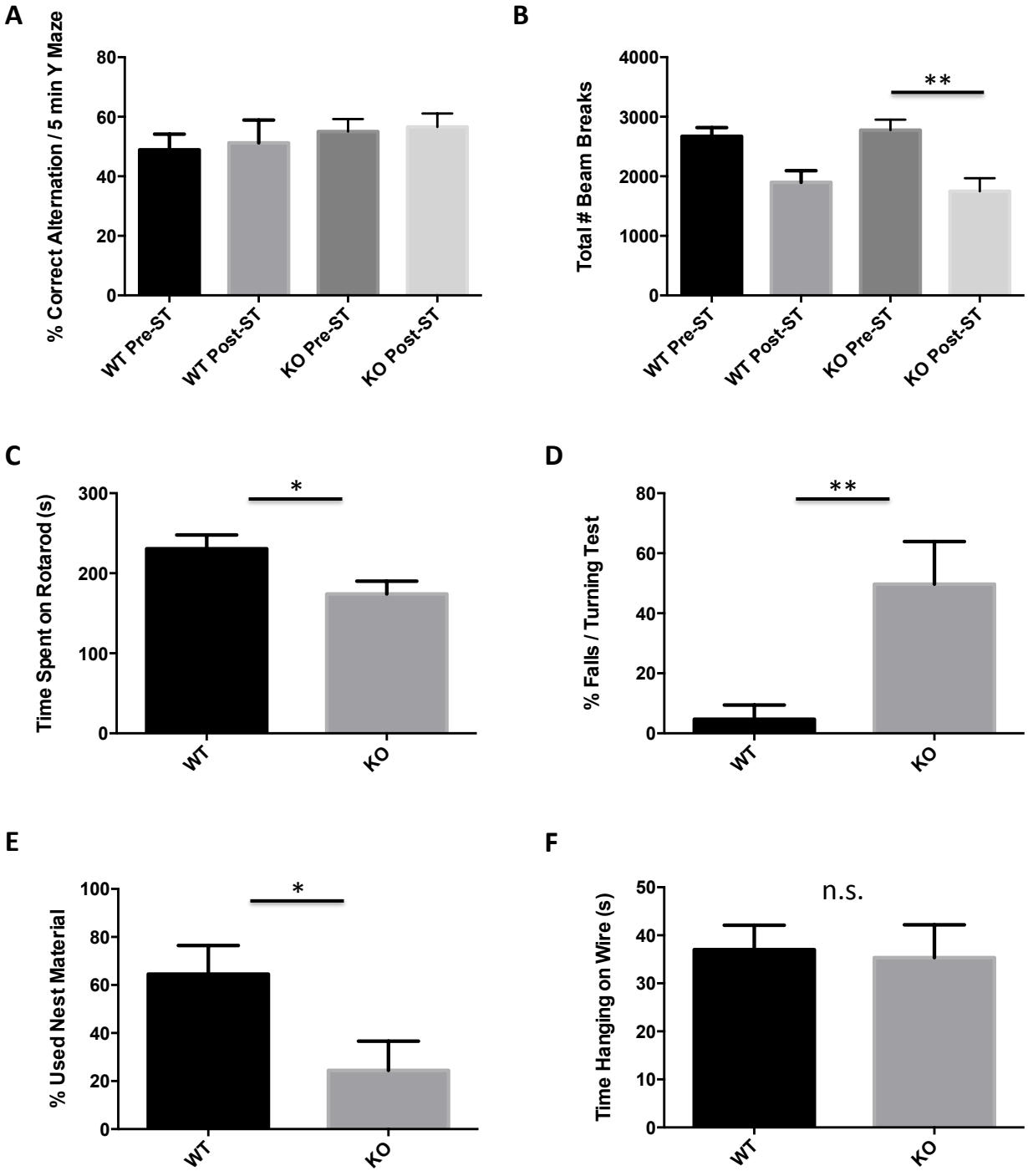

Figure 4-8. (Legend on following page)

Figure 4-8. CD200R1-mediated changes in behavioral recovery after stroke. The percentage of correct alternations/5 min in a Y-maze apparatus on day -3 and day 7 after stroke (A; N=6/group). The total number of beam breaks/20 min were measured in an open field test (B; N=12/group). The total time spent on a rotarod device (2-20 rpm) at day 7 was quantified (C; N=14-15/group) and the percentage of mice that fell off a horizontal cylinder rod during a 180-degree turning test are shown (D; N=7/group). The percentage of used nested material over an 8 hour period was determined on day 7 (E; N=12/group). The total time spent hanging on cage wire at day 7 was quantified (F; N=12/group). Error bars show mean SEM. Abbreviation: SEM standard error of mean, WT wildtype, KO knockout, ST stroke, n.s. not significant. *p≤0.05; **p≤0.01; ***p≤0.001

performance test. CD200R1 knockout mice showed significant impairment in remaining stable on an accelerating cylinder rod over time, having shorter durations before falling (**Figure 4-8C**, p=0.022). Because the rotarod test measures several parameters of motor coordination and stroke may differentially affect motor functions, we assessed motor skills in more detail. Using a static bar to measure the time it takes for a mouse to orient itself 180 degrees, we found that CD200R1 knockout mice failed to successfully orient themselves without falling in approximately half of the trials (**Figure 4-8D**, p=0.008). We next assessed for deficits in the ability to perform activities of daily living such as nest construction. CD200R1 knockout mice showed a significant reduction in nesting activity after stroke compared to wildtype controls (**Figure 4-8E**, p=0.027). This deficit did not appear to be associated with forelimb or grip strength as no difference was found in the length of time that each group of mice could hang from an elevated wire cage top before falling (**Figure 4-8F**). Collectively this data implies that immune-inhibitory interactions between neurons and leukocytes are important for the recovery of motor processes involved with balance and coordination as well as an impaired ability to perform normal daily tasks such as nesting.

CD200-CD200R1 signaling attenuates leukocyte infiltration into the ischemic brain

To determine whether the behavioral deficits found in CD200R1 knockout mice were associated with an increased inflammatory response in the brain following stroke we assessed leukocyte infiltration via flow cytometry. We first demonstrated that infiltrating

(and resident) lymphocyte populations were the predominant CD200R1-expressing cells in the ischemic brain at this time (**Figure 4-9A**). CD200R1-positive T cells in the ischemic brain expressed significantly higher levels of the early activation marker CD69 than CD200R1-negative T cells (**Figure 4-9B-C**, p=0.02). An analysis of total $CD45^{hi}$ peripheral leukocyte counts found that CD200R1 knockout mice had approximately almost three times the number of infiltrating cells as wildtype controls at 7 days (**Figures 4-10A-B**, p=0.009). Despite these changes, no differences in tissue atrophy were observed (**Supplemental Figure 4-1B**). Further analysis revealed that $CD11b^{+}Ly6C^{+}Ly6G^{-}$ monocytes made up the majority of infiltrating myeloid cells whereas $CD3^{+}$ T cells accounted for the majority of infiltrating lymphocytes in CD200R1 knockout mice (**Figures 4-10C-D**). The total number of all leukocyte subsets in the brain was higher in CD200R1 knockout mice. The ratio of infiltrating lymphocytes-to-peripheral myeloid cells was lower in the ischemic brain of CD200R1 knockout mice (**Figures 4-10E-F**). The number of peripheral myeloid cells present in the ischemic brain at day 7 positively correlated with neurological deficit score (**Figure 4-10G**). Interestingly, although CD200R1 knockout mice showed a significant increase in $CD45^{intC}D11b^{+}$ microglia counts one week after stroke (**Figure 4-11A**, p=0.039), there were no differences in either cell size (**Figure 4-11B**) or cellular granularity (**Figure 4-11C**), two characteristic features of microglia activation. These findings suggest that CD200R1 signaling regulates the entry of leukocytes into the ischemic brain, potentiating the delayed recruitment of peripheral myeloid cells. While the prolonged presence of these cells is associated with worse neurological function, the contribution of resident microglia to these outcomes appears to be minimal.

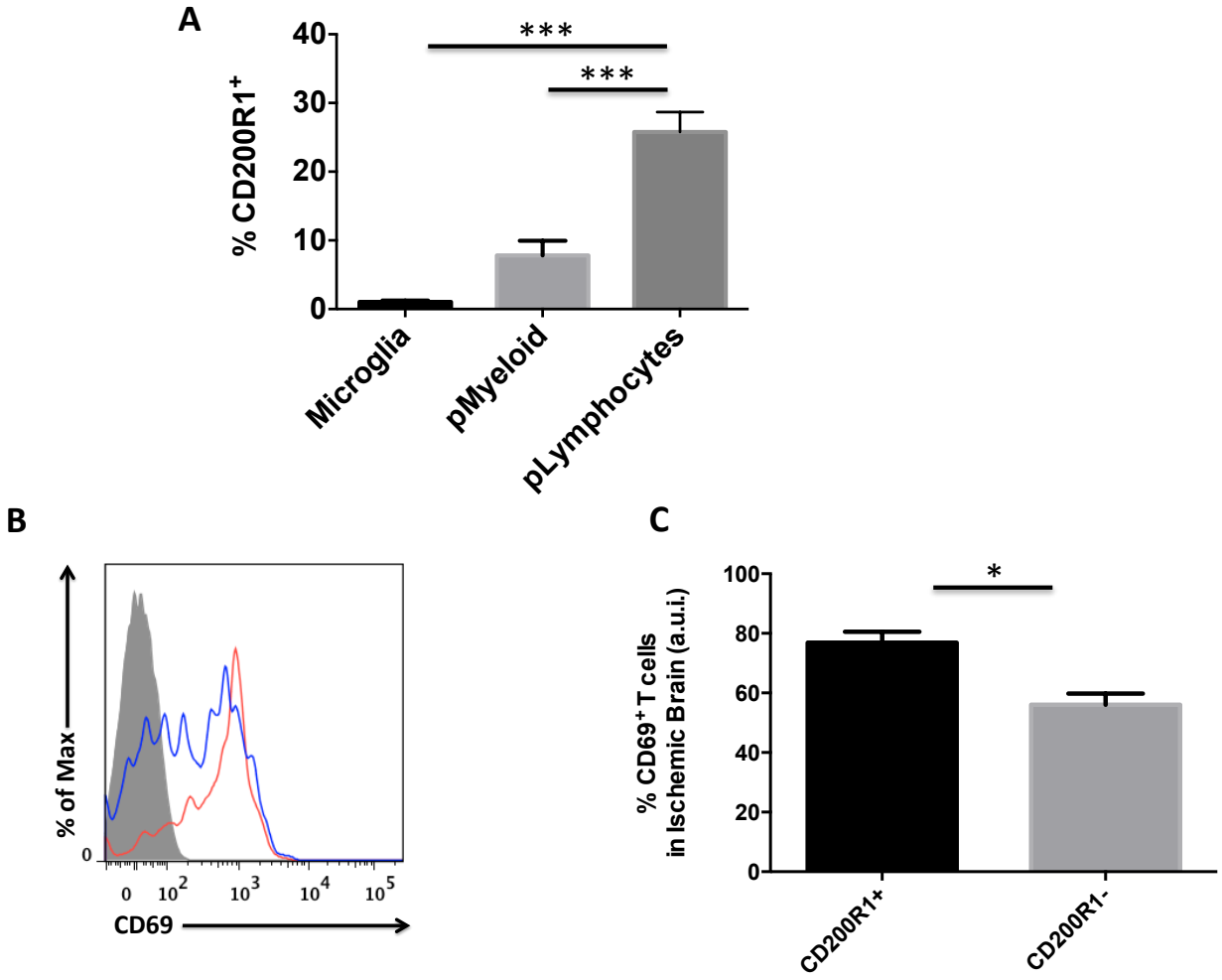

Figure 4-9. Surface expression of CD200R1 on leukocyte subsets in the ischemic brain at 7 days.

The percentage of CD200R1-positive leukocyte populations in the ischemic brain was determined (A). A representative histogram shows the relative expression level of CD200R1-positive (red) and CD200R1-negative (blue) T cells (B). The percentage of CD69-positive T cells for each subset was subsequently quantified (C). Cell-specific FMO controls were used to determine positive gating (shaded gray). For all experiments, N=4-7/group. Error bars show mean SEM. Abbreviation: SEM standard error of mean, p peripheral, Max maximum. *p≤0.05; **p≤0.01; ***p≤0.001

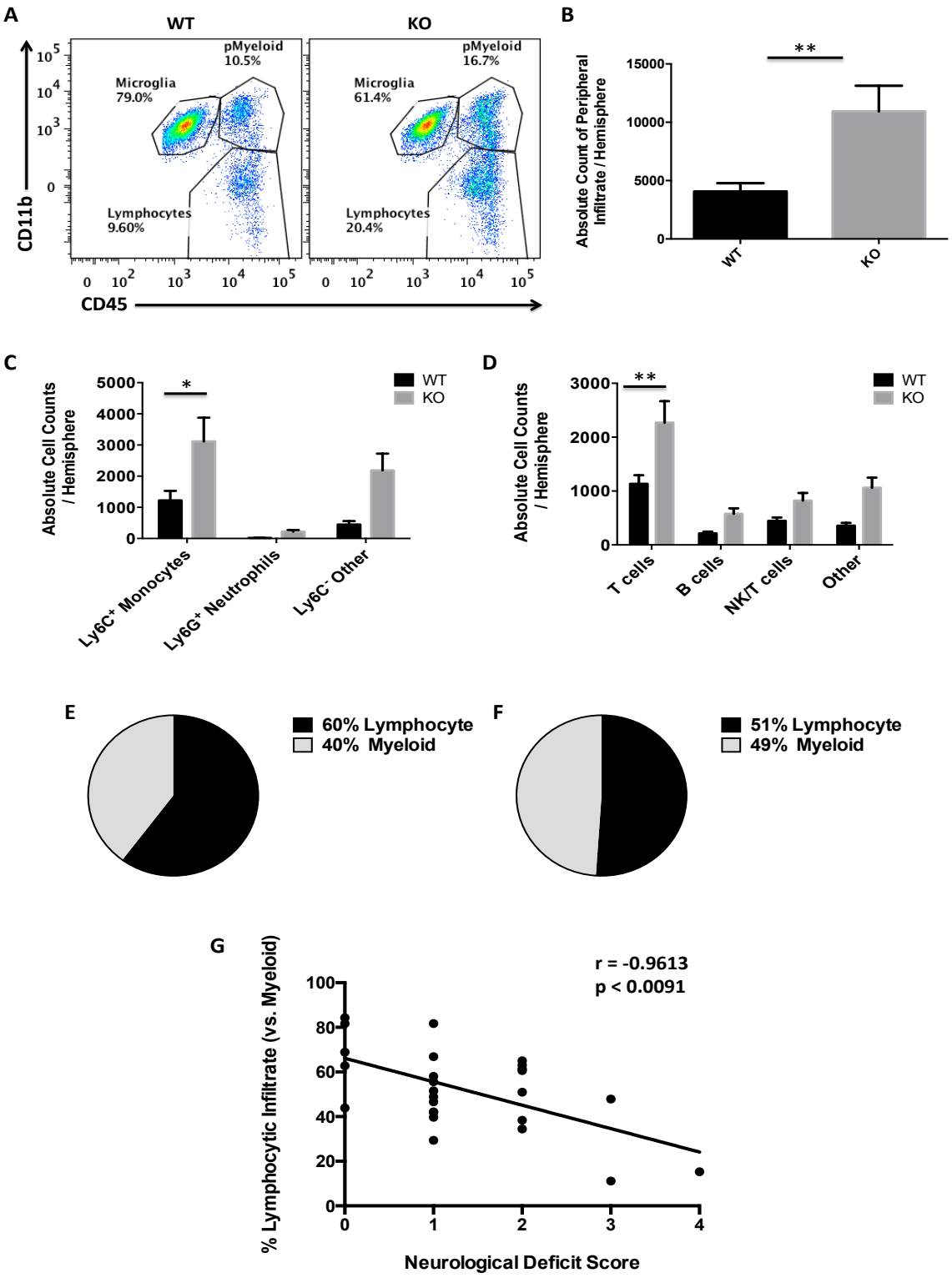

Figure 4-10. (Legend on following page)

Figure 4-10. Effect of CD200R1 deletion on post-acute inflammatory response in ischemic brain.

A representative dot plot depicts the infiltrating leukocytes in the ischemic hemisphere of CD200R1 wildtype and knockout mice at 7 days (A). The overall number of $CD45^{hi}$ peripheral leukocytes was quantified (B). The absolute counts of infiltrating myeloid (C) and lymphocyte (D) subsets were quantified. The relative composition of the brain infiltrate was determined for CD200R1 wildtype (E) and knockout (F) mice (N=12/group). Correlation analysis between lymphocyte (or myeloid) cell count in the ischemic brain and neurological deficit score (G). For all experiments, N=12/group. Cell-specific FMO controls were used to determine positive gating. Error bars show mean SEM. Abbreviation: SEM standard error of mean, WT wildtype, KO knockout. *p≤0.05; **p≤0.01; ***p≤0.001

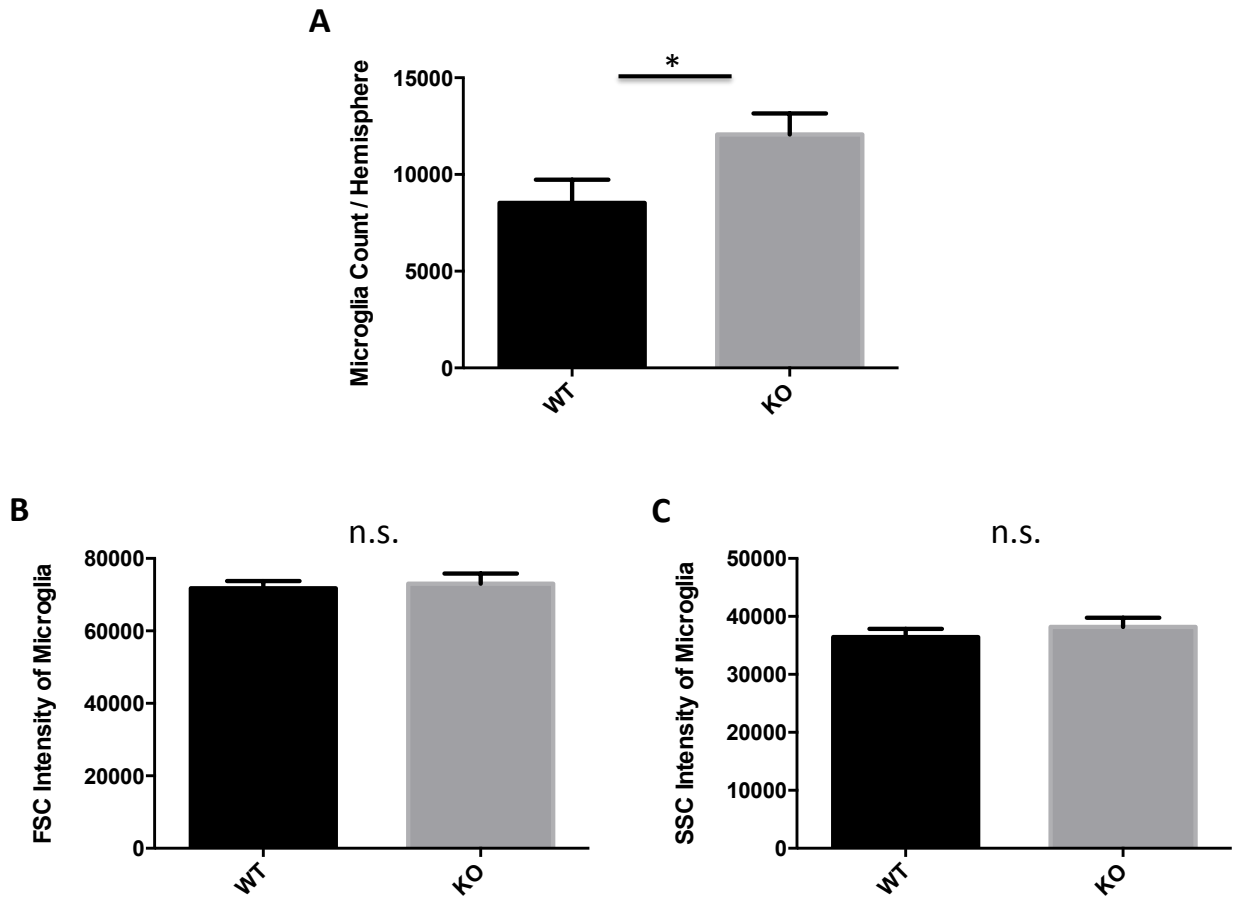

Figure 4-11. CD200R1-mediated changes in post-acute activation of microglia after stroke.

The absolute number of microglia in the ischemic hemisphere at 7 days after stroke was quantified (A). To determine changes in cell size and granularity, the mean intensity of forward (B) and side (C) scatter intensity was quantified (N=12/group). Error bars show mean SEM. Abbreviation: SEM standard error of mean, FSC forward scatter, SSC side scatter, WT wildtype, KO knockout, n.s. not significant. *p≤0.05; **p≤0.01; ***p≤0.001

Lack of CD200R1-mediated inhibition results in exacerbated peripheral immune dysfunction at 7 days after stroke

The peripheral immune response to stroke was first assessed using multiplex ELISA. Out of a panel of 24 targets, we found the plasma concentrations of six cytokines to be altered in CD200R1 knockout mice following stroke. The concentration of TNF was significantly increased in CD200R1 knockout mice at 7 days (**Figure 4-12A**, p=0.05), whereas the concentrations of the anti-inflammatory molecules IL-10 and IL-13 were decreased (**Figure 4-12C**, p=0.002 and **Figure 4-12D**, p=0.02, respectively). CD200R1 knockout mice had significantly lower levels of circulating vascular endothelial growth factor (**Figure 4-12F**, p=0.03), and attenuated levels of IFNγ and IL-17A (**Figure 4-12B**, p=0.05 and **Figure 4-12E**, p=0.002, respectively). To determine whether these alterations in plasma cytokine concentrations were associated with changes in the adaptive immune compartment after stroke we performed a phenotypic analysis of T cells in the blood. A significant increase in lymphopenia was found in CD200R1 knockout mice at 7 days (**Figure 4-13A**, p=0.05). The percentage of circulating $CD4^+$ T cells with effector memory phenotype was dramatically increased in CD200R1 knockout mice compared to wildtype controls (**Figure 4-13B-C**, p=0.05). We performed an analysis of TCR vβ usage using monoclonal antibodies specific to 15 vβ families and found that $CD4^+$ T cells from CD200R1 knockout mice exhibited greater shrinkage in their TCR vβ repertoire after stroke (**Figure 4-13D**). Expression of the early TCR activation marker CD69 was also significantly increased on $CD4^+$ T cells from CD200R1

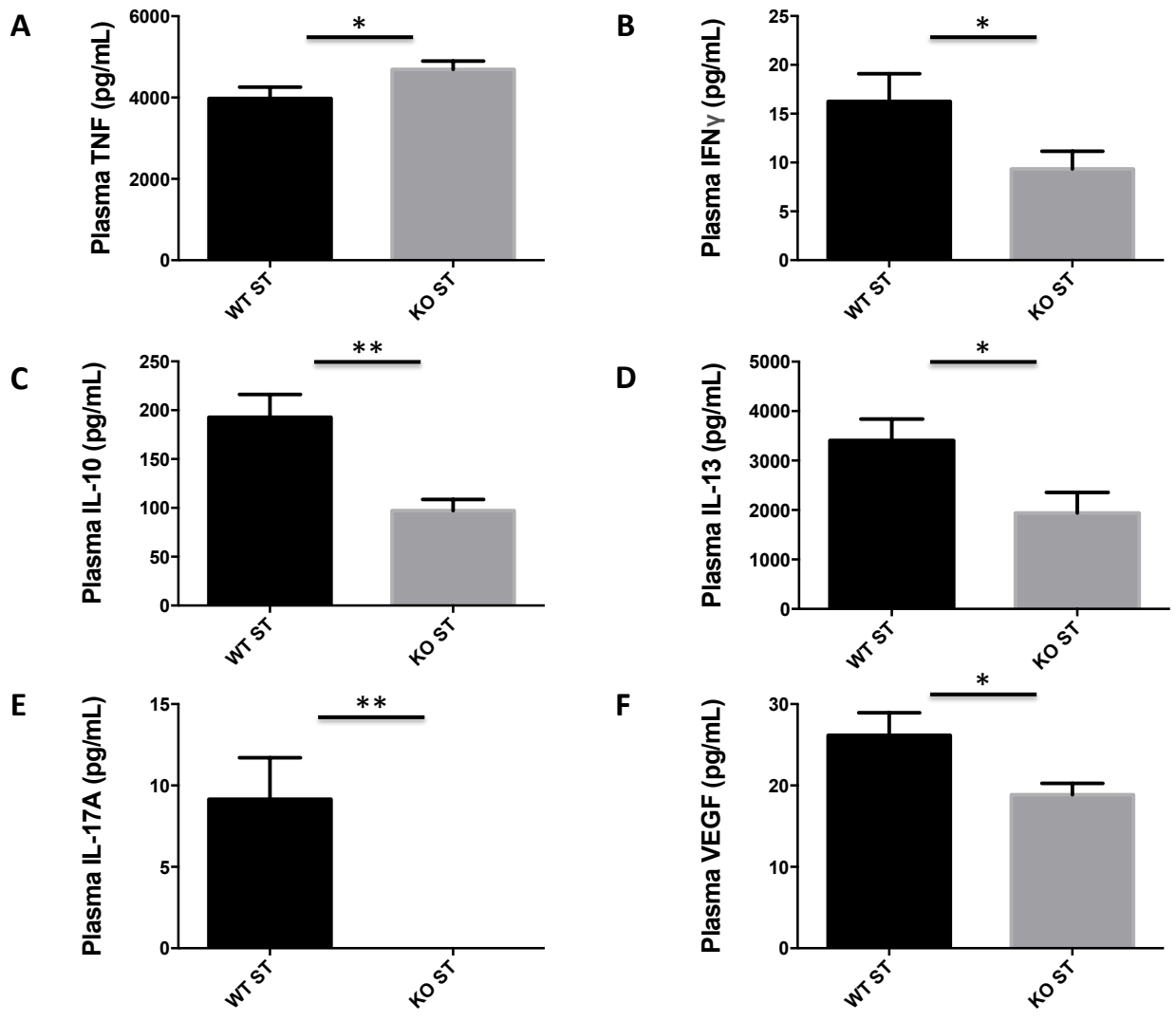

Figure 4-12. Plasma cytokine concentrations in CD200R1 wildtype and knockout mice after stroke.

Plasma concentrations of TNF (A), IFNγ (B), IL-10 (C), IL-13 (D), IL-17A (E), and VEGF (F) are quantified in CD200R1 wildtype and knockout mice at 7 days after stroke (N=9/group). Error bars show mean SEM. Abbreviation: SEM standard error of mean, WT wildtype, KO knockout, ST stroke, TNF tumor necrosis factor, IFNγ interferon gamma, IL-10 interleukin-10, IL-13 interleukin-13, IL-17A interleukin-17A, VEGF vascular endothelial growth factor. *p≤0.05; **p≤0.01; ***p≤0.001

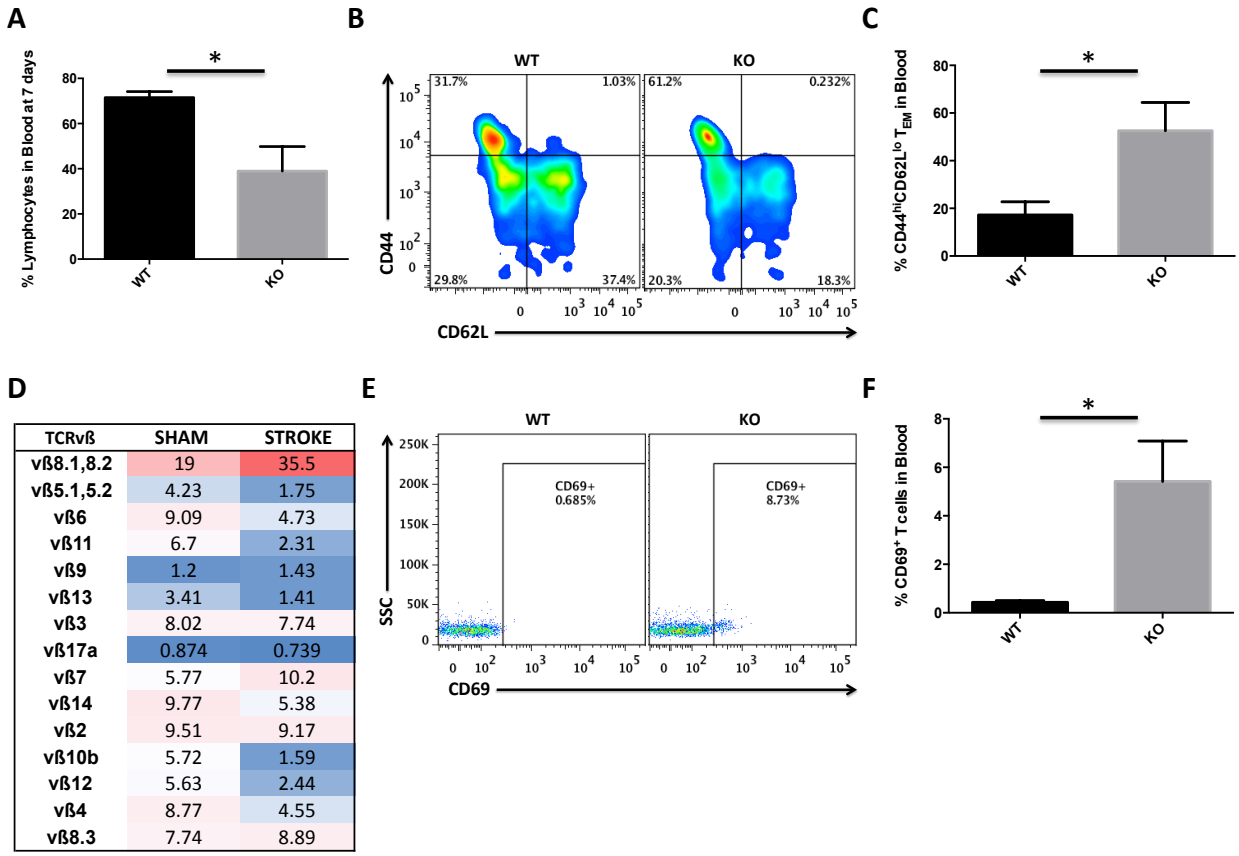

TCRvß	SHAM	STROKE
vß8.1,8.2	19	35.5
vß5.1,5.2	4.23	1.75
vß6	9.09	4.73
vß11	6.7	2.31
vß9	1.2	1.43
vß13	3.41	1.41
vß3	8.02	7.74
vß17a	0.874	0.739
vß7	5.77	10.2
vß14	9.77	5.38
vß2	9.51	9.17
vß10b	5.72	1.59
vß12	5.63	2.44
vß4	8.77	4.55
vß8.3	7.74	8.89

Figure 4-13. Altered peripheral T cell compartment in CD200R1 knockout mice after stroke.

The percentage of lymphocytes (versus myeloid cells) in the blood was quantified at 7 days after stroke. A representative smoothened dot plot shows the percentage of $CD4^+$ T cells with $CD44^{hi}CD62L^{lo}$ effector memory phenotype in the blood (B) and the quantification is shown (C). A representative heat map analysis of 15 TCR vβ families was performed highlighting the narrowing in TCR vβ repertoire of $CD4^+$ T cells in the blood at 7 days after stroke in CD200R1 knockout mice (D). A representative dot plot is shown of CD69-expressing $CD4^+$ T cells in the blood at 7 days (E). The percentage of CD69-positiive $CD4^+$ T cells in the blood was quantified (F). For all experiments, N=5-7/group. Cell-specific FMO controls were used to determine positive gating. Error bars show mean SEM. Abbreviation: SEM standard error of mean, WT wildtype, KO knockout, SSC side scatter, TEM T cell effector memory, TCRvβ T cell receptor variable beta chain region. *p≤0.05; **p≤0.01; ***p≤0.001

knockout mice after stroke (**Figure 4-13F**, p=0.032). These results imply that the peripheral immune environment of mice lacking CD200R1-mediated inhibitory function is generally more pro-inflammatory and likely less capable of mounting an effective response to novel antigenic stimuli, such as a post-stroke infection.

CD200 protein expression is exaggerated after stroke with advanced age

The finding that neuroinflammation was augmented in mice lacking CD200R1 led us to speculate that changes in CD200 expression in the brain may be associated with the gradual increase in CNS inflammation with age, as well as with the exacerbated inflammatory responses found in age-related injuries. We found that there is a significant reduction in CD200 protein expression in normal aged brains compared to their young counterparts (**Figure 4-14A**, p=0.002). Following 90 minutes of MCAO and 72 hours post-reperfusion, a significant decrease in brain CD200 protein levels was seen in aged, but not young mice (**Figure 4-14B**). Although overall levels did not change in the young brain after stroke, increased astrocytic expression of CD200 was observed using immunohistochemistry (**Figure 4-14C**). The decrease in aged brain expression of CD200 following stroke, was accompanied by a dramatic increase in soluble CD200 protein circulating in the plasma (**Figure 4-14D**). These data indicate a potential role for CD200R1 immune-inhibitory signaling in mediating both chronic pro-inflammatory responses in the brain and aggravated peripheral immunosuppression more commonly associated with older mice after stroke.

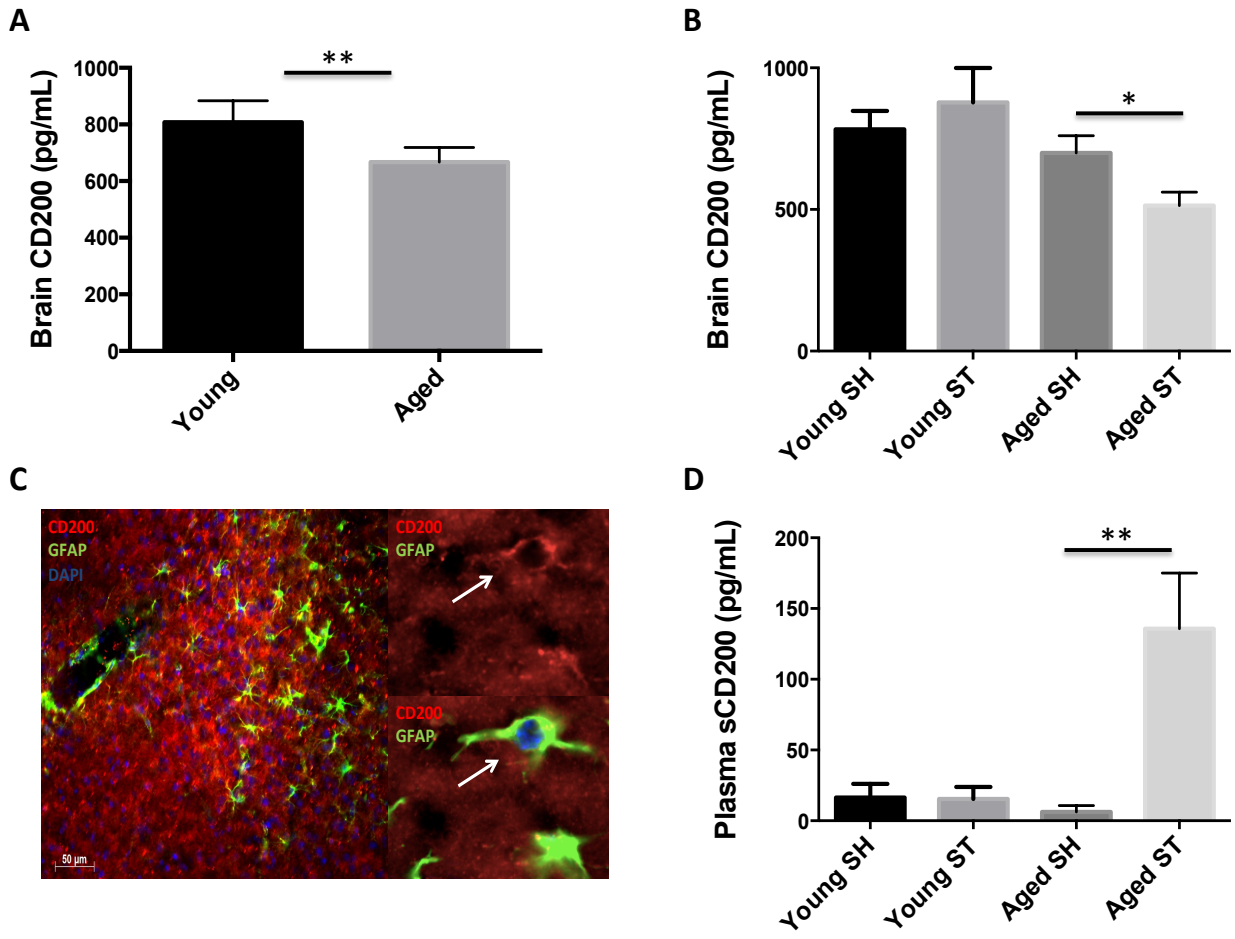

Figure 4-14. CD200 protein concentrations in the brain and plasma of young and aged wildtype mice at 72 hours after stroke.

The concentration of CD200 protein in the brain of naïve young and aged wildtype mice was measured by ELISA (A; N=12/group). CD200 levels in the brain were determined for young and aged, sham and stroke mice at 72 hours after stroke (B; N=5-9/group). A representative 40um-thick brain tissue section depicting areas of enhanced CD200 expression (red) surrounding DAPI-positive (blue) $GFAP^{+}$ astrocytes (green) in the grey matter of the young ischemic cortex at 72 hours (C; N=3-4/group). Plasma concentrations of soluble CD200 in young and aged, sham and stroke mice are shown (D; N=9-14/group). Error bars show mean SEM. Abbreviation: SEM standard error of mean, DAPI 4',6-diamidino-2-phenylindole, GFAP glial fibrillary acidic protein, SH sham, ST stroke. *p≤0.05; **p≤0.01; ***p≤0.001

Discussion

In this study, we provide several pieces of evidence to support the hypothesis that (1) CD200-CD200R1 interactions regulate T cell entry and activation in the brain; (2) function to attenuate brain inflammation and peripheral immune dysfunction following experimental stroke; and (3) are critical for survival and behavioral recovery after stroke. Previous work identified the CD200-CD200R1 signaling axis a major regulator of microglial homeostasis in the healthy and diseased CNS [19,280]. Neuronal-microglial interactions are believed to impart a unidirectional immune-inhibitory signal that suppresses microglia activation and contributes to the immune-privileged status of the CNS [109]. Our work identifies a novel role for CD200R1 in regulating the homeostatic entry of immune-surveillant, effector memory T cells into tertiary tissues, including the CNS. We show for the first time that CD200R1 inhibitory signaling is critical for attenuating brain inflammation and peripheral immune dysfunction after ischemic stroke, as well as promoting survival and behavioral recovery. These findings implicate CD200-CD200R1 immunoregulatory pathway as a novel target for protection from CNS damage in experimental stroke.

The working theory that neuronal-glial interactions function to suppress microglia activation and maintain CNS homeostasis via a constitutively active inhibitory mechanism provides an intriguing explanation for the brain's unique immune privileged status. Moreover, several studies support the notion that after injury these interactions are disrupted, releasing the brake on inflammation. This concept is of translational interest because it implies that chronic inflammation is potentially amenable to

intervention in such a manner that restores homeostasis by enhancing neuronal-glial interactions. Given that this theory is well established in the scientific literature, it is noteworthy that we did not detect surface expression of CD200R1 protein on adult microglia. Despite this surprising finding, it is entirely consistent with the primary literature. Several studies have reported that CD200R1 protein expression in the healthy brain is too weak to detect with western blot and can only be visualized via immunohistochemistry using a signal amplification kit [281]. CD200R1 protein expression is virtually absent in rodent and human microglia [22,84,109,259,282]. Low expression of CD200R1 on microglia has been attributed to receptor down-regulation in response to high levels of neuronal CD200 in the CNS [283]. Although little CD200R1 protein is present on the microglial surface, FACS sorted microglia confirmed the presence of CD200R1 transcript in these cells [109]. Others have reported that CD200R1 gene expression is significantly lower in human microglia than in human blood macrophages [259]. Localization patterns of CD200R1 staining were very distinct, showing high expression on perivascular macrophages in both grey and white matter. Microglial CD200R1 immunoreactivity was not detected in human CNS tissue. These findings are consistent with a recent study by Shrivastava et al (2012) [281] which found no CD200R1-expressing microglia in nervous tissue except in periventricular white matter regions. Instead, they had shown that CD200R1 expression was prominent on perivascular macrophages located in the pial meninges, the ventral lining of lateral ventricles, and surrounding blood vessels in the cortex and hippocampus. In line with this finding, Melief and colleagues (2012) [84] showed that CD200R1 protein expression was highly expressed in choroid plexus macrophages, but virtually absent on human white matter

microglia. We also noted higher expression of CD200R1 on $CD45^{hi}Ly6C^{+}$ perivascular macrophages in the un-injured brain; however, unlike Denieffe S and colleagues (2013) [280] we did not find that these cells were increased in number in CD200R1-deficient brains. Taken together, the lack of surface CD200R1 expression on microglia likely explains our finding that CD200R1-deletion had minimal impact on the microglia compartment. Our work is supported by previous studies that have reported no differences in the number of microglia in the normal brain of CD200 knockout mice [22,280]. Moreover, previous work demonstrated that CD200-deletion had no effect on the secretion of TNF, IL-1b, and IL-6 in un-stimulated glia cultures [21]. After stimulation, however, several studies have noted increased microglia proliferation and exaggerated cytokine production [21,22]. We also observed a similar increase in microglia proliferation after stroke in mice lacking CD200R1, although this could not be attributed to any change in the physical properties of these cells with respect to wildtype controls. In sum, the absence of functional CD200R1 protein in microglia is consistent with the null phenotype found in CD200- and CD200R1-knockout mice. These findings suggest that CD200R1-mediated inhibition of microglia is dispensible for keeping them in a quiescent state, at least under normal conditions.

Expression of CD200R is mainly restricted to cells of the myeloid lineage, however several studies have reported CD200R1 expression on lymphocytes [255,284-286]. CD200R1 is expressed on T cells after TCR activation and upon chronic activation [284,286]. The progressive acquisition of CD200R1 expression coincides with effector cytokine secretion and is found in both Th1 and Th2 subsets. Our finding that CD200R1 expression is confined to the effector memory population is consistent with

these earlier studies. Moreover, our finding that CD200R1-deficient brains have substantially increased numbers of T cells with effector memory phenotype suggest that these cells are in activated state. Thus, it is of potential importance that CD200R1 is expressed on T cells in the healthy brain, and therefore conceivable that the interaction between CD200-positive neurons (and endothelial cells) functions to prevent the activation and extravasation of these cells into the CNS parenchyma. This event would contribute to the maintenance of the immune privileged status of the CNS, in a microglia-independent manner, by limiting the number of T cells surveying the brain at the level of the blood-brain barrier.

Immune-surveillant T cells in the CNS are believed to be tolerized to self-antigen, however it is not known whether the CNS-specific T cells in CD200R1-deficient mice are similarly tolerant. Previous work has shown that CNS-irrelevant (OVA-specific) T cells may enter the brain, cause blood-brain barrier leakiness, but no glial pathology [287]. Indeed, the lack of overt microglia activation or behavioral deficits under normal conditions suggests that these cells may not be deleterious under normal conditions. In the absence of CD200 engagement, T cells are likely more resistant to inhibition at the level of the endothelium and to become chronically activated upon entering the CNS. We demonstrated that immune-surveillant CD8 T cells in CD200R1-deficient mice had significantly higher TNF expression, but greatly diminished IFNγ expression. These findings are consistent with other work showing that CD200-CD200R1 interactions are critical for preventing pathological T cell responses during influenza infection [288,289]. Another study demonstrated that TNF production was increased in splenocytes from CD200R1-deficient mice and that CD200-mediated suppression of graft rejection

requires CD200R1^{+} responder T cells [261]. These data indicate that inhibitory signaling is required to abrogate T cell activation and prevent dysregulated responses to injury and infection. Further studies will be needed to determine the functional role of immune surveillant T cells in the healthy CNS and if they represent a viable therapeutic target.

While there is continuous surveillance of CNS antigens in peripheral lymphoid tissue, antigen-specific T cells do not generally accumulate in CNS tissue in the absence of neuroinflammation [290]. Our finding that there is a higher accumulation of T cells in the normal brain of CD200R1-deficient mice implies there is underlying inflammation. Indeed, blood-brain barrier permeability was found to be increased in naïve CD200-deficient mice [280]. Our findings do not exclude this as a potential explanation for the accumulation of lymphocytes in the CD200R1-deficient CNS, however, leukocyte extravasation is not a passive process, but rather an active one and our results indicate that entry is limited specifically to T cells. In support of this view, the same study showed that CCL2 and IP-10 expression is up-regulated in the brain of CD200-deficient mice. These chemokine signals may facilitate the recruitment of circulating T cells. Moreover, CD200-CD200R1 interactions are involved in T cell adhesion to the endothelium but not macrophages [291]. A recent study found that CD200R1 inhibitory signaling is important in regulating local T cell influx into the ischemic limb, but had no effect on macrophage transmigration [292]. Taken together, CD200-CD200R1 interactions between T cells and the endothelium may function to suppress transmigration and maintain immune privilege in the healthy CNS. In this scenario, any disturbance (e.g., aging, injury) to the CD200-CD200R1 signaling axis would cause immune privilege to be broken. At this time it is not known whether

heightened CNS immune surveillance is predictive of CNS integrity and brain function or if it represents an epiphenomenon. However, our study would suggest that T cell accumulation in the CD200-deficient brain predisposes these mice to have worsened outcomes following injury.

We demonstrated that the CD200-CD200R1 inhibitory signaling pathway is critical for quelling immune cell activation and mitigating transmigration into the brain after stroke. Inflammation plays an important role in the pathogenesis of stroke and other forms of ischemic brain injury [293]. The restoration of brain function after stroke is dependent on the attenuation of inflammatory processes that trigger cell death. Mounting evidence highlights the detrimental impact of chronic inflammation on neuroplasticity and long-term recovery following stroke [2]. We hypothesized that neuroinflammation would be sustained in the absence of inhibitory signals. Although our results unequivocally implicate CD200R1 as a master regulator responsible for slowing the progression of inflammation in the brain after stroke, the cellular basis for this action is not clear. We reported that lymphocytes were the predominant CD200R1-expressors in the ischemic brain at day 7 and that CD200R1$^+$ T cells exhibited a higher level of activation than their CD200R1-negative counterparts. Interestingly, however, similar fold-increases in infiltrating monocyte number were also found in knockout mice and those with higher myeloid-to-lymphocyte ratios had worse outcomes. Previous work has shown that CD200R1 activation suppresses macrophage migration in part by down-regulating expression of the adhesion molecules LFA-1 and VLA-4 [258]. This is consistent with other studies that have reported increased macrophage numbers in both sterile and autoimmune models of brain injury [19,112]. To this end, our observation that

microglia proliferation is increased in CD200R1-deficient mice may reflect accelerated glial scarring. Together, these data imply that CD200R1 signaling may be more powerful in myeloid cells under inflammatory conditions. However, we cannot exclude the possibility that activated T cells potentiate the recruitment and polarization of macrophages.

The results presented in this study bare a striking resemblance to that reported for another immune inhibitory receptor, programmed death-1. Ren X et al (2011) [294] found that PD-1 was up-regulated on macrophages and lymphocytes in the CNS at 96-hours after MCAO. Moreover, deletion of PD-1 resulted in increased infiltration of inflammatory cells into the ischemic brain and augmented cytokine production by peripheral T cells. Ischemic stroke is increasingly recognized as a systemic disease rather than being confined only to a brain lesion [295-298]. Indeed, while acute stroke patients may survive the initial brain insult, infections are the most common cause of morbidity and mortality in the stroke survivor[299-302]. We demonstrated that CD200-CD200R1-mediated regulation of immunity is essential for survival and improved behavioral recovery following stroke. Nearly half of all mice lacking CD200R1 inhibitory signaling did not survive. Although the exact cause of death is not clear, CD200R1-deficient mice exhibited severe weight loss and exacerbated peripheral immune dysfunction. These changes were accompanied by deficits in thermoregulation, neurological function, and impaired motor balance and coordination. Our findings are consistent with other studies that have found CD200-CD200R1 interactions to be essential for attenuating disease progression in the CNS [19,258,283]. CD200R1-deficient mice were found to have an increase in the level of circulating pro-inflammatory factors

and a reduction in anti-inflammatory mediators. Interestingly, we found that CD200R1-deficient mice experience more severe lymphopenia after stroke. A large proportion of CD200R1-defecient T cells acquired an effector memory phenotype, which likely occurred via lymphopenia-induced homeostatic proliferation of existing memory populations or by antigen-driven conversion [303]. Coincident with these changes, we demonstrated that T cells in the blood of CD200R1-deficient mice had a narrowing of the TCR repertoire after stroke. A recent spectratype analysis has shown that clonal expansions of T cells are present in the brain at 7 days after stroke, and to a lesser extent in spleens and lymph nodes [278]. Given that lymphopenia is a prominent feature of stroke and that the majority of infiltrating T cells in the ischemic brain have an effector memory phenotype, it is conceivable that the purported clonal enrichment of T cells in the brain after stroke is a result of the stochastic entry of memory populations that arise from antigen-independent, cytokine-driven homeostatic proliferation rather than a directed autoimmune response to CNS antigen. Although infarct volume is a major determiner of post-stroke immune cell function and susceptibility to infection [304], it is interesting to note that despite having significant T cell dysfunction, CD200R1-deficient brains did not have greater tissue damage, suggesting an important role for inhibitory signaling in regulating the amplitude of peripheral immune responses to stroke. Whether CD200R1-deficient mice display a heightened susceptibility to spontaneous infection following stroke is not clear. It is important to note that the immunosuppressive effects of CD200 are critical to the long-term tolerance and survival of tissue allografts, and is associated with successful outcome of pregnancy [305,306]. Surprisingly, CD200 ablation did not appear to ameliorate post-stroke immune suppression. The paradoxical

role of CD200R1 inhibitory signaling in regulating the peripheral immune environment after stroke is an area that requires further exploration.

Our data show that the regulation of CD200 expression is sensitive to the effects of brain aging. These results are supported by previous work showing CD200 gene expression is decreased in the hippocampus of older mice [307,308]. The age-related reduction in brain CD200 levels may underlie the steady increase in basal inflammatory responses that occurs with age [55]. Although the spatial distribution of CD200 in the aging brain was not assessed, it is possible that the reduction in gray matter volume associated with aging accounts for this decrease [309,310]. Indeed, CD200 expression is diminished in the hippocampus and inferior temporal gyrus of Alzheimer's patients [259]. Moreover, CD200-fusion protein attenuates age-related decreases in LTP, whereas LPS-induced deficits in LTP are exacerbated in CD200-deficient mice [21,113]. CD200-Fc was also shown to attenuate the age-related increase in brain expression of CCL2 and IP-10, implicating CD200R1 as a potential regulator of leukocyte entry in the normal aging CNS [113]. As the integrity of the CD200-CD200R1 signaling axis becomes compromised with age, a concurrent loss of immune privilege and increase in inflammatory mediators may contribute to age-related deficits in brain function. Our finding that CD200 brain protein is significantly decreased at day 3 in the brain of aged mice after stroke, but not young, further strengthens this concept. Our laboratory has previously shown that glial scar formation is exacerbated in older mice after stroke [275]. Thus, it is interesting to note that CD200R1-deficient mice showed a significant increase in microglia proliferation by day 7. This injury-related loss of neuronal CD200 likely contributes to chronic inflammatory responses observed in aged mice [311]. Although

young mice did not exhibit a significant reduction in total brain levels of CD200 at 72 hours, physical disruption of CD200-CD200R1 interactions resulting from neuronal injury presumably account for any loss in immunoregulation. A related study demonstrated that CD200 gene expression is decreased in the ischemic core beginning at 24 hours and returned to baseline after day 7 [23]. While this study did not assess changes in CD200 protein expression, we would predict that due to the increased level of necrosis in the ischemic core, the loss of neurons would likely precipitate a decrease in CD200. Furthermore, we showed that CD200 was up-regulated on reactive astrocytes in young ischemic brain, potentially offsetting any change in overall expression. These findings are consistent with other work showing regional induction of CD200 in astrocytes found in chronic active plaques centers of multiple sclerosis patients and point to a potentially important role for astrocytes in ramping down chronic inflammatory responses [107,109].

Perhaps most strikingly, aged mice exhibited a dramatic increase in circulating soluble CD200 levels following stroke. These results point to a novel mechanism of peripheral immune suppression in which circulating CD200 down-regulates the normal adaptive function of lymphocytes and dendritic cells. More importantly, if this increase in soluble CD200 emanates from dying neurons in the ischemic brain, it would establish a critical link between brain injury and peripheral immune suppression. Indeed, infarct volumes positively correlate with immunosuppression status after stroke [304]. Aged mice also have higher mortality following traumatic CNS injury and are more immunosuppressed than young mice who sustain comparable injuries [312]. The suppressive effects of soluble CD200 are evidenced by its ability to enhance

engraftment of skin and cardiac allografts [313]. It remains to be seen whether soluble CD200 would serve as a useful prognostic marker for brain injury, or if anti-CD200 blockade is a viable approach to attenuating post-stroke immune suppression in older subjects.

To our knowledge, this is the first study to investigate the functional effect of ablating CD200R1 immune-inhibitory signaling in the CNS. Given that the CD200 receptor family has several isoforms, in which all (CD200R2-4) but one (CD200R1) are activating receptors that lack inhibitory motif-bearing proteins, the advantage of using transgenic mice containing a genetic deletion of CD200R1 rather than CD200 is that any observed effect is a result of the absence of inhibitory signaling rather than a combination of activating and inhibitory functions [25,314]. For example, CD200R3 is expressed in basophils and mast cells and cross-linking of CD200R3 induces degranulation and production of IL-4, respectively [315]. The phenotypic similarities in the neuroinflammatory state between CD200- and CD200R1-deficient mice imply that the functional role of the activating CD200R family members may be negligible [25,280]. We did not observe CD200R3 staining of adult microglia, however its expression after stroke and that of the other activating family members (CD200R2 and CD200R4) deserves further study before a complete interpretation can be made.

In conclusion, our observations provide new insights into the contribution of the CD200-CD200R1 inhibitory pathway to immune privilege and the progression of chronic and systemic inflammation following stroke. We propose a revision to the current framework of the CD200 hypothesis to include interactions involving T cells and inflammatory monocytes. It is believed that inhibitory receptors such as CD200R1

evolved as a general strategy to prevent autoimmunity while closely homologous activating receptors are busy combating pathogens [316]. The compensatory increase in inhibitory receptor expression on the surface of chronically activated immune cells implies that this system can be exploited to ameliorate inflammation and restore homeostasis. To this end, our findings suggest that agents that can target the CD200-CD200R1 signaling axis may hold therapeutic potential for the treatment of chronic brain inflammation and peripheral immune depression following stroke.

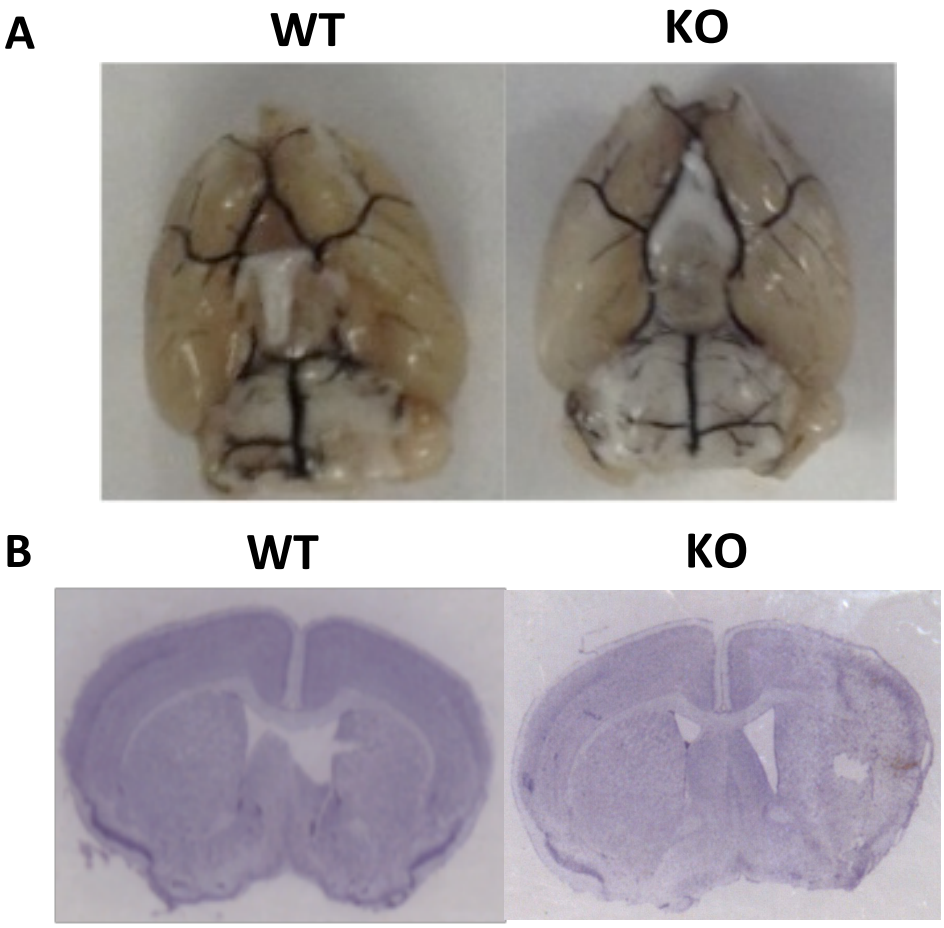

Supplemental Figure 4-1. CD200R1 deletion does not alter gross vasculature of normal brain or post-stroke atrophy.

A representative photograph of a healthy brain perfused with India ink shows no apparent difference in the gross vasculature of adult CD200R1 wildtype and knockout mice (A; N=4/group). Another representative image depicts no difference in cortical atrophy at 7 days after stroke as examined by cresyl violet staining (B; N=8-9/group). Abbreviation: WT wildtype, KO knockout.

Authors' Contributions

RMR and LDM conceived the project. RMR performed most of the experiments and JC, ARP, JG, BK, BF assisted with the flow cytometry preparations. RMR, JC and BK performed the behavioral experiments. RV assisted with the surgeries and statistical analyses. RMR and LDM wrote the paper. All authors read and made comments on the manuscript draft and approved the final manuscript.

Acknowledgements

This work was supported by National Institutes of Health grants R21 NS082906-02 (Louise D. McCullough), R21 NS076293-01A1 (Louise D. McCullough), and F31 NS083244-01A1 (Rodney M. Ritzel).

Chapter 5:

Age- and location-related changes in microglia function

Rodney M. Ritzel[1], Anita R. Patel, Sarah Pan, Joshua Crapser, Matthew D. Hammond, Evan R. Jellison & Louise D. McCullough

This chapter was published in its present form in Neurobiology of Aging; 2015 Jun; 36(6): 2153-106.

Abstract

Inflammation in the central nervous system (CNS) is primarily regulated by microglia. No longer considered a homogenous population, microglia display a high degree of heterogeneity, immunological diversity and regional variability in function. Given their low rate of self-renewal, the microenvironment in which microglia reside may play an important role in microglial senescence. This study examines age-related changes in microglia in the brain and spinal cord. Using ex-vivo flow cytometry analyses, functional assays were performed to assess changes in microglial morphology, oxidative stress, cytokine production, and phagocytic activity with age in both the brain and spinal cord. The regional CNS environment had a significant effect on microglial activity with age. Blood-CNS barrier permeability was greater in the aging spinal cord compared to aging

brain; this was associated with increased tissue cytokine levels. Aged microglia had deficits in phagocytosis at baseline and following stimulus-induced activation. The identification of age-specific, high scatter microglia together with the use of ex-vivo functional analyses provides the first functional characterization of senescent microglia. Age and regional-specificity of CNS disease should be taken into consideration when developing immune-modulatory treatments.

Introduction

Microglia, the resident macrophages of the CNS, actively survey the environment and rapidly respond to homeostatic disturbances. Although microglial responses have been widely studied in the context of injury, changes in microglial phenotype or activation status may also occur under normal conditions. These responses may also vary depending on cues from the local microenvironment [317]. Microglial can have both pro-inflammatory (M1) and wound healing roles (M2) and their phenotype can vary in response to local cues (regional effects) and across the lifespan (aging effects) [318-320]. The brain and spinal cord are distinct CNS environments that serve very specialized functions [321]. However, the degree to which heterogeneity and immunological diversity is present in the microglial population in each area remains an understudied area of glial biology[322].

Regional differences also occur in the response to injury throughout the neuroaxis, with the spinal cord showing a more robust inflammatory response and a greater vulnerability to the detrimental effects of activated microglia [323,324]. For instance, spinal cord lesions produce greater microglia activation and more extensive leukocyte recruitment and blood-CNS barrier breakdown than comparable lesions to the cortex [325,326]. Additionally, injury to white matter results in significantly more inflammation compared to an equivalent injury to gray matter, and caudal regions of the CNS respond with greater microglial activation than forebrain regions after focal cytokine injections [323,327,328]. These findings suggest that the brain and spinal cord, because of their unique structural and functional organization, harbor microglial populations with distinct activation thresholds that are primed to respond differently to stimuli. As many CNS diseases are age-related and manifest in specific CNS regions (e.g., amyloid deposition in Alzheimer's), furthering our knowledge of microglial diversity will increase our understanding of the role played by microglia in the pathogenesis of disease.

Given that microglia have a low rate of self-renewal, the environment in which they reside likely shapes their identity over time. In addition, aging itself has profound effects on cells of the myeloid lineage. Earlier studies have shown microglia senescence is manifested by morphological changes and alterations in immunophenotypic expression and inflammatory profile [54,329-332]. A steady increase in the expression of markers that are up-regulated on young, activated microglia following acute CNS injury is seen at baseline in aged brain. These observations lead to the hypothesis that age-induced microglial dystrophy results in chronic inflammation, a dysregulated or uncontrolled response to injury, and poorer recovery. To better

understand the role played by microglia in age-related diseases, a clearer understanding of the effect aging on baseline microglia function is required. Age-related transitions from ramified to amoeboid morphology have been described [333], but much less is known regarding the functional importance of this phenotypic shift.

The present study examined the effect of aging on mitochondrial activity, reactive oxygen species generation, and phagocytic potential of microglia within the two main CNS compartments, the brain and spinal cord. We hypothesized that microglial identity and function is specified by the environment, and that aging impairs niche function. Our findings indicate that microglia in the aging brain and spinal cord have distinct immunological profiles. A significant enhancement of inflammatory cytokines and markers of oxidative stress, coupled with a loss of phagocytic function was seen, which was more profound in the aged spinal cord. These changes may explain why microglial subsets can differentially contribute to the etiology and pathology of age-related neurodegenerative disease.

Materials and Methods

Mice/Animals: C57BL/6J male mice 8-12 weeks (young adult; 31.5 ± 0.8 grams) and 20-22 months (aged; 37.8 ± 1.0 grams,) of age were pair-housed on sawdust bedding in a pathogen free facility (light cycle 12/12 h light/dark) with free access to chow and water. Animal procedures were performed in accordance with NIH guidelines for the

care and use of laboratory animals and approved by the Animal Care Committee of the University of Connecticut Health Center. All studies were performed blinded to age.

Tissue Harvesting: Mice were euthanized, transcardially perfused with 60 mL cold, sterile PBS, and the brains and spinal cords were harvested. The brainstem, cerebellum, and optic nerve were removed. The brain was then divided along the interhemispheric fissure into two hemispheres. Spinal cords were removed by flushing the spinal column with sterile PBS by hydrostatic pressure and subsequent rinsing with PBS to remove contaminant cells. Samples were then processed in a blinded fashion.

Flow Cytometry: Brains and spinal were placed in complete RPMI 1640 (Lonza) medium and mechanically and enzymatically digested in collagenase/dispase (1 mg/mL) and DNAse (10mg/mL; both Roche Diagnostics) for 1hr at 37C. The cell suspension was filtered through a 70um filter. Leukocytes were harvested from the interphase of a 70%/30% Percoll gradient. Cells were washed and blocked with mouse Fc Block (ebioscience) prior to staining with primary antibody-conjugated flourophores: CD45-eF450, CD11b-APCeF780, Ly6C-PerCP-Cy5.5, and SIRPα-PE. All primary-conjugated antibodies were purchased from eBioscience. For live/dead discrimination, a fixable viability dye, carboxylic acid succinimidyl ester (CASE-AF350, Invitrogen), was diluted at 1:300 from a working stock of 0.3mg/mL. Cells were briefly fixed in 2% paraformaldehyde (PFA). Data were acquired on a LSRII using FACsDiva 6.0 (BD Biosciences) and analyzed using FlowJo (Treestar Inc.). No less than 100,000 events were recorded for each sample. Fluorescence minus one (FMO) controls were used to

determine the positivity of each antibody. Microglia were identified as $CD45^{int}CD11b^{+}$. Subsequently, to ensure that the microglia population was pure, we excluded all $Ly6C^{+}$ bone marrow-derived myeloid populations with overlapping CD45 expression.

To study the phagocytic activity of microglia, fluorescent latex beads (Fluoresbrite Yellow Green (YG) carboxylate microspheres; 1um diameter; Polysciences) were added to freshly isolated microglia in a final dilution of 1:100 as described [207]. After 1-hour at 37°C in an air incubator, the cells were washed three times with FACS buffer, re-suspended in FACS buffer, stained for surface markers, and fixed in PFA (N=7/group). For beta-amyloid peptide and cell stimulation experiments, cells were incubated for 1hr in 37C water bath. Lyophilized fluorescein-labeled (synthetic human) beta-amyloid (1-42) was dissolved in DMSO to a final stock concentration of 500ug/mL (rPeptide, Bogart, GA, USA). This was further diluted 1:1 in PBS to obtain a working stock from which 1ul was added to every 100ul of sample and vortexed to mix. Cell Stimulation Cocktail containing phorbol 12-myristate 13-acetate (PMA) and ionomycin was purchased from eBioscience. Cells were treated with stimulation cocktail (500X) following the addition of phagocytic substrate and subsequently incubated (N=6/group).

To determine mitochondrial activity, MitoTracker Red CM-H2XRos (Life Technologies, Invitrogen; Ex/Em: 579/599), a reduced, nonfluorescent dye that fluoresces upon oxidation was used to stain mitochondria in live cells. Its accumulation is dependent upon membrane potential. Mitotracker was diluted in DMSO to a working concentration of 500nM, at a final volume of 300ul. Cells were incubated for 20 min at

37˚ C and subsequently washed three times with FACS buffer (without NaAz) to remove residual dye (N=6/group).

For detection of reactive oxygen species, microglial cells were incubated with redox-sensitive CM-H2DCFDA (5uM; Ex/Em: 495/520) fluorogenic cell-permeant dye (Life Technologies, Invitrogen). Cells were incubated for 20min at 37C, washed three times with FACS buffer (without NaAz), and then stained for surface markers including CASE (N=5-7/group).

For intracellular cytokine staining, an *in vivo* brefeldin A (BFA) protocol was followed. Briefly, 10mL/kg of BFA (Sigma, 0.5mg/mL in DMSO) was injected via tail vein. Ten hours later, animals were sacrificed and tissue was harvested as noted above. Prior to staining, 1ul of GolgiPlug containing brefeldin A (BD Biosciences) was added to 800ul complete RPMI and cells were incubated for 2h at 37C (5% CO2). Afterward, cells were re-suspended in Fc Block, stained for surface antigens and washed in 100ul of fixation/permeabilization solution (BD Biosciences) for 20 min. Microglia were then washed twice in 300ul permeabilization/wash buffer (BD Biosciences) and resuspended in an intracellular antibody cocktail containing TNF-PE-Cy7 (eBioscience), IL-1β-FITC (eBioscience) and MMP-9-PE (StressMarq Biosciences, Inc.) and subsequently fixed (N=5/group).

ImageStream data were acquired using the Amnis ImageStream Analyzer (Amnis Corporation, WA) equipped with the Amnis INSPIRE software.

Assessment of blood-brain barrier permeability: Two hours before the animals were euthanized, Evans blue (Sigma, 2% in isotonic saline, 4mL/kg) was injected

intraperitoneally. The animals were anesthetized and perfused with 60mL of cold sterile PBS. Spinal cords were syringe-flushed and brain hemispheres were harvested, rinsed with PBS and weighed. Samples were homogenized in 1 ml of PBS using a tissue homogenizer. An equal volume of 100% trichloroacetic acid (TCA) solution was added to each sample and incubated at 37$^{\emptyset}$C for 1 hr. Samples were then centrifuged at 24,000g for 20 minutes at 4$^{\emptyset}$C. The supernatant was plated 100ul per well in triplicate and colormetric absorbance was measured at 608nm (EnSpire 2300 Multilabel Reader, Perkin Elmer). For quantitative measurement of Evans blue leakage, the data was normalized to tissue weight and measured as a concentration (ug/mg tissue weight) of Evan's blue using a standard curve (Evan's blue in 50% TCA). Data were normalized to young brain and expressed as fold change.

Thirty minutes before the animals were euthanized 2ml/kg of a 10% sodium fluorescein (NaF) solution (Sigma) was injected and processed as above. For each sample, 100ul of supernatant was measured in triplicate at ex. 400nm/ em. 516nm. Values obtained from 30% TCA were subtracted from each sample to remove background.

ELISA cytokine measurement: Brain and spinal cord cytokine levels were determined by ELISA (Milliplex Cytokine Assay, EMD Millipore). Brains and spinal cords (n=5/group) were homogenized in ice-cold lysis buffer containing a protease inhibitor cocktail (Roche Diagnostics). Homogenates were sonicated and centrifuged at 4C for 15 min at 14,000 rpm, and supernatants were assayed for total protein using a BCA kit (Pierce, Thermo scientific). 100ug of each sample was loaded into each well in

duplicate. Samples were assayed according to the manufacturer's instructions using a Luminex 200 (Luminex Corporation, Austin, TX, USA) magnetic bead array platform. Inter-and intra-assay coefficients of variation were than less than 10%.

RNA isolation and qPCR: Brain hemispheres and spinal cords were harvested and RNA was extracted using TRIzol Reagent (Invitrogen, Carlsbad, CA). -Gene expression was normalized relative to GAPDH expression. Primer sequences were as follows: GAPDH, forward: 5'-ACCACCATGGAGAAGGC -3', reverse: 5'-GGCATGGACTGTGGTCATGA -3'; CD47, forward: 5'-TGCGGTTCAGCTCAACTACTG-3', reverse: 5'-ACGATGCAAGGGATGACCAC-3'; TNFα, forward: 5'–GACCCTCACACTCAGATCATCTTCT-3', reverse: 5'-CCTCCACTTGGTGGTTTGCT-3'. PCR conditions were as follows: 95$^{\emptyset}$C for 10 min, followed by 40 cycles of 95$^{\emptyset}$C for 15 sec and 60$^{\emptyset}$C for 60 sec. Amplification reactions were performed in triplicate; relative expression levels were calculated from average threshold cycle number using the delta-delta Ct method. The absolute levels of the housekeeping gene GAPDH did not vary significantly with age, consistent with previous findings by Chen, et al. [334] and others [335].

Statistical Analyses: Data from individual experiments are presented as mean ± SEM and age- and region-matched CNS samples were assessed by 2-way ANOVA or one-way ANOVA with Bonferroni corrections for multiple comparisons (GraphPad Prism Software Inc, San Diego, CA, USA). Groups were compared with Student's t-test where appropriate. Significance was set at $p < 0.05$.

Results

Age- and location-related changes were seen in the physical properties and CD45/CD11b expression of microglia

To ensure that all microglia populations under investigation were living and pure, samples were examined by flow cytometry. We identified resident $CD45^{int}$ $CD11b^{+}Ly6C^{-}$ microglia as the predominant myeloid cell population in young and aged C57Bl/6 mouse brain and spinal cord (**Figure 5-1A**) using a defined gating strategy (**Supplemental Figure 5-1A**). We quantified the mean fluorescence intensity (MFI) for each marker. A significant interaction between age and location was seen for CD45 ($F(1,24)=P<0.05$) and CD11b ($F(1,24)=P<0.01$), resulting in an age- and location-dependent increase in expression, with spinal microglia showing highest levels (**Figures 5-1B and 5-1C**). Next we examined the physical properties of microglia using the mean forward scatter (FSC-area) and side scatter (SSC-area) values as relative measures of cell size and granularity, respectively. Spinal cord microglia were larger in size compared to brain microglia ($F(1,24)=P<0.05$), although both increased in size with age (**Figure 5-1E**). Side scatter values were significantly increased with age in both groups, showing a nearly ~50% increase in overall cellular granularity (**Figure 5-1F**; $F(1,24)=P<0.001$). Aged dystrophic microglia were identified as high side scatter populations relative to young microglia, a characteristic that was also observed by

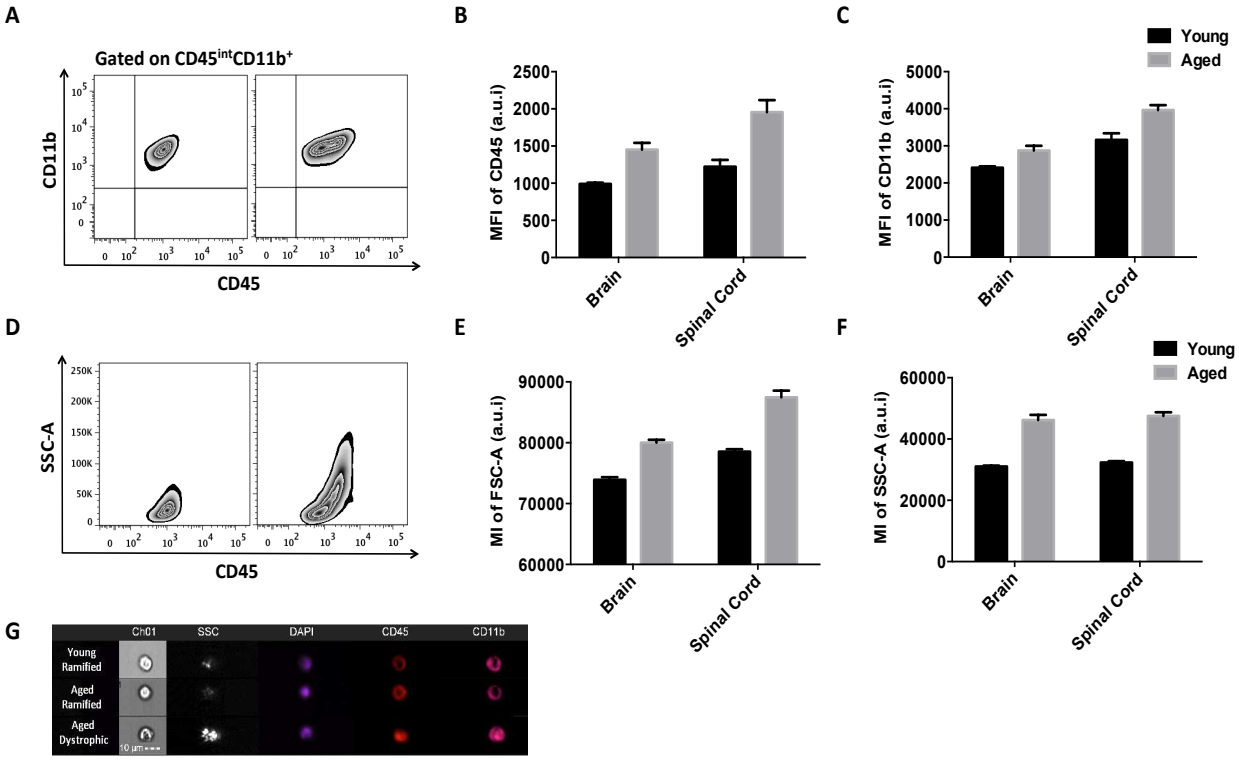

Figure 5-1. Identification of microglial by CD45 and CD11b expression and light scatter properties.

A representative zebra plot showing $CD45^{int}CD11b^{+}$ microglia in young and aged brains (A). The relative expression of microglial CD45 and CD11b were quantified for brain and spinal cord with age (B and C). Physical properties of microglia were measured by flow cytometry. Figure 1D shows a representative zebra plot of microglia in young and aged brains illustrating the increased side scatter properties of aging microglia. Forward scatter area (FSC-A) and side scatter area (SSC-A) mean intensities were quantified revealing a significant interaction between aging and region with regard to cell size (E) and an effect of age on cellular granularity (F) according to 2-way ANOVA statistical analysis. For all experiments N=7/group. Error bars show mean SEM. Abbreviation: SEM, standard error of the mean.

single cell fluorescent microscopy (**Figure 5-1D and 5-1G**). These results suggest that aging is associated with general features of microglia activation, albeit to a greater extent in the spinal cord.

Age- and location-related increases in mitochondrial activity, reactive oxygen species (ROS) production, and expression of the pro-inflammatory cytokines

Aging is associated with altered mitochondrial dynamics [336,337]. Using two commercial dyes, Mitotracker Green and CM-H2XRos, the effects of aging on total mitochondrial content and membrane potential respectively were investigated. Two-way ANOVA revealed a significant interaction between age and region on both mitochondrial content (Mitotracker, $F(1,17)=P<0.0078$) and membrane potential (CM-H2XRos, $F(1,20)=P<0.0055$), primarily driven by relatively large increases in mitochondrial activity of aged spinal cord microglia (**Figure 5-2A-D**). Because both aging and changes in mitochondrial activity have been linked to elevated ROS generation we next measured ROS levels (Finkel T and Holbrook NJ, 2000). A significant age-related increase in the basal production of microglial ROS after incubation with CM-H2DCFDA, was seen, indicating an increase in oxidative stress with age (**Figure 5-2E-F**; $F(1,19)=P<0.0396$).

Increased production of ROS in aging cells is generally associated with increased expression of pro-inflammatory cytokines [338,339]. We measured basal production of M1-associated pro-inflammatory cytokines tumor necrosis factor-alpha (TNF-α) and interleukin 1-beta (IL-1β) in unstimulated microglia by intracellular staining

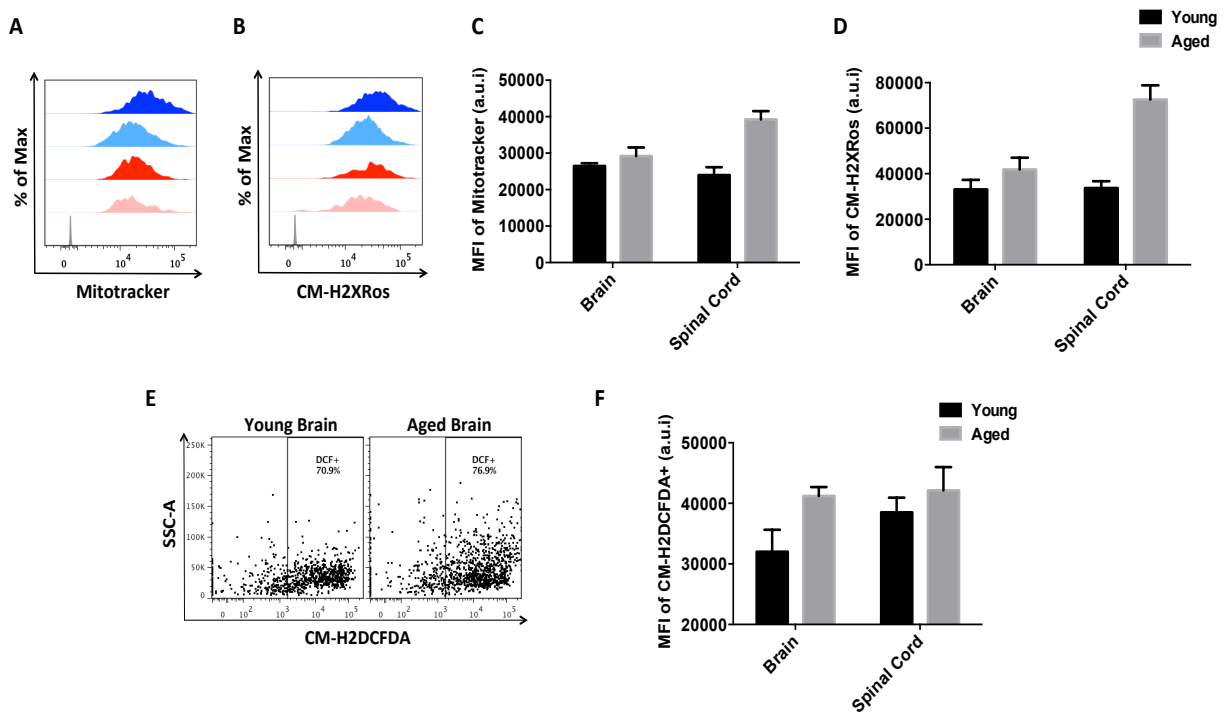

Figure 5-2. Mitochondrial activity and reactive oxygen species production in microglia.

Representative histograms of Mitotracker and CM-H2XRos dye staining of microglia, indicating overall mitochondrial content and mitochondrial membrane potential, respectively (A and B). Quantification of mean fluorescence intensities reveal an effect of aging on mitochondrial mass and activity (C and D). A representative dot plot of the ROS-indicator CM-H2DCFDA, used to assess ROS levels in unstimulated microglia (E). The relative fluorescent intensities of CM-H2DCFDA were significantly altered with age (F). The histogram color key is as follows: gray = microglia FMO dye control, red = brain, blue = spinal cord, light shade = young, dark shade = aged. For all experiments, N=5-7/group. Error bars show mean SEM. Abbreviation: SEM, standard error of the mean.

(**Figure 5-3A and 5-3D**). Significant age- and regional effects were found in the both the percentage and mean intensity of TNF-α- and IL-1β-positive microglia; with aged spinal cord microglia showing relatively greater expression ($F(1,16)=P<0001$). Intracellular production of TNF-α protein was consistent with gene expression levels of TNF-α at the tissue level (**Supplemental Figure 5-1B**; $F(1,9)=P<0.0021$). Together, these findings suggest that microglia adopt a M1 status with age, a transition that is also influenced by the CNS environment.

Age- and location-related changes in phagocytic potential of microglia are associated with changes in the expression of immunoregulatory molecules

The phagocytic potential of microglia was evaluated by phagocytosis substrate assays and microglial expression of signal regulatory protein α (SIRPα). SIRPα serves as a "don't eat me" signal that negatively controls phagocytosis. The percentage of YG bead-positive microglia was significantly higher in the brain compared to the spinal cord (**Figure 5-4A-B**; $F(1,20)=P<0.01$). In addition, a decrease in the percent of bead-positive microglia was seen in aged brain compared to the young. We also observed an age-related decrease in the mean fluorescence intensity of YG bead-positive microglia (**Figure 5-4C**; $F(1,20)=P<0.01$), indicating a decrease in overall phagocytic activity of all bead-positive microglia. The uptake of multiple beads by aged microglia was associated with increased side scatter properties as depicted in **Figure 5-4G**, indicating that side scatter intensity may be a useful indirect measure of phagocytic activity in some situations. Next, to validate these findings using a substrate more reminiscent of

physiological cargo, we assessed phagocytosis of beta-amyloid peptide. Similar effects of age ($F(1,18)=P<0.001$) and region ($F(1,18)=P<0.001$) on the number of phagocytic microglia were observed using beta-amyloid peptide as the substrate (**Figure 5-4D-E**). A significant age-related decrease in the overall amount of beta-amyloid uptake per cell was also found (**Figure 5-4F**; $F(1,18)=P<0.01$). A similar regional effect was found in the expression of SIRPα, with spinal cord showing lower levels compared to brain (**Figure 5-5A-B**; $F(1,24)=P=0.001$). The receptor ligand for SIRPα, CD47, was then evaluated. Gene expression studies showed that endogenous CD47 transcription increases in an age- and region-dependent manner (**Figure 5-5C**; $p<0.05$). Interestingly, PMA/ionomycin stimulation increased phagocytic activity in young and aged microglia for both substrates, albeit to a lesser extent in aged microglia (beads, $P=0.039$; beta-amyloid, $P=0.003$; **Figures 5-5D-F**). These results show that microglial phagocytic activity changes with age both at baseline and after stimulation in a region-specific manner. This may be regulated by the expression of immunoregulatory molecules known to keep microglia in a quiescent state.

The blood-spinal cord barrier exhibits a relatively high degree of vascular leakage

One possible mechanism for age- and location-related differences in microglia activation is increased exposure to systemic factors. We assessed vascular permeability in brain and spinal cord tissue in young and aged mice. Large (Evan's blue, 961Da; bound to albumin, 70kDa) and small (NaF, 400Da) tracers were injected and subsequently analyzed by spectrophotometry (**Figures 5-6A-B**). While vascular

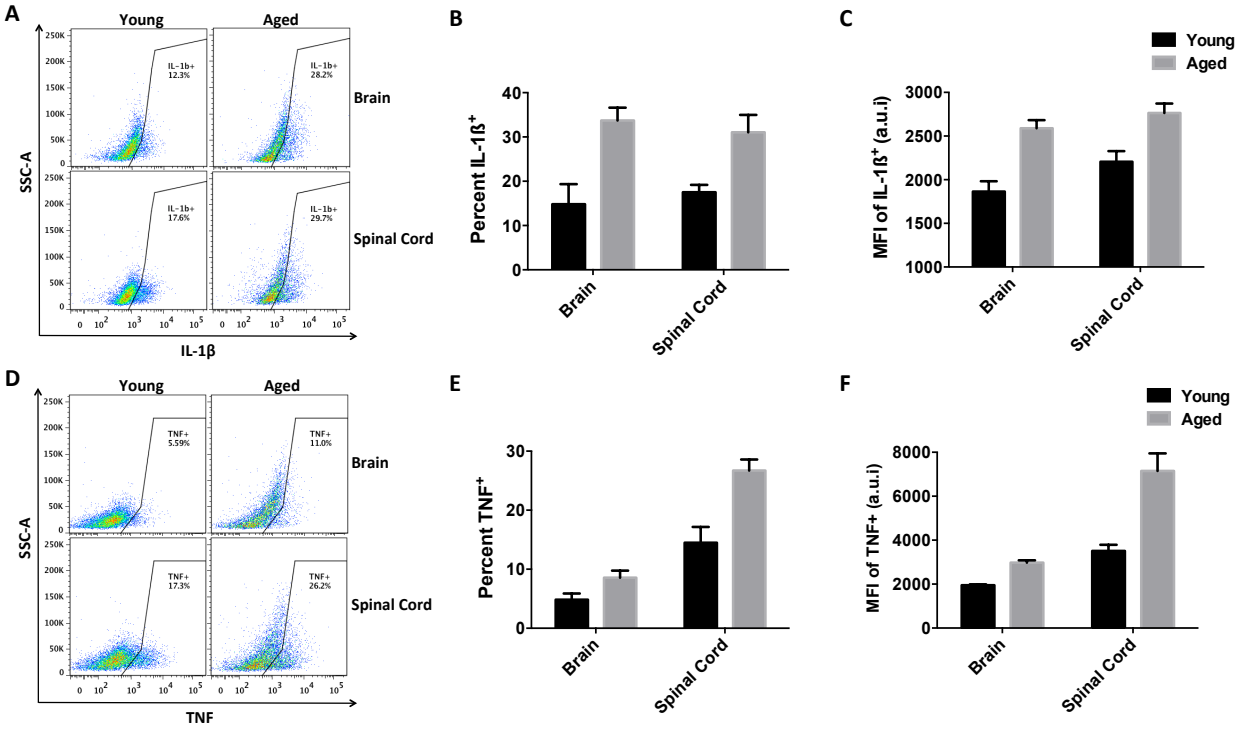

Figure 5-3. Basal cytokine production by microglia is altered with age and region. Representative dot plots illustrate intracellular production of pro-inflammatory cytokines IL-1β and TNF by unstimulated microglia (A and D, respectively). Quantification of these plots show elevated microglial cytokine production with age, which is particularly higher in spinal cord microglia compared to brain microglia (B-C and E-F). Age-specific microglial FMO cytokine controls were used to determine positive gating. For all experiments, N=6/group. Error bars show mean SEM. Abbreviation: SEM, standard error of the mean.

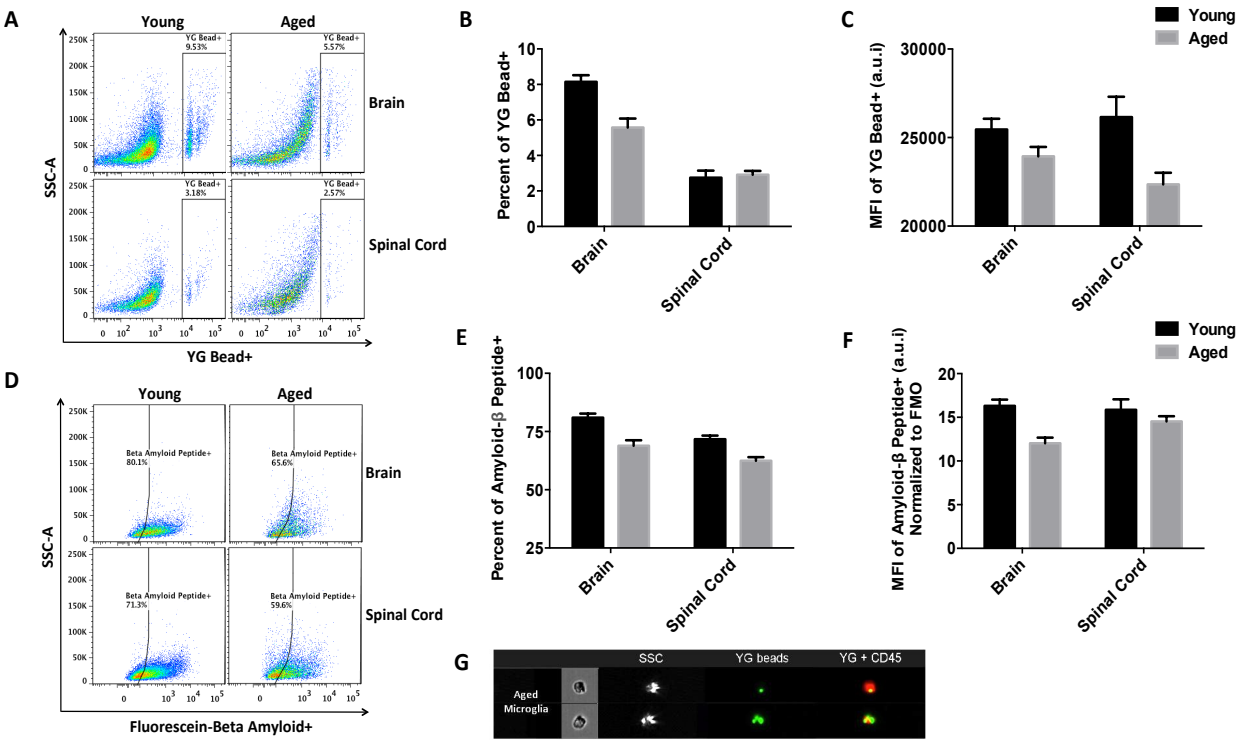

Figure 5-4. Microglia phagocytic activity impairment with age.

A representative dot plot depicting the results of an ex-vivo bead assay to assess phagocytosis (A). Quantification shows that the number of phagocytic microglia (B) and the rate of phagocytosis (C) decreased with age. A representative dot plot depicting the results of an ex-vivo beta-amyloid peptide assay to assess phagocytosis (D). The percent (E) and mean fluorescence intensity (F) of beta-amyloid uptake is quantified (N=6/group). Representative ImageStream cytometer microphotographs of aged microglia that have phagocytized beads (G). Age-specific microglial FMO bead and peptide controls were used to determine positive gating. For bead assay experiment, N=7/group. Error bars show mean SEM. Abbreviation: SEM, standard error of the mean.

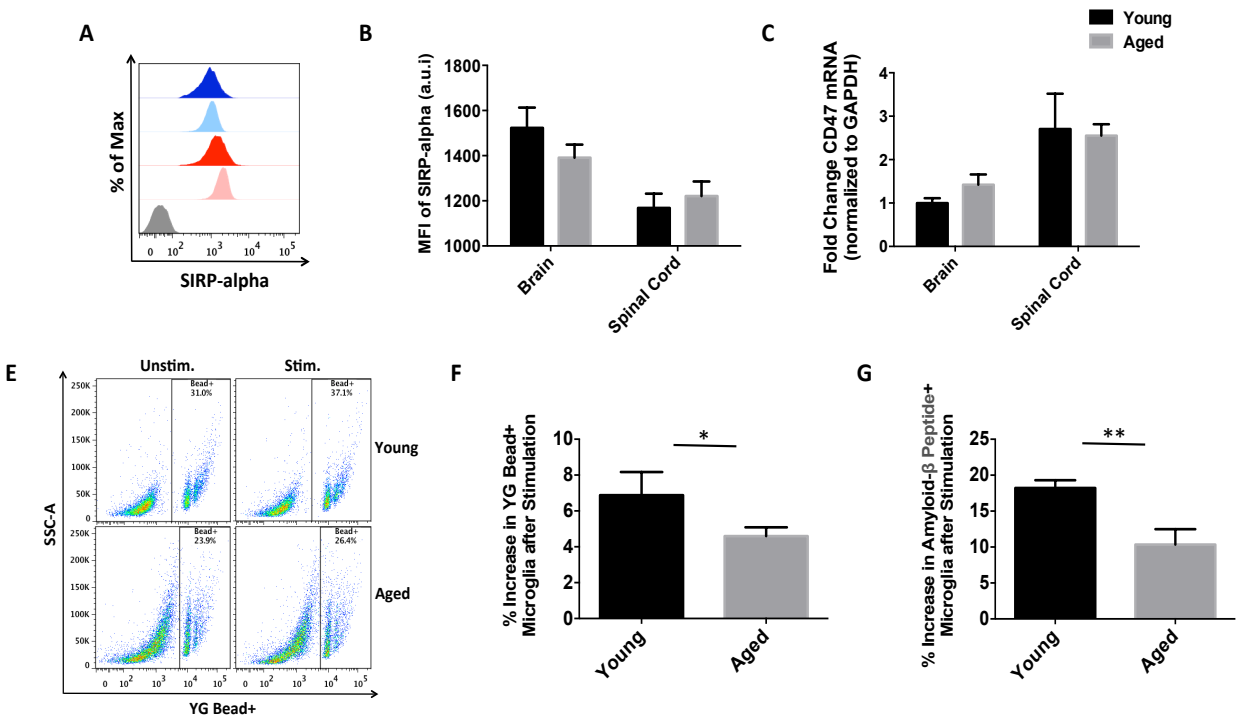

Figure 5-5. Expression of phagocytic-regulatory molecules SIRPα/CD47 and the effects of acute stimulation on uptake.

A representative histogram of the phagocytic regulator SIRP-alpha receptor on microglia (A) illustrates a relative decrease in spinal cord microglial SIRP-alpha expression compared to brain microglia (B). Whole tissue gene expression of its cognate ligand, CD47, a suppressor of phagocytosis, was significantly increased in spinal cord (C; N=5/group). A representative dot plot showing age-related changes in brain microglia after PMA/ionomycin stimulation (D). The percent increase in the number of microglia that phagocytize beads (E) and beta-amyloid peptide (F) after stimulation is quantified (N=6/group). The histogram color key is as follows: gray = age-specific microglia FMO control, red = brain, blue = spinal cord, light shade = young, dark shade = aged. Stars indicate the significance by student T-test (*P≤0.05; **P≤0.01). Error bars show mean SEM. Abbreviation: SEM, standard error of the mean.

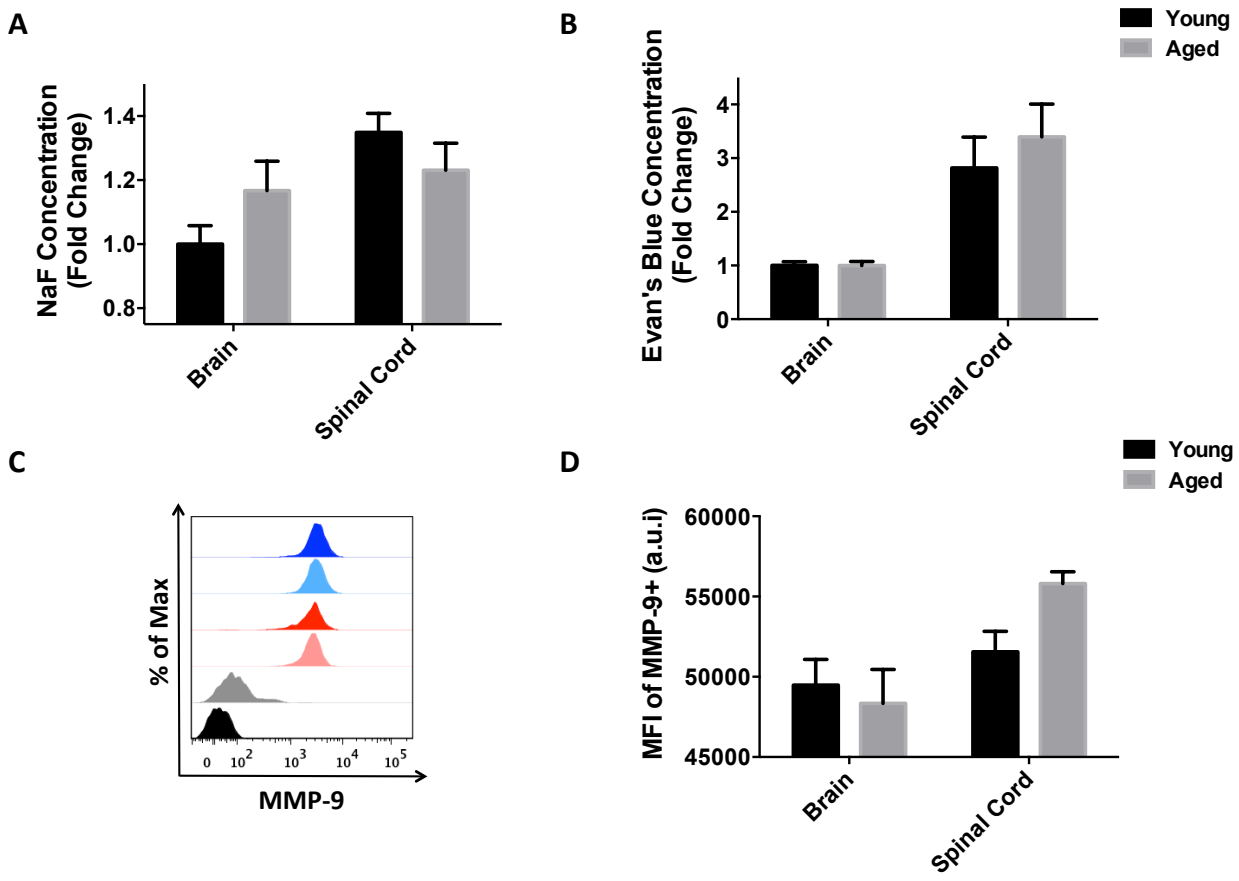

Figure 5-6. Increased blood-CNS barrier permeability in the spinal cord.
The concentrations of small (sodium fluorescein (400Da)) and large (Evan's blue (70kDa)) tracers depict enhanced vascular permeability in normal spinal cord tissue compared to brain (A and B, respectively). For each tracer experiment, N=9-13/group. A representative histogram of intracellular MMP-9 production by microglia (C). The color key is as follows: black = unstained control, gray = microglial FMO MMP-9 control, red = brain, blue = spinal cord, light shade = young, dark shade = aged. Quantification of mean fluorescence intensity of MMP-9^{+} microglia shows higher expression in the spinal cord (D). Error bars show mean SEM. Abbreviation: SEM, standard error of the mean.

integrity was largely preserved with age in both regions, spinal cord tissue exhibited significantly higher permeability to both tracer molecules ($F(1,40)=P<0.0001$ and $F(1,41)=P=0.013$, respectively). Intracellular cytokine staining revealed that spinal cord microglia expressed significantly higher levels of the enzyme matrix metalloproteinase-9, a key player in extracellular matrix remodeling (**Figures 5-6C-D**, $F(1,19)=P=0.005$). These data suggest that factors originating from microglia are associated with changes in CNS vascular integrity and may underlie regional differences in blood-CNS barriers.

Tissue cytokine production in the CNS is profoundly affected by the regional environment

Increased exposure to systemic factors in spinal cord may lead to an enhanced inflammatory state of cord microglia via enhanced cytokine signaling. Total cytokine protein levels in the young and aged brain and spinal cord were measured using multiplex ELISA. Regional differences were found; many pro-inflammatory cytokines were elevated in the spinal cord compared to brain, and remained elevated with age (**Figure 5-7A**). Total tissue levels of TNF, GM-CSF, IL-12p70 and IL-15 were significantly increased ($F(1,14)=P<0.01$) in the spinal cord, while the concentration of two anti-inflammatory cytokines, IL-9 and IL-13, were significantly lower in the cord compared to the brain independent of age ($F(1,14)=P<0.01$). Few age differences in baseline tissue cytokine levels were observed; however, increased expression of the macrophage

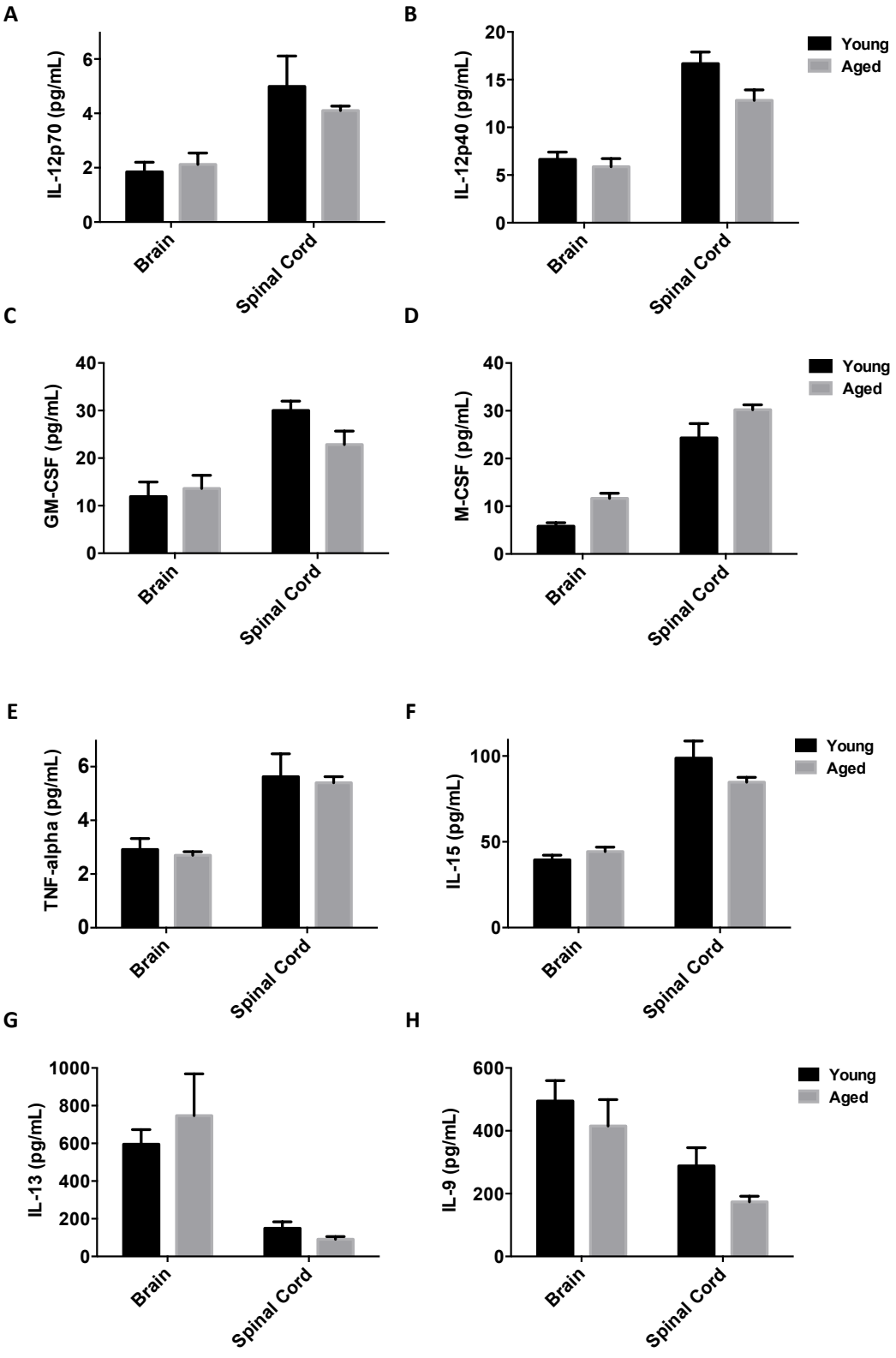

Figure 5-7. (Legend on following page)

Figure 5-7. Tissue-level cytokine production in aging brain and spinal cord. The concentration of several pro-inflammatory cytokines is elevated in the spinal cord compared to the brain. Conversely, the levels of anti-inflammatory cytokines IL-13 and IL-9 are relatively lower in the spinal cord than brain. A significant interaction between aging and region was observed for M-CSF and IL-9. For all experiments, N=5/group. Error bars show mean SEM. Abbreviation: SEM, standard error of the mean.

survival factor M-CSF and IL-12p40 were found in aged samples compared to young ($F(1,14)=P<0.05$).

Discussion

Emerging data suggests the CNS has a unique and significant immunological component. As the resident macrophages of the CNS, microglia perform many important functions required to maintain CNS homeostasis. At the core of microglia function is the ability to sense changes in the microenvironment via expression of a complex functional repertoire of immunological proteins that enable them to react and respond to specific environmental stimuli. Our findings suggest that microglia function is highly influenced by both the microenvironment in which they reside and the cumulative effects of aging. At the tissue level, we found that inflammatory cytokines are present in significant concentrations throughout the CNS, and differ in their expression profile in the brain and spinal cord. Interestingly, pro-inflammatory cytokine concentrations were higher in the spinal cord compared to the brain in both young and aged animals. The elevated basal cytokine level in the spinal cord may contribute to the higher activated state observed in these microglial populations, especially with age, leading to a pro-inflammatory feedback loop that disrupts normal maintenance functions. Despite these findings, age-related diseases of the spinal cord are relatively rare compared to those that manifest in the brain, implying that cytokine concentrations may not accurately reflect cellular function or pathology. Reasons for these regional

differences may reflect increased cytokine transport, or more broadly, altered blood-CNS barrier integrity, exposing vulnerable areas to systemic factors. Importantly, with age, microglia in both CNS regions exhibit a marked increase in cell size, granularity, mitochondrial activity, ROS and cytokine production, as well as defects in phagocytic activity.

A growing body of evidence supports the notion that like neurons, microglia are highly heterogeneous in form and function. In a study examining heterogeneity in the postnatal maturation of microglia, Scheffel, et al. [340] showed that not only do microglia differentially respond to TLR4 and non-TLR challenges, these reactive phenotypes differ with time and within circumscribed CNS regions. Butovsky, et al. [217] have provided further evidence of a unique microglia 'signature' using array profiling at the mRNA and miRNA level, highlighting many differences between microglia isolated from various regions of the adult CNS. We have found that microglia from brain and spinal cord can be distinguished by their physical properties (size, granularity) and their activation status. Spinal cord microglia were larger, more granular, and expressed higher levels of CD45 and CD11b than brain microglia. Regional differences in gene expression of these markers have been previously observed in young mice [341]. Although the functional relevance of these proteins on microglia is currently not known, it likely reflects enhanced translational efforts indicative of a heightened activation state, as evidenced by increased cytokine production [102,342]. Although standard identification of microglia using flow cytometry relies on $CD45^{int}$ and $CD11b^{+}$, our studies indicate that for spinal and aging microglia in particular, the Ly6C antibody may be a useful addition to delineate cell populations when the relative CD45

expression levels of peripheral monocytes overlap with that of resident microglia. Taken together, these data are consistent with previous work showing region-specific increases in oxidative activity and activation markers in white matter and more caudal, adult microglia [332,343].

Our finding that vascular permeability is greater in the spinal cord than brain may help explain regional differences in microglial reactivity and slower recovery after cord lesions [325]. The structure of the blood-spinal cord barrier (BSCB) is different than the blood-brain barrier in that the BSCB has fewer tight- and adherence junction proteins [317,326]. Earlier studies have shown increased transport of TNF and interferons in the spinal cords of healthy mice, compared to brain [344,345]. Schnell et al [325] found that mechanical lesions induced substantially greater and more durable barrier breakdown in the spinal cord compared to brain. This may result from differing entry dynamics of peripheral leukocytes important for repair following injury. However, our observation that MMP-9 production was greater in spinal cord microglia at baseline than in brain suggests that active remodeling of the extracellular matrix may also contribute to increased leakage [346]. Whether these differences are due to the inherent structural features of this barrier or are a detrimental effect of increased microglial activation is not known, but likely involve a combination of both. In a previous study, our laboratory failed to find any difference in cerebral blood flow flux or staining intensity of FITC-dextran and CD31-labeled microvasculature in histological sections of young and aged cohorts [347]. However, we cannot rule out that insults that accrue with aging may increase the potential for temporary opening of the blood-CNS barrier at selective tissue sites. Taken together, our findings provide clear evidence of regional heterogeneity in

microglia activation and highlight the relative leakiness of the blood-spinal cord barrier as a potential mechanism.

Microglia share many functional and phenotypic similarities to peripheral macrophages and have similar surface molecules [78]. Microglia are identified by an intermediate level of CD45 expression and CD11b positivity, but our work suggests that CD45 levels increase with age, further complicating differentiation of microglial from myeloid cells [102]. For example, the relative expression of CD45 and CD11b were significantly higher in the spinal cord compared to the brain and spinal cord microglia also showed comparably higher up-regulation with age. These findings suggest that the inclusion of Ly6C antibody as a peripheral myeloid cell marker may safeguard against mixed populations due to overlapping CD45 expression.

Dystrophic microglia in the aging CNS are defined by altered morphology including enlarged cell bodies, retraction of fine branches, and cytoplasmic processes that appear beady or fragmented [54]. Many of these cellular inclusions contain lipofuscin granules with autofluorescent properties. Similar profiles have been observed in aged rodent microglia, and are reminiscent of young healthy microglia activated after injury [348,349]. We found that aging significantly increased microglial cell size and granularity in both the brain and cord. Importantly, we found that dystrophic (high scatter) and ramified (low scatter) populations of microglia coexisted in a similar ratio as was reported by Streit et al [54] (data not shown). These findings demonstrate that flow cytometry allows for the simple identification of dystrophic microglia based on their physical properties.

Because the CNS has a high-energy demand relative to other tissues, changes in mitochondrial function, ATP production, and oxidative stress may contribute to energy failure and neurodegenerative disease. The increase in mitochondrial content/activity may reflect deficits in mitophagy secondary to the cellular stress induced by aging. Age-associated alterations in mitochondrial activity are also associated with increased production of reactive oxygen species (ROS) by the mitochondrial respiratory chain leading to oxidation of unsaturated fatty acids, proteins, and nucleic acids [350,351]. Increased intracellular ROS may in turn activate microglia, leading to enhanced production of inflammatory mediators and lead to autophagic and lysosomal impairment [352]. The long lifespan of microglia makes them especially vulnerable to the aggregate effects of oxidative stress. We found that microglial ROS and cytokine production increased with age. While the augmented mitochondrial activity found in aged spinal cord did not necessarily translate into similar fold-change increases in ROS production, other factors such as cell volume or tissue-specific demands may account for this discrepancy. Recent work by Youm YH et al [353] has identified Nlrp3 inflammasome-mediated production of IL-1β as a critical link between systemic low-grade inflammation, innate immune activation, and functional decline in the aging CNS. Our studies demonstrating that the blood-brain barrier remains relatively intact with age suggests that the detrimental effects of aging may be intrinsic to the cell and its environment rather than a direct result of systemic modulation.

Deficits in phagocytosis with aging were evident as demonstrated by the reduced number of aged microglia that contained physiological (beta-amyloid peptide) and non-physiological (beads) cargo. This is consistent with prior studies [354,355]. These deficits in

clearance have been implicated in the pathogenesis of age-related diseases such as Alzheimer's [356,357]. Aging is associated with reductions in substrate uptake, proteolytic capacity, and decreased degradation efficiency of beta-amyloid [358]. Beta-amyloid can also trigger microglial production of pro-inflammatory mediators that inhibit phagocytosis [136,359,360]. In this study, we examined basal phagocytic potential of "unstimulated" microglia in an effort to understand the normal homeostatic changes that occur with age. To our knowledge, this is the first study to demonstrate phagocytic deficits in aged microglia. The increased generation of debris and inflammatory mediators in the aging CNS may inhibit mechanisms of microglial phagocytosis. These defects in debris clearance could have several consequences including increased glial activation, as evidenced by the deposition of amyloid plaques in Alzheimer's disease [361], increased cytokine activation, impaired lysosomal function, and disruption of autophagy [362,363]. One limitation pertaining to ex-vivo assays is the possibility that the isolation process itself may 'activate' the cells, and lead to changes in their functional capabilities. Interestingly, we found that ex-vivo stimulation by PMA/ionomycin enhanced the rate of phagocytic activity in all microglia, albeit to a significantly lesser extent in aged microglia. These results suggest that aged microglia may be less responsive to inductive cues and/or more prone to become exhausted from high levels of cellular and inflammatory stress [364]. There are several endogenous mechanisms that also control phagocytosis. SIRPα, a receptor found primarily on myeloid cells, binds to its ligand CD47 and functions as a regulator of phagocytosis [365,366]. This was consistently down-regulated with age. Our results also show that tissue expression of CD47 increased with age, which may account for the age-related inhibition of phagocytosis. Previous

studies have shown that down-regulation of CD47 promotes phagocytosis of compact myelin by microglia *in vitro* [365]. It is possible that age-associated increases in CD47 may serve a compensatory function to prevent unwanted phagocytic removal of myelinated axons by dysregulated microglia. Further studies are required to determine the therapeutic efficacy of targeting phagocytic pathways in aged microglia.

In summary, the normal homeostatic functional status of unstimulated microglia can be assessed using ex-vivo functional assays. We found profound regional differences in microglia function, demonstrating the importance of the local microenvironment to microglial function. *M1-like activation status* increased with age in nearly all microglial populations, although regional differences were preserved. Striking differences were seen in vascular permeability and cytokine levels in the brain versus the spinal cord, with greater potential exposure of spinal cord tissue to systemic factors, mirroring the overall increased activation status of microglia in this region. This work provides the first evidence at the cellular level of a functional decline in microglia homeostasis with age.

A

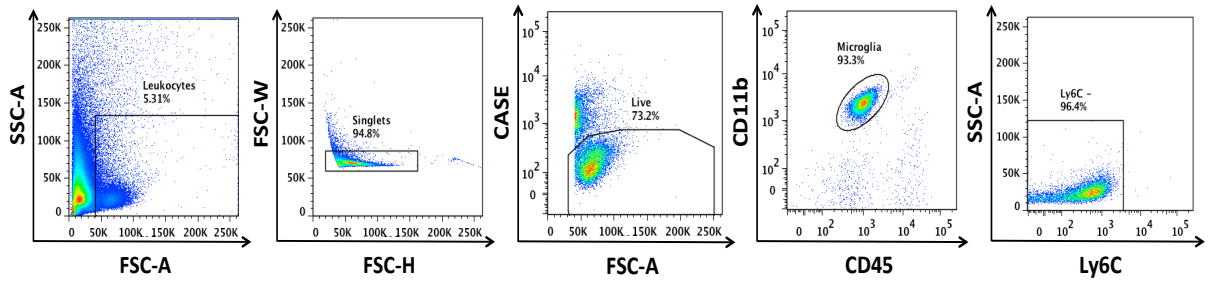

Supplemental Figure 5-1. Gating strategy used for identification of microglia using flow cytometry.

SA1 illustrates the gating strategy used for the definitive identification of microglia (A). Using unstained spleen samples for reference, leukocyte gating was determined by relative scatter (area) identification. To eliminate biased protein expression due to increased event size (doublet or cell clumping) single cells were gated on based on forward scatter (width x height) identification. Living cells were gated on based on the relative exclusion of the viability dye CASE (as determined by FMO). Microglia were subsequently identified based on $CD45^{int}$ CD11b expression. Lastly, to exclude bone marrow-derived macrophage populations, Ly6C+ cells were excluded.

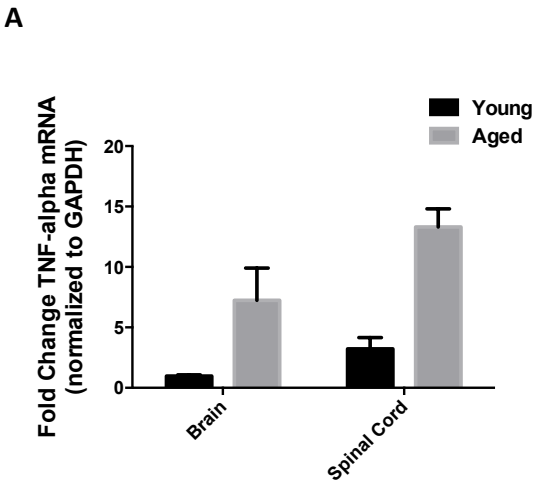

Supplemental Figure 5-2. Age- and region-specific gene expression of TNF. SA2 shows RT-PCR analysis of TNF-alpha mRNA in brain and spinal cord tissue with age. N=4/group. Error bars show mean SEM. Abbreviation: SEM, standard error of the mean.

Authors' Contributions

RMR and LDM conceived the project. RMR performed most of the experiments and ARP, SP, JC assisted with the flow cytometry preparations. RNA and protein expression studies were aided by SP and ARP, respectively. MDH and ERJ assisted the analysis and interpretation of the flow cytometry data. RMR and LDM wrote the paper. All authors read and made comments on the manuscript draft and approved the final manuscript.

Acknowledgements

This work was supported by National Institutes of Health grants R21 NS076293-01A1 (Louise D. McCullough) and F31 NS083244-01A1 (Rodney M. Ritzel).

Chapter 6:

Opposing roles for immune surveillant CD8 T cells in the aging central nervous system

Rodney M. Ritzel[1], Anita R. Patel, Joshua Crapser, Evan R. Jellison, and Louise D. McCullough

Abstract

Aging is associated with an increase in basal inflammatory processes in the central nervous system (CNS) and an overall decline in cognitive function and recovery following injury. Growing evidence suggests that leukocyte recruitment to the CNS is also increased with normal aging, but to date, no systematic evaluation of these "age-associated" leukocytes have been performed. In this work the effect of aging on CNS leukocyte recruitment was examined. Despite no overt change in global blood-brain barrier permeability, aging was associated with an increased number of $CD45^{hi}$ leukocytes, primarily composed of conventional $CD8^{+}$ T cells. These cells were CCR3, CCR5, and CXCR3-positive and coincided with age-related increases in the CNS production of chemokines known to be involved in T cell recruitment (CCL11, CXCL9, CCL5, CXCL10). CD8 T cells in the aged brain expressed significantly higher levels of

the adhesion molecules required for CNS entry, CD11a and CD49d, compared to those in the blood. Intravascular labeling and immunohistology revealed the presence of parenchymal $CD8^+$ T cells in several regions of the brain including the choroid plexus and meninges. These cells had an effector/memory ($CD44^+CD62L^-$) phenotype and expressed markers associated T cell receptor (TCR) activation. This population of CNS-specific CD8 T cells had a similar pattern of TCRvβ family repertoire usage suggesting that entry into the CNS is likely stochastic rather than antigen-driven. Correlational analyses revealed a positive association between CD8 T cell numbers and decreased pro-inflammatory function of microglia. However, the effects of cerebral ischemia and *ex-vivo* stimulation of these cells dramatically increased production of tumor necrosis factor (TNF) and interferon gamma (IFNγ) as well as several chemokines associated with neutrophil chemotaxis. Taken together, we identified a novel population of CNS-specific immunosurveillant CD8 T cells that appear to maintain microglia homeostasis under normal conditions, but are primed to potentiate inflammation and leukocyte recruitment following ischemic brain injury. These cells serve as a hallmark feature of CNS aging and provide an alternative explanation for the noted differences in the neuroinflammatory response of young and aged animals.

Introduction

Aging is associated with cognitive decline, a heightened risk of neurodegenerative disease, and poorer recovery after injury. As the average life expectancy continues to

increase the median age of the population has also increased. People aged 80 and over are the fastest growing segment of the population, projected to reach 19.4 million in 2030 [367]. These statistics highlight growing concerns over the burden to the health services industry as aging affects all of the organ systems in the body. The aging process exerts profound changes on the nervous and immune systems, which extend into nearly all organ systems [368-370]. Indeed, the relationship between these two systems is bidirectional, and the concept of the CNS as an immune privileged organ is evolving [371]. The brain is under constant immune surveillance by resident microglia and trafficking systemic T lymphocytes recruited by the choroid plexus under normal conditions [372-374]. These generally cells serve a protective role, as a rapid response system to detect damaging agents that disrupt homeostasis. Although T lymphocytes transit the CNS at low numbers in healthy brains, the role of these cells and how it changes with age is not well understood [375]. Activated CD4 central memory (T_{cm}) cells reside within human cerebrospinal fluid and circulate in the subarachnoid space and ventricular system of the brain and spinal cord [376,377]. Moreover, CD4 effector memory (T_{EM}) cells with a TCR repertoire specific to CNS antigen are constitutively present in the epithelial layers of the choroid plexus where, at this interface between brain and blood, they are poised to act as immunomodulators of aging and senescence [372,378]. Like neurons, T cells are specified for many unique functions that serve important roles in immunity. For example, Scid mice, which lack functional T cells, show deficits in cognitive abilities compared to WT matched mice, implying that T cell functions can influence CNS functions whether they reside in the CNS itself or outside in the periphery [379-381]. Given the functional importance of T cell subsets implicated in several

neurological diseases, little is known regarding the role and identity of the lymphocytes that traffic throughout the CNS under normal conditions such as aging.

Surveillance is the process whereby the immune system identifies and eliminates cancerous or pre-cancerous cells before they cause harm [382]. Although little is known concerning the role of aging on immune surveillance in the CNS, the increase in basal inflammatory levels indicative of the phenomenon known as “inflammaging” support the notion that the necessity for surveillance may be heightened [55]. The low-grade inflammatory status of the aged CNS may favor their recruitment, but the critical mediators of this phenomenon and the functional role of the immune cell subtypes entering the aged brain in steady state remain to be established. Few studies have provided a comprehensive analysis of the peripheral leukocytes present within the aged CNS. Stichel and Luebbert (2002)[383] showed a significant increase in both $CD11c^+$ dendritic cells and $CD3^+$ T cells with wide distribution throughout the brain beginning at middle age and increasing with advanced age. Although CD4 effector memory cells have been reported in the choroid plexus of aged mice it is not clear whether these populations are confined only to this region. Studies assessing donor human brain tissue have identified the presence of resident $CD8^+$ T cells enriched in white matter and regions of blood-brain barrier leakiness [50,384]. These findings indicate that the observed changes in leukocyte recruitment in the aging mouse brain likely have translational relevance as immune surveillance also occurs in the human CNS, however, our current understanding of these cells is still lacking.

In the present study, we examined for the presence of peripheral leukocytes in the aging CNS to further understand the functional relevance of these cells with regard to

age-related inflammatory signaling in the normal CNS. In order to assess this possibility, we examined blood brain barrier permeability, evaluated the potential for lymphocyte recruitment guidance and response cues, and performed a comprehensive phenotypic analysis of cell subsets found in normal CNS. Lastly, to determine if there was a functional consequence of these CNS-specific leukocytes we assessed production of inflammatory mediators after *ex-vivo* stimulation and in an age-relevant model of ischemic brain injury.

Materials and Methods

Mice/Animals: C57BL/6J mice of 8-12 wks (young adult) and 18-22 months (aged) of age were pair-housed on sawdust bedding in a specific pathogen free facility (light cycle 12/12 h light/dark). The average weight of the naïve, young mice was 29.6 ± 2.3 grams and that of aging mice was 35.7 ± 3.2 grams before sacrifice. All animals had access to chow and water *ad libitium*. Animal procedures were performed in accordance with NIH guidelines for the care and use of laboratory animals and approved by the Animal Care Committee of the University of Connecticut Health Center. *Ex-vivo* studies were performed by an investigator blinded to age.

Tissue Harvesting: Mice were euthanized, transcardially perfused with 60mL cold, sterile PBS, and the brains were harvested. The olfactory bulb, brainstem, and cerebellum were removed. The brain was then divided along the interhemispheric

fissure into two hemispheres and then subsequently rinsed with PBS to remove contaminant cells.

Flow cytometry: Blood was drawn by cardiac puncture with heparinized needles. Red blood cell lysis was achieved by three consecutive 10-minute incubations with Tris-ammonium chloride (Stem Cell Technologies). CNS tissue to be analyzed by flow cytometry was placed in complete Roswell park memorial institute (RPMI) 1640 (Lonza) medium and mechanically and enzymatically digested in collagenase/dispase (1 mg/mL) and DNAse (10mg/mL; both Roche Diagnostics). The cell suspension was filtered through a 70um filter. Leukocytes were harvested from the interphase of a 70%/30% Percoll gradient. Blood and brain leukocytes were washed and blocked with mouse Fc Block (ebioscience) prior to staining with primary antibody-conjugated flourophores (see Supplementary Materials Table 1). For live/dead discrimination, a fixable viability dye, CASE-AF350 (Invitrogen), was diluted at 1:300 from a working stock of 0.3mg/mL. Data were acquired on a LSRII using FACsDiva 6.0 (BD Biosciences) and analyzed using FlowJo (Treestar Inc.). No less than 100,000 events were recorded for each sample. Resident microglia were identified as the $CD45^{int}$ $CD11b^{+}$ population, whereas bone marrow-derived leukocytes were identified as $CD45^{hi}$. Cell-specific fluorescence minus one (FMO) controls were used to determine the positivity of each antibody.

For intracellular cytokine staining, a stock solution of brefeldin A (Sigma) was prepared at 20mg/mL in DMSO, and diluted with PBS to obtain a working solution of 0.5mg/mL. Mice were euthanized 8 hours after intravenous injection of brefeldin A

(250ul). Leukocytes were collected as described above, and 1ul of GolgiPlug containing brefeldin A (BD Biosciences) was added to 800ul complete RPMI. Cells were subsequently stimulated with PBS or Cell Stimulation Cocktail (eBioscience) containing PMA/ionomycin and incubated for 4 hours at 37C (5% CO2). Afterward, cells were resuspended in Fc Block, stained for surface antigens and washed in 100ul of fixation/permeabilization solution (BD Biosciences) for 20 minutes. Cells were then washed twice in 300ul Permeabilization/Wash buffer (BD Biosciences) and resuspended in an intracellular antibody cocktail containing TNF-PE-Cy7, IL-17A-FITC, IL-17F-PerCP-eF710, CCL2-PE, CCL5-PE, Granzyme B-Bv510, and IFNγ-PerCP-Cy5.5 and fixed.

For detection of reactive oxygen species, leukocytes were incubated with redox-sensitive CM-H2DCFDA (5uM; Ex/Em: 495/520) fluorogenic cell-permeant dye (Life Technologies, Invitrogen). Cells were incubated for 20min at 37C, washed three times with FACS buffer (without NaAz), and then stained for surface markers including CASE.

To determine TCRvβ usage, we used a mouse vβ TCR screening panel (BD Pharmingen) according to the manufacturers instructions. Briefly, after collecting blood and tissue leukocytes each sample was divided into 15 separate FACS tubes and stained for the antibody cocktail including one of 15 respective TCRvβ FITC-conjugated monoclonal antibodies. Liver, epididymal adipose, and lung tissue was processed as above using percol gradient.

Phagocytic activity of microglia was performed as described by Ritzel et al (2015). Briefly, fluorescent latex beads (Fluoresbrite Yellow Green (YG) carboxylate microspheres; 1um diameter; Polysciences) were added to sorted microglia in a final

dilution of 1:100 as described [385]. After 1-h incubation at 37 °C, the cells were washed three times with FACS buffer, re-suspended in FACS buffer, stained for surface markers, and fixed in PFA.

ELISA cytokine measurement: Plasma and whole tissue brain chemokine levels were determined by ELISA (Milliplex Cytokine/Chemokine Assay, EMD Millipore). In brief, mice were euthanized by avertin injection and blood was collected by cardiac puncture into heparin-coated syringes. Samples were centrifuged (13,000g for 10min at 4C) and plasma was collected and stored frozen (-80C) until assaying. Brain hemispheres were collected and homogenized in ice-cold lysis buffer containing a protease inhibitor cocktail (Roche Diagnositics). Homogenates were sonicated and centrifuged at 4C for 15 min at 14,000 rpm, and supernatants were assayed for total protein using a BCA protein assay kit (Pierce, Thermo scientific). Using a standard curve, protein concentration was determined and 100ug of each sample was loaded into each well in duplicate. Samples were assayed according to the manufacturer's instructions using a Luminex 200 (Luminex Corporation, Austin, TX, USA) magnetic bead array platform. Inter-and intra-assay coefficients of variation were than less than 10%.

Intravascular staining and cell isolation: A total of 7ug anti-CD3e-PE was injected i.v. At 4 minutes after injection, the animals were sacrificed, and perfused with 40mL PBS. Blood was taken by cardiac puncture prior to perfusion to confirm injection efficiency. The brain hemispheres were harvested within 3 minutes, washed with PBS to remove free antibody, and leukocytes were isolated as described above. Leukocytes

were then stained with CD45-eF450, CD11b-AF700, CD3e-APCeF780, CD4-APC, CD8-PerCPCy5.5 and CASE. Co-labeling was used determine the percentage of peri-vascular/parenchymal (CD3e-PE^-/CD3e-$APCeF780^+$) versus intravascular cells (CD3e-PE^+/CD3e-$APCeF780^+$).

Immunohistochemistry: Following PBS perfusion brains were harvested and embedded in an optimal cutting temperature (OCT) embedding solution and subsequently frozen on dry ice and stored at -80ºC. Brains were sectioned on a 77200187 Issue 5 Thermo cryostat at a thickness of 10 µm at a temperature of 17ºC. These sections were mounted on charged slides and stored at -20ºC until use. After being brought to room temperature the sections were fixed with 4% paraformaldehyde (PFA) for 10 minutes, washed and then blocked in 0.1 mol/L phosphate buffer with 0.3% Triton X-100 (Sigma) and 10% donkey serum for one hour. Primary antibodies rat anti-CD8 (Abcam, 1:200), rabbit anti-myelin basic protein (Abcam, 1:200), mouse anti-NeuN (Millipore, 1:200) and rabbit anti-CD3 (Abcam, 1:100) were added and incubated overnight at 4ºC. These sections were washed and secondary antibodies Alexa Flour 488 anti-rat (Invitrogen, 1:1000), Alexa Flour 594 anti-rabbit (Life Technologies, 1:1000), and Alexa Flour 594 anti-mouse (Invitrogen, 1:1000) as well as conjugated antibodies Texas Red Lycopersicon Esculentum (Tomato) Lectin (Vector, 1:200), mouse anti-glial fibrillary acidic protein (GFAP)-Cy3 (Sigma, 1:200) and 4′,6-diamidino-2-phenylindole, dihydrochloride (DAPI, Invitrogen, 1:1000) were added and incubated at room temperature for one hour, washed and coverslipped for viewing. Images were acquired with a Zeiss Axiovert microscope (Carl Zeiss, Oberkochen, Germany) using a X-Cite

120Q fluorescence illumination system (Lumen Dynamics Group Inc, Mississauga, ON, Canada) and Zeiss image acquisition software (Zeiss LSM 510).

Middle Cerebral Artery Occlusion (MCAO) model of ischemic stroke: Cerebral ischemia was induced by 90 min of reversible middle cerebral artery occlusion under isoflurane anesthesia as previously described [206]. Rectal temperatures were maintained at approximately 37 °C during surgery and ischemia with an automated temperature control feedback system. A midline ventral neck incision was made, and unilateral MCAO was performed by inserting a 0.23mm silicone-coated suture (Doccol Corp, Redlands, CA, USA) into the right internal carotid artery 6 mm from the internal carotid/pterygopalatine artery bifurcation via an external carotid artery stump. Following reperfusion mice were sacrificed at 4 hours after reperfusion. Sham-operated animals underwent the same surgical procedure, but the suture was not advanced into the internal carotid artery.

Statistical Analyses: Data from individual experiments are presented as mean ± SEM and compared with Student's t-test (GraphPad Prism Software Inc, San Diego, CA, USA). Multiple comparisons were assessed by one-way or two-way ANOVA analysis with Tukey post-hoc correction. Correlation analyses were performed using Pearson's correlation. $p < 0.05$ was considered statistically significant.

Results

Aging increases the number of peripheral leukocytes in the CNS

To confirm that aging increases leukocyte trafficking in the CNS we quantified the absolute number of bone marrow-derived cells present in each tissue using the gating strategy shown in **Supplemental Figure 6-1A**. The number of $CD45^{hi}$ leukocytes was significantly increased in the aged brain (**Figure 6-1A**). Absolute cell counts revealed a nearly three-fold increase in peripheral cells in aged brain (**Figure 6-1B**, $p<0.0001$). Similar increases were also observed in the aged spinal cord (**Supplemental Figure 6-2A**). T cells composed the majority of these age-associated leukocytes, wherein the CD8 subset was more numerous than the CD4 subset (**Figure 6-1C-E**, $p<0.001$). These were identified as conventional TCR α/β, CD8 α/β T cells (data not shown). The results show that T lymphocyte trafficking into the CNS is more permissive with age.

Age-related chemokine production is associated with active recruitment of CD8 T cells into the aging brain

To determine whether CD8 T cell recruitment to the aging brain could result from a directed, homeostatic process rather than an indirect result of injury, we examined protein expression of known T cell chemokines. RANTES (CCL5), Eotaxin (CCL11), MIG (CXCL9), and IP-10 (CXCL10) concentrations were all significantly upregulated in

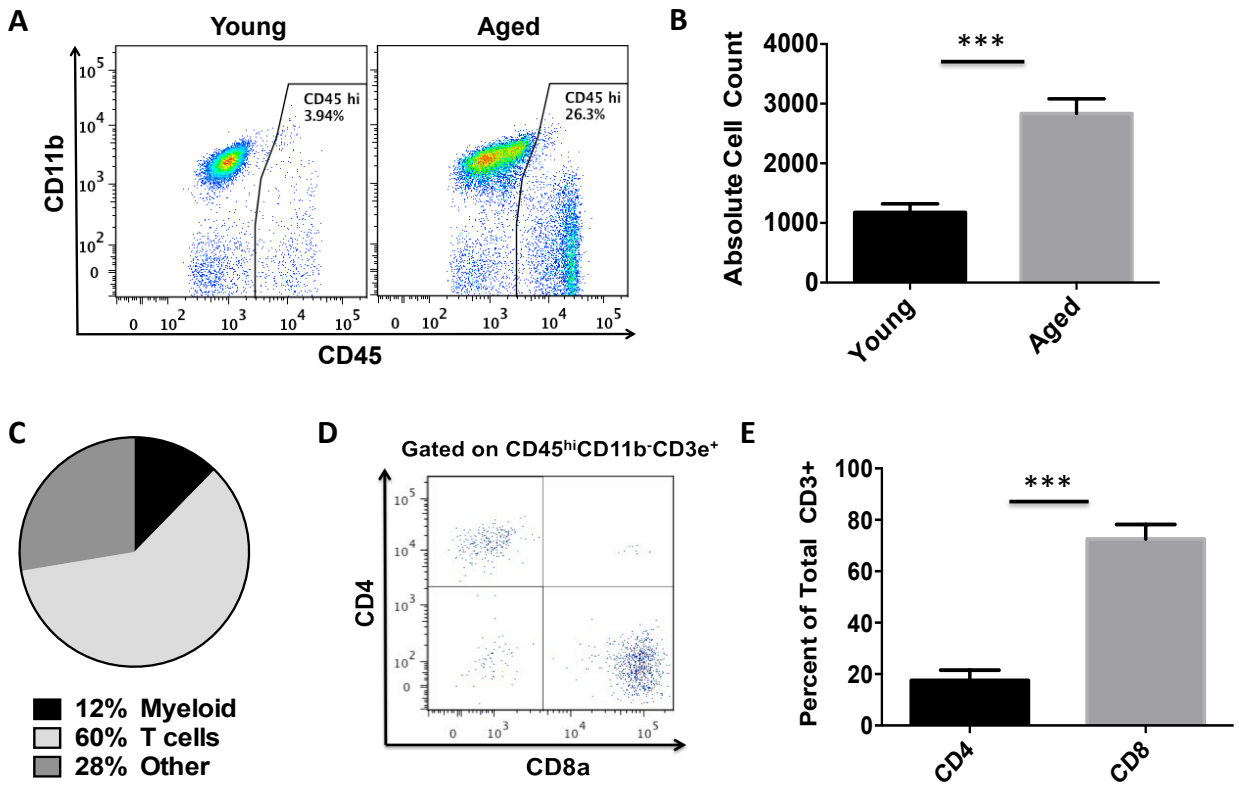

Figure 6-1. CD8 T cell recruitment in the aging CNS.

A representative dot plot depicts an increase in $CD45^{hi}$ peripheral leukocytes in one aged brain hemisphere compared to young (A). The absolute number of $CD45^{hi}$ peripheral leukocytes is quantified (B). A pie chart shows the composition of peripheral leukocytes in the aged brain (C). A representative dot plot shows T cell subsets in the aged brain (D). The percentage of T cell subsets is quantified (E). Error bars show mean SEM. Abbreviation: SEM standard error of mean. *p<0.05; **p<0.01; ***p<0.001

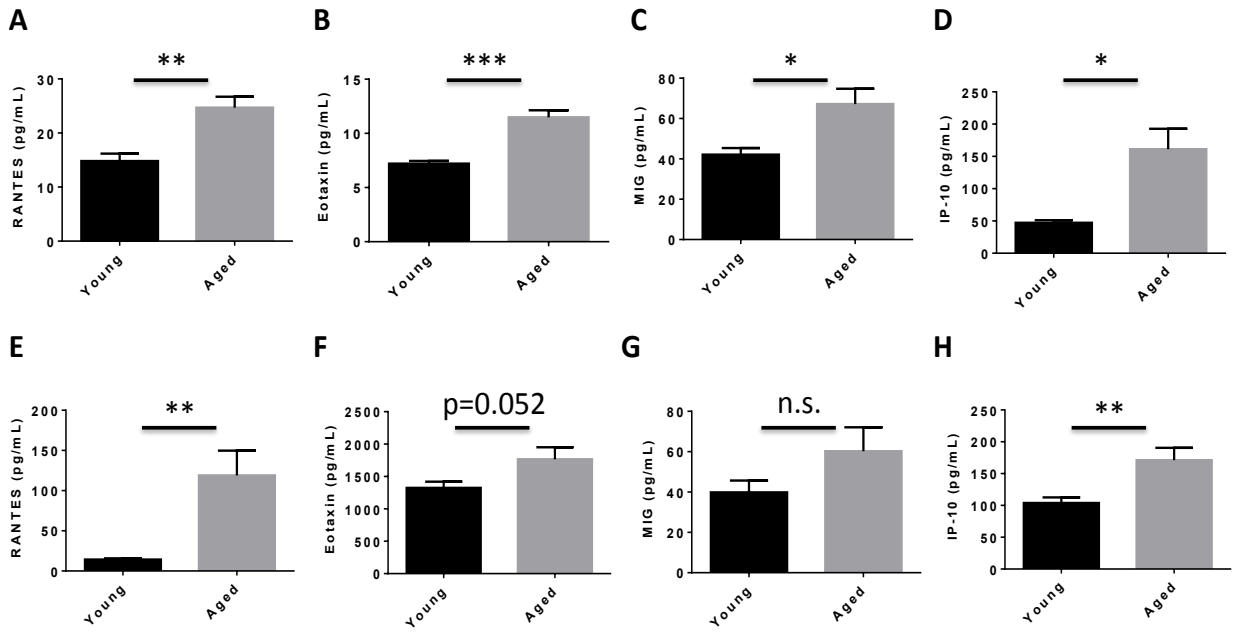

Figure 6-2. T cell chemokine production in the brain with age.

Brain concentrations of RANTES/CCL5 (A), Eotaxin/CCL11 (B), MIG/CXCL9 (C), IP-10/CXCL10 (D) are quantified in young and aged mice. Plasma concentrations of these respective chemokines (E, F, G, and H) are quantified. Error bars show mean SEM. Abbreviation: SEM standard error of mean. *p<0.05; **p<0.01; ***p<0.001

the brain with age by ELISA (**Figure 6-2A-D**). Levels of these chemokines were similarly increased in aged plasma (**Figure 6-2E-H**), suggesting that gradient levels are accessible to circulating T cells. Surface expression of chemokine receptors to these respective chemokines was then assessed on both blood and brain CD8 T cells. An increase in expression of these chemokine receptors was found on blood CD8 T cells with age (**Figure 6-3A-H**). Interestingly, CD8 T cells in the aged brain expressed lower levels of these receptors relative to those in circulation, and levels were comparable to that found in young blood. These results suggest that the aged brain is a source of chemokine cues required for active T cell recruitment, and after migrating to the CNS then down-regulate expression of their chemokine receptors in order to establish residence.

CD8 T cells are present in perivascular and parenchymal regions throughout the aging CNS

T cell extravasation across the endothelium involves a series of adhesion events that include attachment, rolling, and transmigration. Because ICAM-1 expression is reported to be increased in aged brain vasculature [386,387], we examined CD8 T cell expression of CD11a (LFA1) and CD49d (VLA4), adhesion molecules required for T cell entry into peripheral tissues. **Figure 6-4A-B** shows that CD11a and CD49d expression were dramatically increased on brain CD8 T cells compared to those in the blood (N=5, $p<0.0001$ and $p<0.01$, respectively). Vessel capture of T cells implies subsequent extravasation into perivascular and parenchymal CNS tissue. Using tomato-lectin

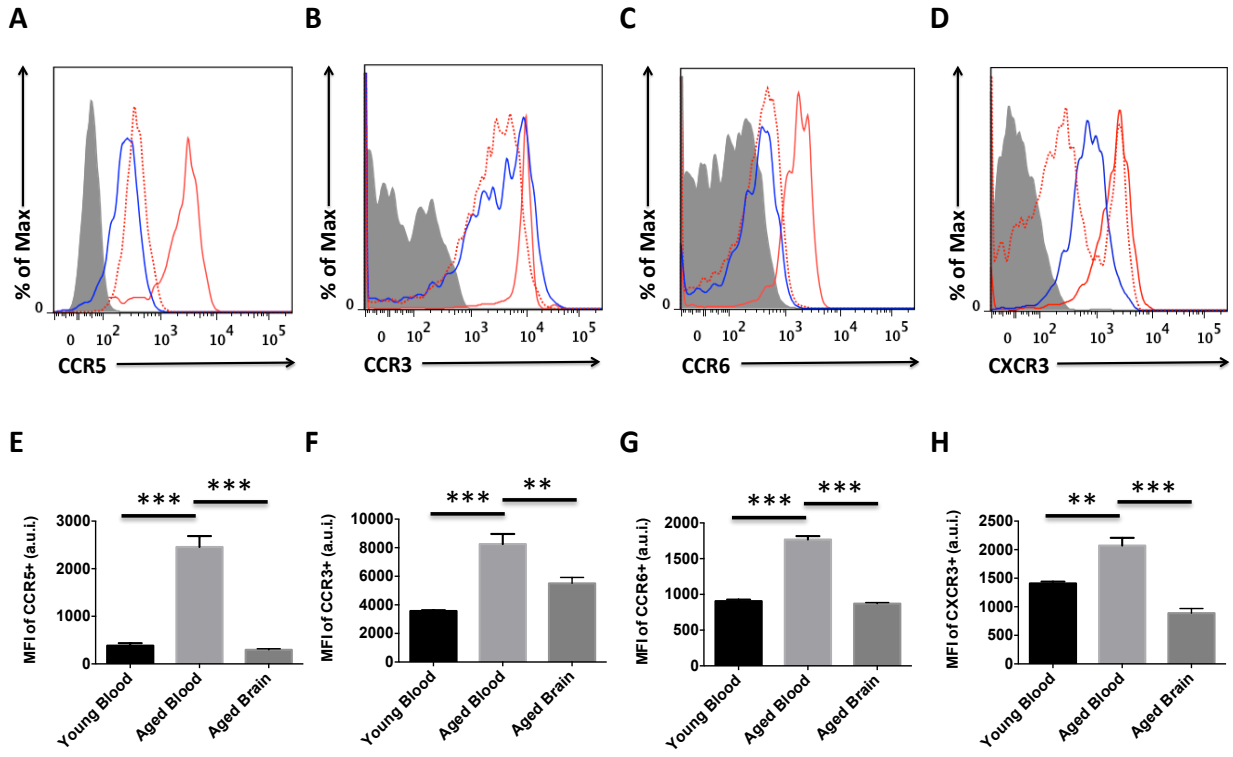

Figure 6-3. CD8 T cell chemokine receptor expression with age.

Representative histograms show higher expression of CCR5 (A), CCR3 (B), CCR6 (C), and CXCR3 (D) on circulating CD8 T cells with age, and down-regulation in the brain. Young blood (dotted red), aged blood (solid red), and aged brain (blue) CD8 T cells are depicted. The mean fluorescence intensity for each of the respective chemokine receptors was quantified (E, F, G, and H; N=5/group). Cell-specific FMO controls were used to determine positive gating (shaded gray). Error bars show mean SEM. Abbreviation: SEM standard error of mean, MFI mean fluorescence intensity. *p<0.05; **p<0.01; ***p<0.001

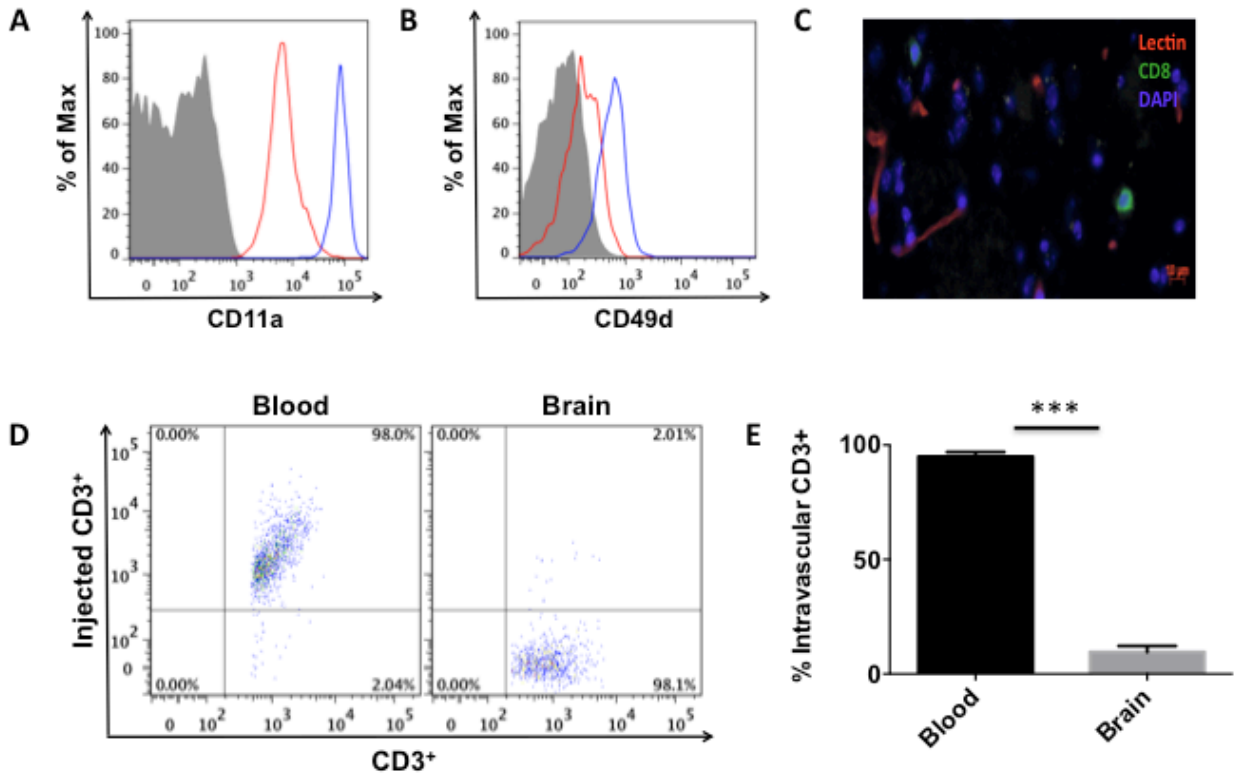

Figure 6-4. Extravasation of CD8 T cells into the aged brain.

A representative histogram depicts higher expression of the adhesion molecules CD11a (A) and CD49d (B) on CD8 T cells in the aged brain (blue) relative to those in the blood (red; N=5/group). Immunohistochemistry shows the presence of CD8-positive cells (green) outside of lectin-positive (red) blood vessels (C). A representative dot plot from the Intravascular labeling experiment shows the absence of injected-CD3+ antibody on CD8 T cells in the aged brain (D). The percentage of intravascular-labeled CD3+ CD8 T cells was quantified in the aged brain and blood (for control). For the intravascular labeling experiment, N= 8/group. Cell-specific FMO controls were used to determine positive gating (shaded gray). Error bars show mean SEM. Abbreviation: SEM standard error of mean. *p<0.05; **p<0.01; ***p<0.001

immunohistochemistry, we identified the putative presence of CD8 T cells outside of lectin-positive lumen of vessels (**Figure 6-4C**). To confirm that T cells resided in the parenchymal tissue, and were not adherent to the brain endothelium, we performed an injection labeling experiment as previously described [388,389]. All circulating and vessel-associated cells bound to transcardially injected PE-conjugated CD3e antibody, processed for leukocyte collection, and subsequently stained with APCeF780-conjugated CD3e antibody. Compared to an injection labeling efficiency of ~98% for all blood CD3e-injected^{+}CD8 T cells, only 7.7±5% of aged brain CD8 T cells were positive for CD3e-injected antibody, suggesting these cells are located outside of the vascular network and in the parenchyma or perivascular spaces (**Figure 6-4D-E**). Immunohistology revealed the presence of CD3^{+}CD8^{+} T cells in circumventricular organs (choroid plexus and meninges) and most gray and white matter regions (cortex, striatum, corpus collosum) throughout the anterior-posterior axis of the brain (**Figure 6-5A-B**). Further, we found that these cells were often associated with astrocytes, although the precise nature of this association is unknown (**Figure 6-5C**).

Age-related, CNS-specific CD8 T cells have memory/effector phenotype and expression markers of T cell-receptor activation

The trafficking of T cells into CNS tissues is thought to occur following antigenic presentation in draining lymph nodes by professional antigen-presenting cells. Antigen-experienced memory T cell subsets are defined by CD44^{+}CD62L^{+} (Central Memory, T_{CM}) and CD44^{+}CD62L^{-} (Effector Memory, T_{EM}) expression, whereas naïve T cells are

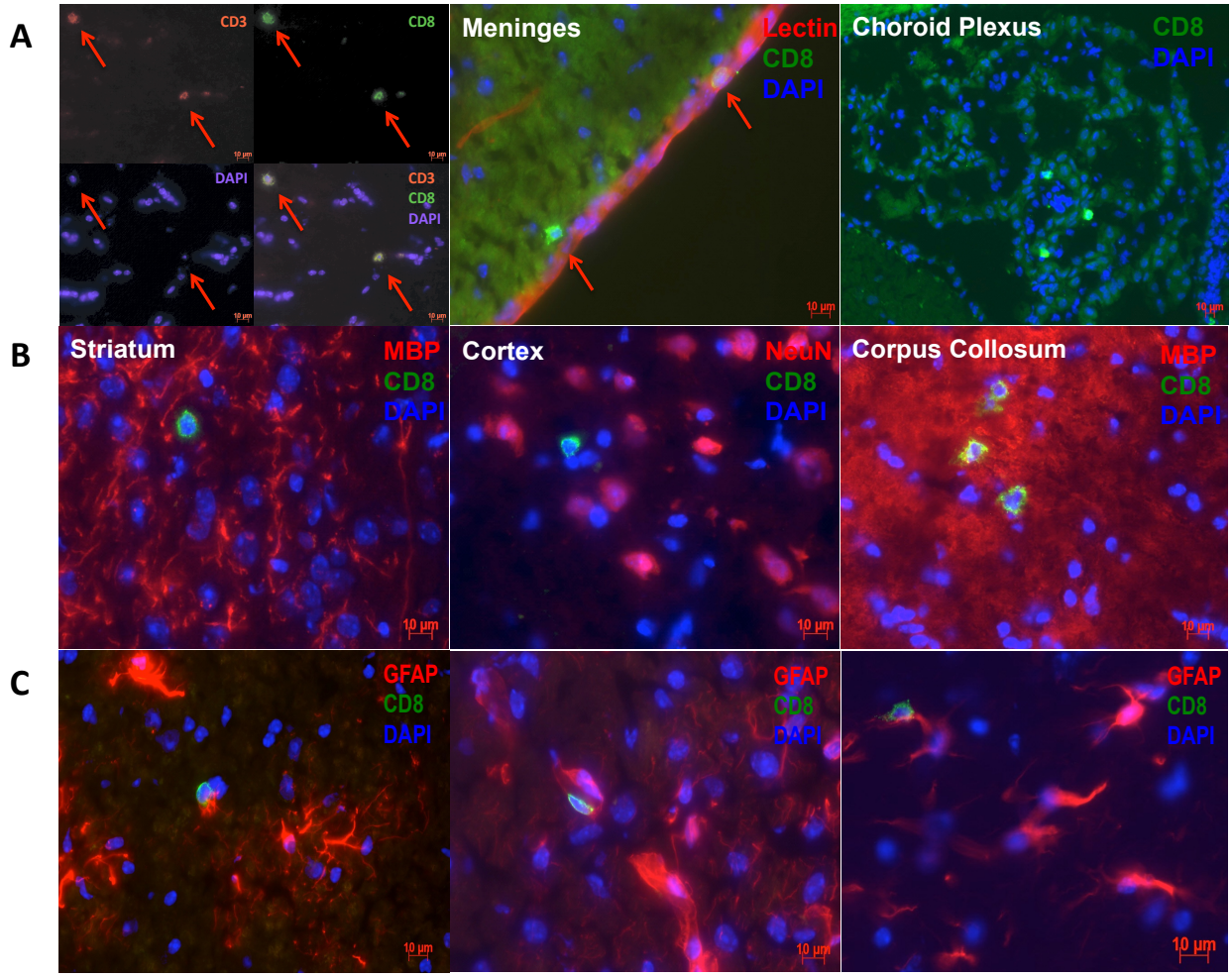

Figure 6-5. Histological assessment of CD8 T cells in the aged brain.
Representative 10um-thick brain tissue sections illustrating the presence of $CD3^{+}CD8^{+}$ T cells in the aged brain, meninges, and choroid plexus (A). CD8+ T cells were found throughout the anterior-posterior axis of the brain, including the striatum, cortex, and corpus collosum (B) and in association with activated astrocytes (C). . Abbreviation: DAPI 4',6-diamidino-2-phenylindole, MBP myelin basic protein, NeuN neuronal nuclei, GFAP glial fibrillary acidic protein.

largely negative for the activation marker CD44 (Roberts AD et al 2004). Applying this paradigm to CD8 T cells in the aging brain we found that the vast majority (87±4%) of all CNS-specific CD8 T cells have an effector memory phenotype (N=5), compared to just 9±4% of blood CD8 T cells (**Figure 6-6A-B**). A similar percentage of T cells with effector memory phenotype was observed in young brains, despite the fact that T cells were found in significantly lower abundance. To determine the general activation state of CNS-specific CD8 T_{EM} cells we probed these cells with known markers of T cell activation. The early activation and tissue-retention marker, CD69, was highly upregulated on CNS-specific CD8 T cells compared to those in the blood (**Figure 6-6C**, N=5, $p<0.001$). Expression of programmed death-1 (PD-1) receptor, which is upregulated on activated T cells, was also dramatically increased on nearly all CNS-specific T cells compared CD8 T cells in aged blood (**Figure 6-6D**, $p<0.0001$), implying the presence of widespread T cell activation in the aged brain. Expression of the resident memory marker alpha E integrin CD103 was also found on a significant fraction of these cells (**Figure 6-6E**). The following data suggest that a pool of activated, antigen-experienced memory effector CD8 T cells are constitutively present throughout adult life in the CNS.

Age-related recruitment of CNS-specific CD8 T cells is mostly stochastic

To determine if CNS-specific CD8 T cells were responding to antigenic signals present in the aging CNS, CD8 T cells in the blood, CNS, liver, adipose, and lung were screened for TCRvβ usage to determine T cell clonality in tertiary tissues. No

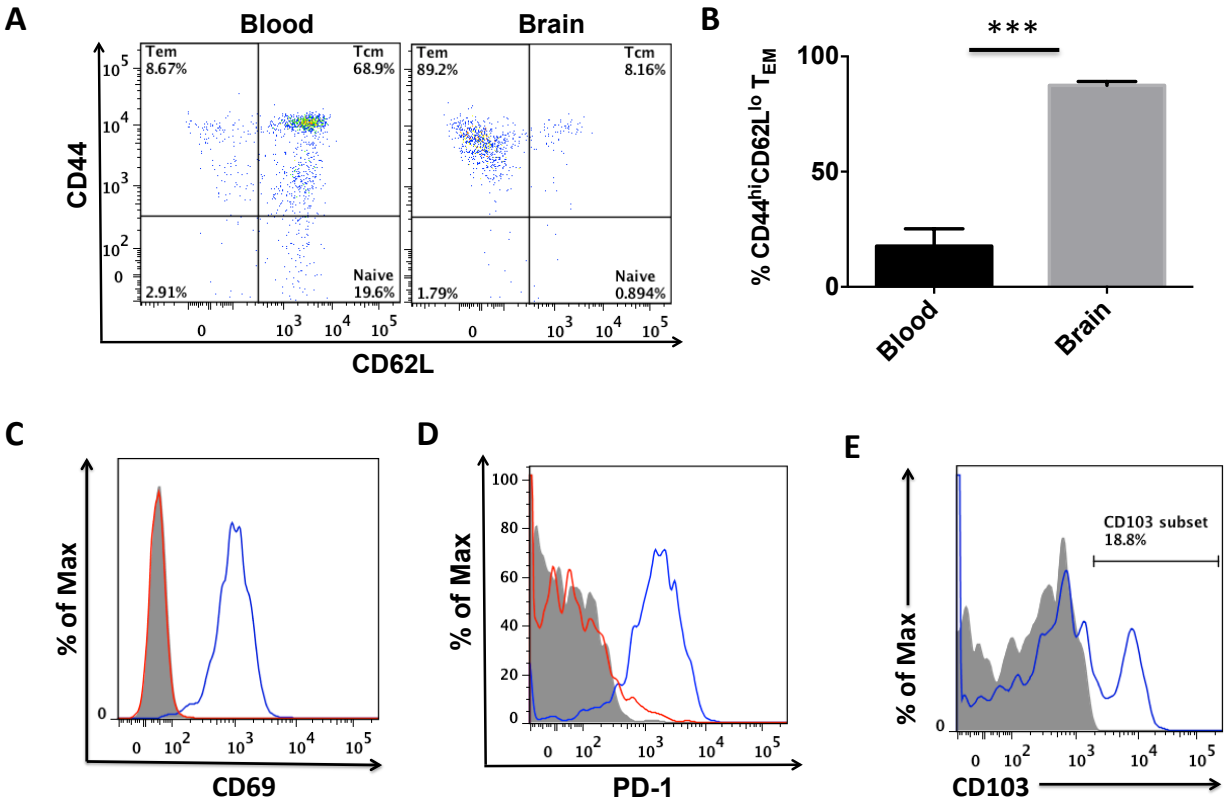

Figure 6-6. CNS-specific CD8 T cells have resident and effector memory phenotypes.

A representative dot plot shows effector memory phenotype of CD8 T cells in the aged brain and central memory phenotype of CD8 T cells in the aged blood (A). The percentage of CD8 T cells with effector memory phenotype ($CD44^{hi}CD62^{lo}$) was quantified (B). Representative histograms depict significant expression of the activation markers CD69 (C) and PD-1 (D) in the brain (blue) relative to blood (red), as well as the resident memory marker CD103 (E). For all experiments, N= 5-6/group. Cell-specific FMO controls were used to determine positive gating (shaded gray). Error bars show mean SEM. Abbreviation: SEM standard error of mean. *p<0.05; **p<0.01; ***p<0.001

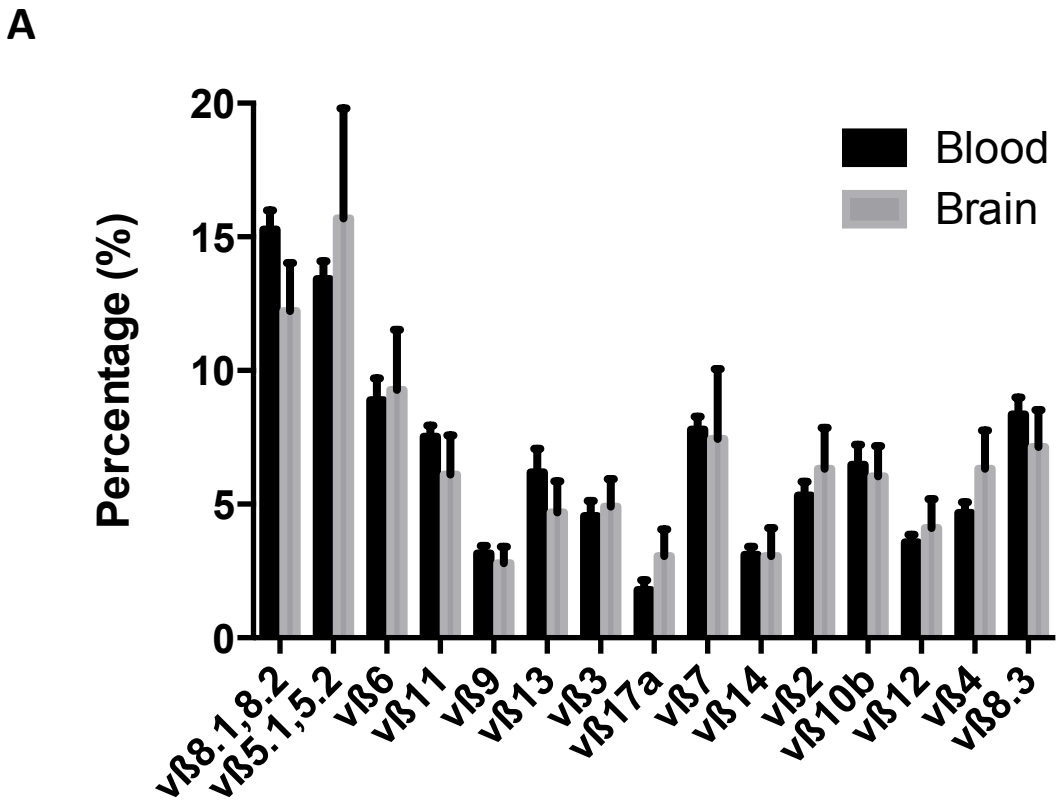

Figure 6-7. Characterization of CD8 T cell receptor v beta usage in the aged brain. A mouse vβ TCR screening panel containing 15 FITC-conjugated monoclonal antibodies was used to assess TCR vβ usage in the blood and brain of aged mice. The mean percentage for each of the 15 subfamilies of T cell receptor vβ (A). No differences were found between groups (N= 11/group). Cell-specific FMO controls were used to determine positive gating. Error bars show mean SEM. Abbreviation: SEM standard error of mean.

differences in TCRvβ usage between CNS-specific CD8 T cells and their blood counterparts was found for any of the 15 TCRvβ families (**Figure 6-7A)**. Based on the absence of major clonal expansions in the CNS, these results suggest that CD8 T cell entry into the aged brain is largely random, rather than antigen-driven.

Increased immune surveillance by CD8 T cells in the aging brain is associated with healthier microglial function

We investigated the functional role of CNS-specific CD8 T cells indirectly by correlating the absolute number in each brain with the activation status of microglia in that brain. Correlation analyses revealed that aged brains with greater numbers of CNS-specific CD8 T cells had significantly more microglia (**Figure 6-8A**, $p<0.05$), indicating that these cells may promote microglia survival or prevent microglial death. Brains that contained large numbers of CNS-specific CD8 T cells were also associated with smaller sized microglia relative to brains with fewer CD8 T cells (**Figure 6-8B**, $p<0.05$), indicative of a more ramified, resting morphology. Functionally, higher numbers of T cells were associated with increased microglia phagocytosis (**Figure 6-8D**, $p<0.001$) and decreased TNF production (**Figure 6-8C**, $p<0.05$). These data imply that CNS-specific CD8 T cells promote an anti-inflammatory, injury-resolving microglia phenotype in the aged brain.

Basal and stimulus-driven production of cytokines and chemokines associated with neutrophil chemotaxis following ischemic stroke

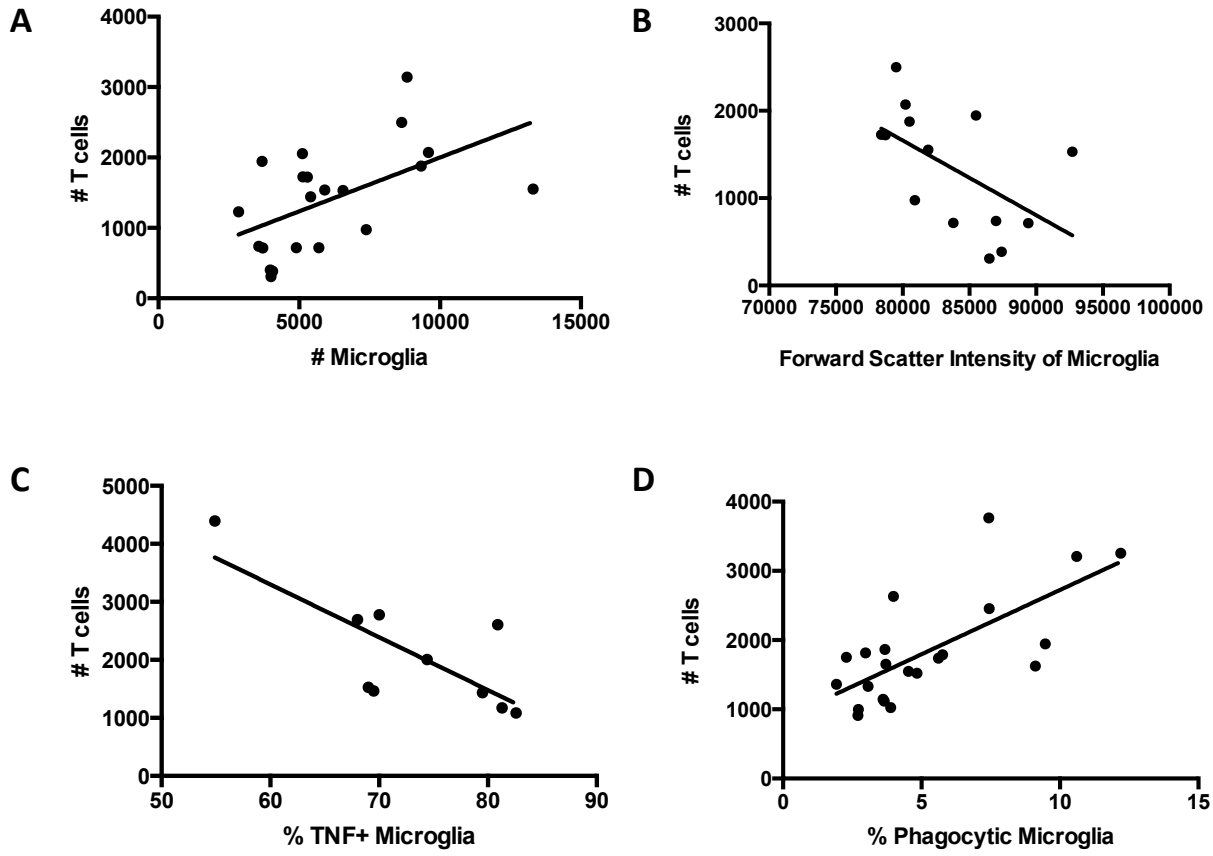

Figure 6-8. Correlational analyses of CNS-specific CD8 T cell counts and microglia function in the aged brain.

Correlation analysis between CD8 T cell count and microglia count (A, p=0.0125 and r=0.534), forward scatter/cell size (B, p=0.0421 and r=-0.5488), percentage TNF-positive (C, p=0.0105 and r=-0.7616), and percentage bead-positive phagocytic (D, p=0.0003 and r=0.6945). For all experiments, N= 10-22/group. Cell-specific FMO controls were used to determine positive gating. Abbreviation: TNF tumor necrosis factor.

T cells are polarized to effector memory cells following TCR reactivation to selected antigenic stimuli. The effector function of these cells is largely specified by cytokine production. An *in vivo* brefeldin protocol was used to measure cytokine production in CNS-specific CD8 T cells as in [390]. Cytokines commonly associated with CD8 T cell pro-inflammatory responses (TNF and IFNγ) were basally produced at significant levels (**Figure 6-9A-C**), whereas granzyme B was not expressed under any conditions (**Supplemental Figure 6-3A**). Both the number and relative expression level of TNF and IFNγ were significantly increased after stimulation in CNS-specific CD8 T cells compared to those in blood (**Figure 6-9D-F**, $p<0.001$). Interestingly, basal production of IL-17A and IL-17F was observed in CNS-specific CD8 T cells but not in blood or spleen (**Figure 6-10D-I**). The mean fluorescence intensities of IL-17A and IL-17F were significantly increased in CNS-specific CD8 T cells after stimulation (**Figure 6-10F and 6-10I**, $p<0.05$ and $p<0.01$, respectively). Given the prominent role of IL-17 in neutrophil chemotaxis we assessed these cells for the heightened production of other chemokines. CCL2 and CCL5 production by CNS-specific CD8 T cells was significantly higher at baseline and after stimulation compared to those in the blood (**Figure 6-9C and 6-9F**, $p<0.001$; **and Figure 6-10A-C**, $p<0.001$). These data suggest that CNS-specific T cells in the aged CNS are a rich source of pro-inflammatory cytokines, likely contributing to the steady increase in overall levels that occurs with advanced age. CNS-specific CD8 T cells appear to be significantly more primed to produce higher levels of pro-inflammatory cytokines and chemokines involved in neutrophil chemotaxis following activation. Next we determined whether these cells were similarly responsive to brain injury. We tested this in an experimental model of ischemic stroke, as this is a disease

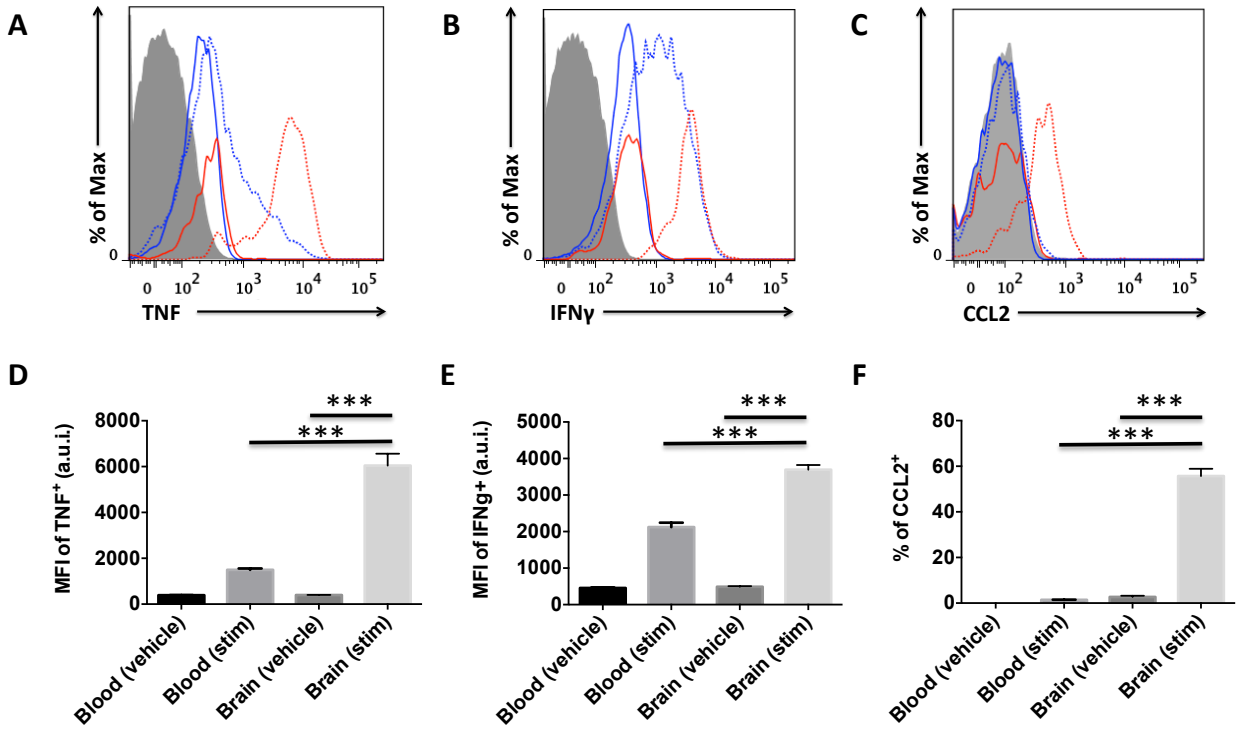

Figure 9. PMA/ionomycin-induced cytokine production of CD8 T cells in the aged brain.

Representative histograms show CD8 T cell expression of TNF (A), IFNγ (B), and CCL2 (C) in blood (solid blue) and brain (solid red) and after stimulation (dotted). The respective mean fluorescence intensities (D, E, F) were quantified. For all experiments, N= 4-10/group. Cell-specific FMO controls were used to determine positive gating (shaded gray). Error bars show mean SEM. Abbreviation: SEM standard error of mean, MFI mean fluorescence intensity, a.u.i. arbitrary units of intensity, TNF tumor necrosis factor, IFNγ interferon gamma, CCL2 monocyte chemoattractant protein-1. *p<0.05; **p<0.01; ***p<0.001

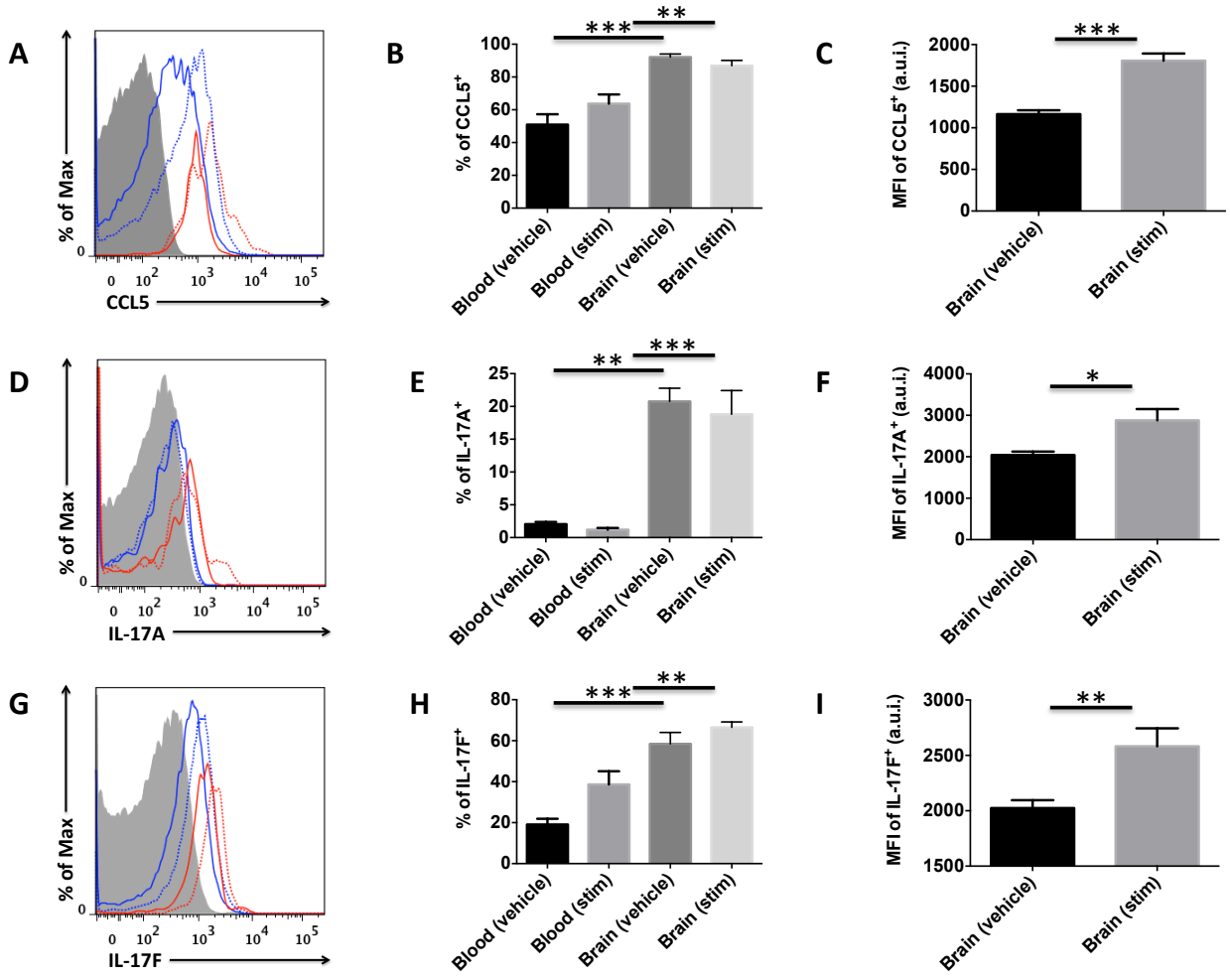

Figure 6-10. PMA/ionomycin-induced production of neutrophil chemokines by CD8 T cells in the aged brain.

Representative histograms show CD8 T cell expression of CCL5 (A), IL-17A (D), and IL-17F (G) in blood (solid blue) and brain (solid red) and after stimulation (dotted). The respective percentages (B, E, H) and mean fluorescence intensities (C, F, I) were quantified. For all experiments, N= 4-10/group. Cell-specific FMO controls were used to determine positive gating (shaded gray). Error bars show mean SEM. Abbreviation: SEM standard error of mean, MFI mean fluorescence intensity, a.u.i. arbitrary units of intensity. *p<0.05; **p<0.01; ***p<0.001

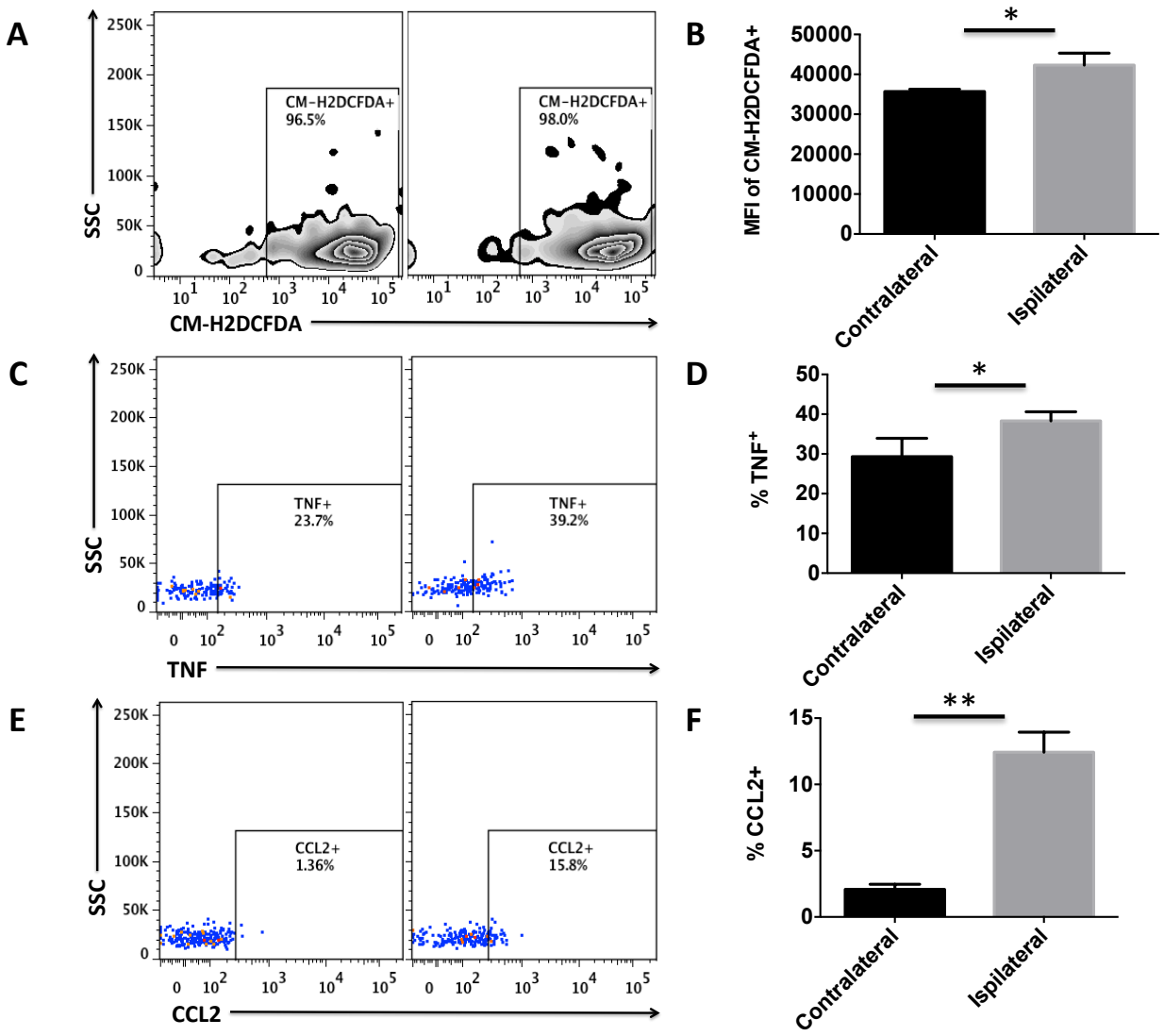

Figure 6-11. (Legend on following page)

Figure 6-11. Acute stimulation of CD8 T cells in an age-relevant model of cerebral ischemia.

Aged mice were subject to 60 minutes of occlusion followed by 2 hours of reperfusion and 1 hour ex-vivo stimulation by PMA/ionomycin. CD8 T cells from the ischemic hemisphere (ipsilateral) were compared to those in the contralateral hemisphere for internal control. A representative zebra plot shows reactive oxygen species levels in CD8 T cells after stroke as measured by CM-H2DCFDA (A) and quantification of mean fluorescence intensity (B). A representative dot plot shows intracellular production of TNF (C) and the percentages quantified (D). A representative dot plot depicts a stroke-induced increase in CCL2 production by CD8 T cells in the aged brain (E). The percentages were quantified (F). For all experiments, N= 4/group. Cell-specific FMO controls were used to determine positive gating. Error bars show mean SEM. Abbreviation: SEM standard error of mean, SSC side scatter intensity, MFI mean fluorescence intensity, CM-H2DCFDA 5-(and-6)-chloromethyl-2',7'-dichlorodihydrofluorescein diacetate, acetyl ester, TNF tumor necrosis factor, CCL2 monocyte chemoattractant protein-1. *p<0.05; **p<0.01; ***p<0.001

that mainly affects the aging population. Cytokine production was assessed at 2 hours post-reperfusion following 60 minutes of occlusion. Reactive oxygen species generation was significantly increased in CD8 T cells subjected to ischemia compared to those in the control contralateral hemisphere, as evidenced by CM-H2DCFDA staining (**Figure 6-11A-**B, $p<0.05$). The percentage of TNF- and CCL2-positive CD8 T cells was also increased in ischemic hemisphere compared to control (**Figure 6-11C-F**, $p<0.05$ and $p<0.01$, respectively). These data suggest that activated CNS-specific CD8 T cells contribute to the age-related exacerbation of acute ischemic brain injury by amplifying production of pro-inflammatory cytokines and promoting recruitment of peripheral leukocytes.

Discussion

This work has identified a novel population of immune surveillant CD8 T cells in the CNS that have opposing roles in health and disease. The present study has added to previous findings confirming that immune privilege in the aging CNS is compromised and more permissive to T cell entry. We base this observation on several criteria: 1) increased production of T cell chemokines, 2) expression of adhesion molecules, 3) extravasation into perivascular and parenchymal regions, 4) activated effector memory phenotype, 5) presence alters microglia function, and 6) primed to elicit strong cytokine and chemokine responses after brain injury. These cells have a phenotype indicative of resident memory cells ($CD44^{hi}$ $CD62L^{-}$ $CD11a^{+}$ $CD69^{+}$ $CD103^{+/-}$). To our knowledge,

this is the first study to systematically characterize CD8 T cells in the normal aging CNS and identify a population of CNS-specific T cells with resident memory phenotype and the potential to influence the neuroimmunological landscape.

We have shown that aging increases production of T cell chemokine signals originating from the brain, providing gradient cues for the directed migration of circulating T cells. Moreover, our findings support other studies that have shown aging to increase chemokine receptor expression on T cells and the chemotactic response to these cues [391-394]. The expression of chemokines is generally associated with increased microglia activation in aging mice, suggesting that chemokines may contribute to decreased brain function that occurs during normal aging. Two of these chemokines, Eotaxin and IP-10, have been recently described as biomarkers for neurodegenerative disease and aging [395,396]. Systemic administration of eotaxin (CCL11) in young mice has been shown to decrease neurogenesis and induce defects in learning and behavior [397]. Chemokines may also play an important role in injury repair as several chemokines have been shown to be essential for the attraction, differentiation, survival, and cytokine production of stem cells [398]. It remains to be seen whether immune surveillance can be abolished using a chemokine blockade and what those effects would have on glial function and cognitive status.

Recent evidence suggests that locoregional leakiness in the hippocampus increases with age [51]. Elahy M et al (2015) [399] have shown that blood-brain barrier tight junction proteins are down-regulated in the cortex and hippocampus with age resulting in regional neuroinflammation, but not leukocyte infiltration. Because sites of leukocyte infiltration do not necessarily correlate with the areas showing the most leakage, it

appears more likely that leukocytes enter the CNS via a specified, active process of extravasation [400]. Indeed, we found that CNS-specific CD8 T cells expressed high levels of the integrins CD11a and CD49d, two adhesion molecules required for entry into tertiary tissues [401]. Because endothelial-ICAM expression has been shown to be enhanced with age [387], we evaluated the potential for these cells to be adherent to vessels. We discovered that the majority of CNS-specific CD8 T cells were not associated with the vascular lumen. In fact, CNS-specific CD8 T cells were largely found to have extravasated beyond the vascular lumen into many parenchymal regions across the CNS. The presence of CNS-specific CD8 T cells in the CNS parenchyma underscores their potential importance to CNS function.

The present study has demonstrated that the normal aging brain contains greater numbers of CD8 than CD4 T cells. A recent study on post-mortem human tissue suggests that CD8 T cells are more enriched in the corpus collosum compared to peripheral blood [384]. The authors noted the distribution of these cells to the perivascular space and parenchyma. The ratio of nearly 3.5:1 of CD8-to-CD4 T cells in the normal aged CNS tissue is intriguing given that the reciprocal ratio is found in cerebrospinal fluid and in the choroid plexus [376,402,403]. The presence of CD8 T cells in the CNS parenchyma suggests they interact with neurons and glial to serve an effector role rather than as sentinels at the interface between the blood and the cerebrospinal fluid. CD8 T cells have received comparably less attention than their CD4 counterparts with regard to CNS disease and aging. This is partly due to their narrowly defined role in anti-viral responses. Yet, emerging data suggests that CD8 T cells may play more diverse roles in disease settings than previously considered. Mounting evidence

supports a role for CD8-mediated immune surveillance in peripheral tissues as part of the body's normal defense against cancer and viral infection [382]. The prevalence of pathogenic and oncogenic insults increases with age, triggering the induction of intrinsic defense mechanisms such as cell death signaling and senescence. Naturally extrinsic mechanisms evolved that alert the immune system to eliminate these cells to prevent further bystander damage. One mechanism through which this occurs is via immune surveillance of tissue-patrolling CD8 T cells. These cells specify elimination of unhealthy cells that increase presentation of non-self peptide. The role of immune surveillance in aging individuals and like-wise the effect of aging on the efficacy of immune surveillance is understudied and warrants further investigation given the relationship between aging and disease.

CD8 T cell-astrocyte interactions have also received growing attention [404,405]. Functional evidence that CD8 T cells are prime candidates for immune surveillance of the CNS is based on the exquisitely specific destruction of transgenic astrocytes expressing MHCI-restricted hemagglutinin [406]. In this study, CD8 T cell-mediated removal of antigen-containing astrocytes occurred in absence of leukocyte infiltration or bystander damage to oligodendrocytes and neurons. Moreover, OVA-expressing oligodendrocytes elicit the proliferation and effector memory conversion of responding OT-1 T cells in healthy mice without infiltrating the CNS, indicating that antigen sampling is performed by CD8 T cells under steady state conditions [290]. Interestingly, the authors found that neuroinflammation augmented the level of antigen sampling and led to the accumulation of OT-1 T cells in the inflamed brain. Thus, it is increasingly evident that CD8 T cells have the capacity to mediate responses against CNS antigens

[407]. While the age-related increase in neuroinflammation likely promotes the recruitment of immune surveillant CD8 T cells, how they impact CNS function is poorly understood. Tissue-resident memory CD8 T cells (T_{RM}) provide superior protection against viral reactivation compared to the circulating memory T cell pool [408,409]. The increased presence of these cells in the aged CNS may reflect an evolutionary need to generate a rapid response to control senescent transformation of cells and/or prevent reactivation of latent neurotropic viruses.

The role of immunosurveillance as a defense mechanism that safeguards the functional integrity of tissues implies that it is an adaptive response to an environment under constant insult. Normal aging is associated with deficits in microglia phagocytosis and increased expression pro-inflammatory mediators [385]. We demonstrated that the increased presence of CNS-specific CD8 T cells in older brains was associated with an attenuation of TNF production and enhanced phagocytic activity by microglia. Although causality cannot be proven, the effects of CD8 T cells on microglia need not occur via direction cell-cell interaction. As well, while T cells are generally associated with CNS injury, several studies have that T cells can enter the brain and not cause glial pathology [287]. Furthermore, emerging data indicates that T cells may function to support learning and memory under normal physiological conditions [379]. It is possible that by eliminating nearby senescent cells CD8 T cells serve to attenuate age-related neuroinflammation, thereby indirectly preventing the chronic activation of microglia.

Antigen-specific CD8 memory T cells remain at stable levels in peripheral tissues for prolonged periods of time in the complete absence of antigen by cytokine-driven homeostatic proliferation [410-412]. Such resident memory cells can enter peripheral

tissues and form the front line of defense against reinfection, but become dependent on the local milieu for function and survival [413]. Our findings indicate that CNS-specific CD8 T cells are not of central memory phenotype, but rather represent a unique subset of effector memory cells. As T_{EM} cells, CNS-specific CD8 T cells have remarkable effector function, but low proliferative potential compared to T_{CM} [414]. Unpublished work from our laboratory also supports the notion that these cells are not mitotically active (data not shown). These findings suggest that CNS-specific CD8 T cells are poised to provide immune surveillance in peripheral tissues.

The question remains whether TCR activation precedes the migration of CD8 T cells into the CNS, or whether activation occurs *in situ*. Our finding that CD69, an early activation marker, and PD-1 expression are induced in CNS-specific CD8 (and CD4) T cells and not circulating T cells, suggests that the putative TCR triggering event occurs primarily *in situ*. However, it is possible CD8 T cells are primed and/or re-activated in the cervical lymph nodes, as some degree of prior activation likely occurs at the level of the blood-CNS barrier interface, enabling the expression of adhesion molecules required for entry.

Given the lack of stereotypical anti-viral responses and recent evidence showing clonal expansion of CNS antigen-specific CD4 T cells in the choroid plexus of aged mice, we hypothesized that CNS-specific CD8 T cell activation is similarly induced by CNS antigen. However, we reported relatively little clonal expansion of TCRvβ subsets in the aged CNS as evidenced by equilibrium in TCRvβ usage between those in the CNS and other non-lymphoid tissues. Thus, our data argue that their migration into the CNS is stochastic and not antigen-driven. Consistent with our findings, studies using

OVA-specific T cells have shown that CNS-irrelevant T cells recognizing non-mammalian antigen also have the capacity to enter the CNS [287]. Similarly, intracranial injection of dendritic cells loaded with OVA peptide resulted in T cell priming in peripheral lymphoid organs and the subsequent infiltration and persistence of OT-1 T cells into the brain for at least 30 days [413]. However, recent findings by Baruch et al (2014)[415] have elegantly demonstrated that splenic CD4 T cells of mice immunized with spinal cord homogenate had a similar TCRβ repertoire composition as CD4 T cells in the aged choroid plexus. Because the age-related accumulation of CD8 memory cells described in our study represent a naturally occurring population of CNS-specific T cells, it may stand as a better model for understanding the biology of this subset of cells. Taken together, migration of effector memory CD8 T cells into the aged CNS does not require stimulation by CNS antigen, although deeper sequencing of the T cell receptor repertoire might be a useful approach in determining the antigenic specificity of these cells.

Memory T cells traffic into inflamed tissues where they can exert effector functions permitting they receive the necessary antigenic signals. Although not reported in this study, we believe it is important to note that CNS-specific CD4 T cells shared many of the same characteristics as CNS-specific CD8 T cells, including effector phenotype and IL-17A expression. These findings illustrate that while there appears to be a select preference for CD8 T cells to migrate into the CNS, the cues and mechanisms underlying T cell recruitment are not exclusively CD8-mediated. Although IL-17-expressing CD4 T cells have been well studied in the context of autoimmune disease, less is known regarding the role of their CD8 counterparts, or Tc17 cells.

Human Tc17 cells have recently been described in healthy individuals [416]. Increased numbers of Tc17 are detectable in cerebrospinal fluid (CSF) from patients with early-stage MS, suggesting their potential contribution to disease progression in human [417-419]. Recent work has shown that the developmental pathways of Tc17 and CTL are mutually exclusive; with Tc17 cells displaying greatly suppressed cytotoxic function and low levels of CTL markers granzyme B and IFNγ [420]. Similarly, CD8 T cells found in the corpus collosum of older individuals exhibited low levels of cytolytic enzymes [384]. Because CTL CD8 T cells have been shown to kill neurons via Fas Ligand and perforin cell death pathways in vitro, the lack of these effector molecules on CNS-specific CD8 T cells does not support a neurotoxic role [421]. Yet, at sites of inflammation IL-17 functions by inducing the expression of IL-1β, IL-6, and TNF by many cells and has an inhibitory effect on neurogenesis. In addition, IL-17 promotes the induction of chemokines important for neutrophil recruitment. The role of IL-17 in the aging CNS requires further investigation.

We demonstrated that upon activation by either PMA/ionomycin stimulation or ischemic brain injury, CNS-specific CD8 T cells in aged brains are prone to highly volatile responses that include the enhanced production of reactive oxygen species, TNF, and IFNγ, as well several chemokines involved in granulocyte recruitment. These cells may therefore predispose the aged brain to overreact to stimuli, further exaggerating the inflammatory response and altering the context of injury via the recruitment of injury-causing neutrophils. This is in contrast to that of the infiltrating CD8 T cell population, which is involved in the delayed response to ischemia during the recovery period. Indeed, the inflammatory milieu and leukocyte response in the

ischemic brain is dramatically different in older mice [422-426]. Furthermore, these exaggerated immune responses are tightly linked to worse outcomes in aged mice [427,428]. For example, unpublished data from our laboratory found that neutrophils are the predominant leukocyte in the ischemic brain of aged mice, whereas monocytes largely comprise the infiltrating population in young mice. Neutrophils contribute to neuronal injury and blood-brain barrier breakdown through the release of oxidative stress signals and matrix metalloproteinases, respectively [429,430]. Whether stroke-induced activation of CNS-specific CD8 T cells results in the biased recruitment of neutrophils in the aged brain by producing elevated levels of chemokines is not known, but would provide an alternative explanation for differences in the kinetics of leukocyte infiltration with age. Moreover, given their role in promoting leukocyte recruitment, CNS-specific CD8 T cells may represent important therapeutic targets in the acute period following stroke.

In this study we have demonstrated that tissue-resident, memory effector CD8 T cells make up the majority of peripherally recruited cells in the aged CNS. To date, our efforts have been focused on resolving the phenotype of these cells in order to understand their role in the CNS; however, more work will be required to ascertain the importance of this population with regard to CNS function. The absolute number of these cells obtained from the aged brain prohibits their utility in adoptive transfer experiments, which require on the order of 500,000 cells to achieve significant engraftment. Nevertheless, our findings suggest that CNS-specific CD8 T cells are poised to influence CNS function by direct interaction with aged glial cells. This data suggests that the working definition of ‘inflamm-aging’ in the CNS be revised to include the increased level of immune surveillance by CD8 T cells. The discovery that resident

microglial function is influenced by the increased presence of these cells leads us to speculate whether this effect is direct or indirect and which mechanisms likely underlie these changes. However, the beneficial role for CD8 T cells in suppressing the pro-inflammatory activity of microglia while increasing phagocytosis is offset by their exaggerated response to stimuli resulting in significant production of pro-inflammatory cytokines and chemokine signals that favor recruitment of granulocytes. As such, the functional role of these cells may be best described as a double-edged sword - advantageous under normal conditions, but prone to exacerbate injury when stimulated. This opposing role may likely account for the observed differences in brain inflammation found in older mice following traumatic injuries such as ischemic stroke. Future studies are needed to determine whether these interactions can be experimentally manipulated to better understand their functional role in normal aging.

A

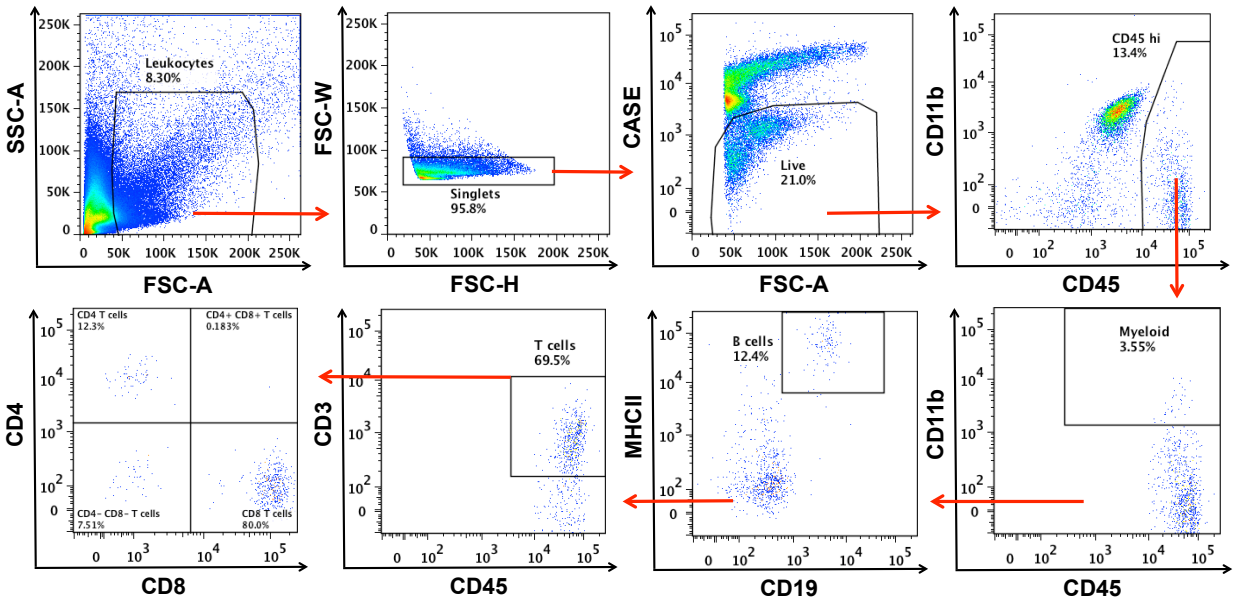

Supplementary Figure 6-1. Flow cytometry gating strategy for identification of leukocytes.

A representative series of dot plots illustrating the gating strategy used in this study (A). The initial leukocyte gate is based on the typical scatter properties for spenocytes. Subsequently, singlets were selected for to eliminate doublets and cell clumping. CASE dye exclusion is used to identify living cells. $CD45^{int}CD11b^{+}$ microglia represent the resident macrophages, whereas the $CD45^{hi}$ leukocyte population is bone marrow-derived and not native to the CNS. $CD45^{hi}CD11b^{+}$ represent the peripheral myeloid population. $CD45^{hi}$CD11b-negative cells are putative lymphocyte populations. The lymphocyte population is generally composed of $CD19^{+}MHCII^{+}$ B cells and $CD3^{+}CD4^{+}$ and $CD3^{+}CD8^{+}$ T cells. FMO controls were used to determine positive gating. Abbreviation: SSC side scatter intensity, FSC forward side scatter, CASE carboxylic acid succinimidyl ester.

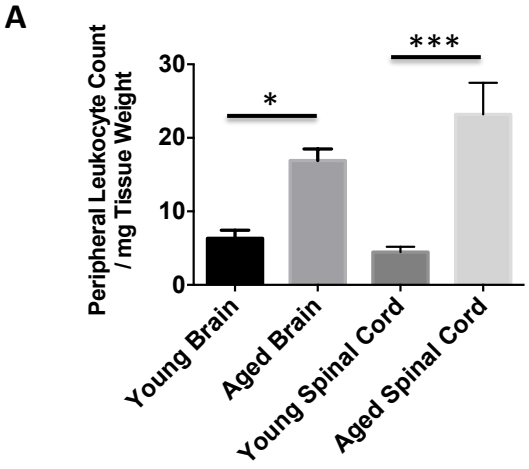

Supplementary Figure 6-2. Peripheral leukocyte counts in the brain and spinal cord with age.

The absolute number of $CD45^{hi}$ peripheral leukocytes in young and aged brain hemispheres and spinal cords normalized to tissue weight (A, N=10-15/group). Error bars show mean SEM. Abbreviation: SEM standard error of mean. *p<0.05; **p<0.01; ***p<0.001

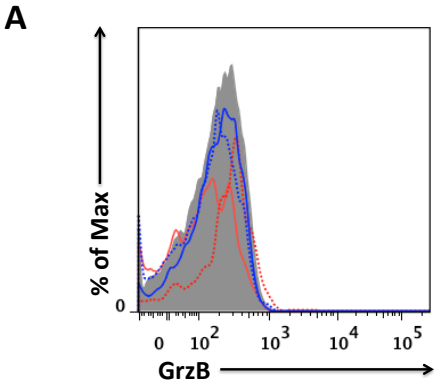

Supplementary Figure 6-3. Lack of granzyme B expression by CD8 T cells in the aged brain.

A representative histogram shows an absence of granzyme B production by CD8 T cells in aged blood (solid blue) and brain (solid red) and following stimulation (dotted, N=4-10, A).

Authors' Contributions

RMR and LDM conceived the project. RMR performed most of the experiments and ARP and JC assisted with the flow cytometry preparations. JC performed the immunohistochemistry experiments. ERJ assisted the analysis and interpretation of the flow cytometry data. RMR and LDM wrote the paper. All authors read and made comments on the manuscript draft and approved the final manuscript.

Acknowledgements

This work was supported by National Institutes of Health grants R21 NS076293-01A1 (Louise D. McCullough) and F31 NS083244-01A1 (Rodney M. Ritzel).

Chapter 7:

Significance and Future Directions

Significance:

To date, the functional contribution of CD200R1 signaling to CNS homeostasis and disease pathogenesis has been mostly limited to expression studies and those examining its role in autoimmune disease models of multiple sclerosis and uveitis (Chapter 1). However, the majority of brain injuries are sterile in nature. This work examined the microglial response to normal aging and ischemic brain injury, with particular emphasis on the role of CD200R1 in regulating these responses. Through our investigations we have made several novel findings, not the least of which is the revelation that CD200 is essential for survival following stroke (Chapter 4). Although we have found a lack evidence of implicating CD200R1 as a major regulator of microglia, its role in the CNS is critical to maintaining the brain's immune privileged status and in preventing chronic brain inflammation and peripheral immune suppression after stroke.

Despite sharing common myeloid origin and phenotypic similarities, our work found that the microglial response to ischemic stroke is unique among macrophages and other cells of this lineage (Chapter 2 and 3). We demonstrated that microglia, likely a result of being resident, are highly vulnerable to the effects of ischemia. These cells tended to become increasingly pro-inflammatory and apoptotic over time. Conversely,

stimulus-driven production of monocytes in the bone marrow favored their recruitment to the ischemic brain where they displayed a remarkable capacity for phagocytosis. These findings are the first to show differential changes in microglia- and monocyte-specific functions after stroke. The sustained inflammatory activity of microglia after ischemia is consistent with the apparent lack of CD200R1 expression on these cells. However, brain-infiltrating monocytes, of which a significant fraction does express this inhibitory receptor, are dramatically increased in CD200R1-deficient mice and are positively correlated with poor outcome (Chapter 4). These data add to our understanding of immunoregulation in the injured brain and suggest that CD200R1 signaling may be more important for controlling peripheral myeloid responses rather than those of tissue-resident microglia.

We demonstrated for the first time that microglia exhibit deficits in phagocytosis with age, which likely contribute to the build-up of fibrillar plaques and toxic by-products of metabolism (Chapter 5). Aged microglia showed not only a poor ability to phagocytize amyloid and other material, but failed to increase this capacity when activated. In comparison to young microglia, the increase in oxidative stress levels and pro-inflammatory cytokine production was reminiscent, albeit to a lesser extent, of what we have observed in younger microglia following stroke. In addition to showing that microglia populations are highly heterogeneous in phenotype and function, we provide evidence for alterations in the blood-brain barrier and cytokine environment as possible explanation for these differences.

In our studies we have discovered a newly identified role for CD200R1 in the regulation of T cell entry into the CNS under steady state conditions (Chapter 4). Given

that effector/memory CD8 T cells made up a significant proportion of this population, we presumed the increase in knockout mice to reflect an increase in CNS immune surveillance. Unlike microglia, CD200R1 was widely expressed on T cells in the wildtype brain, implicating endothelial-T cell interactions as a major determinant of immune privilege. Moreover, we found that CD200 levels were decreased in the brain with age. This was an interesting finding especially given the fact that effector/memory CD8 T cells are significantly increased in aged brains (Chapter 6). Importantly, CNS T cells lacking CD200R1 exhibited increased production of pro-inflammatory mediators after stimulation. This is consistent with our data showing that T cells in the aged brain are primed to produce dramatically elevated levels of pro-inflammatory cytokines and chemokines. Given that a larger population of CD8 T cells expresses CD200R1 in the aged brain, the age-related decrease in CD200 levels likely contributes to this exaggerated response to stimuli. Although the increased presence of CD8 T cells was associated with healthier microglia (M2) function in the naïve brain, we have shown that these cells are equally responsive to an ischemic brain stimulus, further highlighting their importance in the pathogenesis of age-related CNS disease.

Lastly, we have shown that CD200-CD200R1 immune-inhibitory signaling is critical for attenuating brain inflammation after stroke (Chapter 4). By limiting T cell and monocyte infiltration after ischemia, the CD200R1 pathway promoted neurological recovery. CD200R1-deficient mice had severe impairment in motor coordination and balance at 7 days. Moreover, mice lacking CD200R1 had defects in peripheral immunity resulting in severe lymphopenia, T cell receptor activation, and a narrowing of the TCR repertoire. The role of CD200 in the peripheral immune response to stroke is

further highlighted and confounded by data showing aged mice have strikingly increased levels of soluble CD200 in the plasma after stroke. Given that total CD200 levels were significantly decreased in the ischemic brain of aged mice, but not young, we provide evidence for a novel link between brain injury and peripheral immune suppression. Taken together, our data support the hypothesis that CD200-CD200R1 signaling is important for maintaining CNS homeostasis under normal and injury conditions, but extend beyond neuronal-glial interactions in the brain to include monocyte and T cell interactions.

Future directions:

Our findings shine new light on the role of CD200-CD200R1 signaling in the CNS and call for a re-examination of the current model. While this work advances our understanding of CNS regulation of microglia and T cell surveillance, many questions remain outstanding. Specifically, our studies have raised three important questions that require further investigation. These current gaps in knowledge and the strategies designed to fill them will be discussed below.

Is CD200 regulation of microglia an indirect consequence of its ability to control T cell entry and activation in the CNS?

Our initial studies had set out to understand the immunoregulatory role of the CD200-CD200R1 signaling and its ability to suppress microglia activation and maintain homeostasis in the healthy CNS. As is often the case in science, our data pointed us in new directions. Albeit repeatedly proven but rarely discussed in the literature, the lack of CD200R1 expression on microglia presented an early challenge to the notion that this pathway was important for microglia regulation. We have since demonstrated that CD200R1 signaling is important for controlling the activation and entry of T cells in the brain under steady state conditions. Although there were no 'overt' changes in microglia activation in healthy mice lacking CD200R1, we observed increased myeloid responses including microglia proliferation following stroke. Thus, while CD200 may not be essential for keeping microglia in a quiescent state under normal conditions, it may be involved in later stages of injury which require a mechanism to de-escalate inflammatory responses. Previous studies showing that T cells can disrupt the blood-brain barrier while having negligible effects on glia [287] are interesting in light of recent work which suggests CD200-deficient mice have increased blood-brain barrier permeability and greater leukocyte infiltration [280]. To determine the precise role of CD200R1 signaling in microglia, we propose to exploit the use of conditional targeting approaches by generating transgenic mice with cell-specific, promoter-driven control of CD200R1 deletion. Such studies will help to explain whether the effects of CD200 on

microglia are a direct result of CD200 receptor engagement or secondary to its effect on T cells (and other leukocytes).

What is the functional significance of T cell immune surveillance in the CNS?

Our data suggest that heightened immune surveillance has little effect on microglia activation, and may even be beneficial with age. However, brains that have increased numbers of surveillant T cells tend to be predisposed to exacerbated inflammatory responses and worsened outcome after injury. Experimental manipulation of these cells is difficult given their relatively low number. To this end, we propose profiling these cells using RNA sequencing to obtain the transcriptome signature of T cells in healthy and injured brains. These data might then be used to ascertain the signaling pathways that are highly up-regulated in these cells and allow us to further probe these functions using inducible, conditional transgenic mice.

Is CD200 therapy an effective treatment for ischemic stroke and other age-related CNS diseases?

We demonstrated that CD200R1 signaling is essential for limiting inflammation and promoting survival following stroke. Mice that lacked CD200R1-mediated inhibition exhibited a greater severity of brain inflammation and peripheral immune dysfunction. This leads us to believe that given the previous findings in EAE mice, ischemic stroke may also be amenable to treatment with CD200-tailored therapies. Our results suggest

that CD200 therapy may be effective in treating stroke at both acute and chronic timepoints after stroke. Interestingly, CD200's role as a negative regulator of immune cells also enables it to function as a powerful immunosuppressive agent. Thus, while the deleterious effects of inflammation might be mitigated by CD200 therapy, the devastating effects of post-stroke immune suppression could be exacerbated. These unintended side effects could lead to higher rates of infection and greater mortality. Importantly, we discovered that circulating levels of soluble CD200 were dramatically increased in aged mice following stroke. This may also explain in part why aged mice experience greater immune suppression after traumatic brain injury. Aside from establishing a potential link between brain injury and peripheral immune function, this paradoxical role for CD200 in stroke implies that caution is needed in developing its use for treating inflammation. Based on our findings, efforts to target- and promote CD200 signaling in the brain at acute stages may help spare further injury by attenuating inflammation, whereas targeting the peripheral system via CD200-blockade may be more effective at attenuating immune suppression.

Conclusion:

Since it was first proposed by Wright [283] and Hoek [19] at the turn of the century, the hypothesis that neuronal-glial interactions involving the CD200-CD200R1 immune-inhibitory pathway maintain tight control of microglia activation has provided a sound explanation for the brain's unique immune privileged status. The studies presented here have identified several novel roles for this pathway in the regulation of T cell surveillance in the healthy CNS, and in promoting survival following stroke by controlling central and peripheral inflammatory responses. Additionally, its diminished expression with age in both the normal and stroke-injured brain indicate that CD200 serves as an important regulator of age-related changes in immune surveillance and microglia/macrophage activation. As the focus of stroke treatment shifts away from targeting the underlying cause of disease in an effort to manage symptoms and promote rehabilitation, the prospect of a therapeutic candidate that can potentially ameliorate the devastating effects of chronic inflammation may hold great promise for the future.

References

1 Lloyd-Jones, D. *et al.* Heart disease and stroke statistics--2009 update: a report from the American Heart Association Statistics Committee and Stroke Statistics Subcommittee. *Circulation* **119**, 480-486, doi:10.1161/CIRCULATIONAHA.108.191259 (2009).

2 Kamel, H. & Iadecola, C. Brain-immune interactions and ischemic stroke: clinical implications. *Arch Neurol* **69**, 576-581, doi:10.1001/archneurol.2011.3590 (2012).

3 Worthmann, H. *et al.* Linking infection and inflammation in acute ischemic stroke. *Annals of the New York Academy of Sciences* **1207**, 116-122, doi:10.1111/j.1749-6632.2010.05738.x (2010).

4 Iadecola, C. & Alexander, M. Cerebral ischemia and inflammation. *Current opinion in neurology* **14**, 89-94 (2001).

5 Danton, G. H. & Dietrich, W. D. Inflammatory mechanisms after ischemia and stroke. *Journal of neuropathology and experimental neurology* **62**, 127-136 (2003).

6 Macrez, R. *et al.* Stroke and the immune system: from pathophysiology to new therapeutic strategies. *Lancet neurology* **10**, 471-480, doi:10.1016/S1474-4422(11)70066-7 (2011).

7 Yenari, M. A., Kauppinen, T. M. & Swanson, R. A. Microglial activation in stroke: therapeutic targets. *Neurotherapeutics : the journal of the American Society for Experimental NeuroTherapeutics* **7**, 378-391, doi:10.1016/j.nurt.2010.07.005 (2010).

8 Kaminska, B., Gozdz, A., Zawadzka, M., Ellert-Miklaszewska, A. & Lipko, M. MAPK signal transduction underlying brain inflammation and gliosis as therapeutic target. *Anat Rec (Hoboken)* **292**, 1902-1913, doi:10.1002/ar.21047 (2009).

9 Lull, M. E. & Block, M. L. Microglial activation and chronic neurodegeneration. *Neurotherapeutics : the journal of the American Society for Experimental NeuroTherapeutics* **7**, 354-365, doi:10.1016/j.nurt.2010.05.014 (2010).

10 Dheen, S. T., Kaur, C. & Ling, E. A. Microglial activation and its implications in the brain diseases. *Current medicinal chemistry* **14**, 1189-1197 (2007).

11 Vexler, Z. S., Tang, X. N. & Yenari, M. A. Inflammation in adult and neonatal stroke. *Clinical neuroscience research* **6**, 293-313 (2006).

12 Lalancette-Hebert, M., Gowing, G., Simard, A., Weng, Y. C. & Kriz, J. Selective ablation of proliferating microglial cells exacerbates ischemic injury in the brain. *The Journal of neuroscience : the official journal of the Society for Neuroscience* **27**, 2596-2605, doi:10.1523/JNEUROSCI.5360-06.2007 (2007).

13 Watanabe, H., Abe, H., Takeuchi, S. & Tanaka, R. Protective effect of microglial conditioning medium on neuronal damage induced by glutamate. *Neuroscience letters* **289**, 53-56 (2000).

14 Faustino, J. V. *et al.* Microglial cells contribute to endogenous brain defenses after acute neonatal focal stroke. *The Journal of neuroscience : the official journal of the Society for Neuroscience* **31**, 12992-13001, doi:10.1523/JNEUROSCI.2102-11.2011 (2011).

15 Schroeter, M., Jander, S., Huitinga, I., Witte, O. W. & Stoll, G. Phagocytic response in photochemically induced infarction of rat cerebral cortex. The role of resident microglia. *Stroke; a journal of cerebral circulation* **28**, 382-386 (1997).
16 Nathan, C. & Muller, W. A. Putting the brakes on innate immunity: a regulatory role for CD200? *Nature immunology* **2**, 17-19, doi:10.1038/83124 (2001).
17 Kawasaki, B. T. & Farrar, W. L. Cancer stem cells, CD200 and immunoevasion. *Trends in immunology* **29**, 464-468, doi:10.1016/j.it.2008.07.005 (2008).
18 Rosenblum, M. D., Yancey, K. B., Olasz, E. B. & Truitt, R. L. CD200, a "no danger" signal for hair follicles. *J Dermatol Sci* **41**, 165-174, doi:10.1016/j.jdermsci.2005.11.003 (2006).
19 Hoek, R. M. *et al.* Down-regulation of the macrophage lineage through interaction with OX2 (CD200). *Science* **290**, 1768-1771 (2000).
20 Broderick, C. *et al.* Constitutive retinal CD200 expression regulates resident microglia and activation state of inflammatory cells during experimental autoimmune uveoretinitis. *The American journal of pathology* **161**, 1669-1677, doi:10.1016/S0002-9440(10)64444-6 (2002).
21 Costello, D. A. *et al.* Long term potentiation is impaired in membrane glycoprotein CD200-deficient mice: a role for Toll-like receptor activation. *J Biol Chem* **286**, 34722-34732, doi:10.1074/jbc.M111.280826 (2011).
22 Deckert, M., Sedgwick, J. D., Fischer, E. & Schluter, D. Regulation of microglial cell responses in murine Toxoplasma encephalitis by CD200/CD200 receptor interaction. *Acta Neuropathol* **111**, 548-558, doi:10.1007/s00401-006-0062-z (2006).
23 Matsumoto, H. *et al.* Expression of CD200 by macrophage-like cells in ischemic core of rat brain after transient middle cerebral artery occlusion. *Neurosci Lett* **418**, 44-48, doi:10.1016/j.neulet.2007.03.027 (2007).
24 K. Shrivastava, G. L., P. Gonzalez, L. Acarin. in *International Symposium on Cerebral Blood Flow, Metabolism, and Function* 2 (Brain, Barcelona, Spain, 2011).
25 Wright, G. J. *et al.* Characterization of the CD200 receptor family in mice and humans and their interactions with CD200. *J Immunol* **171**, 3034-3046 (2003).
26 Gorczynski, R. M. Transplant tolerance modifying antibody to CD200 receptor, but not CD200, alters cytokine production profile from stimulated macrophages. *Eur J Immunol* **31**, 2331-2337, doi:10.1002/1521-4141(200108)31:8<2331::AID-IMMU2331>3.0.CO;2-# (2001).
27 Jenmalm, M. C., Cherwinski, H., Bowman, E. P., Phillips, J. H. & Sedgwick, J. D. Regulation of myeloid cell function through the CD200 receptor. *J Immunol* **176**, 191-199 (2006).
28 Carter, D. A. & Dick, A. D. CD200 maintains microglial potential to migrate in adult human retinal explant model. *Current eye research* **28**, 427-436, doi:10.1080/02713680490503778 (2004).
29 Simelyte, E. *et al.* CD200-Fc, a novel antiarthritic biologic agent that targets proinflammatory cytokine expression in the joints of mice with collagen-induced arthritis. *Arthritis Rheum* **58**, 1038-1043, doi:10.1002/art.23378 (2008).
30 Wang, Q., Tang, X. N. & Yenari, M. A. The inflammatory response in stroke. *Journal of neuroimmunology* **184**, 53-68, doi:10.1016/j.jneuroim.2006.11.014 (2007).

31 Caso, J. R. *et al.* Toll-like receptor 4 is involved in brain damage and inflammation after experimental stroke. *Circulation* **115**, 1599-1608, doi:10.1161/CIRCULATIONAHA.106.603431 (2007).
32 Villa, P. *et al.* The interleukin-8 (IL-8/CXCL8) receptor inhibitor reparixin improves neurological deficits and reduces long-term inflammation in permanent and transient cerebral ischemia in rats. *Mol Med* **13**, 125-133, doi:10.2119/2007–00008.Villa (2007).
33 Spera, P. A., Ellison, J. A., Feuerstein, G. Z. & Barone, F. C. IL-10 reduces rat brain injury following focal stroke. *Neuroscience letters* **251**, 189-192 (1998).
34 Yilmaz, G., Arumugam, T. V., Stokes, K. Y. & Granger, D. N. Role of T lymphocytes and interferon-gamma in ischemic stroke. *Circulation* **113**, 2105-2112, doi:10.1161/CIRCULATIONAHA.105.593046 (2006).
35 Vila, N., Castillo, J., Davalos, A. & Chamorro, A. Proinflammatory cytokines and early neurological worsening in ischemic stroke. *Stroke; a journal of cerebral circulation* **31**, 2325-2329 (2000).
36 Vila, N. *et al.* Cytokine-induced inflammation and long-term stroke functional outcome. *Journal of the neurological sciences* **162**, 185-188 (1999).
37 Beamer, N. B. *et al.* Persistent inflammatory response in stroke survivors. *Neurology* **50**, 1722-1728 (1998).
38 Clark, W. M., Beamer, N. B., Wynn, M. & Coull, B. M. The initial acute phase response predicts long-term stroke recovery. *Journal of stroke and cerebrovascular diseases : the official journal of National Stroke Association* **7**, 128-131 (1998).
39 Akopov, S. E., Simonian, N. A. & Grigorian, G. S. Dynamics of polymorphonuclear leukocyte accumulation in acute cerebral infarction and their correlation with brain tissue damage. *Stroke; a journal of cerebral circulation* **27**, 1739-1743 (1996).
40 Smith, C. J. *et al.* Peak plasma interleukin-6 and other peripheral markers of inflammation in the first week of ischaemic stroke correlate with brain infarct volume, stroke severity and long-term outcome. *BMC neurology* **4**, 2, doi:10.1186/1471-2377-4-2 (2004).
41 Emsley, H. C. *et al.* Correlation of systemic inflammatory response with infarct volume in acute ischemic stroke patients. *Stroke; a journal of cerebral circulation* **36**, 228-229; author reply 228-229, doi:10.1161/01.STR.0000155197.88944.ac (2005).
42 Rodriguez-Yanez, M. & Castillo, J. Role of inflammatory markers in brain ischemia. *Current opinion in neurology* **21**, 353-357, doi:10.1097/WCO.0b013e3282ffafbf (2008).
43 Chopp, M., Li, Y., Jiang, N., Zhang, R. L. & Prostak, J. Antibodies against adhesion molecules reduce apoptosis after transient middle cerebral artery occlusion in rat brain. *Journal of cerebral blood flow and metabolism : official journal of the International Society of Cerebral Blood Flow and Metabolism* **16**, 578-584, doi:10.1097/00004647-199607000-00007 (1996).
44 Yilmaz, G. & Granger, D. N. Cell adhesion molecules and ischemic stroke. *Neurological research* **30**, 783-793, doi:10.1179/174313208X341085 (2008).
45 del Zoppo, G. J., Becker, K. J. & Hallenbeck, J. M. Inflammation after stroke: is it harmful? *Archives of neurology* **58**, 669-672 (2001).

46 Holmannova, D. *et al.* CD200/CD200R paired potent inhibitory molecules regulating immune and inflammatory responses; Part I: CD200/CD200R structure, activation, and function. *Acta Medica (Hradec Kralove)* **55**, 12-17 (2012).
47 Mozaffarian, D. *et al.* Heart disease and stroke statistics--2015 update: a report from the American Heart Association. *Circulation* **131**, e29-322, doi:10.1161/CIR.0000000000000152 (2015).
48 Lapchak, P. A., Zhang, J. H. & Noble-Haeusslein, L. J. RIGOR guidelines: escalating STAIR and STEPS for effective translational research. *Transl Stroke Res* **4**, 279-285, doi:10.1007/s12975-012-0209-2 (2013).
49 Jenny, N. S. Inflammation in aging: cause, effect, or both? *Discov Med* **13**, 451-460 (2012).
50 Loeffler, C. *et al.* Immune surveillance of the normal human CNS takes place in dependence of the locoregional blood-brain barrier configuration and is mainly performed by CD3(+)/CD8(+) lymphocytes. *Neuropathology* **31**, 230-238, doi:10.1111/j.1440-1789.2010.01167.x (2011).
51 Montagne, A. *et al.* Blood-brain barrier breakdown in the aging human hippocampus. *Neuron* **85**, 296-302, doi:10.1016/j.neuron.2014.12.032 (2015).
52 Streit, W. J. & Xue, Q. S. Human CNS immune senescence and neurodegeneration. *Curr Opin Immunol* **29**, 93-96, doi:10.1016/j.coi.2014.05.005 (2014).
53 Conde, J. R. & Streit, W. J. Microglia in the aging brain. *J Neuropathol Exp Neurol* **65**, 199-203, doi:10.1097/01.jnen.0000202887.22082.63 (2006).
54 Streit, W. J., Sammons, N. W., Kuhns, A. J. & Sparks, D. L. Dystrophic microglia in the aging human brain. *Glia* **45**, 208-212, doi:10.1002/glia.10319 (2004).
55 Franceschi, C. *et al.* Inflamm-aging. An evolutionary perspective on immunosenescence. *Ann N Y Acad Sci* **908**, 244-254 (2000).
56 Deleidi, M., Jaggle, M. & Rubino, G. Immune aging, dysmetabolism, and inflammation in neurological diseases. *Front Neurosci* **9**, 172, doi:10.3389/fnins.2015.00172 (2015).
57 Iadecola, C. & Anrather, J. The immunology of stroke: from mechanisms to translation. *Nat Med* **17**, 796-808, doi:10.1038/nm.2399 (2011).
58 Wang, X. & Feuerstein, G. Z. The Janus face of inflammation in ischemic brain injury. *Acta neurochirurgica. Supplement* **89**, 49-54 (2004).
59 Wood, P. L. Microglia as a unique cellular target in the treatment of stroke: potential neurotoxic mediators produced by activated microglia. *Neurological research* **17**, 242-248 (1995).
60 Neumann, H., Kotter, M. R. & Franklin, R. J. Debris clearance by microglia: an essential link between degeneration and regeneration. *Brain* **132**, 288-295 (2009).
61 Jin, R., Yang, G. & Li, G. Inflammatory mechanisms in ischemic stroke: role of inflammatory cells. *J Leukoc Biol* **87**, 779-789, doi:10.1189/jlb.1109766 (2010).
62 Chan, W. Y., Kohsaka, S. & Rezaie, P. The origin and cell lineage of microglia: new concepts. *Brain Res Rev* **53**, 344-354 (2007).
63 Gomez Perdiguero, E., Schulz, C. & Geissmann, F. Development and homeostasis of "resident" myeloid cells: The case of the microglia. *Glia* **61**, 112-120 (2013).
64 Ginhoux, F. *et al.* Fate mapping analysis reveals that adult microglia derive from primitive macrophages. *Science* **330**, 841-845 (2010).

65 Kissa, K. & Herbomel, P. Blood stem cells emerge from aortic endothelium by a novel type of cell transition. *Nature* **464**, 112-115 (2010).
66 Lichanska, A. M. *et al.* Differentiation of the mononuclear phagocyte system during mouse embryogenesis: the role of transcription factor PU.1. *Blood* **94**, 127-138 (1999).
67 Kierdorf, K. *et al.* Microglia emerge from erythromyeloid precursors via Pu.1- and Irf8-dependent pathways. *Nat Neurosci* (2009).
68 Mizutani, M. *et al.* The fractalkine receptor but not CCR2 is present on microglia from embryonic development throughout adulthood. *J Immunol* **188**, 29-36 (2012).
69 Mukouyama, Y. *et al.* Hematopoietic cells in cultures of the murine embryonic aorta-gonad-mesonephros region are induced by c-Myb. *Curr Biol* **9**, 833-836 (1999).
70 Schulz, C. *et al.* A lineage of myeloid cells independent of Myb and hematopoietic stem cells. *Science* **336**, 86-90 (2012).
71 Labastie, M. C., Cortes, F., Romeo, P. H., Dulac, C. & Peault, B. Molecular identity of hematopoietic precursor cells emerging in the human embryo. *Blood* **92**, 3624-3635 (1998).
72 Erblich, B., Zhu, L., Etgen, A. M., Dobrenis, K. & Pollard, J. W. Absence of colony stimulation factor-1 receptor results in loss of microglia, disrupted brain development and olfactory deficits. *PLoS One* **6**, e26317 (2011).
73 Ovchinnikov, D. A. Macrophages in the embryo and beyond: much more than just giant phagocytes. *Genesis* **46**, 447-462 (2008).
74 Tambuyzer, B. R., Ponsaerts, P. & Nouwen, E. J. Microglia: gatekeepers of central nervous system immunology. *J Leukoc Biol* **85**, 352-370 (2009).
75 Imai, Y., Ibata, I., Ito, D., Ohsawa, K. & Kohsaka, S. A novel gene iba1 in the major histocompatibility complex class III region encoding an EF hand protein expressed in a monocytic lineage. *Biochemical and biophysical research communications* **224**, 855-862 (1996).
76 Ito, D. *et al.* Microglia-specific localisation of a novel calcium binding protein, Iba1. *Brain Res Mol Brain Res* **57**, 1-9 (1998).
77 Ito, D., Tanaka, K., Suzuki, S., Dembo, T. & Fukuuchi, Y. Enhanced expression of Iba1, ionized calcium-binding adapter molecule 1, after transient focal cerebral ischemia in rat brain. *Stroke; a journal of cerebral circulation* **32**, 1208-1215 (2001).
78 Sedgwick, J. D. *et al.* Isolation and direct characterization of resident microglial cells from the normal and inflamed central nervous system. *Proceedings of the National Academy of Sciences of the United States of America* **88**, 7438-7442 (1991).
79 Ford, A. L., Goodsall, A. L., Hickey, W. F. & Sedgwick, J. D. Normal adult ramified microglia separated from other central nervous system macrophages by flow cytometric sorting. Phenotypic differences defined and direct ex vivo antigen presentation to myelin basic protein-reactive CD4+ T cells compared. *J Immunol* **154**, 4309-4321 (1995).
80 Perego, C., Fumagalli, S. & De Simoni, M. G. Temporal pattern of expression and colocalization of microglia/macrophage phenotype markers following brain ischemic injury in mice. *J Neuroinflammation* **8**, 174 (2011).
81 Gesuete, R. *et al.* Recombinant C1 inhibitor in brain ischemic injury. *Ann Neurol* **66**, 332-342, doi:10.1002/ana.21740 (2009).

82 Guillemin, G. J. & Brew, B. J. Microglia, macrophages, perivascular macrophages, and pericytes: a review of function and identification. *J Leukoc Biol* **75**, 388-397 (2004).
83 Ponomarev, E. D., Shriver, L. P., Maresz, K. & Dittel, B. N. Microglial cell activation and proliferation precedes the onset of CNS autoimmunity. *J Neurosci Res* **81**, 374-389 (2005).
84 Melief, J. *et al.* Phenotyping primary human microglia: tight regulation of LPS responsiveness. *Glia* **60**, 1506-1517, doi:10.1002/glia.22370 (2012).
85 Hume, D. A. Applications of myeloid-specific promoters in transgenic mice support in vivo imaging and functional genomics but do not support the concept of distinct macrophage and dendritic cell lineages or roles in immunity. *J Leukoc Biol* **89**, 525-538 (2011).
86 Hirasawa, T. *et al.* Visualization of microglia in living tissues using Iba1-EGFP transgenic mice. *J Neurosci Res* **81**, 357-362 (2005).
87 Saederup, N. *et al.* Selective chemokine receptor usage by central nervous system myeloid cells in CCR2-red fluorescent protein knock-in mice. *PLoS One* **5**, e13693 (2010).
88 Goren, I. *et al.* A transgenic mouse model of inducible macrophage depletion: effects of diphtheria toxin-driven lysozyme M-specific cell lineage ablation on wound inflammatory, angiogenic, and contractive processes. *Am J Pathol* **175**, 132-147, doi:10.2353/ajpath.2009.081002 (2009).
89 Gowing, G., Vallieres, L. & Julien, J. P. Mouse model for ablation of proliferating microglia in acute CNS injuries. *Glia* **53**, 331-337, doi:10.1002/glia.20288 (2006).
90 Tang, X., Zheng Z and Yenari, MA. Bone Marrow Chimeras in the Study of Experimental Stroke. *Transl. Stroke Res* **3**, 341-347 (2012).
91 Monje, M. L., Mizumatsu, S., Fike, J. R. & Palmer, T. D. Irradiation induces neural precursor-cell dysfunction. *Nat Med* **8**, 955-962 (2002).
92 Davoust, N., Vuaillat, C., Androdias, G. & Nataf, S. From bone marrow to microglia: barriers and avenues. *Trends Immunol* **29**, 227-234 (2008).
93 Mildner, A. *et al.* Microglia in the adult brain arise from Ly-6ChiCCR2+ monocytes only under defined host conditions. *Nat Neurosci* **10**, 1544-1553 (2007).
94 Wirenfeldt, M. *et al.* Population control of resident and immigrant microglia by mitosis and apoptosis. *Am J Pathol* **171**, 617-631 (2007).
95 Li, Y. Q., Chen, P., Jain, V., Reilly, R. M. & Wong, C. S. Early radiation-induced endothelial cell loss and blood-spinal cord barrier breakdown in the rat spinal cord. *Radiat Res* **161**, 143-152 (2004).
96 Lambertsen, K. L. *et al.* Microglia protect neurons against ischemia by synthesis of tumor necrosis factor. *J Neurosci* **29**, 1319-1330, doi:10.1523/JNEUROSCI.5505-08.2009 (2009).
97 Linard, C. *et al.* Acute induction of inflammatory cytokine expression after gamma-irradiation in the rat: effect of an NF-kappaB inhibitor. *Int J Radiat Oncol Biol Phys* **58**, 427-434 (2004).
98 Mizumatsu, S. *et al.* Extreme sensitivity of adult neurogenesis to low doses of X-irradiation. *Cancer Res* **63**, 4021-4027 (2003).
99 Davalos, D. *et al.* ATP mediates rapid microglial response to local brain injury in vivo. *Nat Neurosci* **8**, 752-758 (2005).

100 Nimmerjahn, A., Kirchhoff, F. & Helmchen, F. Resting microglial cells are highly dynamic surveillants of brain parenchyma in vivo. *Science* **308**, 1314-1318 (2005).
101 Lawson, L. J., Perry, V. H., Dri, P. & Gordon, S. Heterogeneity in the distribution and morphology of microglia in the normal adult mouse brain. *Neuroscience* **39**, 151-170 (1990).
102 Carson, M. J. *et al.* A rose by any other name? The potential consequences of microglial heterogeneity during CNS health and disease. *Neurotherapeutics* **4**, 571-579 (2007).
103 Biber, K., Neumann, H., Inoue, K. & Boddeke, H. W. Neuronal 'On' and 'Off' signals control microglia. *Trends Neurosci* **30**, 596-602, doi:10.1016/j.tins.2007.08.007 (2007).
104 Cardona, A. E. *et al.* Control of microglial neurotoxicity by the fractalkine receptor. *Nat Neurosci* **9**, 917-924 (2006).
105 Fuhrmann, M. *et al.* Microglial Cx3cr1 knockout prevents neuron loss in a mouse model of Alzheimer's disease. *Nat Neurosci* **13**, 411-413 (2010).
106 Cipriani, R. *et al.* CX3CL1 is neuroprotective in permanent focal cerebral ischemia in rodents. *J Neurosci* **31**, 16327-16335 (2011).
107 Koning, N., Bo, L., Hoek, R. M. & Huitinga, I. Downregulation of macrophage inhibitory molecules in multiple sclerosis lesions. *Ann Neurol* **62**, 504-514, doi:10.1002/ana.21220 (2007).
108 Barclay, A. N., Wright, G. J., Brooke, G. & Brown, M. H. CD200 and membrane protein interactions in the control of myeloid cells. *Trends Immunol* **23**, 285-290 (2002).
109 Koning, N., Swaab, D. F., Hoek, R. M. & Huitinga, I. Distribution of the immune inhibitory molecules CD200 and CD200R in the normal central nervous system and multiple sclerosis lesions suggests neuron-glia and glia-glia interactions. *J Neuropathol Exp Neurol* **68**, 159-167, doi:10.1097/NEN.0b013e3181964113 (2009).
110 Webb, M. & Barclay, A. N. Localisation of the MRC OX-2 glycoprotein on the surfaces of neurones. *J Neurochem* **43**, 1061-1067 (1984).
111 Barclay, A. N. The localization of populations of lymphocytes defined by monoclonal antibodies in rat lymphoid tissues. *Immunology* **42**, 593-600 (1981).
112 Chitnis, T. *et al.* Elevated neuronal expression of CD200 protects Wlds mice from inflammation-mediated neurodegeneration. *Am J Pathol* **170**, 1695-1712, doi:10.2353/ajpath.2007.060677 (2007).
113 Cox, F. F., Carney, D., Miller, A. M. & Lynch, M. A. CD200 fusion protein decreases microglial activation in the hippocampus of aged rats. *Brain Behav Immun* **26**, 789-796, doi:10.1016/j.bbi.2011.10.004 (2012).
114 Ludwig, A. & Weber, C. Transmembrane chemokines: versatile 'special agents' in vascular inflammation. *Thromb Haemost* **97**, 694-703 (2007).
115 Fumagalli, S., Perego, C., Ortolano, F. & De Simoni, M. G. CX3CR1 deficiency induces an early protective inflammatory environment in ischemic mice. *Glia* (2013).
116 Denes, A., Ferenczi, S., Halasz, J., Kornyei, Z. & Kovacs, K. J. Role of CX3CR1 (fractalkine receptor) in brain damage and inflammation induced by focal cerebral ischemia in mouse. *J Cereb Blood Flow Metab* **28**, 1707-1721 (2008).
117 Soriano, S. G. *et al.* Mice deficient in fractalkine are less susceptible to cerebral ischemia-reperfusion injury. *Journal of neuroimmunology* **125**, 59-65 (2002).

118 Jiang, P., Lagenaur, C. F. & Narayanan, V. Integrin-associated protein is a ligand for the P84 neural adhesion molecule. *J Biol Chem* **274**, 559-562 (1999).
119 Fujioka, Y. *et al.* A novel membrane glycoprotein, SHPS-1, that binds the SH2-domain-containing protein tyrosine phosphatase SHP-2 in response to mitogens and cell adhesion. *Mol Cell Biol* **16**, 6887-6899 (1996).
120 Okazawa, H. *et al.* Negative regulation of phagocytosis in macrophages by the CD47-SHPS-1 system. *J Immunol* **174**, 2004-2011 (2005).
121 Yamao, T. *et al.* Negative regulation of platelet clearance and of the macrophage phagocytic response by the transmembrane glycoprotein SHPS-1. *J Biol Chem* **277**, 39833-39839 (2002).
122 Jin, G. *et al.* CD47 gene knockout protects against transient focal cerebral ischemia in mice. *Exp Neurol* **217**, 165-170 (2009).
123 Wang, L. *et al.* SHPS-1 deficiency induces robust neuroprotection against experimental stroke by attenuating oxidative stress. *J Neurochem* **122**, 834-843 (2012).
124 Stefano, L. *et al.* The surface-exposed chaperone, Hsp60, is an agonist of the microglial TREM2 receptor. *J Neurochem* **110**, 284-294 (2009).
125 Piccio, L. *et al.* Blockade of TREM-2 exacerbates experimental autoimmune encephalomyelitis. *Eur J Immunol* **37**, 1290-1301 (2007).
126 Takahashi, K., Rochford, C. D. & Neumann, H. Clearance of apoptotic neurons without inflammation by microglial triggering receptor expressed on myeloid cells-2. *J Exp Med* **201**, 647-657 (2005).
127 Sieber, M. W. *et al.* Attenuated inflammatory response in triggering receptor expressed on myeloid cells 2 (TREM2) knock-out mice following stroke. *PLoS One* **8**, e52982 (2013).
128 Ohsawa, K. *et al.* Involvement of P2X4 and P2Y12 receptors in ATP-induced microglial chemotaxis. *Glia* **55**, 604-616 (2007).
129 Haynes, S. E. *et al.* The P2Y12 receptor regulates microglial activation by extracellular nucleotides. *Nat Neurosci* **9**, 1512-1519, doi:10.1038/nn1805 (2006).
130 Varnum, M. M. & Ikezu, T. The classification of microglial activation phenotypes on neurodegeneration and regeneration in Alzheimer's disease brain. *Arch Immunol Ther Exp (Warsz)* **60**, 251-266 (2012).
131 Hu, X. *et al.* Microglia/macrophage polarization dynamics reveal novel mechanism of injury expansion after focal cerebral ischemia. *Stroke; a journal of cerebral circulation* **43**, 3063-3070, doi:10.1161/STROKEAHA.112.659656 (2012).
132 Ponomarev, E. D., Veremeyko, T. & Weiner, H. L. MicroRNAs are universal regulators of differentiation, activation, and polarization of microglia and macrophages in normal and diseased CNS. *Glia* **61**, 91-103, doi:10.1002/glia.22363 (2013).
133 Liu, H. C. *et al.* N9 microglial cells polarized by LPS and IL4 show differential responses to secondary environmental stimuli. *Cell Immunol* **278**, 84-90, doi:10.1016/j.cellimm.2012.06.001 (2012).
134 Shin, W. H. *et al.* Microglia expressing interleukin-13 undergo cell death and contribute to neuronal survival in vivo. *Glia* **46**, 142-152, doi:10.1002/glia.10357 (2004).

135 Zhou, X., Spittau, B. & Krieglstein, K. TGFbeta signalling plays an important role in IL4-induced alternative activation of microglia. *J Neuroinflammation* **9**, 210, doi:10.1186/1742-2094-9-210 (2012).
136 Hanisch, U. K. & Kettenmann, H. Microglia: active sensor and versatile effector cells in the normal and pathologic brain. *Nature neuroscience* **10**, 1387-1394, doi:10.1038/nn1997 (2007).
137 Pal, G. *et al.* Time course, distribution and cell types of induction of transforming growth factor betas following middle cerebral artery occlusion in the rat brain. *PLoS One* **7**, e46731 (2012).
138 Jimenez, S. *et al.* Inflammatory response in the hippocampus of PS1M146L/APP751SL mouse model of Alzheimer's disease: age-dependent switch in the microglial phenotype from alternative to classic. *J Neurosci* **28**, 11650-11661, doi:10.1523/JNEUROSCI.3024-08.2008 (2008).
139 Katayama, T. *et al.* Accumulating microglia phagocytose injured neurons in hippocampal slice cultures: involvement of p38 MAP kinase. *PLoS One* **7**, e40813 (2012).
140 Denes, A. *et al.* Proliferating resident microglia after focal cerebral ischaemia in mice. *J Cereb Blood Flow Metab* **27**, 1941-1953 (2007).
141 Sakanashi, Y. *et al.* Kinetics of macrophage subpopulations and expression of monocyte chemoattractant protein-1 (MCP-1) in bleomycin-induced lung injury of rats studied by a novel monoclonal antibody against rat MCP-1. *J Leukoc Biol* **56**, 741-750 (1994).
142 Kumar, A. G. *et al.* Induction of monocyte chemoattractant protein-1 in the small veins of the ischemic and reperfused canine myocardium. *Circulation* **95**, 693-700 (1997).
143 Che, X., Ye, W., Panga, L., Wu, D. C. & Yang, G. Y. Monocyte chemoattractant protein-1 expressed in neurons and astrocytes during focal ischemia in mice. *Brain Res* **902**, 171-177 (2001).
144 Ceulemans, A. G. *et al.* The dual role of the neuroinflammatory response after ischemic stroke: modulatory effects of hypothermia. *J Neuroinflammation* **7**, 74 (2010).
145 Dimitrijevic, J. *et al.* [10-year analysis of cerebrovascular accidents at the Neurology Clinic in Sarajevo (before, during and after the war)]. *Medicinski arhiv* **56**, 151-153 (2002).
146 del Zoppo, G. J., Sharp, F. R., Heiss, W. D. & Albers, G. W. Heterogeneity in the penumbra. *J Cereb Blood Flow Metab* **31**, 1836-1851, doi:10.1038/jcbfm.2011.93 (2011).
147 Schilling, M. *et al.* Predominant phagocytic activity of resident microglia over hematogenous macrophages following transient focal cerebral ischemia: an investigation using green fluorescent protein transgenic bone marrow chimeric mice. *Experimental neurology* **196**, 290-297, doi:10.1016/j.expneurol.2005.08.004 (2005).
148 Neher, J. J. *et al.* Inhibition of microglial phagocytosis is sufficient to prevent inflammatory neuronal death. *J Immunol* **186**, 4973-4983 (2011).
149 Franke, H. *et al.* P2X7 receptor expression after ischemia in the cerebral cortex of rats. *J Neuropathol Exp Neurol* **63**, 686-699 (2004).

150 Melani, A. *et al.* ATP extracellular concentrations are increased in the rat striatum during in vivo ischemia. *Neurochem Int* **47**, 442-448, doi:10.1016/j.neuint.2005.05.014 (2005).
151 Monif, M., Reid, C. A., Powell, K. L., Smart, M. L. & Williams, D. A. The P2X7 receptor drives microglial activation and proliferation: a trophic role for P2X7R pore. *J Neurosci* **29**, 3781-3791 (2009).
152 Brough, D., Le Feuvre, R. A., Iwakura, Y. & Rothwell, N. J. Purinergic (P2X7) receptor activation of microglia induces cell death via an interleukin-1-independent mechanism. *Mol Cell Neurosci* **19**, 272-280 (2002).
153 Ferrari, D. *et al.* The P2X7 receptor: a key player in IL-1 processing and release. *J Immunol* **176**, 3877-3883 (2006).
154 Verderio, C. & Matteoli, M. ATP mediates calcium signaling between astrocytes and microglial cells: modulation by IFN-gamma. *J Immunol* **166**, 6383-6391 (2001).
155 Honda, S. *et al.* Extracellular ATP or ADP induce chemotaxis of cultured microglia through Gi/o-coupled P2Y receptors. *J Neurosci* **21**, 1975-1982 (2001).
156 Pellegatti, P., Falzoni, S., Pinton, P., Rizzuto, R. & Di Virgilio, F. A novel recombinant plasma membrane-targeted luciferase reveals a new pathway for ATP secretion. *Mol Biol Cell* **16**, 3659-3665, doi:10.1091/mbc.E05-03-0222 (2005).
157 Chu, K. *et al.* Inhibition of P2X7 receptor ameliorates transient global cerebral ischemia/reperfusion injury via modulating inflammatory responses in the rat hippocampus. *J Neuroinflammation* **9**, 69 (2012).
158 Melani, A. *et al.* P2X7 receptor modulation on microglial cells and reduction of brain infarct caused by middle cerebral artery occlusion in rat. *J Cereb Blood Flow Metab* **26**, 974-982, doi:10.1038/sj.jcbfm.9600250 (2006).
159 Piccinini, A. M. & Midwood, K. S. DAMPening inflammation by modulating TLR signalling. *Mediators Inflamm* **2010**, doi:10.1155/2010/672395 (2010).
160 Ziegler, G. *et al.* Mrp-8 and -14 mediate CNS injury in focal cerebral ischemia. *Biochim Biophys Acta* **1792**, 1198-1204 (2009).
161 Chow, J. C., Young, D. W., Golenbock, D. T., Christ, W. J. & Gusovsky, F. Toll-like receptor-4 mediates lipopolysaccharide-induced signal transduction. *J Biol Chem* **274**, 10689-10692 (1999).
162 Lehnardt, S. *et al.* Toll-like receptor 2 mediates CNS injury in focal cerebral ischemia. *Journal of neuroimmunology* **190**, 28-33 (2007).
163 Bohacek, I. *et al.* Toll-like receptor 2 deficiency leads to delayed exacerbation of ischemic injury. *J Neuroinflammation* **9**, 191 (2012).
164 Hyakkoku, K. *et al.* Toll-like receptor 4 (TLR4), but not TLR3 or TLR9, knock-out mice have neuroprotective effects against focal cerebral ischemia. *Neuroscience* **171**, 258-267, doi:10.1016/j.neuroscience.2010.08.054 (2010).
165 Lalancette-Hebert, M., Phaneuf, D., Soucy, G., Weng, Y. C. & Kriz, J. Live imaging of Toll-like receptor 2 response in cerebral ischaemia reveals a role of olfactory bulb microglia as modulators of inflammation. *Brain* **132**, 940-954, doi:10.1093/brain/awn345 (2009).
166 Suzuki, Y. *et al.* Pharmacological inhibition of TLR4-NOX4 signal protects against neuronal death in transient focal ischemia. *Sci Rep* **2**, 896, doi:10.1038/srep00896 (2012).

167 Chen, Z. *et al.* Lipopolysaccharide-induced microglial activation and neuroprotection against experimental brain injury is independent of hematogenous TLR4. *J Neurosci* **32**, 11706-11715 (2012).
168 Vartanian, K. B. *et al.* LPS preconditioning redirects TLR signaling following stroke: TRIF-IRF3 plays a seminal role in mediating tolerance to ischemic injury. *J Neuroinflammation* **8**, 140, doi:10.1186/1742-2094-8-140 (2011).
169 Lu, C. *et al.* TLR2 ligand induces protection against cerebral ischemia/reperfusion injury via activation of phosphoinositide 3-kinase/Akt signaling. *J Immunol* **187**, 1458-1466.
170 Shichita, T. *et al.* Peroxiredoxin family proteins are key initiators of post-ischemic inflammation in the brain. *Nat Med* **18**, 911-917 (2012).
171 Li, G., Liang, X. & Lotze, M. T. HMGB1: The Central Cytokine for All Lymphoid Cells. *Front Immunol* **4**, 68, doi:10.3389/fimmu.2013.00068 (2013).
172 Vabulas, R. M. *et al.* HSP70 as endogenous stimulus of the Toll/interleukin-1 receptor signal pathway. *J Biol Chem* **277**, 15107-15112, doi:10.1074/jbc.M111204200 (2002).
173 Mitrasinovic, O. M. *et al.* Microglia overexpressing the macrophage colony-stimulating factor receptor are neuroprotective in a microglial-hippocampal organotypic coculture system. *J Neurosci* **25**, 4442-4451 (2005).
174 Lalancette-Hebert, M. *et al.* Galectin-3 is required for resident microglia activation and proliferation in response to ischemic injury. *J Neurosci* **32**, 10383-10395 (2012).
175 McMenamin, P. G. Distribution and phenotype of dendritic cells and resident tissue macrophages in the dura mater, leptomeninges, and choroid plexus of the rat brain as demonstrated in wholemount preparations. *J Comp Neurol* **405**, 553-562 (1999).
176 Bechmann, I. *et al.* Immune surveillance of mouse brain perivascular spaces by blood-borne macrophages. *Eur J Neurosci* **14**, 1651-1658 (2001).
177 Lassmann, H., Schmied, M., Vass, K. & Hickey, W. F. Bone marrow derived elements and resident microglia in brain inflammation. *Glia* **7**, 19-24, doi:10.1002/glia.440070106 (1993).
178 Geissmann, F. *et al.* Blood monocytes: distinct subsets, how they relate to dendritic cells, and their possible roles in the regulation of T-cell responses. *Immunol Cell Biol* **86**, 398-408 (2008).
179 Varvel, N. H. *et al.* Microglial repopulation model reveals a robust homeostatic process for replacing CNS myeloid cells. *Proc Natl Acad Sci U S A* **109**, 18150-18155 (2012).
180 Candelario-Jalil, E., Yang, Y. & Rosenberg, G. A. Diverse roles of matrix metalloproteinases and tissue inhibitors of metalloproteinases in neuroinflammation and cerebral ischemia. *Neuroscience* **158**, 983-994, doi:10.1016/j.neuroscience.2008.06.025 (2009).
181 Walker, E. J. & Rosenberg, G. A. TIMP-3 and MMP-3 contribute to delayed inflammation and hippocampal neuronal death following global ischemia. *Exp Neurol* **216**, 122-131 (2009).
182 Gidday, J. M. *et al.* Leukocyte-derived matrix metalloproteinase-9 mediates blood-brain barrier breakdown and is proinflammatory after transient focal cerebral ischemia. *Am J Physiol Heart Circ Physiol* **289**, H558-568 (2005).

183 Wang, G. *et al.* Bone marrow-derived cells are the major source of MMP-9 contributing to blood-brain barrier dysfunction and infarct formation after ischemic stroke in mice. *Brain Res* **1294**, 183-192 (2009).
184 Dawson, D. A., Martin, D. & Hallenbeck, J. M. Inhibition of tumor necrosis factor-alpha reduces focal cerebral ischemic injury in the spontaneously hypertensive rat. *Neurosci Lett* **218**, 41-44 (1996).
185 Lambertsen, K. L., Biber, K. & Finsen, B. Inflammatory cytokines in experimental and human stroke. *Journal of cerebral blood flow and metabolism : official journal of the International Society of Cerebral Blood Flow and Metabolism* **32**, 1677-1698, doi:10.1038/jcbfm.2012.88 (2012).
186 Fontaine, V. *et al.* Neurodegenerative and neuroprotective effects of tumor Necrosis factor (TNF) in retinal ischemia: opposite roles of TNF receptor 1 and TNF receptor 2. *J Neurosci* **22**, RC216 (2002).
187 Iadecola, C., Zhang, F., Xu, S., Casey, R. & Ross, M. E. Inducible nitric oxide synthase gene expression in brain following cerebral ischemia. *J Cereb Blood Flow Metab* **15**, 378-384, doi:10.1038/jcbfm.1995.47 (1995).
188 Loihl, A. K., Asensio, V., Campbell, I. L. & Murphy, S. Expression of nitric oxide synthase (NOS)-2 following permanent focal ischemia and the role of nitric oxide in infarct generation in male, female and NOS-2 gene-deficient mice. *Brain Res* **830**, 155-164 (1999).
189 Iadecola, C., Zhang, F., Casey, R., Nagayama, M. & Ross, M. E. Delayed reduction of ischemic brain injury and neurological deficits in mice lacking the inducible nitric oxide synthase gene. *J Neurosci* **17**, 9157-9164 (1997).
190 Iadecola, C., Zhang, F. & Xu, X. Inhibition of inducible nitric oxide synthase ameliorates cerebral ischemic damage. *The American journal of physiology* **268**, R286-292 (1995).
191 Pruss, H. *et al.* Inducible nitric oxide synthase does not mediate brain damage after transient focal cerebral ischemia in mice. *J Cereb Blood Flow Metab* **28**, 526-539 (2008).
192 Hu, X. *et al.* Peroxiredoxin-2 protects against 6-hydroxydopamine-induced dopaminergic neurodegeneration via attenuation of the apoptosis signal-regulating kinase (ASK1) signaling cascade. *J Neurosci* **31**, 247-261, doi:10.1523/JNEUROSCI.4589-10.2011 (2011).
193 Rashidian, J. *et al.* Essential role of cytoplasmic cdk5 and Prx2 in multiple ischemic injury models, in vivo. *J Neurosci* **29**, 12497-12505, doi:10.1523/JNEUROSCI.3892-09.2009 (2009).
194 Del Rio Hortega, P. & Penfield, W. Cerebral Cicatrix: the reaction of neuroglia and microglia to brain wounds. *Bulletin of the Johns Hopkins Hospital* **41**, 278-303 (1892).
195 Whiteley, W. *et al.* Inflammatory markers and poor outcome after stroke: a prospective cohort study and systematic review of interleukin-6. *PLoS medicine* **6**, e1000145, doi:10.1371/journal.pmed.1000145 (2009).
196 Di Napoli, M., Papa, F. & Bocola, V. C-reactive protein in ischemic stroke: an independent prognostic factor. *Stroke; a journal of cerebral circulation* **32**, 917-924 (2001).

197 Vila, N. *et al.* Levels of anti-inflammatory cytokines and neurological worsening in acute ischemic stroke. *Stroke; a journal of cerebral circulation* **34**, 671-675, doi:10.1161/01.STR.0000057976.53301.69 (2003).
198 Benakis, C., Garcia-Bonilla, L., Iadecola, C. & Anrather, J. The role of microglia and myeloid immune cells in acute cerebral ischemia. *Front Cell Neurosci* **8**, 461, doi:10.3389/fncel.2014.00461 (2014).
199 Joseph, B. & Venero, J. L. A brief overview of multitalented microglia. *Methods Mol Biol* **1041**, 3-8, doi:10.1007/978-1-62703-520-0_1 (2013).
200 Patel, A. R., Ritzel, R., McCullough, L. D. & Liu, F. Microglia and ischemic stroke: a double-edged sword. *Int J Physiol Pathophysiol Pharmacol* **5**, 73-90 (2013).
201 London, A., Cohen, M. & Schwartz, M. Microglia and monocyte-derived macrophages: functionally distinct populations that act in concert in CNS plasticity and repair. *Frontiers in cellular neuroscience* **7**, 34, doi:10.3389/fncel.2013.00034 (2013).
202 Prinz, M., Priller, J., Sisodia, S. S. & Ransohoff, R. M. Heterogeneity of CNS myeloid cells and their roles in neurodegeneration. *Nat Neurosci* **14**, 1227-1235, doi:10.1038/nn.2923 (2011).
203 Mildner, A. *et al.* Distinct and non-redundant roles of microglia and myeloid subsets in mouse models of Alzheimer's disease. *The Journal of neuroscience : the official journal of the Society for Neuroscience* **31**, 11159-11171, doi:10.1523/JNEUROSCI.6209-10.2011 (2011).
204 Yamasaki, R. *et al.* Differential roles of microglia and monocytes in the inflamed central nervous system. *The Journal of experimental medicine* **211**, 1533-1549, doi:10.1084/jem.20132477 (2014).
205 Tang, X. N., Zheng, Z. & Yenari, M. A. Bone marrow chimeras in the study of experimental stroke. *Translational stroke research* **3**, 341-347, doi:10.1007/s12975-012-0169-6 (2012).
206 McCullough, L. D., Zeng, Z., Blizzard, K. K., Debchoudhury, I. & Hurn, P. D. Ischemic nitric oxide and poly (ADP-ribose) polymerase-1 in cerebral ischemia: male toxicity, female protection. *Journal of cerebral blood flow and metabolism : official journal of the International Society of Cerebral Blood Flow and Metabolism* **25**, 502-512, doi:10.1038/sj.jcbfm.9600059 (2005).
207 Voss, E. V. *et al.* Characterisation of microglia during de- and remyelination: can they create a repair promoting environment? *Neurobiology of disease* **45**, 519-528, doi:10.1016/j.nbd.2011.09.008 (2012).
208 Pul, R., Chittappen, K. P. & Stangel, M. Quantification of microglial phagocytosis by a flow cytometer-based assay. *Methods Mol Biol* **1041**, 121-127, doi:10.1007/978-1-62703-520-0_14 (2013).
209 Schaefer, B. C., Schaefer, M. L., Kappler, J. W., Marrack, P. & Kedl, R. M. Observation of antigen-dependent CD8+ T-cell/ dendritic cell interactions in vivo. *Cellular immunology* **214**, 110-122, doi:10.1006/cimm.2001.1895 (2001).
210 Denes, A. *et al.* Experimental stroke-induced changes in the bone marrow reveal complex regulation of leukocyte responses. *Journal of cerebral blood flow and metabolism : official journal of the International Society of Cerebral Blood Flow and Metabolism* **31**, 1036-1050, doi:10.1038/jcbfm.2010.198 (2011).
211 Chan, P. H. Reactive oxygen radicals in signaling and damage in the ischemic brain. *Journal of cerebral blood flow and metabolism : official journal of the International*

Society of Cerebral Blood Flow and Metabolism **21**, 2-14, doi:10.1097/00004647-200101000-00002 (2001).
212 Chiba, T. & Umegaki, K. Pivotal roles of monocytes/macrophages in stroke. *Mediators of inflammation* **2013**, 759103, doi:10.1155/2013/759103 (2013).
213 Womble, T. A. *et al.* Monocytes are essential for the neuroprotective effect of human cord blood cells following middle cerebral artery occlusion in rat. *Molecular and cellular neurosciences* **59**, 76-84, doi:10.1016/j.mcn.2014.01.004 (2014).
214 Schilling, M., Strecker, J. K., Ringelstein, E. B., Schabitz, W. R. & Kiefer, R. The role of CC chemokine receptor 2 on microglia activation and blood-borne cell recruitment after transient focal cerebral ischemia in mice. *Brain research* **1289**, 79-84, doi:10.1016/j.brainres.2009.06.054 (2009).
215 Schuette-Nuetgen, K., Strecker, J. K., Minnerup, J., Ringelstein, E. B. & Schilling, M. MCP-1/CCR-2-double-deficiency severely impairs the migration of hematogenous inflammatory cells following transient cerebral ischemia in mice. *Experimental neurology* **233**, 849-858, doi:10.1016/j.expneurol.2011.12.011 (2012).
216 Hughes, P. M. *et al.* Monocyte chemoattractant protein-1 deficiency is protective in a murine stroke model. *Journal of cerebral blood flow and metabolism : official journal of the International Society of Cerebral Blood Flow and Metabolism* **22**, 308-317, doi:10.1097/00004647-200203000-00008 (2002).
217 Butovsky, O. *et al.* Identification of a unique TGF-beta-dependent molecular and functional signature in microglia. *Nature neuroscience* **17**, 131-143, doi:10.1038/nn.3599 (2014).
218 Hashimoto, D. *et al.* Tissue-resident macrophages self-maintain locally throughout adult life with minimal contribution from circulating monocytes. *Immunity* **38**, 792-804, doi:10.1016/j.immuni.2013.04.004 (2013).
219 Getts, D. R. *et al.* Ly6c+ "inflammatory monocytes" are microglial precursors recruited in a pathogenic manner in West Nile virus encephalitis. *The Journal of experimental medicine* **205**, 2319-2337, doi:10.1084/jem.20080421 (2008).
220 Grathwohl, S. A. *et al.* Formation and maintenance of Alzheimer's disease beta-amyloid plaques in the absence of microglia. *Nature neuroscience* **12**, 1361-1363, doi:10.1038/nn.2432 (2009).
221 Derecki, N. C. *et al.* Wild-type microglia arrest pathology in a mouse model of Rett syndrome. *Nature* **484**, 105-109, doi:10.1038/nature10907 (2012).
222 Chouery, E. *et al.* Mutations in TREM2 lead to pure early-onset dementia without bone cysts. *Human mutation* **29**, E194-204, doi:10.1002/humu.20836 (2008).
223 Neumann, H. & Takahashi, K. Essential role of the microglial triggering receptor expressed on myeloid cells-2 (TREM2) for central nervous tissue immune homeostasis. *Journal of neuroimmunology* **184**, 92-99, doi:10.1016/j.jneuroim.2006.11.032 (2007).
224 Baba, T. *et al.* Electrical stimulation of the cerebral cortex exerts antiapoptotic, angiogenic, and anti-inflammatory effects in ischemic stroke rats through phosphoinositide 3-kinase/Akt signaling pathway. *Stroke; a journal of cerebral circulation* **40**, e598-605, doi:10.1161/STROKEAHA.109.563627 (2009).
225 Sugawara, T., Lewen, A., Noshita, N., Gasche, Y. & Chan, P. H. Effects of global ischemia duration on neuronal, astroglial, oligodendroglial, and microglial reactions

in the vulnerable hippocampal CA1 subregion in rats. *Journal of neurotrauma* **19**, 85-98, doi:10.1089/089771502753460268 (2002).
226 Yenari, M. A. & Giffard, R. G. Ischemic vulnerability of primary murine microglial cultures. *Neuroscience letters* **298**, 5-8 (2001).
227 Panickar, K. S. & Norenberg, M. D. Astrocytes in cerebral ischemic injury: morphological and general considerations. *Glia* **50**, 287-298, doi:10.1002/glia.20181 (2005).
228 Dewar, D., Underhill, S. M. & Goldberg, M. P. Oligodendrocytes and ischemic brain injury. *Journal of cerebral blood flow and metabolism : official journal of the International Society of Cerebral Blood Flow and Metabolism* **23**, 263-274 (2003).
229 Courties, G. *et al.* Ischemic stroke activates hematopoietic bone marrow stem cells. *Circulation research* **116**, 407-417, doi:10.1161/CIRCRESAHA.116.305207 (2015).
230 Zhang, Q. *et al.* Cell cycle inhibition attenuates microglial proliferation and production of IL-1beta, MIP-1alpha, and NO after focal cerebral ischemia in the rat. *Glia* **57**, 908-920, doi:10.1002/glia.20816 (2009).
231 Ishimura, R., Martin, G. R. & Ackerman, S. L. Loss of apoptosis-inducing factor results in cell-type-specific neurogenesis defects. *The Journal of neuroscience : the official journal of the Society for Neuroscience* **28**, 4938-4948, doi:10.1523/JNEUROSCI.0229-08.2008 (2008).
232 Schilling, M. *et al.* Microglial activation precedes and predominates over macrophage infiltration in transient focal cerebral ischemia: a study in green fluorescent protein transgenic bone marrow chimeric mice. *Experimental neurology* **183**, 25-33 (2003).
233 Li, T. *et al.* Proliferation of parenchymal microglia is the main source of microgliosis after ischaemic stroke. *Brain : a journal of neurology* **136**, 3578-3588, doi:10.1093/brain/awt287 (2013).
234 Rose, S., Misharin, A. & Perlman, H. A novel Ly6C/Ly6G-based strategy to analyze the mouse splenic myeloid compartment. *Cytometry. Part A : the journal of the International Society for Analytical Cytology* **81**, 343-350, doi:10.1002/cyto.a.22012 (2012).
235 Butovsky, O. *et al.* Modulating inflammatory monocytes with a unique microRNA gene signature ameliorates murine ALS. *The Journal of clinical investigation* **122**, 3063-3087, doi:10.1172/JCI62636 (2012).
236 Peters, O. *et al.* Increased formation of reactive oxygen species after permanent and reversible middle cerebral artery occlusion in the rat. *Journal of cerebral blood flow and metabolism : official journal of the International Society of Cerebral Blood Flow and Metabolism* **18**, 196-205, doi:10.1097/00004647-199802000-00011 (1998).
237 Manzanero, S., Santro, T. & Arumugam, T. V. Neuronal oxidative stress in acute ischemic stroke: sources and contribution to cell injury. *Neurochemistry international* **62**, 712-718, doi:10.1016/j.neuint.2012.11.009 (2013).
238 Tang, X. N., Zheng, Z., Giffard, R. G. & Yenari, M. A. Significance of marrow-derived nicotinamide adenine dinucleotide phosphate oxidase in experimental ischemic stroke. *Annals of neurology* **70**, 606-615, doi:10.1002/ana.22476 (2011).
239 Moskowitz, M. A., Lo, E. H. & Iadecola, C. The science of stroke: mechanisms in search of treatments. *Neuron* **67**, 181-198, doi:10.1016/j.neuron.2010.07.002 (2010).

240 Clausen, B. H. *et al.* Interleukin-1beta and tumor necrosis factor-alpha are expressed by different subsets of microglia and macrophages after ischemic stroke in mice. *Journal of neuroinflammation* **5**, 46, doi:10.1186/1742-2094-5-46 (2008).
241 Sumbria, R. K., Boado, R. J. & Pardridge, W. M. Brain protection from stroke with intravenous TNFalpha decoy receptor-Trojan horse fusion protein. *Journal of cerebral blood flow and metabolism : official journal of the International Society of Cerebral Blood Flow and Metabolism* **32**, 1933-1938, doi:10.1038/jcbfm.2012.97 (2012).
242 Abulafia, D. P. *et al.* Inhibition of the inflammasome complex reduces the inflammatory response after thromboembolic stroke in mice. *Journal of cerebral blood flow and metabolism : official journal of the International Society of Cerebral Blood Flow and Metabolism* **29**, 534-544, doi:10.1038/jcbfm.2008.143 (2009).
243 Zhang, N. *et al.* Chrysophanol inhibits NALP3 inflammasome activation and ameliorates cerebral ischemia/reperfusion in mice. *Mediators of inflammation* **2014**, 370530, doi:10.1155/2014/370530 (2014).
244 Tanaka, R. *et al.* Migration of enhanced green fluorescent protein expressing bone marrow-derived microglia/macrophage into the mouse brain following permanent focal ischemia. *Neuroscience* **117**, 531-539 (2003).
245 Woo, M. S. *et al.* Genetic deletion of CD36 enhances injury after acute neonatal stroke. *Annals of neurology* **72**, 961-970, doi:10.1002/ana.23727 (2012).
246 Fang, H. *et al.* CD36-mediated hematoma absorption following intracerebral hemorrhage: negative regulation by TLR4 signaling. *J Immunol* **192**, 5984-5992, doi:10.4049/jimmunol.1400054 (2014).
247 Rausch, M. *et al.* Dynamic patterns of USPIO enhancement can be observed in macrophages after ischemic brain damage. *Magnetic resonance in medicine : official journal of the Society of Magnetic Resonance in Medicine / Society of Magnetic Resonance in Medicine* **46**, 1018-1022 (2001).
248 Geissmann, F. *et al.* Development of monocytes, macrophages, and dendritic cells. *Science* **327**, 656-661, doi:10.1126/science.1178331 (2010).
249 Hammond, M. D. *et al.* CCR2+ Ly6C(hi) inflammatory monocyte recruitment exacerbates acute disability following intracerebral hemorrhage. *The Journal of neuroscience : the official journal of the Society for Neuroscience* **34**, 3901-3909, doi:10.1523/JNEUROSCI.4070-13.2014 (2014).
250 Mallat, M., Marin-Teva, J. L. & Cheret, C. Phagocytosis in the developing CNS: more than clearing the corpses. *Current opinion in neurobiology* **15**, 101-107, doi:10.1016/j.conb.2005.01.006 (2005).
251 Lauber, K., Blumenthal, S. G., Waibel, M. & Wesselborg, S. Clearance of apoptotic cells: getting rid of the corpses. *Molecular cell* **14**, 277-287 (2004).
252 Murray, P. J. *et al.* Macrophage activation and polarization: nomenclature and experimental guidelines. *Immunity* **41**, 14-20, doi:10.1016/j.immuni.2014.06.008 (2014).
253 Towfighi, A. & Saver, J. L. Stroke declines from third to fourth leading cause of death in the United States: historical perspective and challenges ahead. *Stroke* **42**, 2351-2355, doi:10.1161/STROKEAHA.111.621904 (2011).
254 Ransohoff, R. M. & Cardona, A. E. The myeloid cells of the central nervous system parenchyma. *Nature* **468**, 253-262, doi:10.1038/nature09615 (2010).

255 Gorczynski, R. M. CD200 and its receptors as targets for immunoregulation. *Curr Opin Investig Drugs* **6**, 483-488 (2005).
256 Mihrshahi, R., Barclay, A. N. & Brown, M. H. Essential roles for Dok2 and RasGAP in CD200 receptor-mediated regulation of human myeloid cells. *J Immunol* **183**, 4879-4886, doi:10.4049/jimmunol.0901531 (2009).
257 Mihrshahi, R. & Brown, M. H. Downstream of tyrosine kinase 1 and 2 play opposing roles in CD200 receptor signaling. *J Immunol* **185**, 7216-7222, doi:10.4049/jimmunol.1002858 (2010).
258 Liu, Y. *et al.* CD200R1 agonist attenuates mechanisms of chronic disease in a murine model of multiple sclerosis. *J Neurosci* **30**, 2025-2038, doi:10.1523/JNEUROSCI.4272-09.2010 (2010).
259 Walker, D. G., Dalsing-Hernandez, J. E., Campbell, N. A. & Lue, L. F. Decreased expression of CD200 and CD200 receptor in Alzheimer's disease: a potential mechanism leading to chronic inflammation. *Exp Neurol* **215**, 5-19, doi:10.1016/j.expneurol.2008.09.003 (2009).
260 Wang, X. J., Ye, M., Zhang, Y. H. & Chen, S. D. CD200-CD200R regulation of microglia activation in the pathogenesis of Parkinson's disease. *J Neuroimmune Pharmacol* **2**, 259-264, doi:10.1007/s11481-007-9075-1 (2007).
261 Boudakov, I. *et al.* Mice lacking CD200R1 show absence of suppression of lipopolysaccharide-induced tumor necrosis factor-alpha and mixed leukocyte culture responses by CD200. *Transplantation* **84**, 251-257, doi:10.1097/01.tp.0000269795.04592.cc (2007).
262 Bederson, J. B. *et al.* Rat middle cerebral artery occlusion: evaluation of the model and development of a neurologic examination. *Stroke* **17**, 472-476 (1986).
263 Abe, T. *et al.* The neuroprotective effect of prostaglandin E2 EP1 receptor inhibition has a wide therapeutic window, is sustained in time and is not sexually dimorphic. *J Cereb Blood Flow Metab* **29**, 66-72, doi:10.1038/jcbfm.2008.88 (2009).
264 Li, X. *et al.* Chronic behavioral testing after focal ischemia in the mouse: functional recovery and the effects of gender. *Exp Neurol* **187**, 94-104, doi:10.1016/j.expneurol.2004.01.004 (2004).
265 Hattori, K. *et al.* Cognitive deficits after focal cerebral ischemia in mice. *Stroke* **31**, 1939-1944 (2000).
266 Wahl, F., Allix, M., Plotkine, M. & Boulu, R. G. Neurological and behavioral outcomes of focal cerebral ischemia in rats. *Stroke* **23**, 267-272 (1992).
267 Deacon, R. M. Measuring motor coordination in mice. *J Vis Exp*, e2609, doi:10.3791/2609 (2013).
268 van Dellen, A., Blakemore, C., Deacon, R., York, D. & Hannan, A. J. Delaying the onset of Huntington's in mice. *Nature* **404**, 721-722, doi:10.1038/35008142 (2000).
269 Galante, M. *et al.* Impairments in motor coordination without major changes in cerebellar plasticity in the Tc1 mouse model of Down syndrome. *Hum Mol Genet* **18**, 1449-1463, doi:10.1093/hmg/ddp055 (2009).
270 Bouet, V. *et al.* Sensorimotor and cognitive deficits after transient middle cerebral artery occlusion in the mouse. *Exp Neurol* **203**, 555-567, doi:10.1016/j.expneurol.2006.09.006 (2007).
271 Truong, D. T., Venna, V. R., McCullough, L. D. & Fitch, R. H. Deficits in auditory, cognitive, and motor processing following reversible middle cerebral artery

occlusion in mice. *Exp Neurol* **238**, 114-121, doi:10.1016/j.expneurol.2012.08.011 (2012).
272 Deacon, R. Assessing burrowing, nest construction, and hoarding in mice. *J Vis Exp*, e2607, doi:10.3791/2607 (2012).
273 Deacon, R. M. Assessing nest building in mice. *Nat Protoc* **1**, 1117-1119, doi:10.1038/nprot.2006.170 (2006).
274 Liu, F., Schafer, D. P. & McCullough, L. D. TTC, fluoro-Jade B and NeuN staining confirm evolving phases of infarction induced by middle cerebral artery occlusion. *J Neurosci Methods* **179**, 1-8, doi:10.1016/j.jneumeth.2008.12.028 (2009).
275 Manwani, B. *et al.* Functional recovery in aging mice after experimental stroke. *Brain Behav Immun* **25**, 1689-1700, doi:10.1016/j.bbi.2011.06.015 (2011).
276 Ritzel, R. M. *et al.* Functional differences between microglia and monocytes after ischemic stroke. *J Neuroinflammation* **12**, 106, doi:10.1186/s12974-015-0329-1 (2015).
277 Liesz, A., Hu, X., Kleinschnitz, C. & Offner, H. Functional role of regulatory lymphocytes in stroke: facts and controversies. *Stroke* **46**, 1422-1430, doi:10.1161/STROKEAHA.114.008608 (2015).
278 Liesz, A., Karcher, S. & Veltkamp, R. Spectratype analysis of clonal T cell expansion in murine experimental stroke. *J Neuroimmunol* **257**, 46-52, doi:10.1016/j.jneuroim.2013.01.013 (2013).
279 Shichita, T. *et al.* Pivotal role of cerebral interleukin-17-producing gammadeltaT cells in the delayed phase of ischemic brain injury. *Nat Med* **15**, 946-950, doi:10.1038/nm.1999 (2009).
280 Denieffe, S., Kelly, R. J., McDonald, C., Lyons, A. & Lynch, M. A. Classical activation of microglia in CD200-deficient mice is a consequence of blood brain barrier permeability and infiltration of peripheral cells. *Brain Behav Immun* **34**, 86-97, doi:10.1016/j.bbi.2013.07.174 (2013).
281 Shrivastava, K., Gonzalez, P. & Acarin, L. The immune inhibitory complex CD200/CD200R is developmentally regulated in the mouse brain. *J Comp Neurol* **520**, 2657-2675, doi:10.1002/cne.23062 (2012).
282 Dentesano, G. *et al.* Inhibition of CD200R1 expression by C/EBP beta in reactive microglial cells. *J Neuroinflammation* **9**, 165, doi:10.1186/1742-2094-9-165 (2012).
283 Wright, G. J. *et al.* Lymphoid/neuronal cell surface OX2 glycoprotein recognizes a novel receptor on macrophages implicated in the control of their function. *Immunity* **13**, 233-242 (2000).
284 Rijkers, E. S. *et al.* The inhibitory CD200R is differentially expressed on human and mouse T and B lymphocytes. *Mol Immunol* **45**, 1126-1135, doi:10.1016/j.molimm.2007.07.013 (2008).
285 Minas, K. & Liversidge, J. Is the CD200/CD200 receptor interaction more than just a myeloid cell inhibitory signal? *Crit Rev Immunol* **26**, 213-230 (2006).
286 Caserta, S. *et al.* Chronic infection drives expression of the inhibitory receptor CD200R, and its ligand CD200, by mouse and human CD4 T cells. *PLoS One* **7**, e35466, doi:10.1371/journal.pone.0035466 (2012).
287 Smorodchenko, A. *et al.* CNS-irrelevant T-cells enter the brain, cause blood-brain barrier disruption but no glial pathology. *Eur J Neurosci* **26**, 1387-1398, doi:10.1111/j.1460-9568.2007.05792.x (2007).

288 Rygiel, T. P. *et al.* Lack of CD200 enhances pathological T cell responses during influenza infection. *J Immunol* **183**, 1990-1996, doi:10.4049/jimmunol.0900252 (2009).
289 Snelgrove, R. J. *et al.* A critical function for CD200 in lung immune homeostasis and the severity of influenza infection. *Nat Immunol* **9**, 1074-1083, doi:10.1038/ni.1637 (2008).
290 Harris, M. G. *et al.* Immune privilege of the CNS is not the consequence of limited antigen sampling. *Sci Rep* **4**, 4422, doi:10.1038/srep04422 (2014).
291 Ko, Y. C. *et al.* Endothelial CD200 is heterogeneously distributed, regulated and involved in immune cell-endothelium interactions. *J Anat* **214**, 183-195, doi:10.1111/j.1469-7580.2008.00986.x (2009).
292 van den Borne, P. *et al.* The CD200-CD200 receptor inhibitory axis controls arteriogenesis and local T lymphocyte influx. *PLoS One* **9**, e98820, doi:10.1371/journal.pone.0098820 (2014).
293 Ahmad, M. *et al.* Inflammation in ischemic stroke: mechanisms, consequences and possible drug targets. *CNS Neurol Disord Drug Targets* **13**, 1378-1396 (2014).
294 Ren, X., Akiyoshi, K., Vandenbark, A. A., Hurn, P. D. & Offner, H. Programmed death-1 pathway limits central nervous system inflammation and neurologic deficits in murine experimental stroke. *Stroke* **42**, 2578-2583, doi:10.1161/STROKEAHA.111.613182 (2011).
295 Chamorro, A., Urra, X. & Planas, A. M. Infection after acute ischemic stroke: a manifestation of brain-induced immunodepression. *Stroke* **38**, 1097-1103, doi:10.1161/01.STR.0000258346.68966.9d (2007).
296 Meisel, C. *et al.* Preventive antibacterial treatment improves the general medical and neurological outcome in a mouse model of stroke. *Stroke* **35**, 2-6, doi:10.1161/01.STR.0000109041.89959.4C (2004).
297 Offner, H., Vandenbark, A. A. & Hurn, P. D. Effect of experimental stroke on peripheral immunity: CNS ischemia induces profound immunosuppression. *Neuroscience* **158**, 1098-1111, doi:10.1016/j.neuroscience.2008.05.033 (2009).
298 Prass, K. *et al.* Stroke-induced immunodeficiency promotes spontaneous bacterial infections and is mediated by sympathetic activation reversal by poststroke T helper cell type 1-like immunostimulation. *J Exp Med* **198**, 725-736, doi:10.1084/jem.20021098 (2003).
299 Klehmet, J. *et al.* Stroke-induced immunodepression and post-stroke infections: lessons from the preventive antibacterial therapy in stroke trial. *Neuroscience* **158**, 1184-1193, doi:10.1016/j.neuroscience.2008.07.044 (2009).
300 Meisel, A., Meisel, C., Harms, H., Hartmann, O. & Ulm, L. Predicting post-stroke infections and outcome with blood-based immune and stress markers. *Cerebrovasc Dis* **33**, 580-588, doi:10.1159/000338080 (2012).
301 Westendorp, W. F., Nederkoorn, P. J., Vermeij, J. D., Dijkgraaf, M. G. & van de Beek, D. Post-stroke infection: a systematic review and meta-analysis. *BMC Neurol* **11**, 110, doi:10.1186/1471-2377-11-110 (2011).
302 Kwan, J. *et al.* IL-6 is a predictive biomarker for stroke associated infection and future mortality in the elderly after an ischemic stroke. *Exp Gerontol* **48**, 960-965, doi:10.1016/j.exger.2013.07.003 (2013).

303 Sandau, M. M., Winstead, C. J. & Jameson, S. C. IL-15 is required for sustained lymphopenia-driven proliferation and accumulation of CD8 T cells. *J Immunol* **179**, 120-125 (2007).
304 Hug, A. *et al.* Infarct volume is a major determiner of post-stroke immune cell function and susceptibility to infection. *Stroke* **40**, 3226-3232, doi:10.1161/STROKEAHA.109.557967 (2009).
305 Gorczynski, R. M. Evidence for an immunoregulatory role of OX2 with its counter ligand (OX2L) in the regulation of transplant rejection, fetal loss, autoimmunity and tumor growth. *Arch Immunol Ther Exp (Warsz)* **49**, 303-309 (2001).
306 Rygiel, T. P. & Meyaard, L. CD200R signaling in tumor tolerance and inflammation: A tricky balance. *Curr Opin Immunol* **24**, 233-238, doi:10.1016/j.coi.2012.01.002 (2012).
307 Frank, M. G., Baratta, M. V., Sprunger, D. B., Watkins, L. R. & Maier, S. F. Microglia serve as a neuroimmune substrate for stress-induced potentiation of CNS pro-inflammatory cytokine responses. *Brain Behav Immun* **21**, 47-59, doi:10.1016/j.bbi.2006.03.005 (2007).
308 Lyons, A. *et al.* CD200 ligand receptor interaction modulates microglial activation in vivo and in vitro: a role for IL-4. *J Neurosci* **27**, 8309-8313, doi:10.1523/JNEUROSCI.1781-07.2007 (2007).
309 Taki, Y. *et al.* A longitudinal study of gray matter volume decline with age and modifying factors. *Neurobiol Aging* **32**, 907-915, doi:10.1016/j.neurobiolaging.2009.05.003 (2011).
310 Taki, Y. *et al.* Correlations among brain gray matter volumes, age, gender, and hemisphere in healthy individuals. *PLoS One* **6**, e22734, doi:10.1371/journal.pone.0022734 (2011).
311 Howcroft, T. K. *et al.* The role of inflammation in age-related disease. *Aging (Albany NY)* **5**, 84-93 (2013).
312 Kovacs, E. J., Duffner, L. A. & Plackett, T. P. Immunosuppression after injury in aged mice is associated with a TH1-TH2 shift, which can be restored by estrogen treatment. *Mech Ageing Dev* **125**, 121-123, doi:10.1016/j.mad.2003.11.007 (2004).
313 Gorczynski, R., Chen, Z., Khatri, I. & Yu, K. sCD200 present in mice receiving cardiac and skin allografts causes immunosuppression in vitro and induces Tregs. *Transplantation* **95**, 442-447, doi:10.1097/TP.0b013e3182754c30 (2013).
314 Gorczynski, R. M. *et al.* Structural and functional heterogeneity in the CD200R family of immunoregulatory molecules and their expression at the feto-maternal interface. *Am J Reprod Immunol* **52**, 147-163, doi:10.1111/j.1600-0897.2004.00192.x (2004).
315 Kojima, T. *et al.* Mast cells and basophils are selectively activated in vitro and in vivo through CD200R3 in an IgE-independent manner. *J Immunol* **179**, 7093-7100 (2007).
316 Arase, H. & Lanier, L. L. Virus-driven evolution of natural killer cell receptors. *Microbes Infect* **4**, 1505-1512 (2002).
317 Zhang, B. & Gensel, J. C. Is neuroinflammation in the injured spinal cord different than in the brain? Examining intrinsic differences between the brain and spinal cord. *Experimental neurology* **258**, 112-120, doi:10.1016/j.expneurol.2014.04.007 (2014).

318 Nayak, D., Roth, T. L. & McGavern, D. B. Microglia development and function. *Annual review of immunology* **32**, 367-402, doi:10.1146/annurev-immunol-032713-120240 (2014).
319 Wong, W. T. Microglial aging in the healthy CNS: phenotypes, drivers, and rejuvenation. *Frontiers in cellular neuroscience* **7**, 22, doi:10.3389/fncel.2013.00022 (2013).
320 Ransohoff, R. M. & Perry, V. H. Microglial physiology: unique stimuli, specialized responses. *Annual review of immunology* **27**, 119-145, doi:10.1146/annurev.immunol.021908.132528 (2009).
321 Baskar Jesudasan, S. J., Todd, K. G. & Winship, I. R. Reduced inflammatory phenotype in microglia derived from neonatal rat spinal cord versus brain. *PloS one* **9**, e99443, doi:10.1371/journal.pone.0099443 (2014).
322 Hanisch, U. K. Functional diversity of microglia - how heterogeneous are they to begin with? *Frontiers in cellular neuroscience* **7**, 65, doi:10.3389/fncel.2013.00065 (2013).
323 Schnell, L., Fearn, S., Schwab, M. E., Perry, V. H. & Anthony, D. C. Cytokine-induced acute inflammation in the brain and spinal cord. *Journal of neuropathology and experimental neurology* **58**, 245-254 (1999).
324 Batchelor, P. E., Tan, S., Wills, T. E., Porritt, M. J. & Howells, D. W. Comparison of inflammation in the brain and spinal cord following mechanical injury. *Journal of neurotrauma* **25**, 1217-1225, doi:10.1089/neu.2007.0308 (2008).
325 Schnell, L., Fearn, S., Klassen, H., Schwab, M. E. & Perry, V. H. Acute inflammatory responses to mechanical lesions in the CNS: differences between brain and spinal cord. *The European journal of neuroscience* **11**, 3648-3658 (1999).
326 Bartanusz, V., Jezova, D., Alajajian, B. & Digicaylioglu, M. The blood-spinal cord barrier: morphology and clinical implications. *Annals of neurology* **70**, 194-206, doi:10.1002/ana.22421 (2011).
327 Phillips, L. M., Simon, P. J. & Lampson, L. A. Site-specific immune regulation in the brain: differential modulation of major histocompatibility complex (MHC) proteins in brainstem vs. hippocampus. *The Journal of comparative neurology* **405**, 322-333 (1999).
328 Phillips, L. M. & Lampson, L. A. Site-specific control of T cell traffic in the brain: T cell entry to brainstem vs. hippocampus after local injection of IFN-gamma. *Journal of neuroimmunology* **96**, 218-227 (1999).
329 Vaughan, D. W. & Peters, A. Neuroglial cells in the cerebral cortex of rats from young adulthood to old age: an electron microscope study. *Journal of neurocytology* **3**, 405-429 (1974).
330 Samorajski, T. How the human brain responds to aging. *Journal of the American Geriatrics Society* **24**, 4-11 (1976).
331 Perry, V. H., Matyszak, M. K. & Fearn, S. Altered antigen expression of microglia in the aged rodent CNS. *Glia* **7**, 60-67, doi:10.1002/glia.440070111 (1993).
332 Hart, A. D., Wyttenbach, A., Perry, V. H. & Teeling, J. L. Age related changes in microglial phenotype vary between CNS regions: grey versus white matter differences. *Brain, behavior, and immunity* **26**, 754-765, doi:10.1016/j.bbi.2011.11.006 (2012).

333 von Bernhardi, R., Tichauer, J. E. & Eugenin, J. Aging-dependent changes of microglial cells and their relevance for neurodegenerative disorders. *Journal of neurochemistry* **112**, 1099-1114, doi:10.1111/j.1471-4159.2009.06537.x (2010).
334 Chen, J. *et al.* Neuroinflammation and disruption in working memory in aged mice after acute stimulation of the peripheral innate immune system. *Brain, behavior, and immunity* **22**, 301-311, doi:10.1016/j.bbi.2007.08.014 (2008).
335 Tanic, N., Perovic, M., Mladenovic, A., Ruzdijic, S. & Kanazir, S. Effects of aging, dietary restriction and glucocorticoid treatment on housekeeping gene expression in rat cortex and hippocampus-evaluation by real time RT-PCR. *Journal of molecular neuroscience : MN* **32**, 38-46 (2007).
336 Chan, D. C. Mitochondria: dynamic organelles in disease, aging, and development. *Cell* **125**, 1241-1252, doi:10.1016/j.cell.2006.06.010 (2006).
337 Balaban, R. S., Nemoto, S. & Finkel, T. Mitochondria, oxidants, and aging. *Cell* **120**, 483-495, doi:10.1016/j.cell.2005.02.001 (2005).
338 Chung, H. Y., Sung, B., Jung, K. J., Zou, Y. & Yu, B. P. The molecular inflammatory process in aging. *Antioxidants & redox signaling* **8**, 572-581, doi:10.1089/ars.2006.8.572 (2006).
339 de Gonzalo-Calvo, D. *et al.* Differential inflammatory responses in aging and disease: TNF-alpha and IL-6 as possible biomarkers. *Free radical biology & medicine* **49**, 733-737, doi:10.1016/j.freeradbiomed.2010.05.019 (2010).
340 Scheffel, J. *et al.* Toll-like receptor activation reveals developmental reorganization and unmasks responder subsets of microglia. *Glia* **60**, 1930-1943, doi:10.1002/glia.22409 (2012).
341 de Haas, A. H., Boddeke, H. W. & Biber, K. Region-specific expression of immunoregulatory proteins on microglia in the healthy CNS. *Glia* **56**, 888-894, doi:10.1002/glia.20663 (2008).
342 Carson, M. J., Reilly, C. R., Sutcliffe, J. G. & Lo, D. Mature microglia resemble immature antigen-presenting cells. *Glia* **22**, 72-85 (1998).
343 Ensinger, E. M. *et al.* Regional topographical differences of canine microglial immunophenotype and function in the healthy spinal cord. *Journal of neuroimmunology* **227**, 144-152, doi:10.1016/j.jneuroim.2010.07.017 (2010).
344 Pan, W., Banks, W. A. & Kastin, A. J. Permeability of the blood-brain and blood-spinal cord barriers to interferons. *Journal of neuroimmunology* **76**, 105-111 (1997).
345 Pan, W., Banks, W. A. & Kastin, A. J. Blood-brain barrier permeability to ebiratide and TNF in acute spinal cord injury. *Experimental neurology* **146**, 367-373, doi:10.1006/exnr.1997.6533 (1997).
346 Gaudet, A. D. & Popovich, P. G. Extracellular matrix regulation of inflammation in the healthy and injured spinal cord. *Experimental neurology* **258**, 24-34, doi:10.1016/j.expneurol.2013.11.020 (2014).
347 Manwani, B. *et al.* Perfusion of ischemic brain in young and aged animals: a laser speckle flowmetry study. *Stroke* **45**, 571-578, doi:10.1161/STROKEAHA.113.002944 (2014).
348 Ogura, K., Ogawa, M. & Yoshida, M. Effects of ageing on microglia in the normal rat brain: immunohistochemical observations. *Neuroreport* **5**, 1224-1226 (1994).
349 Godbout, J. P. *et al.* Exaggerated neuroinflammation and sickness behavior in aged mice following activation of the peripheral innate immune system. *FASEB journal :*

official publication of the Federation of American Societies for Experimental Biology **19**, 1329-1331, doi:10.1096/fj.05-3776fje (2005).
350 Stadtman, E. R. Protein oxidation and aging. *Free radical research* **40**, 1250-1258, doi:10.1080/10715760600918142 (2006).
351 Clausen, A., Doctrow, S. & Baudry, M. Prevention of cognitive deficits and brain oxidative stress with superoxide dismutase/catalase mimetics in aged mice. *Neurobiology of aging* **31**, 425-433, doi:10.1016/j.neurobiolaging.2008.05.009 (2010).
352 Terman, A., Gustafsson, B. & Brunk, U. T. The lysosomal-mitochondrial axis theory of postmitotic aging and cell death. *Chemico-biological interactions* **163**, 29-37, doi:10.1016/j.cbi.2006.04.013 (2006).
353 Youm, Y. H. *et al.* Canonical Nlrp3 inflammasome links systemic low-grade inflammation to functional decline in aging. *Cell metabolism* **18**, 519-532, doi:10.1016/j.cmet.2013.09.010 (2013).
354 Orre, M. *et al.* Isolation of glia from Alzheimer's mice reveals inflammation and dysfunction. *Neurobiology of aging*, doi:10.1016/j.neurobiolaging.2014.06.004 (2014).
355 Lucin, K. M. *et al.* Microglial beclin 1 regulates retromer trafficking and phagocytosis and is impaired in Alzheimer's disease. *Neuron* **79**, 873-886, doi:10.1016/j.neuron.2013.06.046 (2013).
356 Sokolowski, J. D. & Mandell, J. W. Phagocytic clearance in neurodegeneration. *The American journal of pathology* **178**, 1416-1428, doi:10.1016/j.ajpath.2010.12.051 (2011).
357 Selkoe, D. J. Toward a comprehensive theory for Alzheimer's disease. Hypothesis: Alzheimer's disease is caused by the cerebral accumulation and cytotoxicity of amyloid beta-protein. *Annals of the New York Academy of Sciences* **924**, 17-25 (2000).
358 Li, W. Phagocyte dysfunction, tissue aging and degeneration. *Ageing research reviews* **12**, 1005-1012, doi:10.1016/j.arr.2013.05.006 (2013).
359 Pyo, H., Jou, I., Jung, S., Hong, S. & Joe, E. H. Mitogen-activated protein kinases activated by lipopolysaccharide and beta-amyloid in cultured rat microglia. *Neuroreport* **9**, 871-874 (1998).
360 Halle, A. *et al.* The NALP3 inflammasome is involved in the innate immune response to amyloid-beta. *Nature immunology* **9**, 857-865, doi:10.1038/ni.1636 (2008).
361 Napoli, I. & Neumann, H. Microglial clearance function in health and disease. *Neuroscience* **158**, 1030-1038, doi:10.1016/j.neuroscience.2008.06.046 (2009).
362 Floden, A. M. & Combs, C. K. Beta-amyloid stimulates murine postnatal and adult microglia cultures in a unique manner. *The Journal of neuroscience : the official journal of the Society for Neuroscience* **26**, 4644-4648, doi:10.1523/JNEUROSCI.4822-05.2006 (2006).
363 Salminen, A. *et al.* Impaired autophagy and APP processing in Alzheimer's disease: The potential role of Beclin 1 interactome. *Progress in neurobiology* **106-107**, 33-54, doi:10.1016/j.pneurobio.2013.06.002 (2013).
364 Norden, D. M. & Godbout, J. P. Review: microglia of the aged brain: primed to be activated and resistant to regulation. *Neuropathology and applied neurobiology* **39**, 19-34, doi:10.1111/j.1365-2990.2012.01306.x (2013).

365 Han, M. H. *et al.* Janus-like opposing roles of CD47 in autoimmune brain inflammation in humans and mice. *The Journal of experimental medicine* **209**, 1325-1334, doi:10.1084/jem.20101974 (2012).
366 Gitik, M., Liraz-Zaltsman, S., Oldenborg, P. A., Reichert, F. & Rotshenker, S. Myelin down-regulates myelin phagocytosis by microglia and macrophages through interactions between CD47 on myelin and SIRPalpha (signal regulatory protein-alpha) on phagocytes. *Journal of neuroinflammation* **8**, 24, doi:10.1186/1742-2094-8-24 (2011).
367 Ortman, J. M., Velkoff, V. A. & Hogan, H. An aging nation: the older population in the United States. *Washington, DC: US Census Bureau*, 25-1140 (2014).
368 Cribbs, D. H. *et al.* Extensive innate immune gene activation accompanies brain aging, increasing vulnerability to cognitive decline and neurodegeneration: a microarray study. *J Neuroinflammation* **9**, 179, doi:10.1186/1742-2094-9-179 (2012).
369 Schwartz, M., Kipnis, J., Rivest, S. & Prat, A. How do immune cells support and shape the brain in health, disease, and aging? *J Neurosci* **33**, 17587-17596, doi:10.1523/JNEUROSCI.3241-13.2013 (2013).
370 Wrona, D. Neural-immune interactions: an integrative view of the bidirectional relationship between the brain and immune systems. *J Neuroimmunol* **172**, 38-58, doi:10.1016/j.jneuroim.2005.10.017 (2006).
371 Banks, W. A. The blood-brain barrier in neuroimmunology: Tales of separation and assimilation. *Brain Behav Immun* **44**, 1-8, doi:10.1016/j.bbi.2014.08.007 (2015).
372 Baruch, K. *et al.* CNS-specific immunity at the choroid plexus shifts toward destructive Th2 inflammation in brain aging. *Proc Natl Acad Sci U S A* **110**, 2264-2269, doi:10.1073/pnas.1211270110 (2013).
373 Louveau, A. *et al.* Structural and functional features of central nervous system lymphatic vessels. *Nature*, doi:10.1038/nature14432 (2015).
374 Sierra, A. *et al.* Surveillance, phagocytosis, and inflammation: how never-resting microglia influence adult hippocampal neurogenesis. *Neural Plast* **2014**, 610343, doi:10.1155/2014/610343 (2014).
375 Gemechu, J. M. & Bentivoglio, M. T Cell Recruitment in the Brain during Normal Aging. *Front Cell Neurosci* **6**, 38, doi:10.3389/fncel.2012.00038 (2012).
376 de Graaf, M. T. *et al.* Flow cytometric characterization of cerebrospinal fluid cells. *Cytometry B Clin Cytom* **80**, 271-281, doi:10.1002/cyto.b.20603 (2011).
377 de Graaf, M. T. *et al.* Central memory CD4+ T cells dominate the normal cerebrospinal fluid. *Cytometry B Clin Cytom* **80**, 43-50, doi:10.1002/cyto.b.20542 (2011).
378 Kivisakk, P. *et al.* Human cerebrospinal fluid central memory CD4+ T cells: evidence for trafficking through choroid plexus and meninges via P-selectin. *Proc Natl Acad Sci U S A* **100**, 8389-8394, doi:10.1073/pnas.1433000100 (2003).
379 Kipnis, J., Gadani, S. & Derecki, N. C. Pro-cognitive properties of T cells. *Nat Rev Immunol* **12**, 663-669, doi:10.1038/nri3280 (2012).
380 Radjavi, A., Smirnov, I., Derecki, N. & Kipnis, J. Dynamics of the meningeal CD4(+) T-cell repertoire are defined by the cervical lymph nodes and facilitate cognitive task performance in mice. *Mol Psychiatry* **19**, 531-533, doi:10.1038/mp.2013.79 (2014).

381 Radjavi, A., Smirnov, I. & Kipnis, J. Brain antigen-reactive CD4+ T cells are sufficient to support learning behavior in mice with limited T cell repertoire. *Brain Behav Immun* **35**, 58-63, doi:10.1016/j.bbi.2013.08.013 (2014).
382 Swann, J. B. & Smyth, M. J. Immune surveillance of tumors. *J Clin Invest* **117**, 1137-1146, doi:10.1172/JCI31405 (2007).
383 Stichel, C. C. & Luebbert, H. Inflammatory processes in the aging mouse brain: participation of dendritic cells and T-cells. *Neurobiol Aging* **28**, 1507-1521, doi:10.1016/j.neurobiolaging.2006.07.022 (2007).
384 Smolders, J. *et al.* Characteristics of differentiated CD8(+) and CD4 (+) T cells present in the human brain. *Acta Neuropathol* **126**, 525-535, doi:10.1007/s00401-013-1155-0 (2013).
385 Ritzel, R. M. *et al.* Age- and location-related changes in microglial function. *Neurobiol Aging* **36**, 2153-2163, doi:10.1016/j.neurobiolaging.2015.02.016 (2015).
386 Miguel-Hidalgo, J. J., Nithuairisg, S., Stockmeier, C. & Rajkowska, G. Distribution of ICAM-1 immunoreactivity during aging in the human orbitofrontal cortex. *Brain Behav Immun* **21**, 100-111, doi:10.1016/j.bbi.2006.05.001 (2007).
387 Xu, Y. Z., Nygard, M., Kristensson, K. & Bentivoglio, M. Regulation of cytokine signaling and T-cell recruitment in the aging mouse brain in response to central inflammatory challenge. *Brain Behav Immun* **24**, 138-152, doi:10.1016/j.bbi.2009.09.006 (2010).
388 Anderson, K. G. *et al.* Intravascular staining for discrimination of vascular and tissue leukocytes. *Nat Protoc* **9**, 209-222, doi:10.1038/nprot.2014.005 (2014).
389 Anderson, K. G. *et al.* Cutting edge: intravascular staining redefines lung CD8 T cell responses. *J Immunol* **189**, 2702-2706, doi:10.4049/jimmunol.1201682 (2012).
390 Liu, F. & Whitton, J. L. Cutting edge: re-evaluating the in vivo cytokine responses of CD8+ T cells during primary and secondary viral infections. *J Immunol* **174**, 5936-5940 (2005).
391 Biber, K., Zuurman, M. W., Dijkstra, I. M. & Boddeke, H. W. Chemokines in the brain: neuroimmunology and beyond. *Curr Opin Pharmacol* **2**, 63-68 (2002).
392 Chen, J. *et al.* Aging is associated with increased T-cell chemokine expression in C57BL/6 mice. *J Gerontol A Biol Sci Med Sci* **58**, 975-983 (2003).
393 Felzien, L. K., McDonald, J. T., Gleason, S. M., Berman, N. E. & Klein, R. M. Increased chemokine gene expression during aging in the murine brain. *Brain Res* **890**, 137-146 (2001).
394 Mo, R. *et al.* T cell chemokine receptor expression in aging. *J Immunol* **170**, 895-904 (2003).
395 Mo, F. M., Proia, A. D., Johnson, W. H., Cyr, D. & Lashkari, K. Interferon gamma-inducible protein-10 (IP-10) and eotaxin as biomarkers in age-related macular degeneration. *Invest Ophthalmol Vis Sci* **51**, 4226-4236, doi:10.1167/iovs.09-3910 (2010).
396 Shurin, G. V. *et al.* Dynamic alteration of soluble serum biomarkers in healthy aging. *Cytokine* **39**, 123-129, doi:10.1016/j.cyto.2007.06.006 (2007).
397 Villeda, S. A. *et al.* The ageing systemic milieu negatively regulates neurogenesis and cognitive function. *Nature* **477**, 90-94, doi:10.1038/nature10357 (2011).
398 Jaerve, A. & Muller, H. W. Chemokines in CNS injury and repair. *Cell Tissue Res* **349**, 229-248, doi:10.1007/s00441-012-1427-3 (2012).

399 Elahy, M. *et al.* Blood-brain barrier dysfunction developed during normal aging is associated with inflammation and loss of tight junctions but not with leukocyte recruitment. *Immun Ageing* **12**, 2, doi:10.1186/s12979-015-0029-9 (2015).
400 Floris, S. *et al.* Blood-brain barrier permeability and monocyte infiltration in experimental allergic encephalomyelitis: a quantitative MRI study. *Brain* **127**, 616-627, doi:10.1093/brain/awh068 (2004).
401 Greenwood, J. *et al.* Review: leucocyte-endothelial cell crosstalk at the blood-brain barrier: a prerequisite for successful immune cell entry to the brain. *Neuropathol Appl Neurobiol* **37**, 24-39, doi:10.1111/j.1365-2990.2010.01140.x (2011).
402 Vrethem, M. *et al.* CD4 and CD8 lymphocyte subsets in cerebrospinal fluid and peripheral blood from patients with multiple sclerosis, meningitis and normal controls. *Acta Neurol Scand* **97**, 215-220 (1998).
403 Baruch, K. *et al.* Aging. Aging-induced type I interferon response at the choroid plexus negatively affects brain function. *Science* **346**, 89-93, doi:10.1126/science.1252945 (2014).
404 Barcia, C. *et al.* T cells' immunological synapses induce polarization of brain astrocytes in vivo and in vitro: a novel astrocyte response mechanism to cellular injury. *PLoS One* **3**, e2977, doi:10.1371/journal.pone.0002977 (2008).
405 Sasaki, K. *et al.* Relapsing-remitting central nervous system autoimmunity mediated by GFAP-specific CD8 T cells. *J Immunol* **192**, 3029-3042, doi:10.4049/jimmunol.1302911 (2014).
406 Cabarrocas, J., Bauer, J., Piaggio, E., Liblau, R. & Lassmann, H. Effective and selective immune surveillance of the brain by MHC class I-restricted cytotoxic T lymphocytes. *Eur J Immunol* **33**, 1174-1182, doi:10.1002/eji.200323492 (2003).
407 Sun, D. *et al.* Myelin antigen-specific CD8+ T cells are encephalitogenic and produce severe disease in C57BL/6 mice. *J Immunol* **166**, 7579-7587 (2001).
408 Ariotti, S. *et al.* Tissue-resident memory CD8+ T cells continuously patrol skin epithelia to quickly recognize local antigen. *Proc Natl Acad Sci U S A* **109**, 19739-19744, doi:10.1073/pnas.1208927109 (2012).
409 Ariotti, S., Haanen, J. B. & Schumacher, T. N. Behavior and function of tissue-resident memory T cells. *Adv Immunol* **114**, 203-216, doi:10.1016/B978-0-12-396548-6.00008-1 (2012).
410 Jameson, S. C. Maintaining the norm: T-cell homeostasis. *Nat Rev Immunol* **2**, 547-556, doi:10.1038/nri853 (2002).
411 Lau, L. L., Jamieson, B. D., Somasundaram, T. & Ahmed, R. Cytotoxic T-cell memory without antigen. *Nature* **369**, 648-652, doi:10.1038/369648a0 (1994).
412 Tan, J. T. *et al.* Interleukin (IL)-15 and IL-7 jointly regulate homeostatic proliferation of memory phenotype CD8+ cells but are not required for memory phenotype CD4+ cells. *J Exp Med* **195**, 1523-1532 (2002).
413 Wakim, L. M., Woodward-Davis, A. & Bevan, M. J. Memory T cells persisting within the brain after local infection show functional adaptations to their tissue of residence. *Proc Natl Acad Sci U S A* **107**, 17872-17879, doi:10.1073/pnas.1010201107 (2010).
414 Wolint, P., Betts, M. R., Koup, R. A. & Oxenius, A. Immediate cytotoxicity but not degranulation distinguishes effector and memory subsets of CD8+ T cells. *J Exp Med* **199**, 925-936, doi:10.1084/jem.20031799 (2004).

415 Baruch, K. & Schwartz, M. CNS-specific T cells shape brain function via the choroid plexus. *Brain Behav Immun* **34**, 11-16, doi:10.1016/j.bbi.2013.04.002 (2013).
416 Kondo, T., Takata, H., Matsuki, F. & Takiguchi, M. Cutting edge: Phenotypic characterization and differentiation of human CD8+ T cells producing IL-17. *J Immunol* **182**, 1794-1798, doi:10.4049/jimmunol.0801347 (2009).
417 Huber, M. *et al.* IL-17A secretion by CD8+ T cells supports Th17-mediated autoimmune encephalomyelitis. *J Clin Invest* **123**, 247-260, doi:10.1172/JCI63681 (2013).
418 Peelen, E. *et al.* Fraction of IL-10+ and IL-17+ CD8 T cells is increased in MS patients in remission and during a relapse, but is not influenced by immune modulators. *J Neuroimmunol* **258**, 77-84, doi:10.1016/j.jneuroim.2013.02.014 (2013).
419 Tzartos, J. S. *et al.* Interleukin-17 production in central nervous system-infiltrating T cells and glial cells is associated with active disease in multiple sclerosis. *Am J Pathol* **172**, 146-155, doi:10.2353/ajpath.2008.070690 (2008).
420 Huber, M. *et al.* A Th17-like developmental process leads to CD8(+) Tc17 cells with reduced cytotoxic activity. *Eur J Immunol* **39**, 1716-1725, doi:10.1002/eji.200939412 (2009).
421 Melzer, N., Meuth, S. G. & Wiendl, H. CD8+ T cells and neuronal damage: direct and collateral mechanisms of cytotoxicity and impaired electrical excitability. *FASEB J* **23**, 3659-3673, doi:10.1096/fj.09-136200 (2009).
422 Doyle, K. P., Cekanaviciute, E., Mamer, L. E. & Buckwalter, M. S. TGFbeta signaling in the brain increases with aging and signals to astrocytes and innate immune cells in the weeks after stroke. *J Neuroinflammation* **7**, 62, doi:10.1186/1742-2094-7-62 (2010).
423 Liu, F. & McCullough, L. D. Interactions between age, sex, and hormones in experimental ischemic stroke. *Neurochem Int* **61**, 1255-1265, doi:10.1016/j.neuint.2012.10.003 (2012).
424 Popa-Wagner, A. *et al.* Accelerated infarct development, cytogenesis and apoptosis following transient cerebral ischemia in aged rats. *Acta Neuropathol* **113**, 277-293, doi:10.1007/s00401-006-0164-7 (2007).
425 Sieber, M. W., Claus, R. A., Witte, O. W. & Frahm, C. Attenuated inflammatory response in aged mice brains following stroke. *PLoS One* **6**, e26288, doi:10.1371/journal.pone.0026288 (2011).
426 Sieber, M. W. *et al.* Age-specific transcriptional response to stroke. *Neurobiol Aging* **35**, 1744-1754, doi:10.1016/j.neurobiolaging.2014.01.012 (2014).
427 Manwani, B. *et al.* Differential effects of aging and sex on stroke induced inflammation across the lifespan. *Exp Neurol* **249**, 120-131, doi:10.1016/j.expneurol.2013.08.011 (2013).
428 Shapira, S., Sapir, M., Wengier, A., Grauer, E. & Kadar, T. Aging has a complex effect on a rat model of ischemic stroke. *Brain Res* **925**, 148-158 (2002).
429 Famakin, B. M. The Immune Response to Acute Focal Cerebral Ischemia and Associated Post-stroke Immunodepression: A Focused Review. *Aging Dis* **5**, 307-326, doi:10.14336/AD.2014.0500307 (2014).
430 Jickling, G. C. & Sharp, F. R. Improving the translation of animal ischemic stroke studies to humans. *Metab Brain Dis* **30**, 461-467, doi:10.1007/s11011-014-9499-2 (2015).